Development of new chemical strategies for the site selective conjugation of native proteins

Valentine Vaur

UNIVERSITÉ DE STRASBOURG

ÉCOLE DOCTORALE DES SCIENCES CHIMIQUES

Laboratoire de Conception et Application de Molécules Bioactives

THÈSE présentée par :

Valentine VAUR

Soutenue le : **24 octobre 2023**

pour obtenir le grade de : **Docteur de l'université de Strasbourg**

Discipline/ Spécialité : Chimie Biologique et thérapeutique

Développement de nouvelles méthodes de conjugaison chimiques pour la modification site-sélective de protéines natives

THÈSE dirigée par :

M CHAUBET Guilhem	Chargé de Recherche, Université de Strasbourg

RAPPORTEURS :

Mme VIAUD-MASSUARD Marie-Claude	Professeur, Université de Tours
M ALBADA Bauke	Professor, University of Wageningen

AUTRES MEMBRES DU JURY :

M HERNANDEZ-ALBA Oscar	Chargé de Recherche, Université de Strasbourg
M MARUANI Antoine	Chargé de Recherche, Université Paris Cité
M WAGNER Alain	Directeur de Recherche, Université de Strasbourg

« Y’a un truc qui existe, en gros tu branches un anticorps et un médicament et tu obtiens une chimiothérapie sans effet secondaires ! C’est dingue non ? Si jamais y’a de la chimie là-dedans et que je fais une thèse je veux que ce soit sur ça ! »

Valentine, 19 ans

Table of contents

Remerciements :

Avant toute chose je souhaite remercier les membres du Jury : Pr Marie-Claude Viaud-Massuard, Dr Bauke Albada, Dr Oscar Hernandez-Alba, Dr Antoine Maruani et Dr Alain Wagner qui ont accepté d'évaluer mes travaux de thèse, j'espère que cela mènera à une belle discussion le 24 octobre.

Merci bien entendu aux plateformes techniques de la faculté de pharmacie, aux différents membres du laboratoire de Conception et Applications de Molécules Bioactives et plus particulièrement aux membres de l'équipe de Chimie Bio-Fonctionnelle qui m'ont accueilli et aidé pendant ces trois années de thèse.

Guilhem, merci d'avoir rendu cette thèse possible et de m'avoir fait confiance. Ton implication dans le projet mais aussi la liberté que tu m'as laissée m'ont permis de vivre une thèse dont je garderais un excellent souvenir, merci pour ça. Merci bien évidement aussi pour les innombrables corrections que tu as apporté à ce manuscrit et surtout, merci de vouloir rester un chimiste qui s'amuse. « Pour la science !! »

Alain c'est toi qui m'as fait passer mon premier entretien pour intégrer le labo et ça a été un plaisir de travailler dans ton équipe. Merci d'avoir toujours une nouvelle idée sous le coude et de (presque) tout aborder avec humour.

Aux quatre doctorants arrivés en même temps que moi, merci pour ces trois ans.

Jessica et Robin, on l'a fait les gars !! On a commencé ensemble, on a souvent craqué (je pense particulièrement à la chanson de l'otarie qui tourne à 19 h dans le couloir) mais on peut être fiers de nous et du chemin parcouru en trois ans.

Lorenzo, thank you for being so attentive and kind it was a pleasure to share a lab with you. And pleeeeease remember that football is not the only reason to go home before 8 pm !

Ilias, we shared a research project which is a really uneasy task and I think we nailed it mate ! Thanks a lot for your kindness and for giving me my moments alone with Martine the centrifuge (haha sorry from inside out). I was really happy to be part of the Ugi Dream Team with you and I am sure we'll share another Lily and "une pinte de blonde" soon enough.

Aux doctorants arrivés après moi : Safae, Indréalie et Louis merci d'assurer l'avenir du labo. Je vous souhaite de passer une belle fin de thèse.

Finalement Julien, petit Juli, merci pour tout. Ma thèse aurait été bien différente sans un voisin de paillasse tel que toi. Merci d'avoir eu un an d'expérience en plus, d'avoir tout dédramatisé et de m'avoir tant aidé pendant ces trois années. Merci aussi de ne pas avoir mis que du gros métal

dans le labo, de m'avoir prêté ta sœur (et Agathe), de m'avoir toujours libérée quand tu me mettais en prison (et même de m'avoir libéré de la chambre froide une fois), d'être toujours chaud pour une bière ou une raclette et d'être mon ami.

Merci également aux biologistes du labo Marc, Isabelle et Fanny d'avoir partagé une partie de leurs connaissances en avec moi, j'espère avoir été une élève digne. Je me dois également de remercier Agathe, qui ne fait pas partie intégrante du labo mais qui m'a appris la culture cellulaire pendant des cours du soir.

Héloïse merci d'avoir partagé ton expérience du domaine de la conjug, merci pour ton humour et bon courage pour tes projets un peu louphoques (you got this !).
Ketty merci pour ta bonne humeur et ton entrain qui m'ont bien souvent remonté le moral. Michel, merci pour tes fonds de fritté de quelques grammes, tes précieux conseils en synthèse et ta gentillesse. Françoise, merci de gérer tous les soucis du quotidien.

Je souhaite également remercier quelques alumnis de l'équipe :
Charlotte, on a finalement peu travaillé ensemble (bientôt un peu plus) mais tu resteras la fondatrice du Ugi bitches club. Merci de m'avoir appris la bioconj, merci de me faire confiance et de te rendre toujours disponible pour répondre à mes (trop) nombreuses questions. Victor et Tony, je me sens chanceuse d'avoir commencé ma thèse aux cotés de deux passionnés tels que vous. Victor merci de m'avoir introduit toutes les techniques du labo et d'avoir été là pour discuter pendant mes heures de dessalage. Tony merci d'être toujours disposé à parler de sciences et aussi de pas avoir été trop méchant lors de tes relectures.

Merci également aux membres du laboratoire de Spectrométrie de Masse Bio-Organique (LSMBO), ils ont permis d'emmener le projet plus loin. Merci au Dr Sarah Cianférani et Dr Oscar Hernandez-Alba pour leur disponibilité pour discuter de nouvelles méthodes d'analyse. Merci au Dr Helene Diemer d'avoir réalisé toutes ces campagnes de peptide mapping dans un temps record. Et enfin merci à Rania et à Stéphane qui ont accepté beaucoup trop d'analyses toutes les semaines. Stéphane merci particulièrement de m'avoir tout expliqué avec patience et pédagogie.

Finalement merci à toutes les autres personnes ayant suivi cette thèse d'un peu plus loin.
Gemma, Joris, Michou et Romé, merci d'avoir été là au quotidien pour se changer les idées, partir en vacances pendant le pont du 14 Juillet ou découvrir de nouveaux restaurants. Aux autres membres du master : Louis, Johanna, Ioana, Micka merci pour les belles années du master et venez nous voir plus souvent wesh !

Merci Xu et Sauce de m'écouter patiemment parler de chimie depuis toutes ces années, merci d'être toujours là pour se changer les idées et d'être des humains aussi cool. Merci Léo d'être toujours chaud pour parler Sciences, peu importe l'heure, l'endroit ou l'état. Et merci à tous les autres copaings de la bande d'avoir été là depuis toutes ces années, de m'avoir fait redescendre

sur terre avec des choses de la vrai vie (bienvenue au petit Ismaël). Sarah, CeyCey, Pruno, Marco, Paupaulito, Tev un grand merci à vous.

Merci à mes parents de m'avoir supporté toute au long de mes études et ce malgré une humeur particulièrement mauvaise en périodes de révisions. Merci à ma sœur de m'avoir ouvert à pleins d'autres choses que la science et de me donner toujours plus envie de voyager. Merci au reste de ma famille, ma tante, mon grand-père et mes cousins pour votre soutien.

Et puis merci Pierre. Je ne vais pas m'étendre ici sur tout ce que tu m'as apporté pendant cette thèse mais je te remercie particulièrement pour ces derniers mois de rédaction pendant lesquels tu as été aux petits soins.

Preface

This thesis, founded by the Agence Nationale de la Recherche, was supervised by Dr Guilhem Chaubet, co-director of the BioFunctional Chemistry team along with Dr Alain Wagner.

The BFC team is part of the «Laboratoire de Conception et Applications de Molécules Bioactives » (UMR7199) located in the Faculty of Pharmacy of Strasbourg, in Illkirch-Graffenstaden. The team's main research interest lies in the field of chemical biology and aims to investigate novel bio-compatible and bio-responsive chemical systems to study biological processes and design alternative therapeutic strategies. In this context, research mainly revolves around three main axes:

Single Cell Omic: focused on developing novel capture systems of biomolecules and phase inversion microfluidic technologies, which paves the way toward advanced single cell multi-omic approaches (e.g., transcriptomic, proteomic, secretomic, surfacomic). This technology provides a unique insight into cancer heterogeneity and differentiation processes and led to the recent creation of a start-up company, 'Micro-omix'.

In vivo chemistry: focused on understanding the rules guiding chemical reactions in complex biological media, taking into account reagent transport, bio-distribution and pharmacokinetics. This field opens new opportunities toward alternative therapeutic and chemo-omics approaches *via in vivo* modification of biotics (metabolites) or xenobiotics (drugs, imaging agents).

Bio-specific chemical reactions: dedicated to precise chemical conjugation and controlled delivery of drugs or payloads. Mastering the selectivity in protein conjugation opens exciting prospects toward novel formats of hybrid bimolecular constructs for drug delivery or biophysical studies.

My research work fits in this third area of research and was only made possible thanks to a very close collaboration with the « Laboratoire de Spectrométrie de Masse Bio-organique » (LSMBO; UMR7178) headed by Dr Sarah Cianferani and located in Strasbourg.

The main objective of my thesis was to develop new chemical methods for to the selective labeling of proteins and explore the different application it might have. This led to two main projects, whose initial goals and main results will be detailed in this manuscript.

The first one was the exploration of multicomponent reactions (MCR) for the labeling of protein. The labelling of lysine residues through Robinson-Schöpf 3-component reaction as well as the labeling of lysine and aspartate or glutamate using the Ugi 4 components 3 centers reaction were explored. This led to the development of site-selective conditions for the labeling of human and humanized monoclonal antibodies.

Finally, my second main research project was dedicated to the generation of high molecular weight complexes such as bispecific antibodies. The developed method was based on our site-selective conditions and on bioorthogonal chemistry leading to the efficient formation of different bispecifics, starting from off the shelf antibodies.

An experimental section is provided at the end of this manuscript, listing all experimental procedures used to carry this work as well as the characterization of all new compounds produced during the course of these last three years.

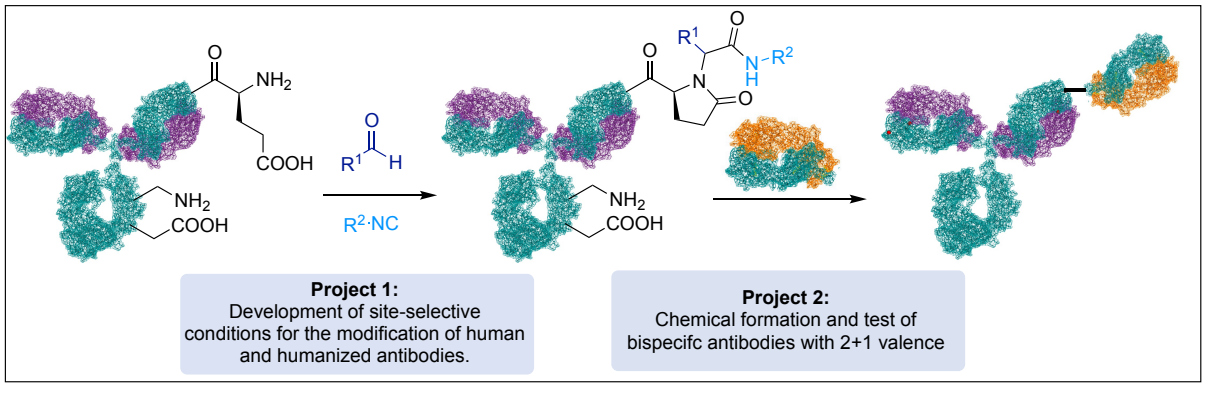

Abbreviations

2-DPBA	2-(diphenylphosphino)benzoic acid
2-FBPA	2-formylphenylboronic acid
2-PCA	2-pyridinecarboxyaldehyde
3-CR	3 component reaction
4C-3CR	4 component-3 center reaction
aa	amino acid
Ac	Acetyl
ADC	antibody-drug conjugate
APB	Activity based probe
APC	allophycocyanin
app	apparent
av. DoC	Average degree of conjugation
BBS	borate-buffered saline
BCN	bicyclo[6.1.0]non-4-yne
br	broad
BSA	Bovine serum albumin
bsAb	bispecific antibody
C, cys	cysteine
CDR	complementary determining regions
cHex	cyclohexane
CID	collision induced dissociation
conv.	conversion
CPP	cell penetrating peptide
CuAAC	copper(I)-catalysed alkyne-azide cycloaddition
Cy5	sulfocyanine-5
d	doublet
D, Asp	acid aspartic
Da	Dalton
DAR	Drug to antibody ratio
DBCO	dibenzylcyclooctyne
DBM	Dibromomaleimide
DCC	N,N'-dicyclohexylcarbodiimide
DCM	Dichloromethane
DIFP	diisopropyl fluorophosphate
DMEM	Dulbecco's modified eagle media
DMF	N,N-dimethylformamide
DMSO	Dimethyl sulfoxide
DNA	desoxyribonucleic acid
DoC	Degree of conjugation

DTNB	5,5’-dithiobis-(2-nitrobenzoic acid)
DTT	Dithitreitol
E, Glu	acid glutamic
E:T	effector to target
e.g.	For example
EBA	2-ethynylbenzaldehyde
EC_{50}	half maximal effective concentration
EDTA	2,2',2'',2'''-(Ethane-1,2-diyldinitrilo)tetraacetic acid
EEDQ	2-ethoxy-1-ethoxycarbonyl-1,2-dihydroquinoline
EGFR	epidermal growth factor receptor
ELISA	enzyme-linked immunosorbent assay
EMA	European Medicine Agency
EpCAM	epithelial cell adhesion molecule
equiv.	equivalent
ESI	electrospray ionisation
Et	ethyl
eV	electronvolt
Fab	antigen binding fragment
F_{ave}	Fab avelumab
F_{durva}	Fab durvalumab
F_{muro}	Fab muromonab
F_{rit}	Fab rituximab
F_{tra}	Fab trastuzumab
FBS	Fetal bovine serum
Fc	Fraction cristaline
FCS	Fœtal calf serum
FDA	Food and Drug Administration
FITC	fluorescein isothiocyanate
Frit	Fab rituximab
Fv	variable fragments
FVS	Fœtal veal serum
GAPDH	glyceraldehyde-3-phosphate dehydrogenase
GFP	green fluorescent protein
Gly	Glycine
GSH	Glutathione
HC	heavy chain
HCD	higher-energy collisional dissociation
HDMS	high definition mass spectrometer
HER-2	Human epidermal growth factor receptor 2
HIC	Hydrophobic interaction chromatography
His	Histidine
HPLC	high performance liquid chromatography

HRMS	high resolution mass spectrometry
HRP	Horseradish peroxidase
HSA	Human serum albumin
HSAB	Hard-soft acide-base
i.e.	id est
IEDDA	Inverse electron demand Diels-Alder
IgG	Immunoglobulin G
IR	infrared
J	coupling constant
K, lys	Lysine
KiH	knobs-into-holes technology
LC	Light chain
LC/MS	liquid chromatography couple to mass spectrometry
Ldchem	ligand-directed chemistry
LPG	linear polyglycerols
LT	Ligand tracer
m	multiplet
m/z	mass-to-charge ratio
mAb	Monoclonal antibody
MALDI	matrix-assisted laser desorption/ionization
MCR	Multicomponent reaction
Me	Methyl
MET	mesenchymal-epithelial transition
MS	Mass spectrometry
nanoESI	nanoelectrospray ionization
NaOAc	sodium acetate
NCS	N-chlorosuccinimide
NGM	Next generation maleimide
NHS	N-hydroxysuccinimide
NMR	Nuclear magentic resonnance
OSAE	o-salicaldehyde ester
PB	Phosphate buffer
PBM	Petasis Borono Mannich
PBS	Phosphate-buffered saline
PD	dibromopyridazinediones
PD-L1	programmed death-ligand 1
PE	phycoerythrin
PEGs	polyethylene glycols
PFP	pentafluorophenyl
Ph	phenyl
pH	potential of hydrogen
PMA	Phosphomolybdic acid

PNP	paranitrophenol
POI	protein of interest
ppm	part per million
PTH	phenylthiohydantoin
q	quartet
QTOF	quadrupole time-of-flight
Ramu	ramucirumab
r.t.	Room temperature
RML	*Rhizomucor miehei* lipase
rpm	round per minute
σ	standard deviation
s	singulet
SASP	Secondary amine-selective Petasis
SDS-page	Sodium dodecyl sulfate-polyacrylamide gel electrophoresis
SEC	Size exclusion chromatography
SPAAC	Strain-promoted azide-alkyne cycloaddtion
SPIEDAC	strain-promoted inverse electron demand Diels-Alder cycloaddition
sulfoCy5	sulfo-cyanine 5
t	triplet
TCEP	*tris*(2-carboxyethyl)phosphine
TCO	transcyclooctene
TDCC	T-cell dependant cellular cytotoxicity
TEA	triethylamine
TFA	trifluoroacetic acid
THF	tetrahydrofuran
TLC	Thin layer chromatography
TMPP	tris(2,4,6-trimethoxyphenyl)phosphonium bromide
TNB	5-thio-2-nitrobenzoic acid
TNBS	trinitrobenzenesulfonate
TOP-ABPP	tandem orthogonal proteolysis-activity-based protein profiling
Tra	trastuzumab
Tyr	tyrosine
U-4C-3CR	Ugi four-components-three-centers reaction
U-4CR	Ugi four component reaction
UV	ultra-violet
VEGFR	vascular endothelial growth factor
VEGFR-2	vascular endothelial growth factor 2
V_H	heavy chain variable domain
V_L	Light chain variable domain
w	Wide

INTRODUCTION

I. Protein bioconjugation

Bioconjugation consists in the development of a chemical linkage between a biomolecule — in this work, a protein — and any other molecule,[1] depending on the applications sought: cytotoxic drugs, small nucleic acids or oligonucleotides, fluorophores, nanoparticles or even another protein or fragments thereof. Chemistry is involved all along the development of bioconjugates, from the design and synthesis of small organic payloads to the comprehension of the constraints of the biochemical microenvironment of the protein and to the analysis and characterisation of the modified proteins. This truly interdisciplinary field forces the collaboration between actors of different fields of research, fostering creativity and innovation and paving the way to fruitful applications impacting our everyday lives.

I.1.Applications

The first known application of bioconjugation goes back to mid nineteenth century with the use of chromium(III) salts in the tanning industry. By cross-linking collagen in animal's hide, the resulting leather was found to be more resistant and durable. While it is highly likely that early-day bioconjugation chemists were lacking the comprehension of the process at the molecular scale, the development of characterization tools paralleled the appearance of novel conjugation techniques, helping to gain better mechanistic insights.[2]

I.1.a. Characterization:

Over the twentieth century, the development of protein purification techniques such as ion exchange (IEX), size exclusion (SEC) and affinity chromatography set bases for a strong collaboration between bioconjugation and analysis by allowing the characterization of peptide and proteins.[2] Those bioconjugation reagents were designed to present a chromophore motif, allowing the quantification of bound reagent to the protein as well as a reactive function — usually an electrophilic group — responsible for the attachment of the chromophore on the protein. One can cite the reaction of trinitrobenzenesulfonate (TNBS, **R1**) (Scheme 1) with primary amines proposed by Fields leading to the formation of trinitroaniline complexes **R2** quantified by their absorbance at 420 nm or Ellman's reagent — 5,5'-dithiobis-(2-nitrobenzoic acid) (DTNB) **R3** (Scheme 1) — used to measure the concentration of thiols through their transformation into 5-thio-2-nitrobenzoic acid (TNB) **R4** absorbing at 412 nm.[3,4] Later on, the determination of peptide sequence became possible by using Edman degradation (1967), a process in which phenyl isothiocyanate **R5** reacts with the α-amine of the *N*-terminal residue of a peptide under alkaline conditions resulting in a phenylthiocarbamoyl derivative **R6**. Following acidic treatment, cleavage of the *N*-terminal residue under the form of a thiazolinone derivative **R7** occurs, the latter being isolated by liquid-liquid extraction as its phenylthiohydantoin (PTH)

isomer **R8** which can be detected, isolated and characterized using chromatography techniques. Automated versions of this process were developed through the years that helped accelerate this analytical process and allowed the development of more advanced technologies for the modification and characterization of proteins.[5,6]

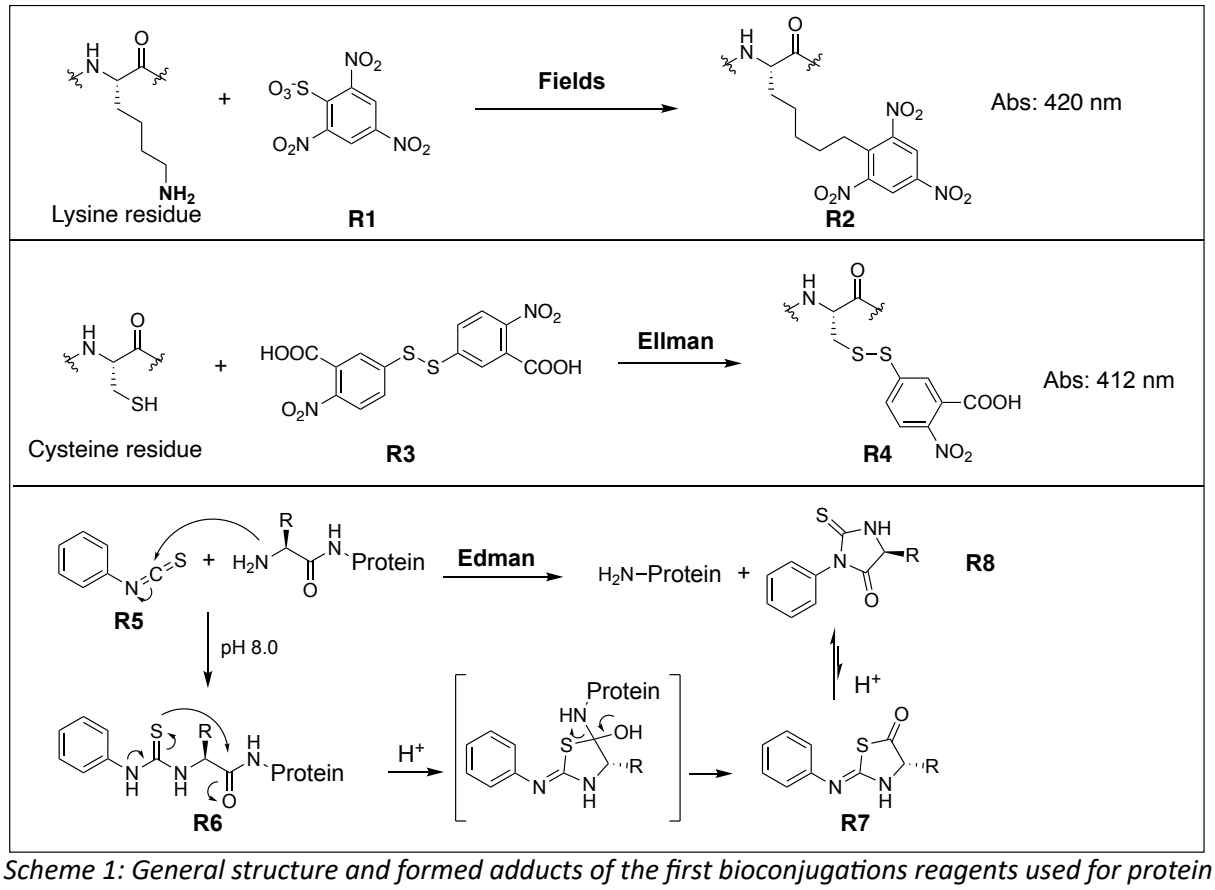

Scheme 1: General structure and formed adducts of the first bioconjugations reagents used for protein characterization.

Based on the observation that protein's behaviour might be biased by its isolation from its native environment, proteomics studies were developed. It consists in the quantification and characterization of the proteome – i.e., the entire set of proteins produced and/or modified by an organism or a system which varies from one cell to another and through time. Precise bioconjugation methods as well as analytical tools are hence needed to be created for such analysis. In the early days, proteins of interest (POI) were detected using antibodies, able to recognise with great affinity one precise motif — the antigen — borne by another protein, the presence of a chromophore on the detection antibody helping the detection of the protein complex. Such characterization techniques are still used nowadays like enzyme-linked immunosorbent assay (ELISA) or western blots. Limited by the available library of antibodies, antibody-free protein detection techniques were developed, leading to the democratisation of mass spectrometry-based techniques. Coupled or not with chromatography techniques, the development of 'soft ionization' methods in the 1980's such as matrix-assisted laser desorption/ionization (MALDI) and electrospray ionization (ESI), allowed mass spectrometry (MS) analysis of proteins while preserving their primary structure. Such analyses have now become pivotal for the development of new bioconjugation methods — for mechanistic comprehension and quantification and their development largely rely on the production of pure

and well-defined conjugates to assess the accuracy and resolution of the conditions.[7–9] In addition to identification and characterization of a protein, such information can give great insights on the metabolic pathway followed by a protein as well as its mechanism within the concerned organism.[7,10]

I.1.b. Determination of biological mechanism

Having powerful analytical tools is key to the determination of biological mechanisms and of the nature of the different partners involved. For example, the idea that a particular amino acid is responsible for the biological activity of an enzyme can be demonstrated by the use of appropriate bioconjugation reagents, such as the seminal diisopropyl fluorophosphate (DIFP) **R9** (Figure 1) developed in 1952 by Balls and Jensen. This reagent was shown to react in a chemoselective manner with serines leading to the formation of compound **R10**, thus inhibiting the activity of several proteases such as chymotrypsin and cholinesterases.[11,12]

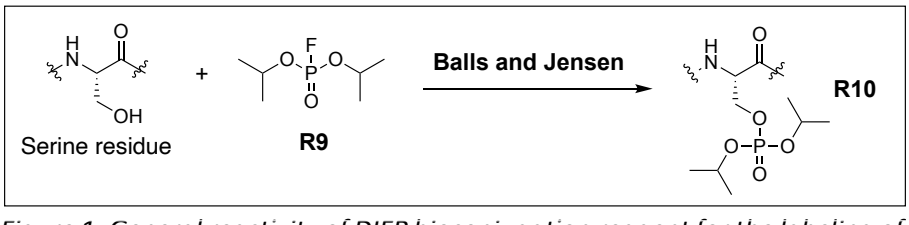

Figure 1: General reactivity of DIFP bioconjugation reagent for the labeling of serines.

Pursuing the development of chemoselective reagents for low abundant residues allowed to analyse more complex environments. For example, Cravatt and co-workers developed a method called isotopic tandem orthogonal proteolysis-activity-based protein profiling (TOP-ABPP) that enabled to quantify the thiol groups of free-cysteines in a given proteome.[13] In order to do so, they used iodoacetamide alkyne **R12** (Scheme 2), whose chemoselectively had been previously demonstrated, forming stable thioethers adducts **R13** that were further functionalized by copper(I)-catalysed alkyne-azide cycloaddition (CuAAC) with an azido-functionalized biotin tag **R14**, leading to biotinylated protein **R15**. Based on the strong non-covalent interactions between biotin and streptavidin (K_D up to 10^{-15} M), they were able not only to isolate but also to concentrate the cysteine-containing proteins and characterize them by tandem MS. As an alternative to activity-based probes, ligand-directed chemistry (LDchem) was also developed, mostly by Hamachi and co-workers. The idea behind this strategy it to link a fluorophore or an affinity tag to the native ligand of a POI using a cleavable linker (**R16**). The ligand part of the construct will play a "carrier" role and bring the desired chemical in spatial proximity to the POI's surface. The cleavable function borne by the linker — usually an electrophilic moiety such as tosylate ester — will then undergo a nucleophilic attack resulting in the covalent attachment of the target chemical to the protein's surface (**R17**) and possible traceless restitution of the intact protein's active site (**R18**) (Scheme 2).[14] Such approaches gave key information for the identification of small therapeutic molecules — covalent inhibitors/activators of key enzymes

— but also paved the way toward the production of biomolecule-based therapeutics such as protein carriers in drug delivery systems.

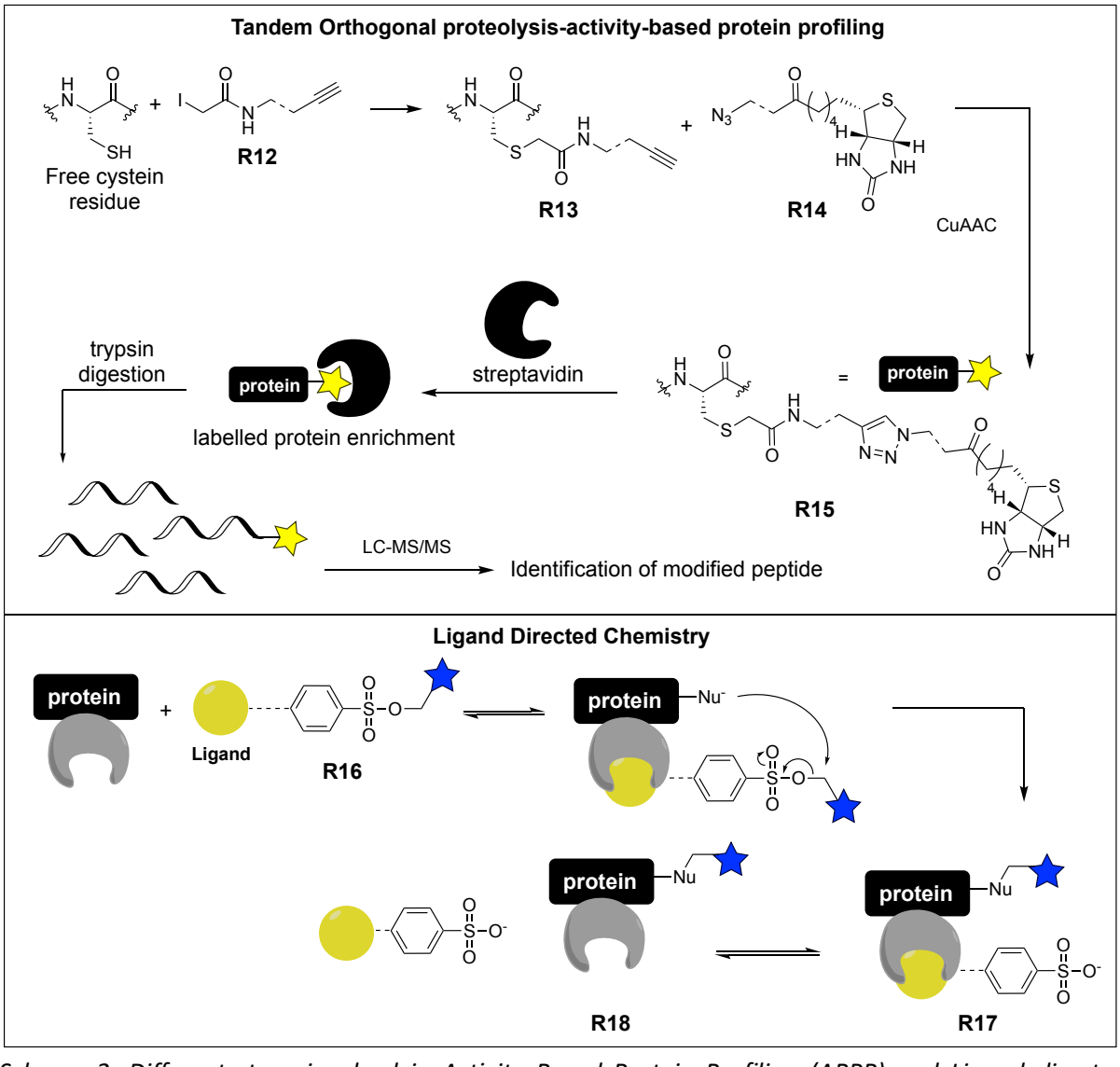

Scheme 2: Different steps involved in Activity Based Protein Profiling (ABPP) and Ligand directed chemistry (LDchem)

I.1.c. Development for therapy:

One of the first application of bioconjugation for therapy is the development of vaccines for tetanus and diphtheria developed in 1920's. Such vaccines called toxoids are inactivated bacterial toxins whose molecular markers responsible for the immune response have been preserved. Such inactivation can be performed thermally or chemically by using fixation reagents such as formaldehyde.[15] The high efficacy of toxoids paved the way towards the development of conjugate vaccines which combine a weak antigen — usually a polysaccharide — to a strong antigen — usually diphtheria or tetanus toxoids described before — as a carrier to provoke stronger response from the immune system. The two biomolecules are usually conjugated using cross-linking reagent such as squaric acid diethyl ether that can react with primary amines of both partners.[16]

If toxoid and conjugate vaccines are good examples of pharmaceutical applications of bioconjugation, the main class of protein conjugates developed for therapy are antibody-drug conjugates (ADC). Those immunoconjugates — *viz.* bioconjugates of immunoglobulins G (IgG) and more precisely monoclonal antibodies (mAb) — are mostly used in oncology. Such constructs combine the high affinity of the mAb for a target receptor — the antigen, overexpressed at the surface of tumor cells — with highly cytotoxic payloads — e.g., DNA intercalating reagents, microtubular disrupting agents, or more recently oligonucleotides —, connected through a linker (Figure 2).

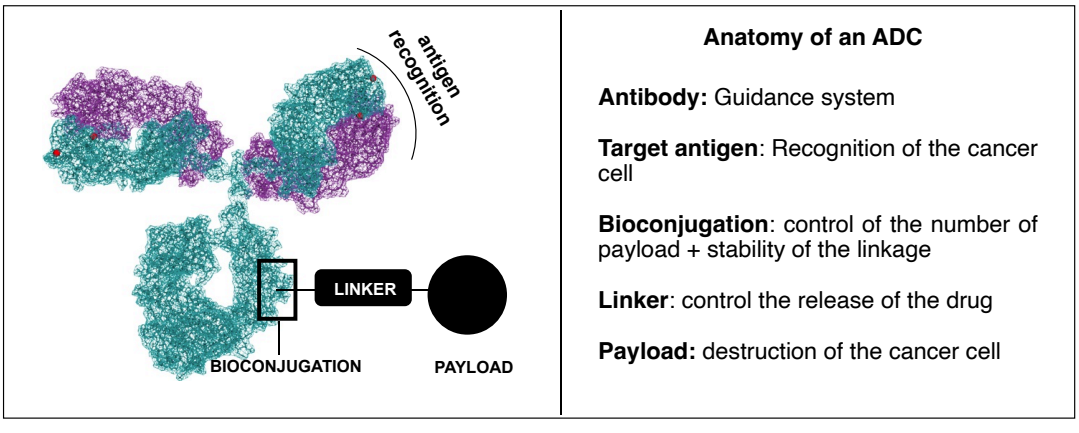

Figure 2: General anatomy of an ADC and principal characteristics of its key components.

The mAb constituent, a protein of around 150 kDa, allows to mask the cytotoxic character of the payload when it is linked to it while delivering it selectivity in the tumor; the linker then allows the usually traceless release of the drug, free to exert its cytotoxic activity.[17] The efficacy of the ADC is strongly correlated with the choice of the target antigen, the payload and the linker but the bioconjugation method also plays a crucial role in the pharmacokinetics and the pharmacodynamics of the whole complex: unstable adducts can lead to early release of the payload in the circulation, resulting in off-target cytotoxicity, whilst the uncontrolled conjugation may impair the affinity of the mAb for its target antigen.[18,19,20]

Currently, there are 10 ADCs approved by the European Medicine Agency (EMA), 2 more were approved by the Food and Drug Administration (FDA) and another has reached market in China.[21] Besides these marketed ADCs, hundreds of others have reached clinical trials, mostly for oncologic applications. This is highly encouraging for the future of immunoconjugates, and it has been made possible thanks to the prolonged efforts of researchers to address the many challenges of antibody conjugation.

I.2. Challenges

Classical organic chemistry offers a great choice of solvents, temperature, pH and pressure to the experimenter, with the possibility of working with a wide range of concentrations, and usually deals with small molecules that can benefit from many different purification and

analytical techniques. Proteins on the contrary are gigantic entities that can only withstand aqueous buffered solution, small variations in pH (5 < pH < 9) or temperature (4 °C < T° < 37 °C) and low concentration (□M range). Moreover, being highly polar, proteins cannot be functionalized with too many organic compounds as this might cause the protein's denaturation or precipitation.

The simplest parameters used to define a bioconjugation reaction are the conversion — i.e., the amount of protein that reacted — and the average degree of conjugation (av. DoC) — i.e., the number of modifications introduced per biomolecule on average — that can be obtained by LC-MS using techniques such as soft ionisation. In addition, depending on its resolution, this analysis can help validate the molecular weight of the introduced payload and confirm or disconfirm the conjugation mechanism. On the other hand, determination of the modified amino acid(s) — the modification site(s) — on the protein's sequence is more challenging as it requires its digestion into peptides prior to their separation by liquid chromatography (LC) and analysis by tandem mass spectrometry (MS/MS) to characterize the modified peptides according to their fragmentation. Such peptide mapping analysis is time consuming and requires high resolution instruments; however, as it is the most precise method developed for this purpose, its use becomes mandatory in order to validate the chemo- and site-selectivity of the conjugation reaction.

Bioconjugation of proteins consists in the formation of covalent bonds with the side chains of some of their constitutive amino acids, multiple copies of which can be found in their primary sequence. Depending on the properties of the side-chain reactive groups (e.g. abundance, polarity, ionization), these will be more or less surface exposed and thus available for modification. Hence the selection of the target amino acids leads to a first – and the easiest to address – issue of selectivity in the development of precise bioconjugation methods: chemo-selectivity. In this case, the bioconjugation reagent must react selectively with the target chemical function without affecting other reactive groups. However, depending on the size of the protein, multiple copies of the amino acid bearing the targeted chemical function can be present on its surface, which can lead to the formation of various regio-isomers.

Gautier *et al*. showed for example that in the case of a big protein such as IgG, possessing 88 primary amines (i.e., 84 ε-amines borne by lysines' side-chains, plus four *N*-terminal α-amines), 69 were shown to be reactive enough to be modified.[22] All sites considered equal, the modification of 1 equivalent of IgG with 6 equivalent of amine-selective reagent can lead to a mixture of unmodified IgG (D0), IgG modified once (D1), twice (D2) up to n times (Dn). Each of those Dn species contains a mixture of regio-isomers, which combined for millions different regio-isomers. While this gives a rapid insight into the complexity and challenges of the selective bioconjugation of native proteins, isolation and characterization can also represent a hurdle in its own right.

When detecting a particular protein within a complex mixture — as it is the case in proteomics study — is the final goal of the bioconjugation step, the homogeneous labelling of the protein is not problematic for detection, hence chemo-selective methods can be used. Another example being the conjugate vaccines, as long as the injected mixture does not present any global toxicity the vaccine is efficient no matter the conjugation site. If the lack of global toxicity was considered sufficient in the case of marketed ADCs such as Mylotarg or Kadcyla, each regio-isomer might present a different pharmacokinetic and pharmacodynamic that might result in premature release and off-target cytotoxicity. In this case, a second degree of selectivity can be reached by thinking the protein as the biological object it is. For instance, post-translational modifications happen in a very reproducible and selective way which means all the reactive sites are not equal, biologically speaking. Inspired by this reflexion, bioconjugation chemists developed new type of reagents — site-selective reagents — that target one site of the protein based on its physico-chemical environment allowing to reduce the number of formed regio-isomers and increasing the reproducibility of the conjugation step leading to the formation of characterized and molecularly defined conjugates.

Hence, protein conjugation reagents can be separated in two main categories based on their degree of selectivity: either chemo-selective — targeting precise chemical functions present on the surface of the target protein — or site-selective — targeting one precise site based on its environment, accessibility or reactivity. Depending on the application of the conjugate, one might focus on the development of site-selective method or on the development of a chemo-selective method. As site-selective methods are difficult to develop and more importantly to characterize, the more easily accessible — and empirical — chemo-selective methods are still being investigated nowadays and used on an everyday basis in many domains of research.

II. Chemo-selective bioconjugation reagents

At the end of 2021, our team published a review of the different chemo- and site-selective strategies and reagents developed for the conjugation of proteins.[23] The results presented in the following sections are a condensed version of this review focused on chemo-selective methods considered as the most relevant for the research work presented in this thesis manuscript — purely chemical modification of native protein — and features additional methods reported in the literature since its publication.

II.1. Lysine conjugation

Lysine residues are a target of choice for chemo-selective bioconjugation reagents because they are abundant in proteins (> 5%) and possess a nucleophilic ε-amine side-chain, the pK_a of which varies from 9.3 to 9.5, meaning they are mostly positively charged at physiological pH (Scheme 3).[24] This cationic character makes them essentially located on the protein's surface and thus easily accessible for conjugation. Chemo-selective reagents targeting amines can be separated into three main categories, i.e., carbonyls, activated esters and iso(thio)cyanates.[25–29]

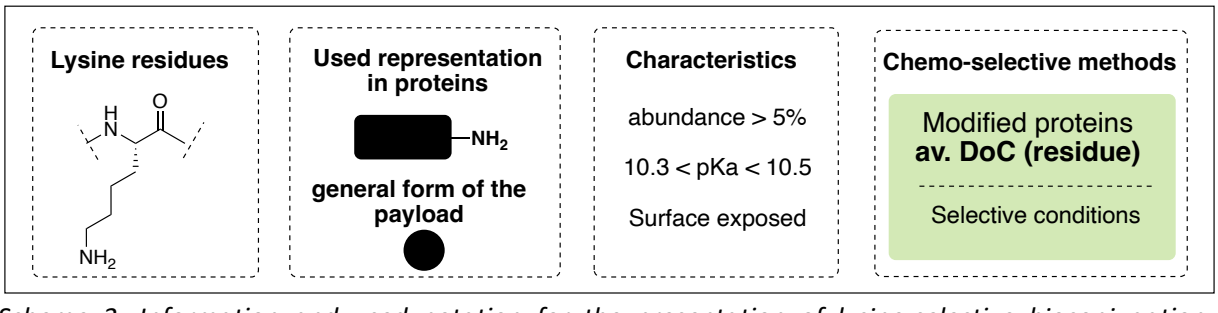

Scheme 3: Information and used notation for the presentation of lysine-selective bioconjugation reagents.

The reaction of a carbonyl derivative **R19** with the primary amine of a lysine residue leads to the well described formation of a Schiff base. However, under aqueous basic conditions the formed imines are unstable, and their formation is disfavoured. Consequently, conjugation methods using carbonyl derivatives are usually accompanied with an irreversible reduction step using sodium cyanoborohydride ($NaBH_3CN$) and leading to the formation of a stable secondary amine **R20** (Figure 3).[25,30]

As an alternative to carbonyls, activated carboxylates — such as pentafluorophenyl (PFP) ester **R21** or *N*-hydroxysuccinimidyl (NHS) esters **R22** —can react with primary amines to form amides **R23 (**Figure 3). [31–36,37,38] Those linkages are extremely stable in water — with an half-life estimated to be around 600 years in neutral aqueous solution — making them particularly interesting for bioconjugation.[39] However such activated compounds get rapidly hydrolysed in water — for example the half-life of NHS esters at pH 8.4 at 4 °C is around 10 minutes —[40], amide bonds can still be obtained using very mild conjugation conditions — mostly by variation of the reaction's temperature and pH.[41] The main drawback of this conjugation method —

beside hydrolysis of the activated carboxylate that is overcome by careful design and modulation of the reaction conditions — is the alteration of the overall charge at the surface of the modified protein.

The use of isothiocyanate **R24** derivatives is also considered a standard for the labelling of lysines (Figure 3). If those reagents were found to be more resistant toward hydrolysis than the activated esters, the formed thiourea **R25** is less stable than an amide bond. [42–44] Its main representant is the fluorescein isothiocyanate (FITC) that is widely used for fluorescent labelling of proteins.

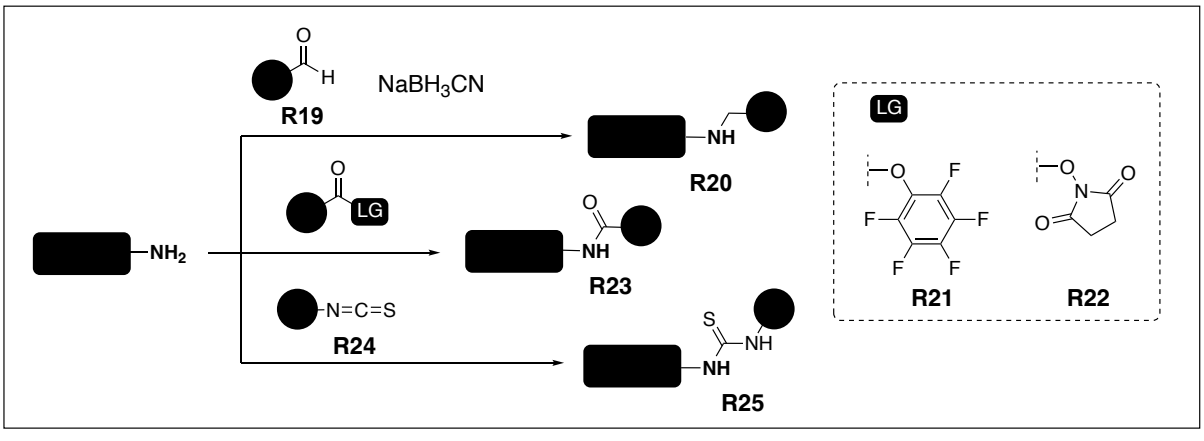

Figure 3: General structure of amine-selective bioconjugation reagents and of the resulting products.

Given the efficacy of these strategies and their facile implementation, with reagents often being cheap and easily accessible, they remain a method of choice for protein conjugation whenever heterogeneity in conjugation sites is not an issue.

Having described the main lysine-targeting strategies, we analysed the most recent publications of new amine-selective reagents or the adaptation of the previously described standard reagents for specific applications.

Among the few new reagents reported recently, it is worth mentioning the azaphilones **R26** developed by Yi *et al*. in 2022, reacting through a sequential ring-opening/ring closure mechanism leading to the formation of UV-active vinylogous γ-pyridones **R27** (Figure 4).[45] Because this reagent led to stable adduct, they were able to label all the available amines of small proteins thus reaching very high degrees of conjugation (DoC) — up to 14 in the case of Histone 2A. However, in the case of bigger proteins such as mAbs, the number of surface exposed amines was found too high to imagine targeting them all without stability issues and the method thus led to a classical DoC distribution resulting in mixtures of various regioisomers just like the other classical methods.

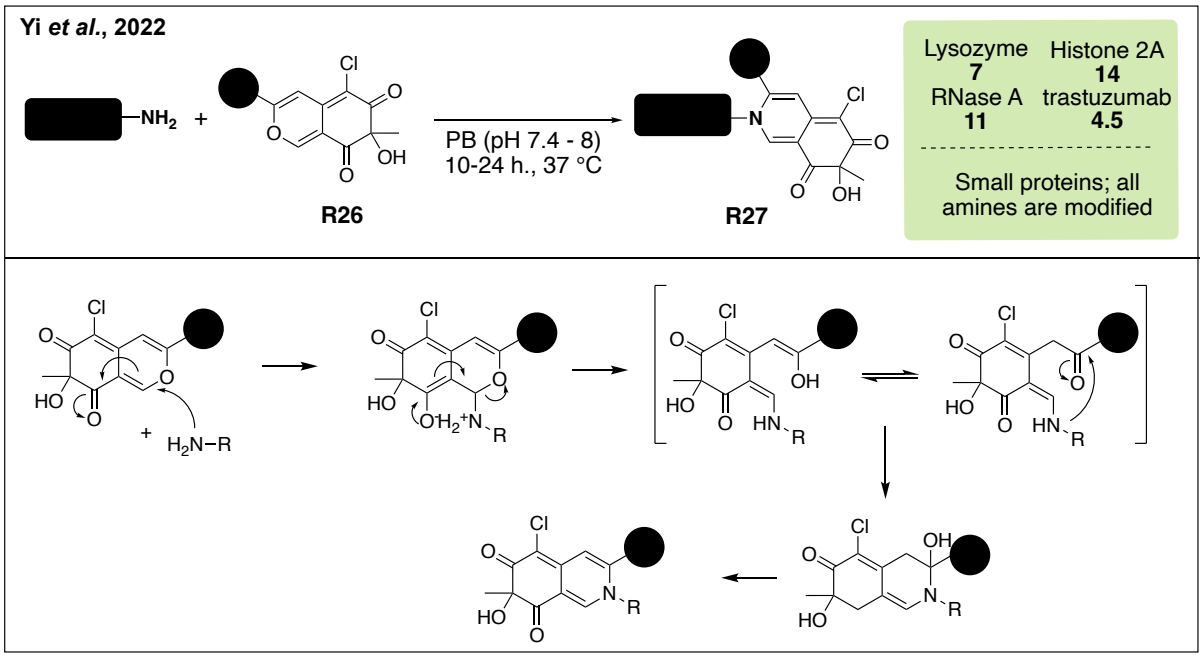

Figure 4: Chemo-selective modification of native proteins using azaphilone reagent R26. Homogeneous labelling can be reached by saturation of available primary amines but is lost when applied to big proteins.

Drifting away from such strategies targeting high degrees of functionalization, the development of DoC-selective methods emerged. In this case, a mono-disperse mixture of regio isomer is obtained, leading to easier characterization of the formed species. Most of the methods recently described focus on the use of already existing lysine-selective reagent and DoC selectivity is reached by fine tuning of the labelling conditions and/or purification.

For example, reductive amination is used for the conjugation of large polymers such as polyethylene glycols (PEGs) and linear polyglycerols (LPG) of high molecular weights (> 10 kDa) onto a POI in order to increase its solubility and stability in living organisms (Figure 5).[46,47] The introduction of an aldehyde on the polymer is trivial in comparison with more sophisticated motives and, more interestingly, the steric hindrance induced by the linkage of one PEG chain results in observed av. DoC around 1. Because of the high polarity and molecular weight of the introduced payload, the different formed DoC species (D1, D2 etc..) can be separated by hydrophobic interaction chromatography (HIC) or size exclusion chromatography (SEC) resulting in mono-disperse mixture of regio isomers (Figure 5).

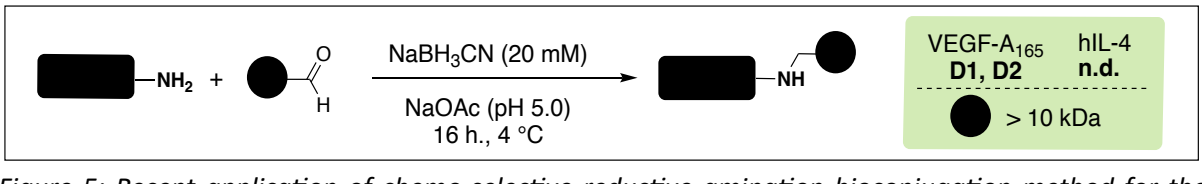

Figure 5: Recent application of chemo-selective reductive amination bioconjugation method for the modification of native proteins. The use of high molecular weight payloads allows the reduction of bioconjugation sites and/or separation of the formed species.

Based on a similar thought, the introduction of large payloads such as quantum dots,[48] polymers,[49] and supramolecular machines[50] functionalized with NHS-esters has also been reported, allowing isolation of mono-disperse species, facilitated by the size of the payload.

Such DoC selective technique has also been explored in the case of small payloads. For instance our team developed in 2020 the equimolar native chemical tagging (ENACT) technology.[51] This process affords mono-disperse protein conjugate using NHS ester **R28** with large excess of proteins, in so called 'low conversion' conditions, in order to obtain a mixture comprising 95% of unconjugated protein and 5% of protein modified with only one payload (**R29**) (Figure 6). Because **R28** contains a biotin tag, conjugate **R29** can be immobilized on a streptavidin column and the unconjugated protein can be recycled. After 20 cycles, trans-tagging of the iminosydnone motive with a strained alkyne — such as bicyclo[6.1.0]non-4-yne (BCN), dibenzylcyclooctyne (DBCO) or 3,3,6,6-tetramethylthiacycloheptyne (TMTH) — allowed to release the mono-disperse conjugate **R30** from the streptavidin column. This technique was shown applicable to various proteins — i.e., trastuzumab, bevacizumab, HSA and lysozyme however, peptide mapping analysis of mono-disperse trastuzumab D1 showed a mixture of 12 regio-isomers that could not be separated.

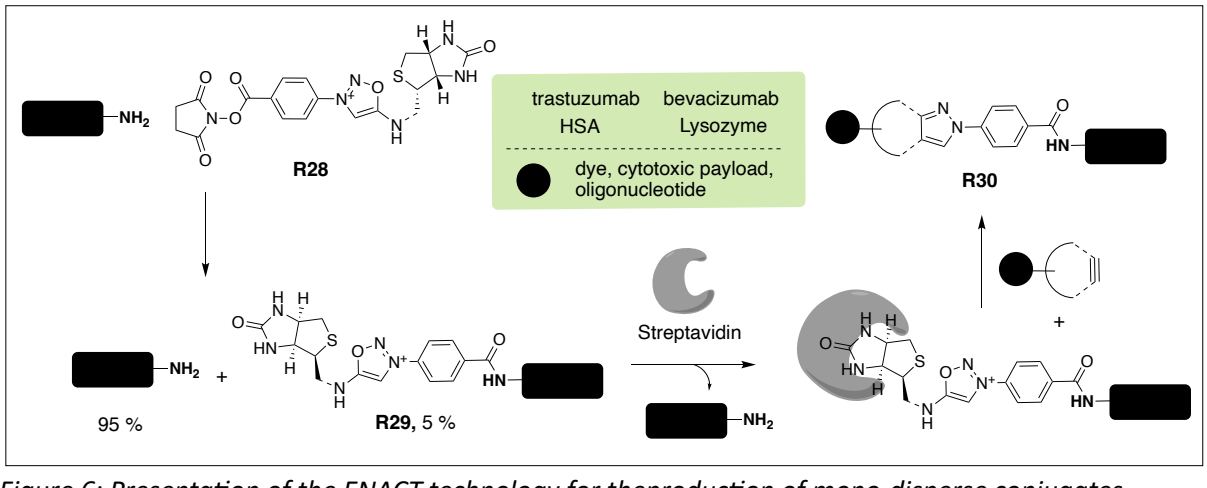

Figure 6: Presentation of the ENACT technology for theproduction of mono-disperse conjugates.

If no studies compared yet the interest of those mono-disperse species with conjugates obtained by traditional chemo-selective methods — presenting a DoC distribution — or site selective conjugates — containing a single regio-isomer —, those methods present an intermediate degree of selectivity.

Interestingly, Kreusser *et al.* recently developed a method for the separation of regioisomers resulting from the FITC-labelling of lysozyme using HIC.[52] After incubation of lysozyme with 1.5 equiv. of FITC at 7 °C for 3 hours they observed an av. DoC around 1. Using finely tuned HIC purification conditions, they managed to separate four lysozyme containing fractions. The first one was found to contain pure unlabelled lysozyme and the three others coined C1, C2 and C3 were found to contain lysozyme modified with only one FITC according to ESI-MS analysis. Based on a previous study of Schnaible and Przybylski which showed that lysozyme labelling with FITC was preferentially happening on its α-NH_2 and on ε-NH_2 borne by K33 and K97 they

hypothesized that their C1, C2 and C3 fractions might contain those three regioisomers.[53] If their study lacks peptide mapping characterization to support this hypothesis, it is however a promising approach that would allow the to reach highly homogeneous conjugates using already widely described chemo-selective conjugation methods.

Another important part of the research concerning lysine bioconjugation focused on the development and rationalisation of site-selective conjugation of proteins, using widely described chemo-selective reagents. Weil and co-workers showed for example that the use of biotinylated NHS-ester **R31** could lead to regio-selective conjugation of RNase A and lysozyme C when it is added portion wise at 4 °C which allow kinetic control of the reaction (Figure 7).[54] The resulting biotinylated proteins **R32** were separated from the unconjugated protein using avidin columns and good yields > 90% were obtained. Peptide mapping experiments validated that the isolated product was exclusively modified on their K1 residues however the modification of the α- or ε-amine was not discussed.

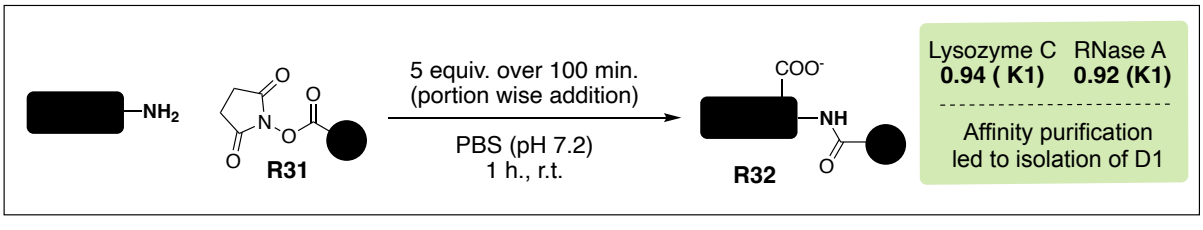

Figure 7: Recent application of the chemo-selective NHS-ester mediated bioconjugation method for the modification of native proteins. Kinetically controlled addition of the reagent associated to affinity purification allows to control the modification site.

On a similar note, Cellitti and co-workers showed that careful control of the reaction's temperature, using PFP ester **R33** on the antigen binding fragment (Fab) of trastuzumab — a human IgG — could lead to the formation of amide **R34** on a single lysine residue (K188) (Figure 8).[36] Directed mutagenesis studies showed the importance of the surrounding residues H189 and D151 in the selective labelling of K188 but no exact mechanism was proposed. D151 might activate H189 to act as an acid-base catalyst and accelerate K188 labelling in comparison with the other lysine residues of the protein. This observed site-selectivity is linked to the environment of the labelled residue and is lost upon increased temperature or use of more reactive reagents such as NHS esters, showing the kinetic character of this method.

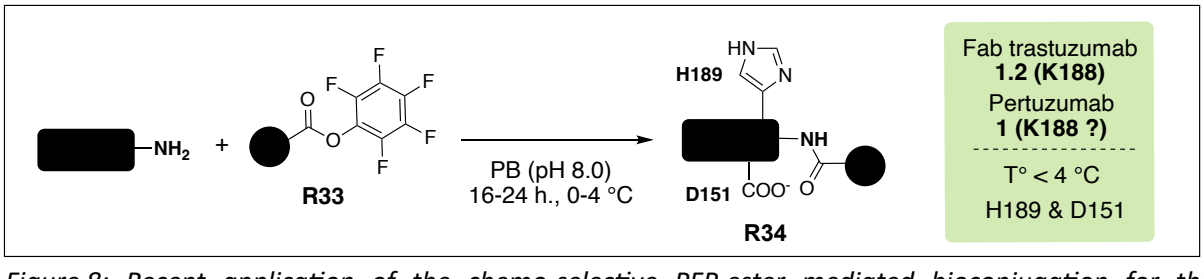

Figure 8: Recent application of the chemo-selective PFP-ester mediated bioconjugation for the modification of native proteins. Selectivity of site is obtained by kinetic controlled addition of the reagent in addition to spatial proximity of a histidine and an aspartate residue.

Based on the thought that such site is highly conserved within human κ-light chains, Sarrett *et al* applied similar conditions to the site-selective labelling of pertuzumab — a humanized mAb presenting the target light chain (Figure 8).[37] If no peptide mapping of the labelling site was performed thus preventing to validate the K188 modification, remarkable D1 labeling of the light chain was observed in comparison with the NHS labeling.

Finally, recent publications about lysine-selective bioconjugation are mostly focused on the development of novel 'more selective' conditions using widely described chemo-selective reagents. The generation — or isolation — of mono-disperse conjugates seems to gain interest lately presenting an intermediate degree of selectivity that can be placed in between chemo- and regio- selectivity. The development of regio-selective conditions using the widely described and easily accessible chemo-selective reagents illustrates well the growing interest for the isolation of pure regio-isomers. For such application, and especially in the case of large proteins such as monoclonal antibodies, the functionalization of less abundant amino acids using chemo-selective reagents is often more effective.

II.2. Cysteine conjugation

In Nature, thiols are mainly found as part of disulfide bonds, connecting two cysteine's side chains. Those disulfide bridges can be reduced thus generating thiolate groups that are highly nucleophilic at physiological pH, making them good candidates for functionalization. Because of the low abundance of cysteines in Nature (1.5 %) chemo-selective targeting of free thiols was largely explored (Scheme 4).[41,55] Thiolate selective reagents are electrophilic compounds, whose reactivity has to be finely controlled as competition with more abundant nucleophilic lysines can happen. The most widely described are alkyl and aryl halides, disulfide, electron-deficient alkenes and alkynes, among which maleimides are considered as the golden standard.[26–28,56]

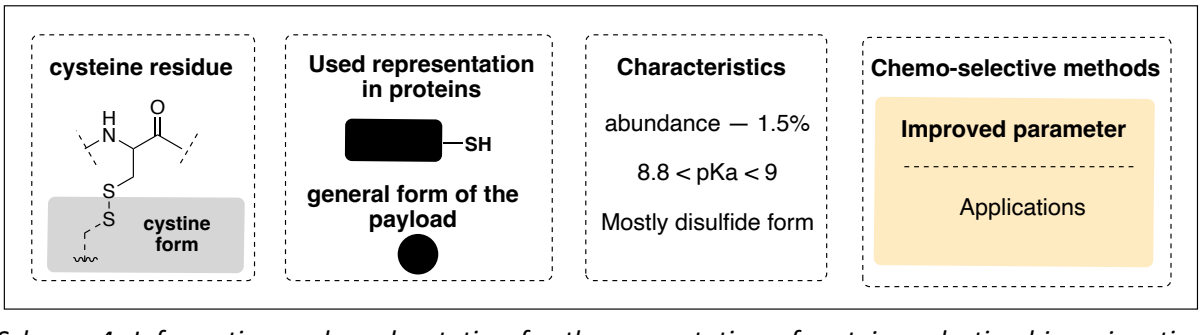

Scheme 4: Information and used notation for the presentation of cysteine-selective bioconjugation reagents.

The targeting of this residue presents great interest when large proteins such as mAbs, are targeted. Indeed, they only contain eight accessible free thiols in comparison with sixty-nine accessible amines. Analytical chemistry also represents a field of research in need for thiol-selective reagents, especially when complex mixture of proteins or protein digestate are analysed.

Indeed, the presence of free thiols in such mixture can lead to the formation of artefacts due to random disulfide formation. In this context, thiol-selective reagents must display fast kinetics of reaction and great selectivity as they are used in complex, highly diluted solutions. Alkyl halides and especially iodoacetamide derivatives have been employed for such application for decades, however lack of chemo-selectivity has been reported thus illustrating the need for new reagents.[57,58]

Recently, the use of thiomethyltetrazine **R35** (Figure 9) was reported for proteomics studies in live cell. The reagent can undergo thiol exchange, labelling any thiol-containing protein **R36** with high and tuneable kinetic rates, from 1 to 100 $M^{-1}s^{-1}$, depending on the side-chain borne by the tetrazine ring. More interestingly, thiol exchange can be stopped by the addition of a transcyclooctene (TCO)-containing reagent in the mixture, leading to an inverse electron demand Diels-Alder (IEDDA) reaction and to the formation of dihydropyridazine products **R37**, insensitive to thiol exchange.[59] This methodology allowed time-course proteomic studies as it allowed to study the thiol content of a mixture at a given time, upon addition of TCO, with great sensitivity.

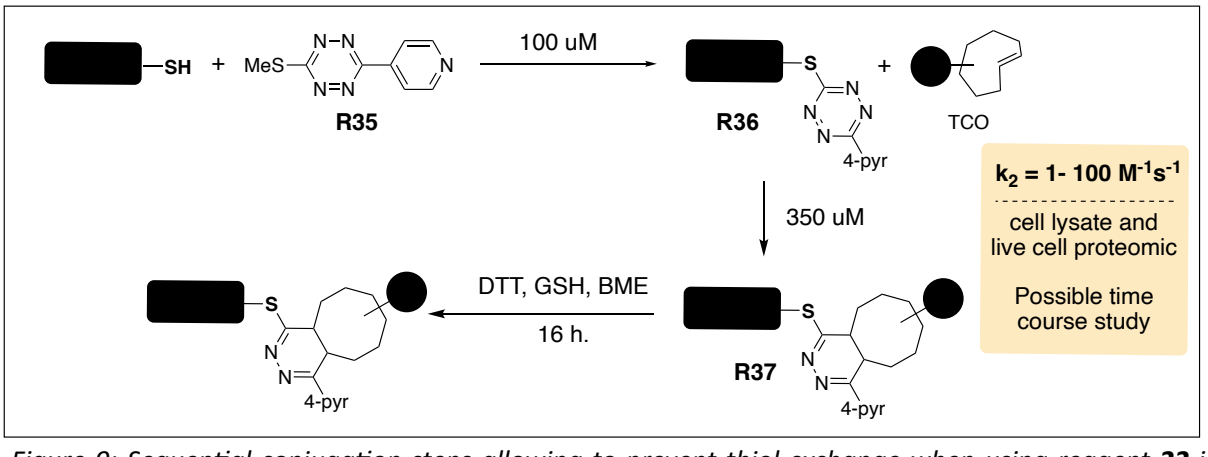

*Figure 9: Sequential conjugation steps allowing to prevent thiol exchange when using reagent **22** in proteomic studies.*

In the same vein, the use of nitrile oxide **R38** (Figure 10) — generated in situ by the oxidation of an oxime precursor **R39** or by the use of an α-chlorooxime reagent **R40** — displayed fast kinetics and good chemo-selectivity resulting in oxime labelled proteins **R41**. It was used for a variety of applications, from the labelling of small proteins such as bovine serum albumin (BSA) and engineered KRAS protein (MW = 24 kDa) to wide scale proteomic studies where it allowed the

Figure 10: Methods for the generation of nitrile oxides reagents leading to cysteine-selective labeling of native proteins in proteomic assays.

detection of glyceraldehyde-3-phosphate dehydrogenase (GAPDH), an enzyme involved in glycolysis usually hard to label in such study due to its low abundance.[60,61]

If analysis and more precisely proteomic study is one of the most recent applications of cysteine-selective reagents, their main application remains the labelling of large proteins, especially the formation of ADCs, with 7 out of the 10 approved by the EMA being functionalized with maleimides (Table 1, Figure 11).

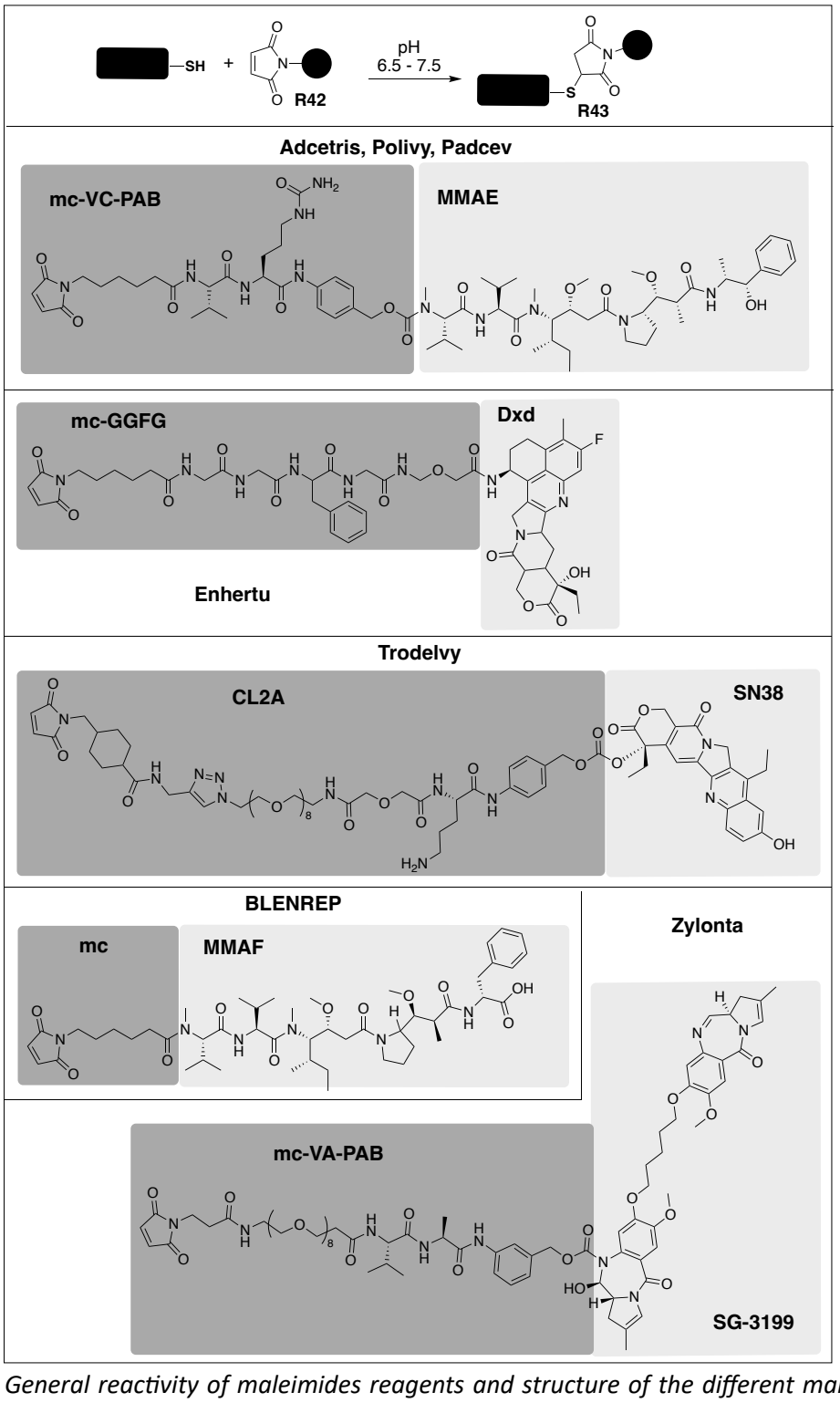

Figure 11: General reactivity of maleimides reagents and structure of the different maleimide based reagents used for the generation of ADCs.

Maleimides **R42** can react with thiolates via thio-Michael addition to form thioethers **R43**,[62,63] with optimal chemo-selectivity being observed at pH values comprised between 6.5 and 7.5 (competitive aza-Michael addition starts to occur at pH above 8.5).[64–66] Maleimides also display fast kinetics, with second-order rate constants oscillating between 100 and 1000 M^{-1} s^{-1}, depending on the structure of the thiol and the pH of the reaction mixture.[62,67,68] Except for Enhertu and Trodelvy, all the maleimide-based ADCs present av. DoC below 8, usually due to the high hydrophobicity of the drug-linker payload causing the immunoconjugates with elevated DoC to precipitate. Moreover, some maleimide-based conjugates were shown to undergo retro-Michael under physiological conditions, resulting in thiol exchange and off-target toxicity.

Table 1: List of the different ADC based on cysteine-selective bioconjugation methods.

Trade name	Year of first approval	mAb	Drug	Linker	Av. DAR
Polivy	2020	Polatuzumab	MMAE	mc-VC-PAB	3.8
Enhertu	2021	Trastuzumab	Dxd	mc-GGFG	7.7
Trodelvy	2021	Sacituzumab	SN-38	CL2A	7.6
Adcetris	2012	Brentuximab	MMAE	mc-VC-PAB	4
Padcev	2022	Enfortumab	MMAE	mc-VC-PAB	4
BLENREP	2020	Belentamab	MMAF	mc	4
Zylonta	2022	Loncastuximab	SG-3199	mc-VA-PAB	2.3

Considering the relative fragility of the maleimide motif, research has been mostly focused on the development of more stable thiol-selective reagents with maintained reactivity. Based on the observation that the formed thioether - maleimides **R43** were prone to hydrolysis, forming ring-opened maleamic acids that are unreactive towards *retro*-thio-Michael,[69,70] Kalia *et al.* developed *o*-CH_2NH^iPr phenyl maleimides **R44** that can be easily hydrolysed to ring-opened derivatives **R45** thanks to both the electron-withdrawing effect of the phenyl ring and the intramolecular maleimide activation from the appended ammonium group (Figure 12).[71]

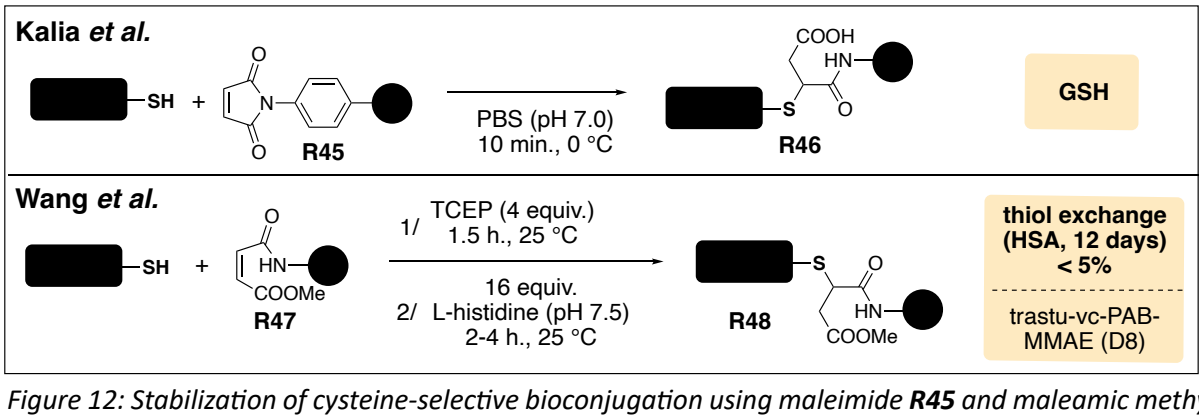

*Figure 12: Stabilization of cysteine-selective bioconjugation using maleimide **R45** and maleamic methyl esters **R47**.*

Interestingly, while maleamic acids are unreactive toward thiol addition, Wang *et al.* recently proved that maleamic methyl ester **R47** were effective conjugation reagents, leading to stable thioethers **R48**, thus preventing further thiol exchange (Figure 12).[72] After installation of their methyl maleamic ester to the classical VC-PAB-MMAE linker, they successfully produced a DAR 8 trastuzumab-based ADC and proved its stability toward thiol exchange in the presence of glutathione and albumin for 14 days with good improvement in comparison to their maleimide analogues.

Hackenberger and co-workers reported in 2019 the use of ethynylphosphonamidate reagent **R49** which, despite slow kinetics (0.6 $M^{-1}.s^{-1}$), was shown to lead to conjugate **R50** that is stable toward thiol exchange in the presence of BSA for up to 5 days (Figure 13).[73]

In 2022, the same team showed that when using similar P(V) reagent functionalized with two alkynes, these displayed different kinetics and that pre-functionalization of the reagent by CuAAC — resulting in the triazole-functionalized phosphinate **R51** — could considerably increase the second order rate constant of this reaction (from 0.47 $M^{-1}s^{-1}$ to 4.61 $M^{-1}s^{-1}$), showcasing the tuneable reactivity of those reagents (Figure 13).[74]

Following another goal, they also recently proposed a Staudinger-based functionalization of their phosphorus reagents with long PEG chains (12 units) resulting in compound **R53** as a way to facilitate the introduction of large hydrophobic payloads, yielding conjugates **R54**. As a proof of the advantages of their approach, they easily obtained D8 brentuximab functionalized with VC-PAB-MMAE, which displayed higher hydrophilicity compared to its D4 maleimide analogue Adcetris (Figure 13).[75]

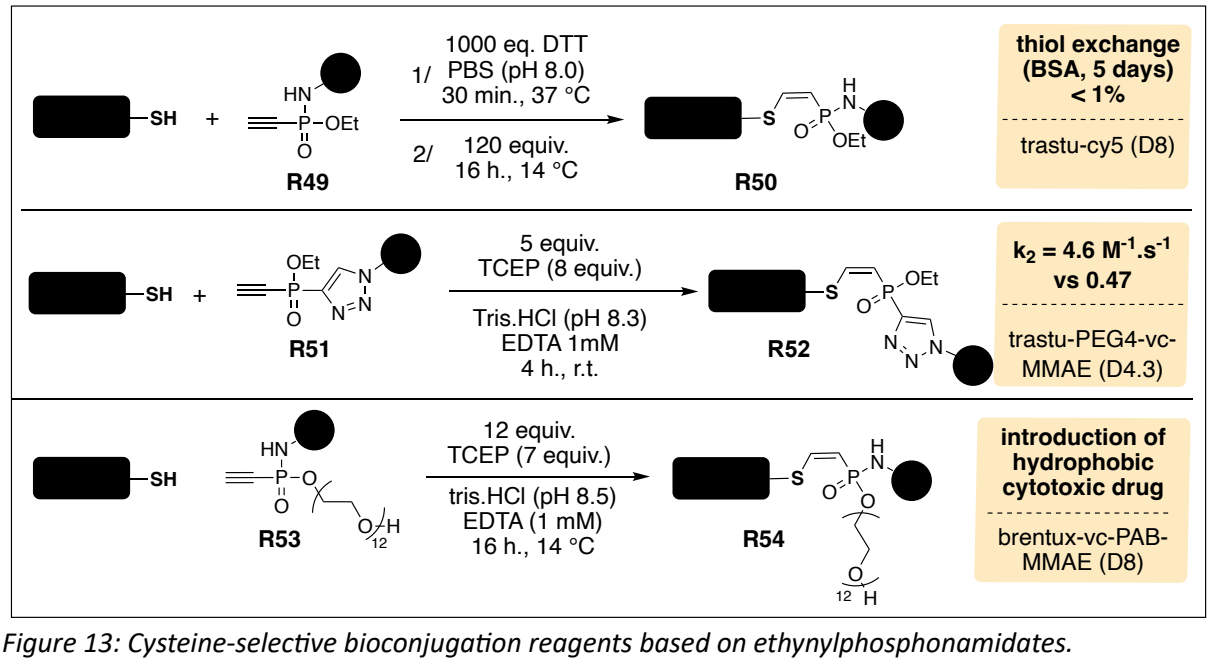

Figure 13: Cysteine-selective bioconjugation reagents based on ethynylphosphonamidates.

With a different view, a recent study showed that reversible CO_2 adsorption in aqueous media might improve *S*-selectivity by slight acidification of the medium thus preventing hydrolysis of the used electrophile and leading to the reversible blockage of amine residues that might compete with the thiolate residue. However this study was only conducted on HSA using a maleimide as electrophile, the in vitro analysis seems promising to allow the use of highly reactive reagents that were set aside due to a lack of chemo-selectivity.[76]

Those recent publications show that the tendency for chemo-selective cysteine conjugation is to the development of highly reactive reagent — useful for in cell proteomics studies — or to the development of homogeneous and stable ADCs sometimes to the detriment of kinetic rates. The main competitor of those conjugation methods is the development of engineered mAbs in which an additional readily available free thiol has been inserted so that stable ADCs with low DAR can be produced easily. If such constructs are hot topic in the bioconjugation domain lately, they will not be discussed in this manuscript, where the focus will be on the chemical modification of native proteins.

This quick overview of the evolution of the two main chemo-selective strategies shows how the field of protein bioconjugation continues to thrive, offering now dozens — if not hundreds — of diverse ways to label selectively amines and thiols. In response to the increasing demand for homogeneous conjugates, the scientific community also took an increasing interest in the domain of bioconjugation, which fostered creativity and promoted the development of alternative methods for the conjugation of less abundant and reactive amino acid residues.

II.3. Aspartate, glutamate and other residues

Besides lysine and cysteine, other residues have been the targets of new conjugation methods, notably the electron-rich histidines and tyrosines. If several methods have been developed, they were extensively discussed in our previously published review and will thus not be discussed in this manuscript.[23]

It is however worth mentioning the work of Raines and co-workers, who recently reported the use of diazo compound **R55** targeting carboxylates with elevated pK_a values, such as the side chains of aspartate and glutamate residues (Figure 14).[77,78] Those residues are often poorly reactive under physiological conditions and involved in structural integrity or catalytic sites of proteins thus they are not often targeted for bioconjugation. Raines took advantages of the instability of formed ester **R56** for transient conjugation of cytochrome-c and green fluorescent protein (GFP) with thiolated cellular delivery moieties such as cell penetrating peptides (CPP), integrin targeting ligands and large polysaccharides leading to conjugate **R57**. Upon arrival in the cell, conjugate **R57** can undergo esterase-triggered deconjugation after cleavage of the self-immolative carbonate allowing the cytosolic delivery of the native POI. In the case of diazo reagent **R58**, they observed rather slow hydrolysis of ester **R59** and they developed conditions

using 2-(diphenylphosphino) benzoic acid (2-DPBA) to generate self-immolative compound **R60** via Staudinger mechanism (Figure 14).

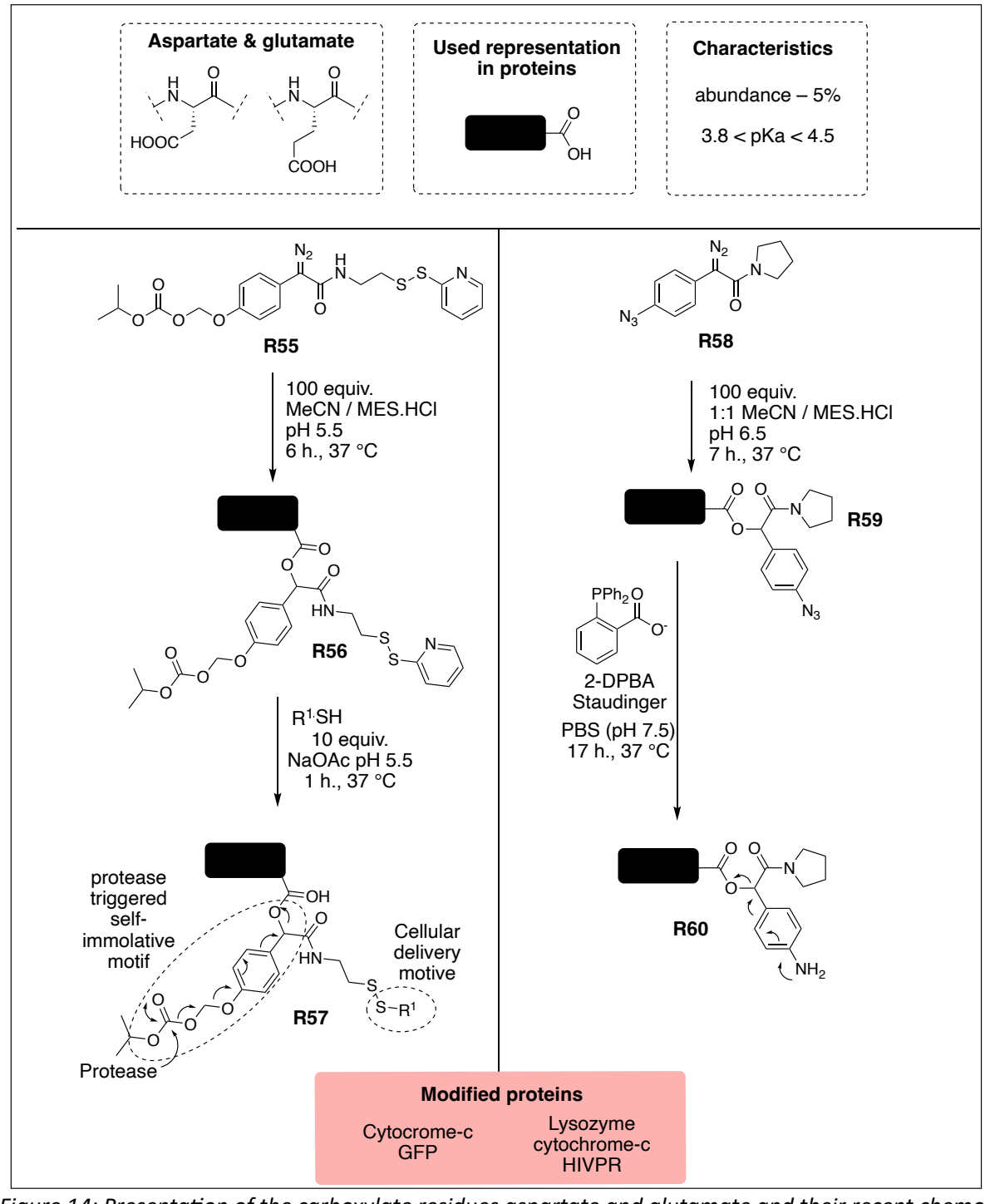

Figure 14: Presentation of the carboxylate residues aspartate and glutamate and their recent chemo-selective bioconjugation methods.

Many chemo-selective strategies have been developed over the past decades and we depicted here the most recent ones. The main targeted chemical functions are primary amines — often with no distinction between ε- and α- amines borne by lysines and *N*-ter residues — and sulfhydryl groups borne by cysteines. However, those chemo-selective methods lead to a distribution of payloads resulting in mixtures of different regio-isomers. If this contained level of heterogeneity is not problematic for some applications such as the generation of vaccines or proteomics studies and was even shown to be efficient for the generation of therapeutic conjugates such as ADCs, the different species might display different pharmacokinetics and pharmacodynamics and, consequently, efforts were made in order to reduce the number of obtained regio-isomers. Among the developed techniques, chemo-selective strategies yielding mono-disperse conjugates and saturation of the targeted chemical function were considered. However, the development of regio-selective methods — that will be considered equivalent to site-selective methods in this manuscript — allowed to reach more homogeneous and molecularly defined conjugates facilitating their characterization and thus their application for medical use.

III. Site selective approaches for the modification of proteins

Various site selective bioconjugation methods are based on protein engineering — and more precisely on directed mutagenesis — with the introduction of unnatural amino acids (UAA) bearing bioorthogonal handles or, as mentioned earlier, with the introduction of easily accessible natural amino acids. This PhD work being focused on the conjugation of native and natural proteins, those strategies will not be discussed in this manuscript. The focus will be made on the recent development of regio-selective strategies such as the labelling of *N*-terminal residues — based on their accessibility or spatial proximity of two reactive functions — or the labelling of dual residues, based on their spatial proximity.

III.1. *N*-terminal residue labelling

With a lower pK_a than the ε-amino side chain of lysine, α-amino groups of *N*-terminus possess a peculiar reactivity of particular interest in this context, explaining why it has gained increasing attention in recent years (Scheme 5). In a great majority of cases, the first labelled residues are the most accessible ones which are often positioned at the beginning or at the end of the protein sequence. In nature, these *N*-terminal and *C*-terminal residues are subjected to post-translational modification thus necessitating their accessibility to the protein's environment.[54]

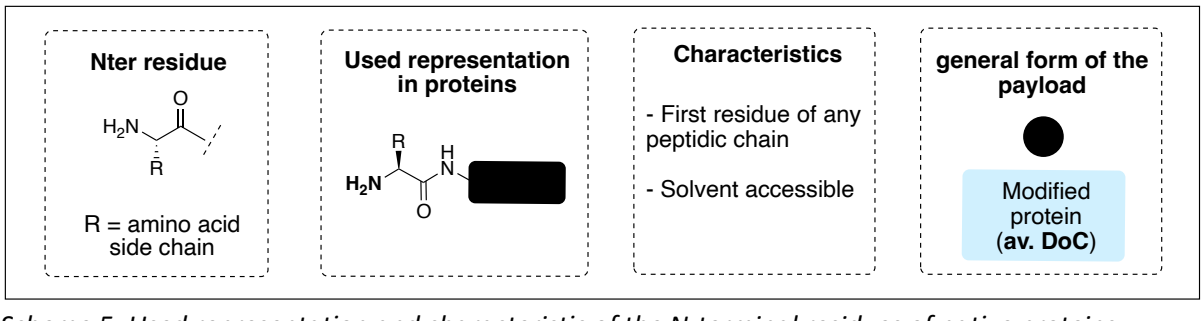

Scheme 5: Used representation and characteristic of the N-terminal residues of native proteins.

III.1.a. General labelling of N-ter residues

A first strategy considered for the modification of *N*-terminal residues is the acylation of the α-NH_2. Ketenes **R61**, developed by Chan *et al.* were reported for *N*-terminal acylation **R62** of proteins but poor conversions (between 20 and 40%) and lack of selectivity was observed on native proteins (Figure 15).[79]

Jensen's team reported in 2022 a new method for the *N*-acylation of proteins, using phenol esters **R63**, resulting in the formation of the stable amide **R64** (Figure 15).[80] This reagent was shown to selectively label α-NH_2 of various isolated amino acids — with no interference from their side chains — at physiological pH. Small proteins such as human growth hormone (HGH), insulin, lysozyme and RNAse A were selectively labelled using this reagent, with conversions varying from 39 to 61%. If low levels of aspecific labelling could still be detected (< 10% in all tested proteins), this reagent allowed the *N*-terminal incorporation of various payloads on small proteins.

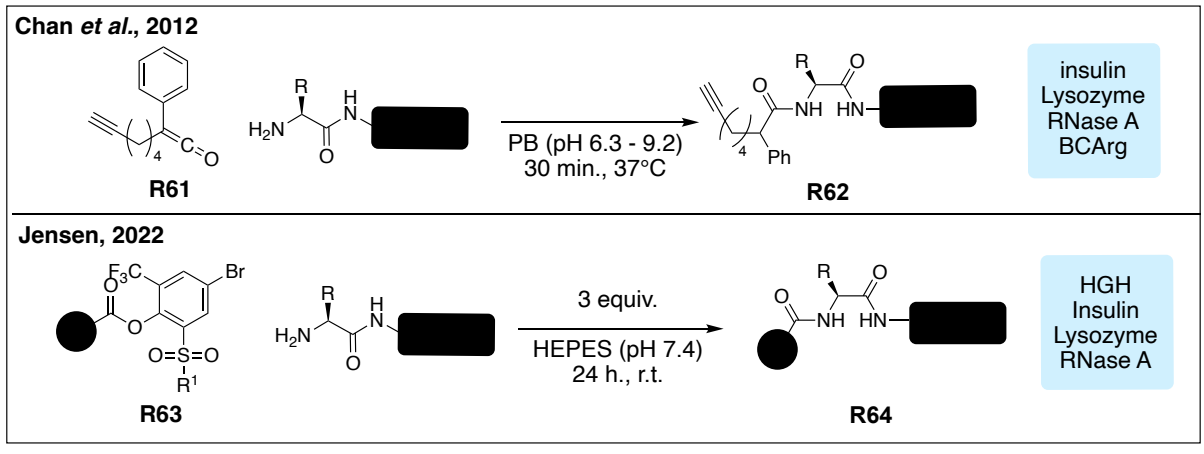

Figure 15: Reagents and reaction conditions used for acylation of N-terminal residues in native proteins.

Recently, Sugai and co-workers reported the use of 2-pyridinecarboxyaldehyde (2-PCA) azido derivative **R65** in the presence of copper(II) for the *N*-terminal-selective labelling of various proteins (Figure 16).[81]

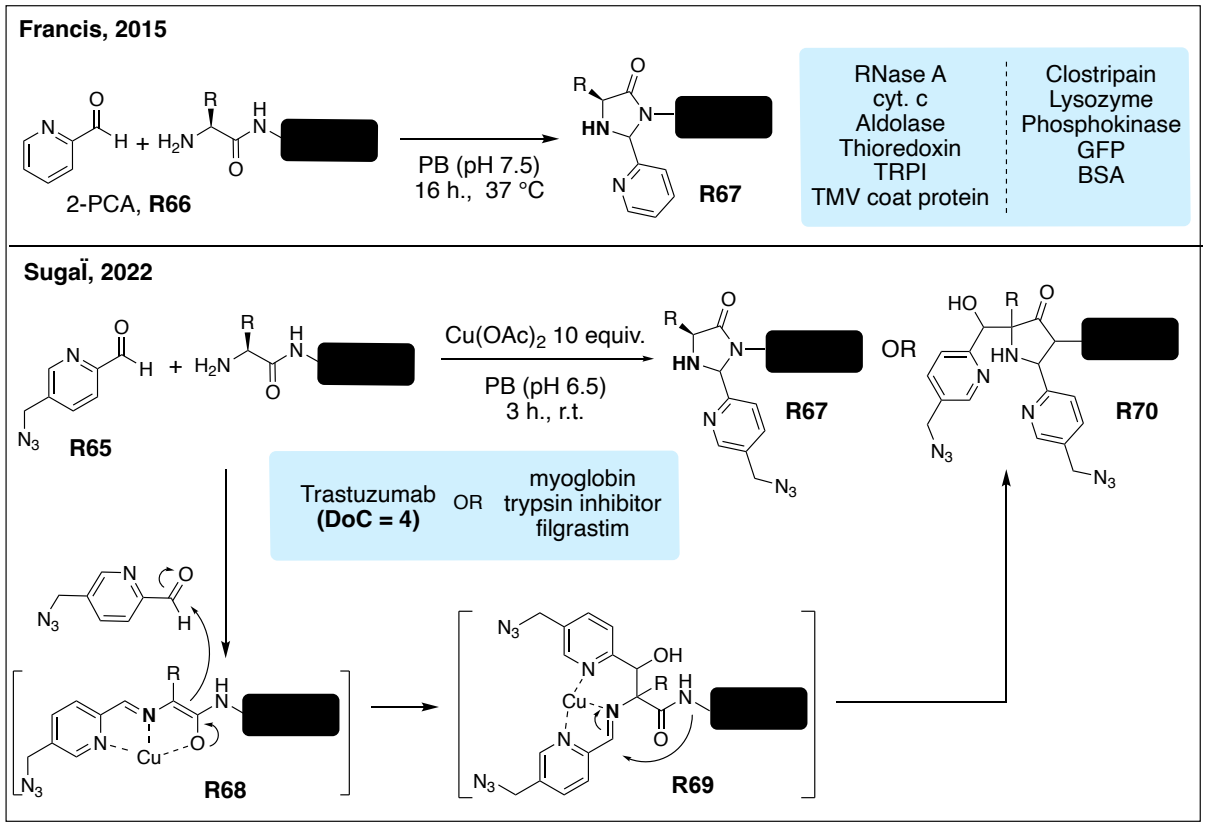

Figure 16: Mechanism and reagents used for the formation of imidazolidinones on N-terminus of native proteins.

2-PCA **R66** had previously been reported by Francis and co-workers with a similar site-selectivity on 11 proteins, conjugated with good conversions thanks to the formation of imidazolidinones **R67,** obtained via cyclization of the imine precursor with the α-amino group of the n + 1 residue in 16 hours at 37 °C (Figure 16).[82] Despite being similar in terms of reactants, the mechanism proposed by the Sugai group is yet rather different; they hypothesized that the presence of

copper would result in the stabilisation of the transient imine in the form of the pseudo-enolate **R68**, favouring the addition of a second equivalent of 2-PCA via an aldol addition mechanism mimicking the catalytic site of aldolases. If such double addition, leading to structure **R70** could indeed be observed on peptides and small proteins, its application to larger proteins such as trastuzumab led to the sole mono-addition of 2-PCA leading to conjugate **R67**, following the mechanism previously described by Francis.

In this last case, however, the kinetics of the reaction was found to be accelerated by the addition of copper in the reaction media, probably thanks to the increased electrophilicity of the copper(II)-bound imine. The presence of an azide group on **R65** even allowed the formation of an ADC — av. Drug to antibody ratio (DAR) 2.8 — using the SN-38 cytotoxic drug functionalized with a terminal alkyne, pre-coupled with R65 by CuAAC before its conjugation. The resulting ADC presented an IC_{50} of 10.2 nM which is comparable to that of free SN-38 (3.6 nM), but surprisingly no comparison with existing ADC was done. The only limitation found for the use of 2-PCA for the *N*-terminal labelling of protein was the presence of a proline residue in n+1 position thus preventing the imidazolidinone formation as, in this case, the amine of the n+1 residue is not available.

With the exception of 2-PCA, being one of the few reagents known to tolerate various side-chains, the development of *N*-terminal selective conjugation methods is often hampered by the exact nature of the residue, whose side-chain can lead to side reactions. Based on this observation, bioconjugation methods were thus developed in order to take advantage of this spatial proximity between the grafted reagent and the side chain. If such methodology limits the scope of the developed method, it greatly improves its selectivity resulting in highly homogeneous modifications.

III.1.b. Specific N-ter residue

Building on this idea, Gois and Gao independently reported in 2016 the use of 2-formylphenyl boronic acid **R71** (2-FPBA) for the modification of *N*-terminal cysteines through the formation of thioazolidines **R72** with high second-order kinetic rates comprised between 10^2 and $10^3\ M^{-1}.s^{-1}$ (Figure 17).[83,84] Unfortunately, the reaction was found to be reversible in the presence of free cysteines or under mildly acidic conditions.

To address this limitation, Gao and co-workers hypothesized in 2020 that the acylation of the thiazolidine nitrogen would prevent imine reformation and ring-opening thus leading to more stable conjugates.[85] Using boronic acid reagents **R73** based on an acetylated salicylaldehyde motif, they managed to observe formation of the expected adducts **R74**, with the *O*-to-*N*-acetyl shift from boron reagent **R73** being the rate limiting step (Figure 17).

Gois team proposed in 2022 a DFT-based mechanism confirming Gao's observation and even showed that boron-free *o*-salicylaldehyde esters (OSAEs) **R75** could accelerate the formation of

phenolic thiazolidines **R76** in comparison with 2-PCA **R66** for the selective modification of *N*-terminal cysteines on peptides.[86]

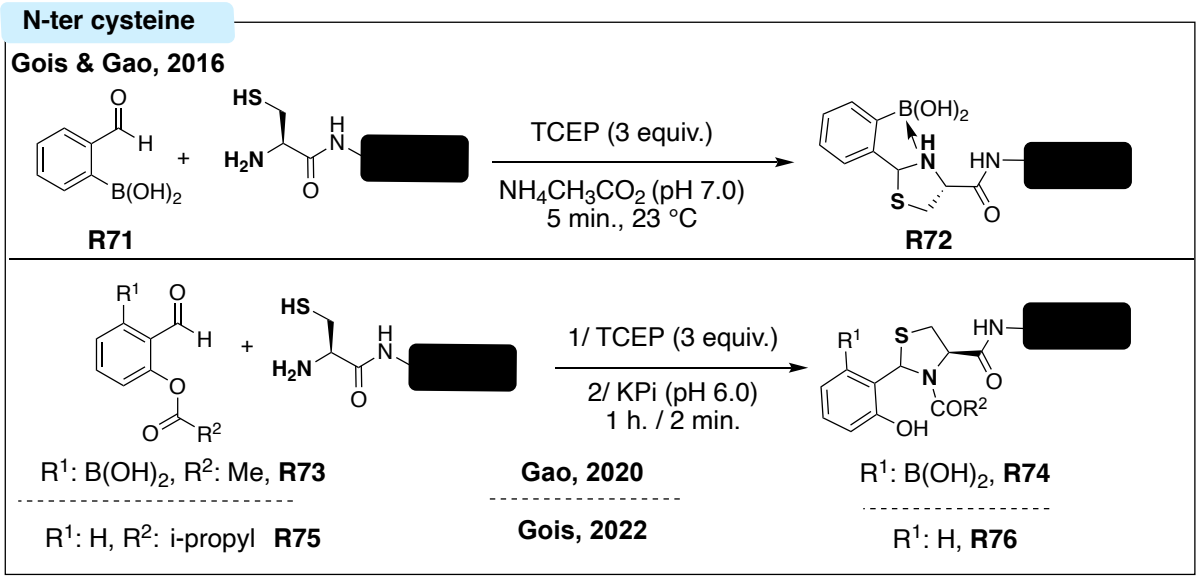

Figure 17: Reagents and conditions used for the formation of thiazolidines on N-terminal cysteines

Gois team also developed in 2021 a NHS-activated acrylic ester **R77** that combines two chemical functions and is used for the selective modification of amines on one side and of thiols on the other side, the reactivity of the reagent being based on the spatial proximity of the two functions and accessibility of a *N*-terminal residue (Figure 18).[87] Few proteins possess *N*-terminal cysteines hence they tested and validated the formation of *N*-terminal adduct **R78** on a model octapeptide (laminin fragment) and calcitonin salmon (3.5 kDa). Interestingly, they showed that **R77** could be used as stapling reagent in absence of *N*-ter cysteine and presence of free thiol, as in BSA. They also observed an inter-residue mechanism between a free cysteine and a neighbouring lysine thus opening new directions toward the site-selective labelling of native proteins.

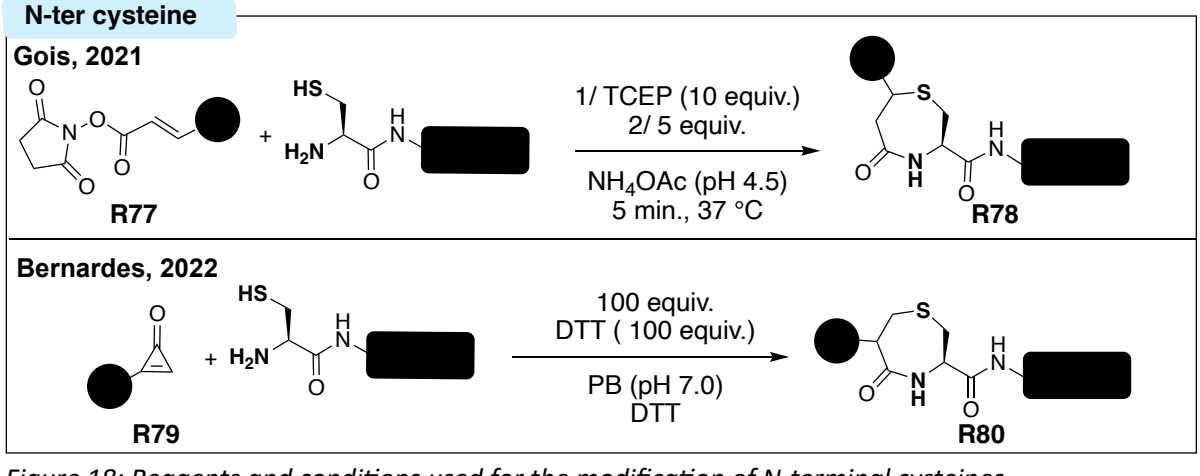

Figure 18: Reagents and conditions used for the modification of N-terminal cysteines.

In the same vein, cyclopropenone reagents of general structure **R79**, developed by Bernardes and co-workers in 2022, led to the *N*-terminal cysteine-selective formation of 1,4-thiazepan-5-one **R80** (Figure 18).[88] The reagent was proven to show excellent selectivity and > 90% conversions albeit with a slight decrease when hydrophobic payloads were used.

Switching to another family of residues, Rai and co-workers showed in 2019 that, using *o*-substituted benzaldehydes **R81**, *N*-terminal glycines could selectively be modified as 1,2-amino alcohols **R82** (Figure 19).[89] Notwithstanding the excessive amount of reagent employed (500 equivalents), the reaction proceeded under smooth conditions — pH 7.8, 24 h, 25 °C — and proved to be selective for *N*-terminal glycines as proteins exhibiting C_α-substituted *N*-terminal residues were not labelled in competition experiments.

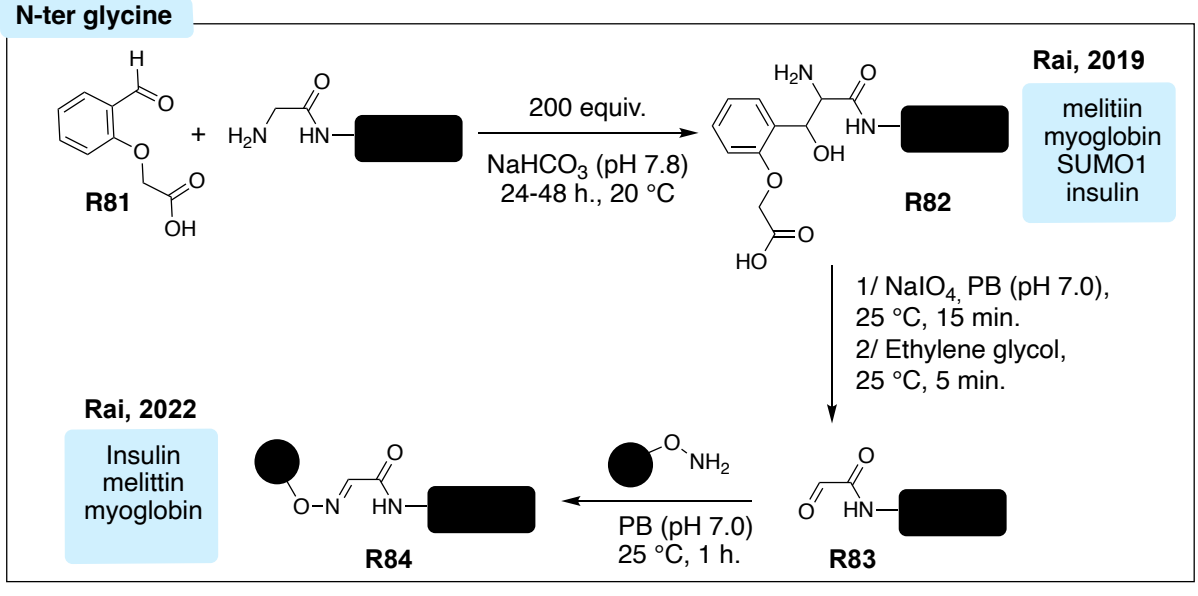

Figure 19: Reagents and conditions developed for the selective conjugation of N-terminal Glycines.

In order to facilitate the functionalization of conjugates **R82**, the same team developed in 2022 a $NaIO_4$-mediated oxidative cleavage protocol to generate the glyoxyamide moiety **R83**. This allowed a final functionalization/purification step thanks to the addition of an *o*-alkoxyamine allowing functionalization of the POI in the form of conjugates **R84** — a procedure that also gave the possibility of trapping and isolating pure mono-labelled conjugates on hydrazide-based resins before operating a trans-tagging release with *O*-alkoxyamine probes (Figure 19).[90]

III.2. Dual residue targeting

III.2.a. Disulfide rebridging

As previously mentioned, cysteines with free side-chain thiols are relatively scarce in nature, usually forming homo- or hetero-dimers via oxidized disulfide bonds, such as the cystine residues bridging heavy and light chains in antibodies (Scheme 6). While reduction of the inter-chain disulfide bonds of IgGs can give access to eight free thiols, their chemo-selective labelling can have a detrimental impact on the structure, shape, stability and activity of the protein, while still leading to heterogeneous mixtures of conjugates due to incomplete conversion.[91] Thus, chemical methods to conjugate covalently free cysteines 'in pairs', taking advantage on their close spatial proximity, have been proposed as a way to address this issue and have been coined "rebridging" strategies.[92]

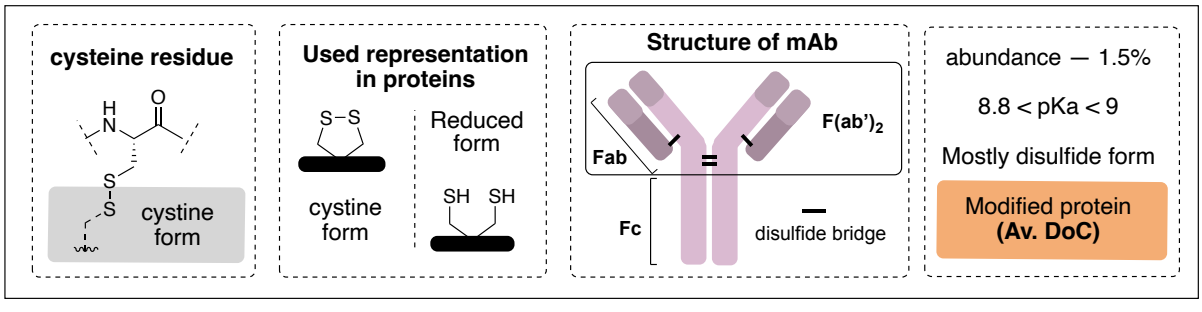

Scheme 6: Structure, properties and used notation for cystine residue modification.

This strategy has been widely explored in the past decade with next-generation maleimides (NGM) developed by Caddick and co-workers in 2014 — such as dibromomaleimides (DBM) **R85** and dithiphenolmaleides **R86** yielding conjugate **R87**— and dibromopyridazinediones (PDs) **R88** yielding conjugate **R89**, developed by the same team in 2015 (Figure 20). In comparison with

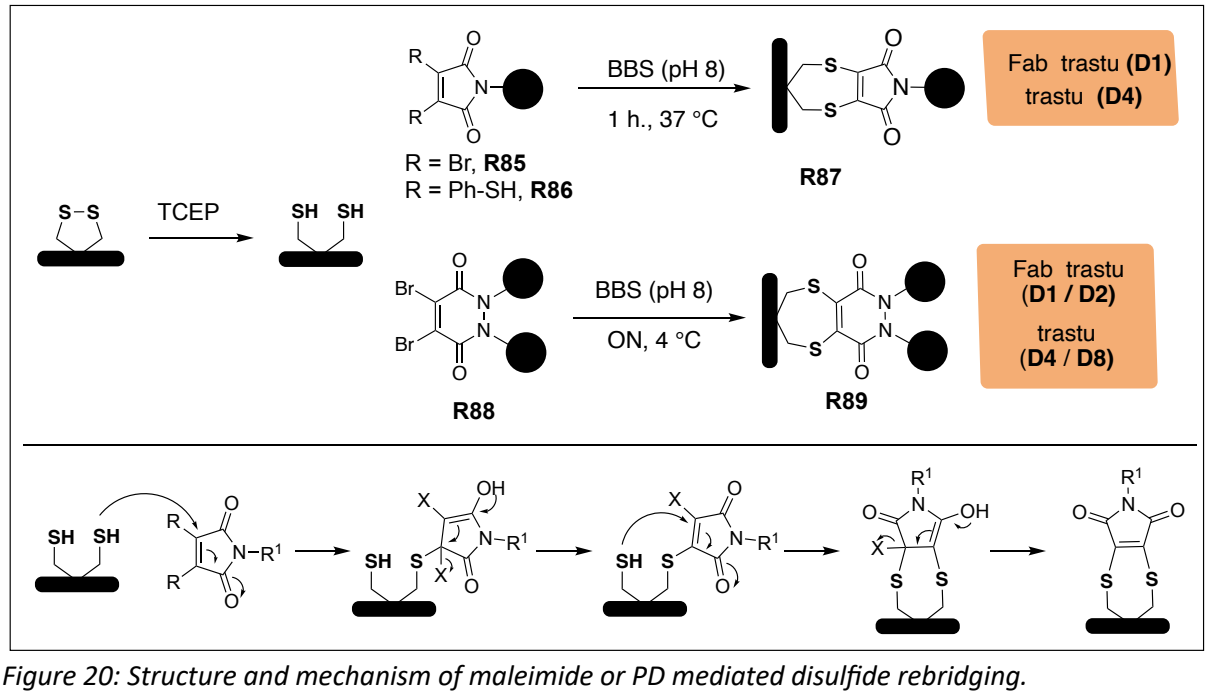

Figure 20: Structure and mechanism of maleimide or PD mediated disulfide rebridging.

analogous maleimides, the introduction of two nucleofuges across the double bond allow consecutive thio-Michael addition.[93–96,97]

These reagents helped construct numerous ADCs, some with improved properties over conventional maleimide-conjugated species in terms of efficacy, toxicity and pharmacokinetics. Excellent yields and conversion have been reported for both types of reagents, with DAR 4 or DAR 8 being the sole immunoconjugates detected in certain cases. Even if concurrent generation of half-antibody isoforms via intra-chain rebridging and disulfide scrambling could systematically be observed with NGM, it could be only restricted to less than 5% in most cases when using PDs. Besides this greater regioselectivity, PDs can also be functionalized by two different bioorthogonal handles on the two nitrogens of the pyridazinedione scaffold and can thus be easily tuned to reach homogeneous D4 or D8 functionalized mAbs.[98,99] This remarkable rebridging ability of PDs even opened the possibility of conducting disulfide reduction and rebridging in a single step with a so called 'two-in-one' procedure.[100]

The remarkable rebridging ability of PD reagent was used and extensively applied by Chudasama and co-workers. Being capable of fully rebridging mAbs as well as Fab and Fc fragments, PD-based reagents were largely derivatized in order to reach tuneable amounts of payload per protein or protein fragment but also tuneable ratio of payloads.[101,102] One of the most recent examples is the development of reagent **R90**, composed of two PD motives, two azido functions and one tetrazine function (Figure 21).[103] This reagent was shown to lead to fully rebridged mAb, Fc and half F(ab')$_2$ and, based on the difference in reactivity between azido

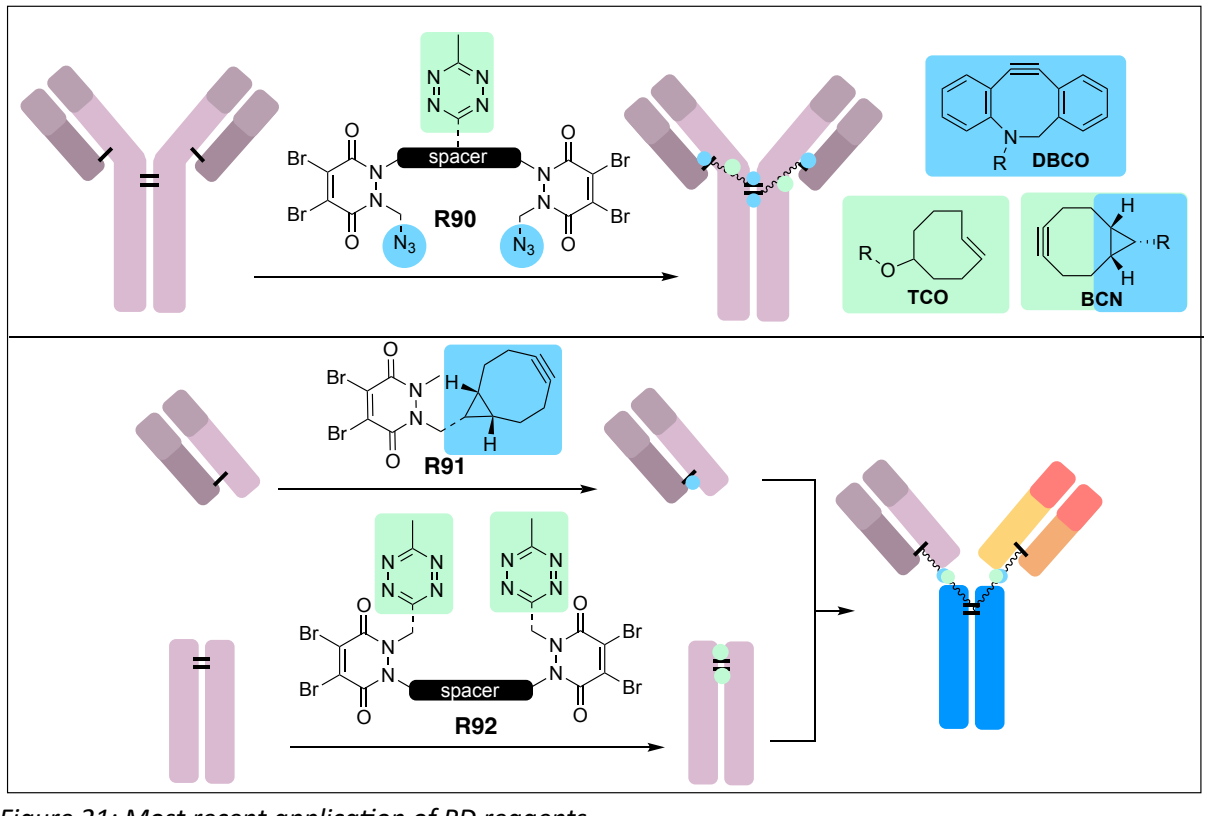

Figure 21: Most recent application of PD reagents.

and tetrazine functions, differently labelled species were obtained after careful choice of click partner —BCN for both azido and tetrazine functionalization, DBCO for selective azido functionalization and TCO for selective tetrazine functionalization. Earlier this year, Thoreau *et al.* pushed the reaction further by creating an artificial bispecific mAb (2 Fab + 1 Fc) using click chemistry between reagent **R91** and **R92** (Figure 21). [104]

Structurally related to this strategy, addition to electron-deficient alkenes — such as divinyl triazine — and alkynes was also explored by several groups developing various rebridging reagents that were tested on native proteins — mostly whole antibodies.[105–108] While potent ADCs could be produced in this way, disulfide scrambling was systematically observed, as evidenced by the formation of half-antibodies in all cases.

Recently, Spring and co-workers managed to overcome this issue, based on the observation that the maximal distance between any two cysteines engaged in an interchain disulfide bond was approximately 20 Å. They therefore designed a tetra-divinylpyrimidine reagent **R93** with a matching linker length, allowing the rebridging of all four accessible disulfide bridges of trastuzumab with a single reagent, thus preventing disulfide scrambling (Figure 22). In addition to the four divinylpyrimidines, they also included a terminal alkyne to their reagent, allowing its further functionalization by CuAAC.

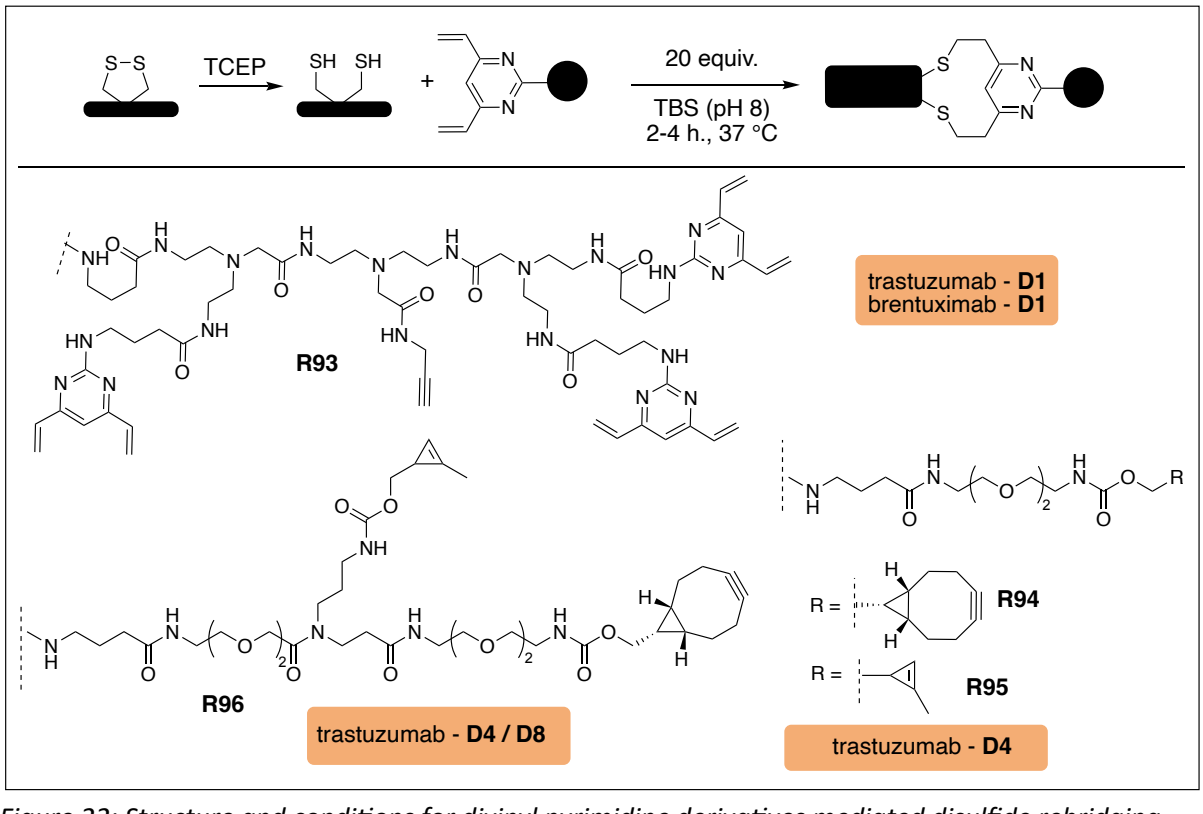

Figure 22: Structure and conditions for divinyl pyrimidine derivatives mediated disulfide rebridging.

Soon afterwards, the same group also reported divinylpyrimidine reagents functionalized with BCN **R94**, cyclopropylene **R95** and both functions **R96**, allowing metal free bioorthogonal functionalization of the resulting conjugation reagents.[109,110]

New rebridging reagents are still being developed among which α-thioester **R97** reported by Baker and co-workers is worth mentioning (Figure 23). Its use on Fab fragment led to the formation of a stable α-thio-thioether, with both sulfur atoms originating from the two cysteines' side-chains, resulting in conjugate **R98**. The formed thioester was further functionalized through native chemical ligation (NCL), resulting in conjugate **R99**, whose disulfide bond can be reduced and rebridged with PD **R91** yielding conjugate **R100**. It is interesting to underline that such method can be used to modify the reactivity of a cysteine implicated in a disulfide bridge into a more *C*-ter like reactivity. This way the "new" introduced residue will present a free carboxylic acid in β of the thiol which can be used for example, to dissociate the reactivity of those two thiols.[111]

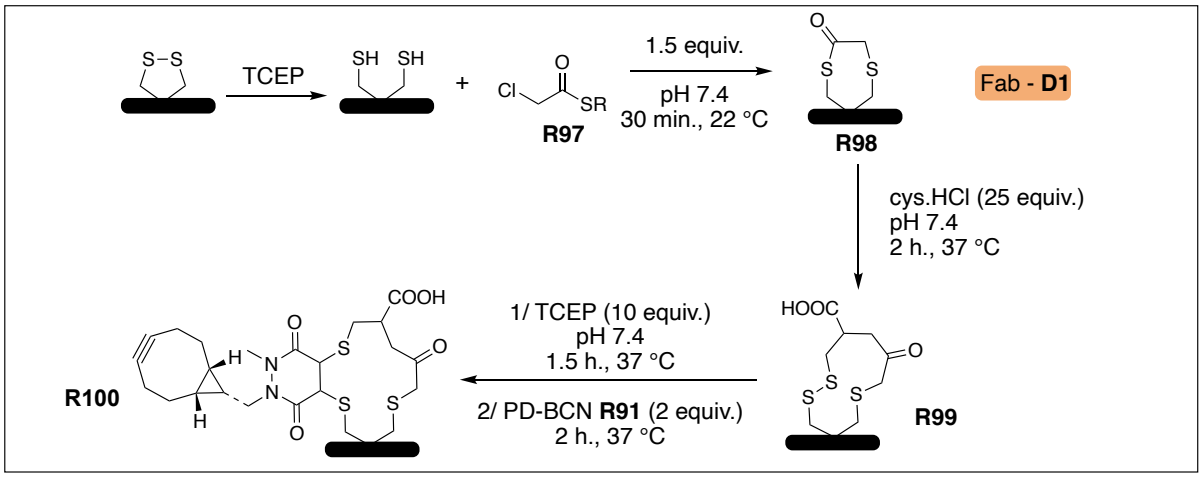

Figure 23: Use of α -thioester for asymmetrical rebridging of native proteins.

Cystine-rebridging reagents have thus offered access to site-selectively conjugated native proteins in excellent yields. NGM and PD have been the most studied reagents in this regard and were shown to be the most effective at minimizing disulfide scrambling. More interestingly, varying their structure permitted a controlled access to DAR 8, 6, 4 and 2 ADCs.

III.2.b. Template directed approach.

Another prominent site-selective strategy uses the concept of template-directed approach. In this case, the procedure follows a two-step approach: a heterobifunctional reagent is developed to first react with one residue in a quick but reversible manner, before a second irreversible conjugation to a neighbouring residue occurs. The number of reactive sites that can partake in this reaction is thus highly limited as it relies on the flexibility and length of the linker connecting the two reactive electrophiles.

This idea was first developed by Gothelf and co-workers in 2014, when they took advantage of histidine-rich regions in different proteins to form transient metal complexes with divalent cations, helping to direct a NHS ester equipped with a *tris*-nitrilotriacetic acid chelating handle to label only a handful of neighbouring lysines.[112]

This idea of using another amino acid as a temporary anchor point to direct — via electrostatic interactions or covalent bond formation — the modification of a spatially close lysine residue can also be found in subsequent studies. Rai and co-workers developed in 2020 a bifunctional conjugation reagent **R101** featuring an aldehyde and an activated phenol ester for lysine-directed lysine conjugation (Figure 24). The *o*-hydroxy-substituted benzaldehyde first leads to the rapid but reversible formation of stabilized imines with multiple solvent-accessible lysines, helping to direct the intramolecular acylation of a neighbouring lysine with the activated ester in a slow but irreversible second step (conjugate **R102**). A final addition of an *O*-alkoxyamine solution permits the removal of all remaining imines while functionalizing the POI (reagent **R103**) following the procedure mentioned in paragraph III.1.b. Site-selectivity was achieved on different proteins: RNase A was selectively modified on K7 (34% conversion), insulin on K29 (48%), aprotinin on K41 (86%), ubiquitin on K6 (35%), α-lactalbumin on K16 (37%) and myoglobin on K42 (26%).[113] Variation of the size of the linker led to the modification of different lysines on the same proteins mentioned above which illustrates the great modularity of those strategies.

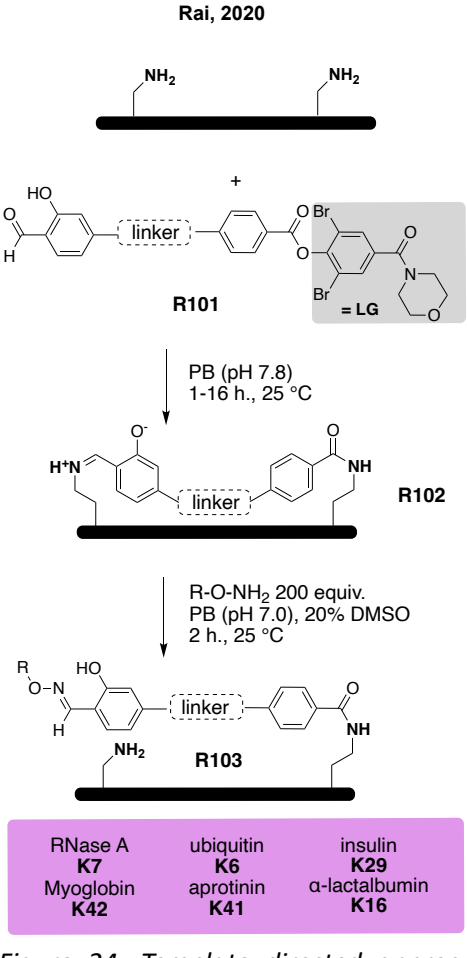

Figure 24: Template directed approach using bi-functional linker published by Rai in 2020.

The Gothelf group proposed in 2022 a bioconjugation reagent **R104** based on similar reactivity. The lysine-targeting moiety consisted in the same salicylaldehyde scaffold, thus allowing the stabilization of the formed imine **R105** and the pre-orientation of the phenol ester, facilitating

the site-selective acylation of a neighbouring lysine leading to conjugate **R106** (Figure 25). In this case though, the phenol ester is constructed in such manner that the phenolate leaving group is part of the linker, which can be seen as the traceless variant of Rai's method. While they proved that the method could be applied to different IgGs, no actual evidence of the site selectivity of the method was given.[114]

In the same vein, the group of Vishal Rai reported in 2022 a reduced version of their previous bifunctional reagent, with a terminal benzaldehyde instead of a benzoic ester (Figure 25, reagent **R107**). In this case, the formation of the second imine does not benefit from the stabilizing effect of the proximal hydroxyl group, making it more reactive toward nucleophiles such as $P(OEt)_3$ leading to the formation of stable secondary amines **108** through a Kabachnik-Fields reaction. Addition of an *O*-alkoxyamine solution allowed the same functionalization as mentioned above and the isolation of monoconjugates **109**. Site-selectivity was observed, depending on the size of the used linker on cytochrome C K60 (35%) or K27 (37%), myoglobin K50 (39%) or K42 (72%) and RNase A K1 (27%).[115]

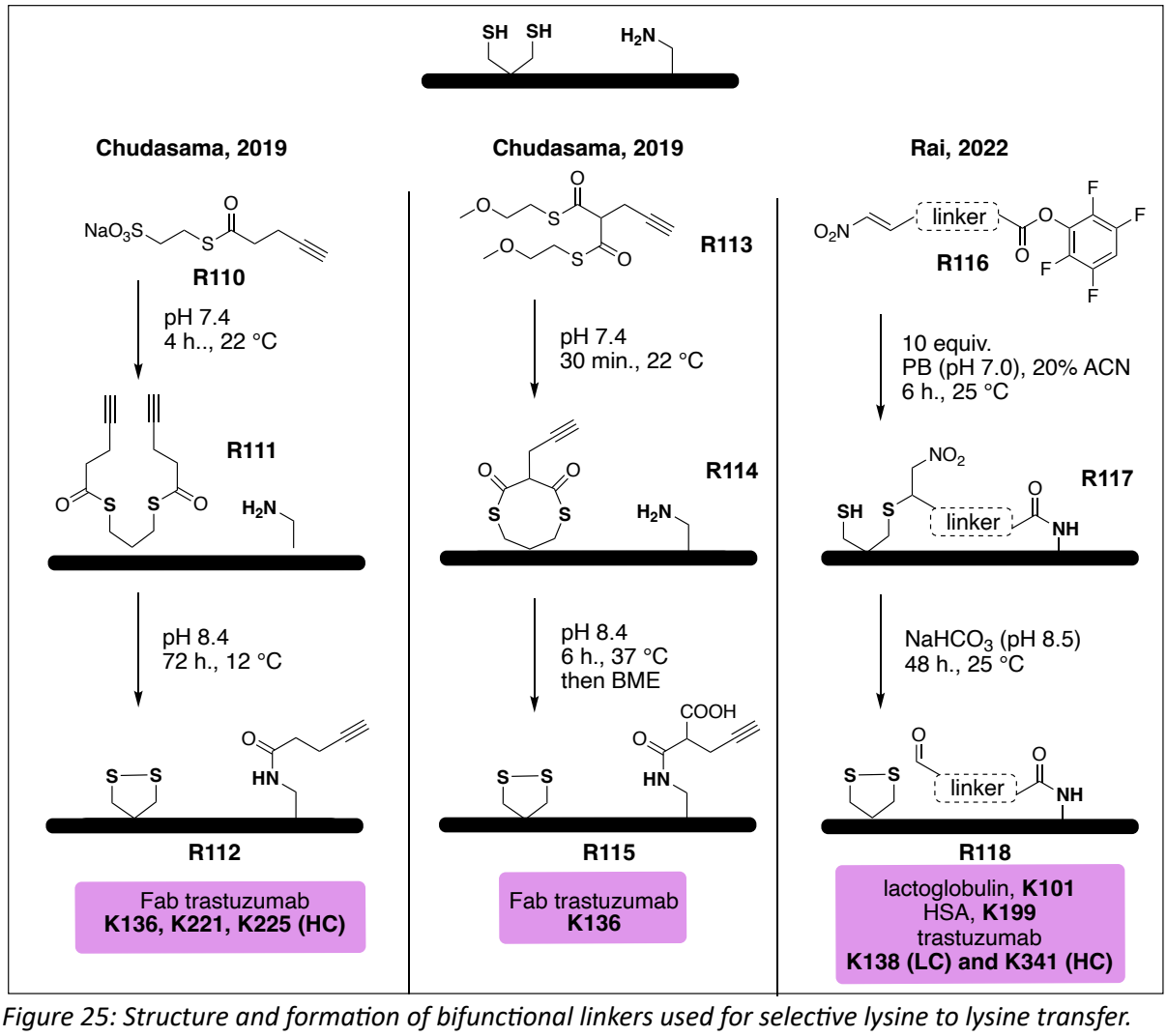

Figure 25: Structure and formation of bifunctional linkers used for selective lysine to lysine transfer.

Chudasama and co-workers showed in 2019 that cysteines could act as valuable relays for the site-selective modification of lysines on the Fab fragment of trastuzumab with thioesters **R110**,[116] in a strategy reminiscent of native chemical ligation (Figure 26). After reduction of the disulfide bond of the Fab fragment, a first trans-thioesterification between the cysteine thiol and the thioester leading to conjugate **R111** is followed with a 'cysteine-to-lysine transfer' (i.e. *S*,*N*-acyl migration) on a proximal lysine leading to conjugate **R112**. While this first approach could not be coined site-selectively per se, with three labelled lysines in the vicinity of the disulfide bond being identified (K136, K221 and K225), the use of *bis*-thioester **R113** for the formation of the intermediate bridged conjugate **R114** led to the sole conjugation of K136 of structure **R115** (80% conversion), presumably thanks to conformational effects.

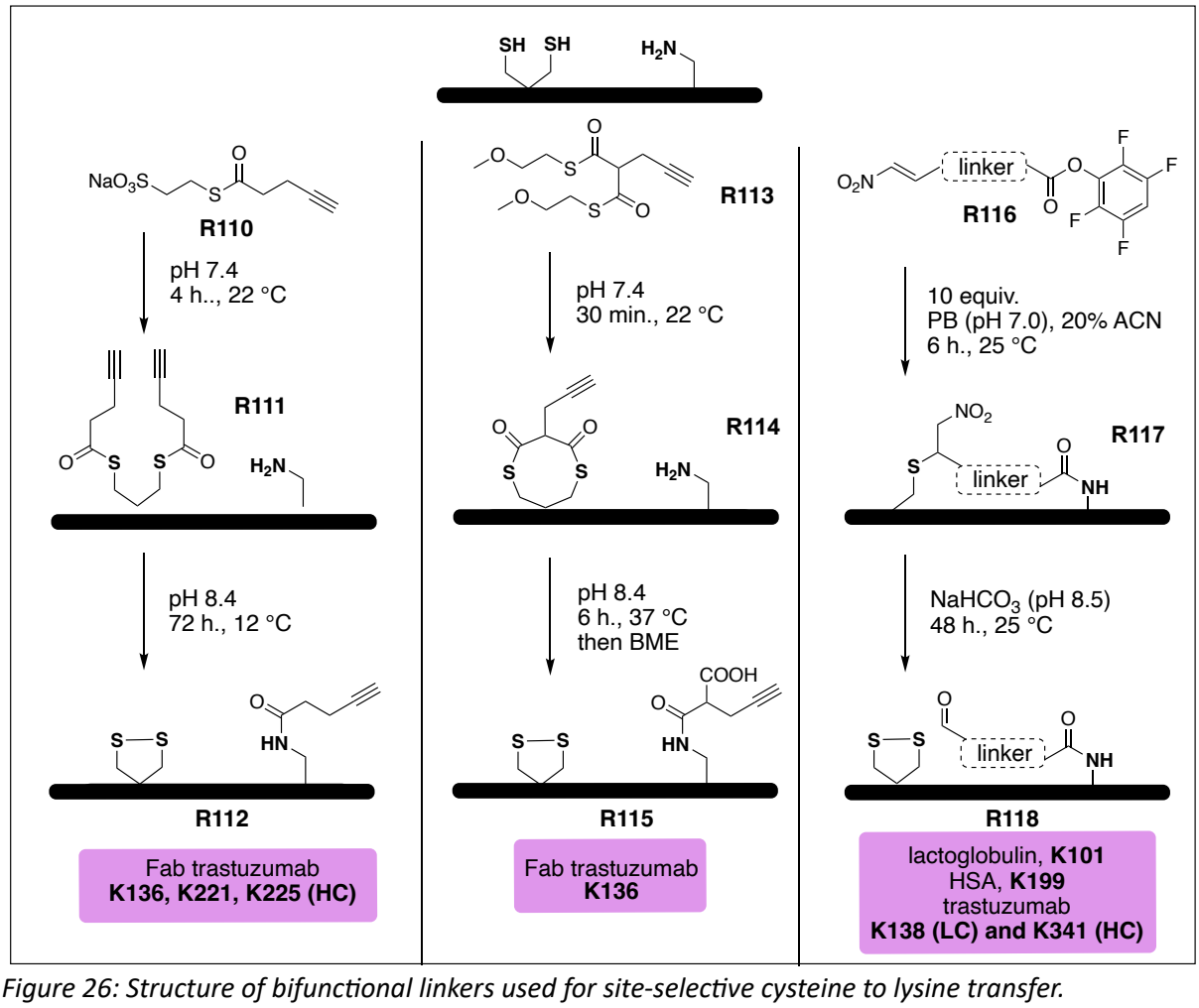

Figure 26: Structure of bifunctional linkers used for site-selective cysteine to lysine transfer.

Based on a similar strategy, Rai and co-workers also exploited the *S*,*N*-acyl migration previously mentioned. They developed reagent **R116** comprising a cysteine-selective nitroolefin linked to a lysine-selective tetra-fluorophenoxide ester through linkers of various lengths (Figure 26). They then developed conditions for the release of the thioester linkage of the cyclic conjugate **R117** by a *retro*-Henry reaction, resulting in a C-C bond dissociation and formation of an aldehyde **R118** that can be further functionalized with an *O*-alkoxyamine as mentioned above.

They were able to demonstrate site selectivity on K101 of β-lactoglobulin (87 % conv.), HSA K199 (conv. not provided by the author) and on full trastuzumab with K138 (LC) and K341 (HC) being identified as favoured sites (25% conv.). They also raised an interesting point which is protein selectivity as they were able to show that in cell lysate, only HSA was modified despite the abundance of competiting functions thus illustrating the extended selectivity of the method.[117]

The same team developed a variation of such reagent, **R119**, for the modification of histidines thanks to the addition of a monosubstituted epoxide as the "irreversibly coupling" partner leading to conjugate **R120** (Figure 27).[118] Site-selective, mono-labelling of various proteins was demonstrated, albeit on different histidines and in lower conversion compared with a previously published cyclohexenone approach for the same targets. This degree of selectivity seems to depend on both the linker structure and the protein size: while the Fab fragment of trastuzumab could be site-selectively conjugated (H189; light chain) with **R119**, this site-selectivity eroded when the full antibody was used instead. Interestingly, single labelling of a unique protein (cytochrome C) could be achieved when reacted in a mixture with six other proteins.

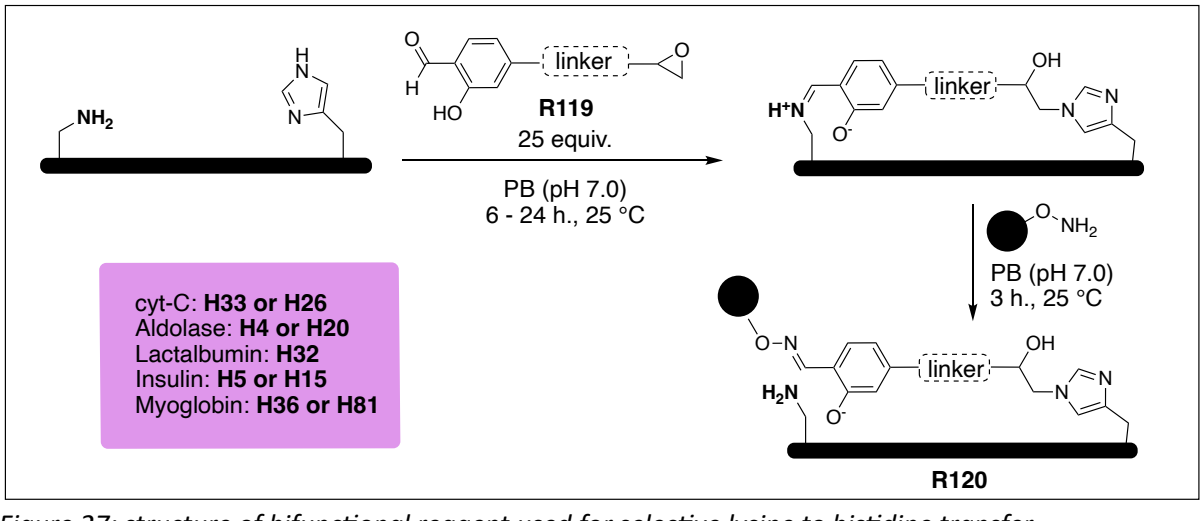

Figure 27: structure of bifunctional reagent used for selective lysine to histidine transfer.

Our team published in 2020 an alternative to this template-directed approach by focusing on dual-residue functionalisation in a Ugi four-component three-centre reaction (4C-3-CR). In our case, the two targeted chemical groups — i.e., an amine and a carboxylic acid — are conjugated upon addition of an aldehyde and an isocyanide, in a single reaction and both targeted chemical functions are involved in the final structure of the Ugi adduct.[119] This multi-component approach will be further developed in the following chapter.

IV. Conclusion

The chemical conjugation of proteins has thus gone a long way since its first applications in the tanning industry more than 150 years ago thanks to the progressive understanding of proteins' structure and composition, which fostered the development of chemical reagents and techniques with improved selectivity. With many applications in analytics, biology and therapy, bioconjugation is a truly interface domain, necessitating various transversal knowledge and comprehension.

The challenge in the case of native proteins lies in the understanding of the slight variations in reactivity of the various surface-exposed reactive entities, governed by the three-dimensional conformation of the protein and the microenvironment surrounding the residues and affecting their nucleophilicity, basicity and access. Working with these constraints, innovation in the site-selective conjugation of native proteins has been driven by two main approaches: the development of new reagents and that of novel techniques with a clear overlap between these two areas in several cases. Recent advances in the development of site-selective conjugation method, in combination with bioorthogonal chemistry allowed to extend the used payloads from the conjugation of small molecules to protein fragments allowing the construction of artificial proteins with new properties such as bispecific antibodies (bsAbs).

While predicting what the future holds in store for the field is nearly impossible, as it might depend heavily on the applications of all reported strategies to date, one can assume that the involvement of new techniques and new fields of research can lead to improved conjugation strategies. Having transitioned from an exotic oddity to an industrially applicable method, one can imagine it could lead to new reactivity profiles by modifying local microenvironments at the surface of the protein. As shown by a recent work from the Bernardes group,[120] computational chemistry can help design tailored reagents for site-selective applications. Coupled with X-ray crystallography or AI-powerded techniques such as alpha-fold to decipher proteins' three-dimensional structure, it could facilitate our understanding of the key factors influencing reactivity and lead to new synthetic strategies taking advantage of the spatial proximity between two or more reactive residues to narrow down the potential number of conjugation sites.

Multicomponent reactions for bioconjugation of native proteins

I. Introduction

I.1. History and applications of multicomponent reactions

A multicomponent reaction (MCR) is a chemical reaction where three or more compounds react together sequentially to selectively give a single product.[121] If a concerted mechanism is not a requirement, the reaction has to happen in a 'one pot' manner to be considered as multicomponent. Moreover, a catalyst, or a reagent who will not structurally contribute to the formed product, is not considered as part of the components. There are many advantages with the use of such reactions, such as low amounts of by-products — providing high atom economy — and simple procedures and equipment — allowing cost, time and energy savings — while allowing to reach high diversity of products in a rapid manner. Most of the time, the product is assembled following a network of elementary reactions equilibria which all converge into an irreversible last step yielding the final product. Fine tuning of the reaction conditions — solvent, temperature and concentration — is thus mandatory.[122,123]

The first rationalized MCR — the condensation of aldehyde **R121**, ammonia **R122** and hydrogen cyanide **R123** allowing the formation of an α-aminocyanide **R124** that can be hydrolysed into the desired α-amino acids **R125** — was exemplified by Adolf Strecker in 1850 and would later be dubbed after him: the Strecker amino acid synthesis (Figure 28).[124]

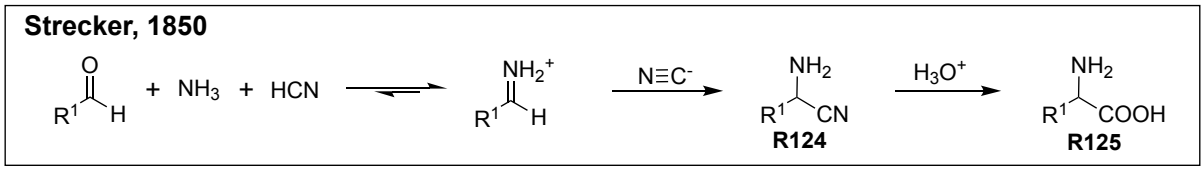

Figure 28: First reported multicomponent reaction.

This followed an observation made 12 years before by Laurent and Gerhardt who had isolated benzoylazotide from bitter almond oil, as the benzaldehyde source, liquid ammonia and hydrogen cyanide.[125] Many other MCRs were reported in the following years, now named after their discoverers and inventers, such as the Hantzsch reaction (1882), the Biginelli reaction (1883), the Mannich condensation (1912) or the Passerini reaction (1921).[126–129] Almost 100 years after the Strecker synthesis was published, application of such reactions was found in the multistep synthesis of biologically active compounds, greatly increasing the synthesis yields. At this time, such reactions started to be coined as MCRs and classified according to similarity in their mechanisms.[130]

I.1.a. Hantzsch type MCR

In 1882, Hantzsch reported the condensation of aldehyde **R126**, two equivalents (equiv.) of β-ketoesters **R127** and ammonia **R128** yielding a 1,4-dihydropyridine dicarboxylate **R129** that can be oxidized into pyridine **R130** in a subsequent step driven by aromatization (Figure 29).[126] This reaction found applications in the production of therapeutics, as dihydropyridines are an important class of calcium channel blockers as epitomised by commercial drugs such as Nifedipin, Amlodipine and Nimodipine.[131] While the mechanism of the reaction is not clearly elucidated, with at least five different pathways suggested, it was shown that polar protic solvents and basic pH were required for the reaction to happen. Monitoring of the reaction by NMR spectroscopy validated the formation of enamine **R130** and a chalcone **R131** intermediates, which would be consistent with the mechanism presented in figure 29, whose strategic steps are based on enolization of carbonyls and Knovenagel condensation.[132,133]

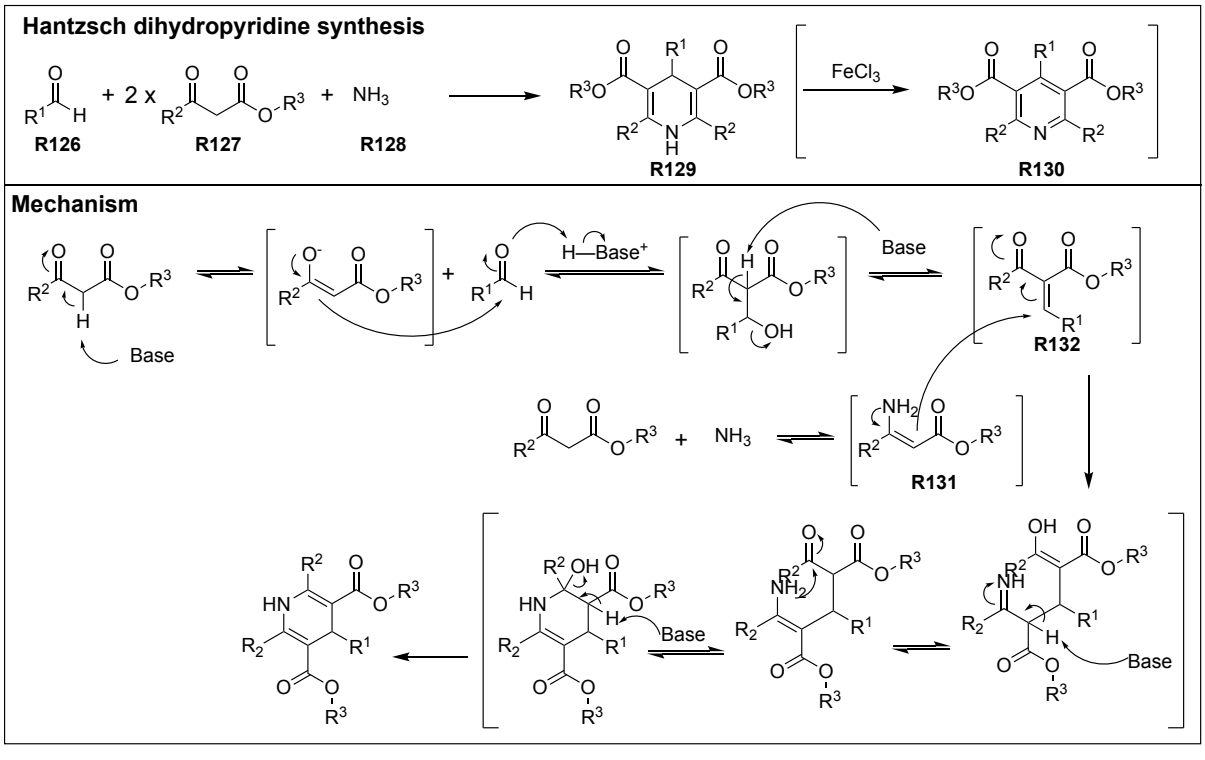

Figure 29: Conditions and presumed mechanism of the Hantzsch 1,4-dihydropyridine synthesis

This tri-component reaction (3-CR) was shown to tolerate good variation of the used reagents — carbonyls, malonate derivatives (α-keto ester or malonitrile) and heteroatom donors (nitrogen or sulfure) — allowing the rapid formation of various aromatic heterocycles.

Among the many proposed variations, the Hantzsch pyrrole synthesis, the Biginelli synthesis as well as the Gewald synthesis are worth mentioning (Figure 30).

The Hantzch pyrrole synthesis proposed in 1890 consists in the replacement of the aldehyde used in the original synthesis by an α-chloroketone **R133**.[134] This carbonyl is a soft electrophile, allowing its selective nucleophilic attack by enamine **R134** — based on the hard-soft acid base (HSAB) Pearson principle — and the formation of pyrrole **R135** (Figure 30).

Biginelli proposed in 1883 a version of this reaction where the primary amine is replaced by (thio)urea **R136**.[127] The addition of **R136** on benzaldehyde **R137** allows the formation of Schiff base **R138** which undergoes an aldol condensation with α-ketoester **R127**. A second nucleophilic addition of the free amine of the urea motif allows cyclization into hexadibromopyridine **R139** which is then aromatized into the corresponding 3,4-dihydropyrimidin-2(1*H*)-ones **R140** (Figure 30).

Finally, the Gewald reaction involves α-ketone **R141**, malonitrile **R142** and a source of sulfur. First, Knoevenagel condensation between **R141** and **R142** leads to intermediate **R143**. The mechanism of the following sulfur addition is still unknown but postulated intermediates are proposed in figure 30, with a final tautomerization step yielding the final 2-amino thiophene **R144** product.[135]

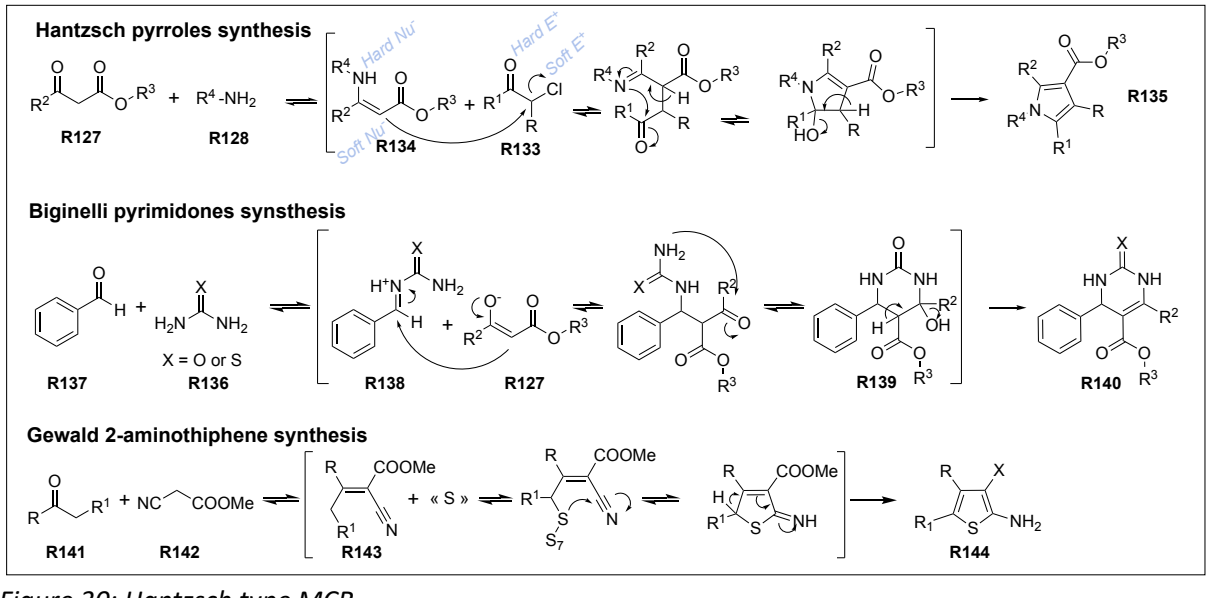

Figure 30: Hantzsch type MCR

All those heterocycles are found in many bioactive molecules and the development of those reactions allowed simple and rapid access to libraries of drug-like compounds, a process highly used in drug discovery.[136–138] A second family of 3-CR, allowing to reach an even higher diversity of products was described by Mannich in 1903.

I.1.b. Mannich type MCR

Mannich-type MCR are all based on the preliminary formation of a Schiff base followed by its nucleophilic attack by a soft nucleophile such as an enolizable carbonyl.[139] Based on the observation made by Tollens and Van Marle in 1903 that reacting acetophenone, formaldehyde and ammonium chloride would lead to a tertiary amine product,[140] Mannich studied the general reaction between carbonyl **R145** — aldehyde or ketone —, primary amine **R146** and enolizable carbonyl **R147** leading to alkylated β-ketoamines **R148** (Figure 31).

This reaction, often used for the synthesis of natural products, can be performed under both acidic or basic conditions and the use of chiral catalysts allowed the development of enantio-selective conditions.[128,139,141,142]

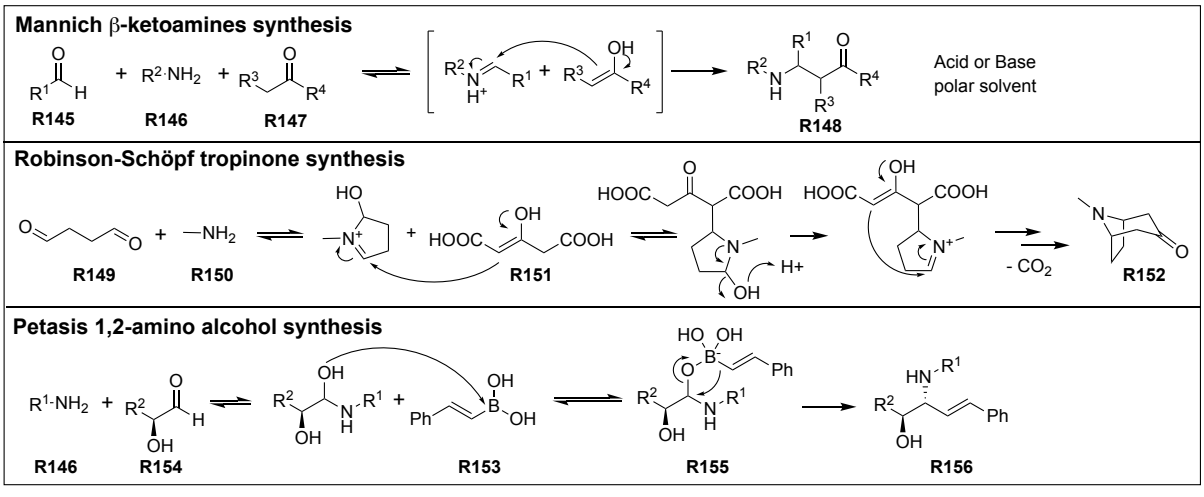

Figure 31: Mannich MCR general mechanism and presentation of Mannich type MCR

Robinson reported in 1917 a three-component reaction between a dialdehyde **R149**, methylamine **R150** and 3-oxoglutaric acid **R151** and a primary amine for the one-pot formation of tropinone **R152** through a double Mannich reaction (Figure 31).[143] This reaction was later optimized by Schöpf, allowing it to be performed under smoother, physiological conditions, and it is thus named after those two researchers.[144] This reaction was found to highly reduce the number of steps in the synthesis of alkaloids such as atropine, often used as antidote for gaz poisoning or in order to slow heart rate during surgery, properties highly needed during the first World Wars (when it was developped).

A mechanistically related reaction is the Petasis reaction, also called the Petasis Borono-Mannich (PBM) reaction, first reported in 1993. In this case, the terminal nucleophile is a vinyl- or aryl-boronic acid **R153** instead of an enolizable carbonyl, leading to allylamines instead of β-amino carbonyls (Figure 31).[145] Diastereoselective variants have been documented, notably when using α-hydroxy aldehydes **R154**, with the hydroxyl group helping to form a transient boronate anion **R155**, orienting the alkylation (or arylation) of the Schiff base and resulting in the exclusive formation of *anti*-1,2-aminoalcohols **R156**.[145]

If those 3-CR were proven to give access to a large variety of compounds, access to the largest variety of backbones rose along with the access to wide variety of isocyanides.[146] Isocyanides are an extraordinary functional group that can act both as an electrophile and a nucleophile according to its resonance form between tetravalent and divalent form. Because of this remarkable property, their use in MCRs was widely explored, with the Passerini and the Ugi reactions being the most representative examples.

I.1.c. Isocyanide based MCR

The Passerini reaction, described in 1921, consists in the reaction of a carbonyl **R157** — aldehyde or ketone — carboxylic acid **R158** and a isocyanide **R159** leading to the formation of α-acyloxycarboxamide **R160** (Figure 32).[129] The reaction is often performed at room temperature and is known to proceed best with high concentrations in reagents and in aprotic solvents. The latter feature suggests that the reaction does not follow an ionic pathway and that hydrogen bonding between the different reagents is crucial.[147] It is notably used in the synthesis of therapeutic reagents such as azynomycines used in cancer treatment.[121,148]

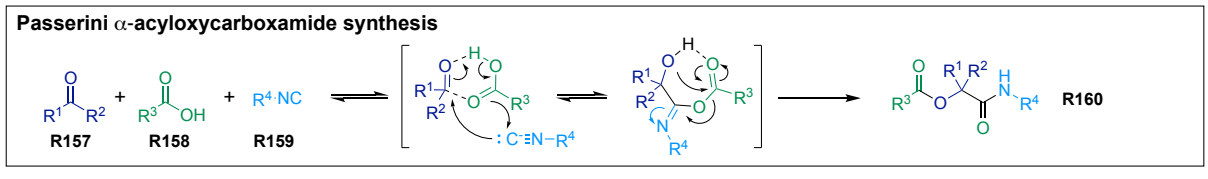

Figure 32: Presumed mechanism of Passerini MCR

In 1959, Ivar Ugi reported a four-component alternative to the Passerini reaction also involving carbonyl **R157**, carboxylic acid **R158** and isocyanide **R159** but also primary amine **R161** (Figure 33).[146,149–151] The reaction mechanism, quite different from that of the Passerini reaction, is believed to consist first in the condensation of **R157** and **R161** to yield imine **R162**, in equilibrium with its iminium analogue **R163** upon deprotonation of carboxylic acid **R158**. Following the nucleophilic addition of isocyanide **R159**, the resulting isonitrilium can then react with carboxylate **R164** to give carboximidate **R165**, which undergoes an irreversible Mumm rearrangement to form α-aminoacylamide **R166**.[152,149]

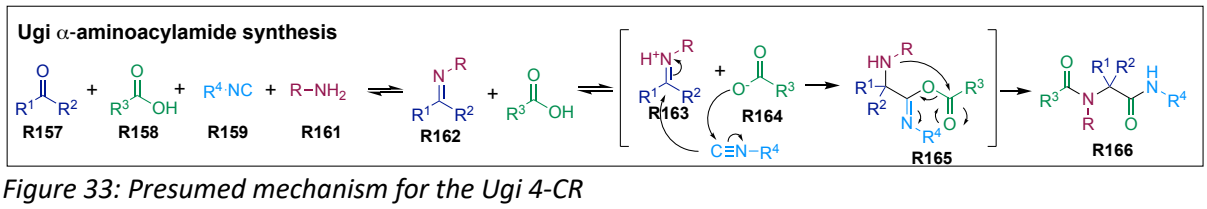

Figure 33: Presumed mechanism for the Ugi 4-CR

The Ugi reaction was largely derivatized as it was shown to tolerate great variability on the reagents' side chains. For instance, conserved reactivity was observed whenever the amine and the carboxylic acid were borne by a single reagent (typically, β-amino acid **R167**). The so-called Ugi 4-component 3-centre reaction (Ugi-4C-3CR) allowed for example the access to β-lactams **R168** libraries upon variation of the aldehydes' side chain (Figure 34).[153]

Keeping in mind this idea of multifunctional reagents, the Ugi reaction was shown to tolerate reactive functions on the side chain of the used reagent as exemplified by the Ugi-Diels-Alder reaction, were the Ugi reaction is used to bring in spatial proximity a diene **R169** and a dienophile **R170** for intra-molecular Diels-Alder to happen (Figure 34).[154,155]

The Ugi-smile reaction on the other hand consists in the replacement of the carboxylic acid with a substituted phenol **R171**.[156] In this case, the final Mumm rearrangement is replaced by a Smile rearrangement, yielding compound **R172** (Figure 34).

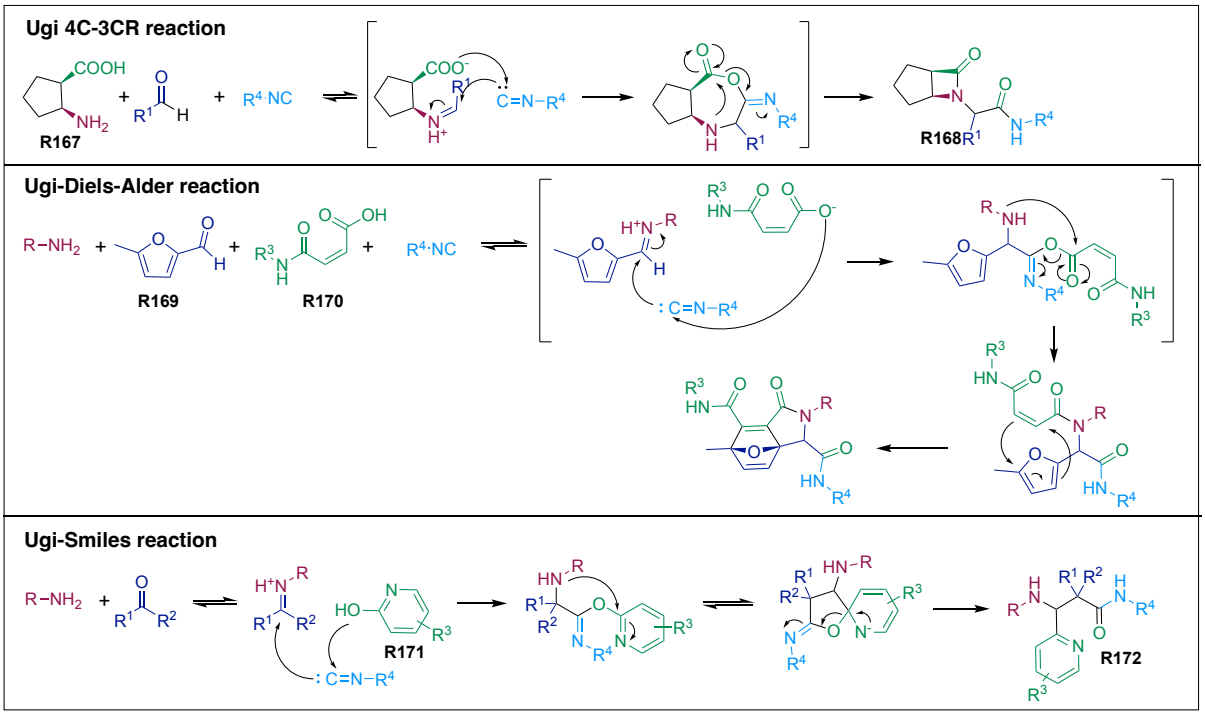

Figure 34: Mechanisms of the different variants of the Ugi 4-CR

Multicomponent reactions were shown to tolerate various side chains and their high degree of selectivity made them highly versatile and ideal steps in the synthesis of complex molecules such as natural products or drugs but also in combinatorial chemistry, for the rapid synthesis of libraries of small molecules. This versatility in reagents coupled with the low amounts of by-products and good tolerance for polar solvents made those equilibrium-oriented reactions good candidates for bioconjugation application. Considering that the key families of reagents employed in most MCRs can also be found in biomolecules, bioconjugation chemists quickly turned their attention toward their use.

I.2. Multicomponent reactions for bioconjugation

Francis and co-workers were the first to use the Mannich reaction for the chemoselective labeling of tyrosine residues, using the side chain phenol group as surrogate for the traditional enolate nucleophile.[157,158] Introduction of a large excess of formaldehyde **R173** and aniline **R174** led to the labeling of different surface-accessible tyrosines of three different proteins — i.e., chymotrypsinogen A, lysozyme, and RNase A— at pH 6.5 and in 18 hours (Figure 35). The undesired imines resulting from the reaction of formaldehyde with available amines (*N*-ter and

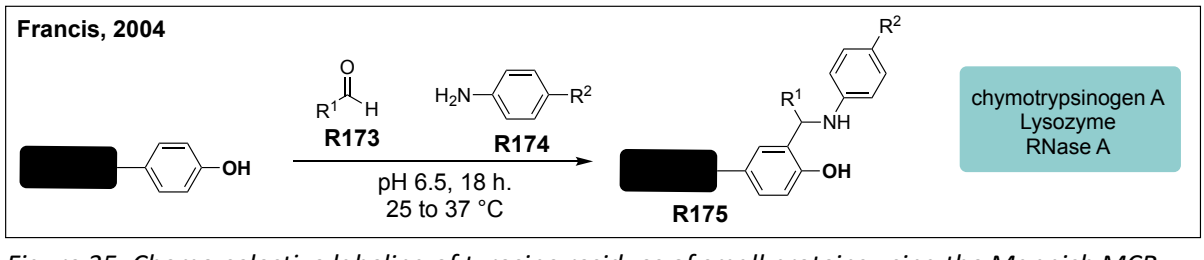

Figure 35: Chemo-selective labeling of tyrosine residues of small proteins using the Mannich MCR.

lysines) were hydrolyzed using hydroxylamine resulting in homogeneous conjugates. This method was later used for the attachment of peptide sequences of interest on small proteins.

Rai and co-workers adapted the Mannich MCR for the site-selective conjugation of lysines. Using either formaldehyde **R176** or benzaldehyde derivatives **R177**, ε-amino groups were first converted to latent imines, which reacted in a subsequent step with carefully selected nucleophiles — either in-situ formed copper(I) phenylacetylide **R178** (A^3 coupling)[159] or triethylphopshine **R179** (phospha-Mannich),[160] respectively — with excellent chemo- and site-selectivity (Figure 36). Among the various proteins evaluated in both studies, some were shown to be labelled on the same lysine residue, irrespective of the MCR employed under identical reaction conditions: ubiquitin (on K48) and α-chymotrypsinogen A (K79).

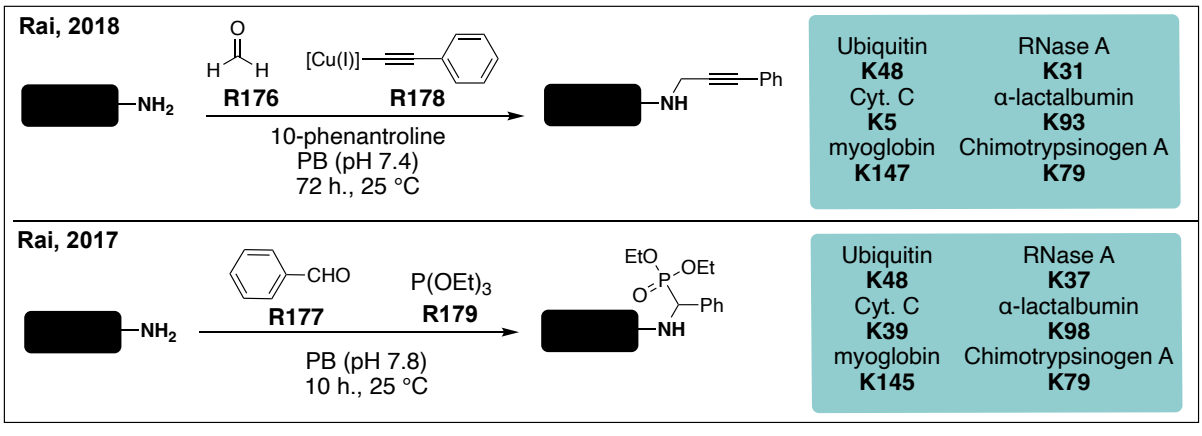

Figure 36: Site-selective labeling of native proteins using adaptations of the Mannich MCR.

The majority, however, showed dissimilar conjugation sites depending on the strategy employed — RNase A (phospha-Mannich: K37; A^3 coupling: K31), α-lactalbumin (phospha-Mannich: K98; A^3 coupling: K93), cytochrome C (phospha-Mannich: K39; A^3 coupling: K5), myoglobin (phospha-Mannich: K145; A^3 coupling: K147)—, as the first step of the reaction consists in the formation of a Schiff base, the most accessible lysine of each protein should react first, those results stress the prevalence of the reagent structure on the conjugation site.

In 2019, Raj *et al.* proposed to use the secondary amine-selective Petasis (SASP) reaction for the labelling of peptides and small proteins such as creatinine kinase and aldolase, presenting *N*-terminal prolines.[161] The Schiff base formed between 2-PCA **R180** and the proline can undergo a nucleophilic attack from a boronate reagent **R181** leading to the formation of a stable tertiary amine **R182** (Figure 37). However, they mentioned that this reaction could be used to label other

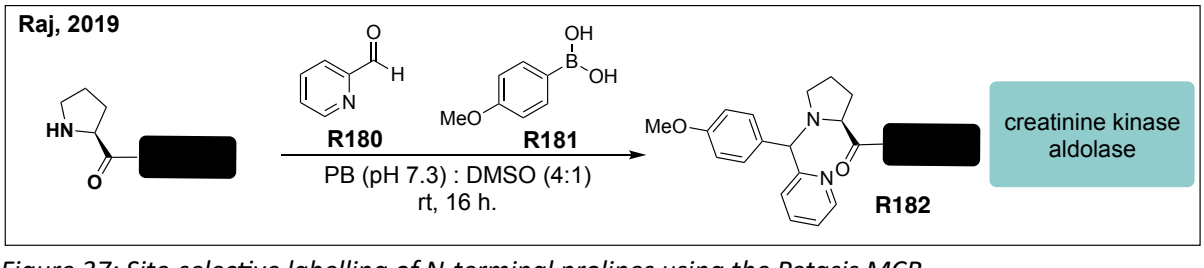

Figure 37: Site-selective labelling of N-terminal prolines using the Petasis MCR.

N-terminal amino acids, but that better conversions were obtained with prolines, probably due to their higher nucleophilicity linked to their secondary amine character.

Encouraged by the successful application of the Mannich-type reactions for the selective labelling of proteins, other MCR were explored for protein labelling. Among the different MCR mentioned above, the isocyanide-based strategies have retained researchers' attention and especially the Ugi 4-CR as it was shown to work in water, and polar protic solvents in general.

The first report of its use for protein conjugation dates back to 1974, with the immobilization of trypsin on isocyanide-containing nylon (poly-isocyanide nylon).[162] It was shown that in the presence of large excess of reagents — i.e., acetaldehyde and acetate — trypsin could be immobilized by one of its lysine residues. If such immobilization seems to have a slightly detrimental effect on the trypsin activity, probably due to a lower accessibility of the protein, it was shown that such stappling did increase the stability of the enzyme toward both pH and temperature variation. The same team reported four years later good transferability of the method on a different isocyanide based support: poly(ethylene tetraphtalate). Immobilization of different enzymes — such as horseradish peroxidase (HRP) and *Rhizomucor miehei* lipase (RML) — as source of amine for an Ugi reaction was performed using carboxylate-containing resins and[163,164] aldehyde-functionalized resins with maintained enzymatic activity.[165] Immobilization of RML as source of carboxylate on an amine containing resin by addition of an aldehyde and an isocyanide was also reported.[166] Those studies show that proteins can easily partake in a Ugi reaction through both their lysine and their aspartate and glutamate with no impact on their activity.

In 2000, Ziegler and coworkers reported the preparation of bioconjugates with the Ugi reaction (Figure 38).[167] Bovine serum albumin (BSA) and HRP were reacted with different carboxylic acids, isocyanides, carbonyls and amines and the two proteins were found to react either via

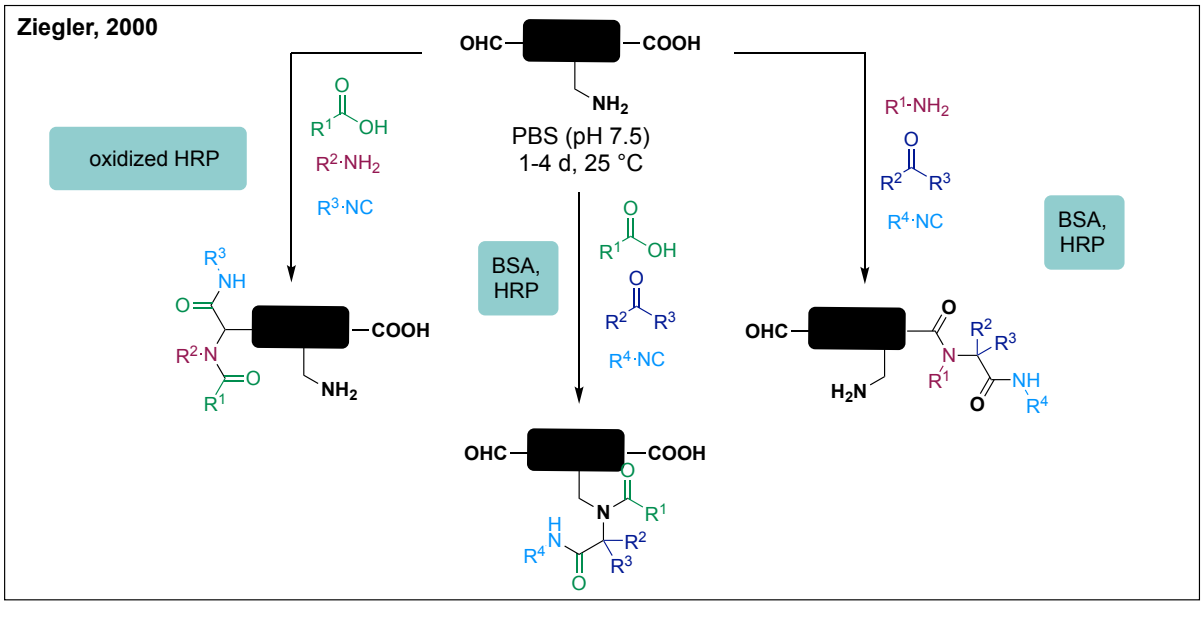

Figure 38: Selective labeling of proteins using the Ugi MCR.

their amino or carboxylate groups, in their native form, or via aldehyde groups after oxidation of the HRP's carbohydrates with sodium periodate, depending on the used conditions. To achieve good conversions, up to 4000 equivalents of reagents were necessary, with incubation times of 1 to 4 days at 25 °C.

Rivera *et al.* proposed to use the U-4CR for the development of glycoconjugate vaccine candidates (Figure 39).[168] In order to do so, two bacterial capsular polysaccharides (CPs) from *Streptotoccus Pneumoniae* and *Streptotoccus Typhi* were oxidized and chosen as the aldehyde component and conjugated to carrier proteins– tetanus toxoid (TT) and diphtheria toxoid (DT) – acting here as the amine source in the MCR. Acetic acid and *tert*-butyl isocyanide were chosen as the two other components for the reaction. Because only 41% conversion was obtained after 48 hours, a more nucleophilic hydrazide group was introduced on the proteins, via the modification of aspartate / glutamate residues, allowing for complete conversion after 4 hours. Two years later, based on the same strategy, they were able to increase the complexity of their vaccines by making multivalent glycoconjugates from four different capsular polysaccharides.[169]

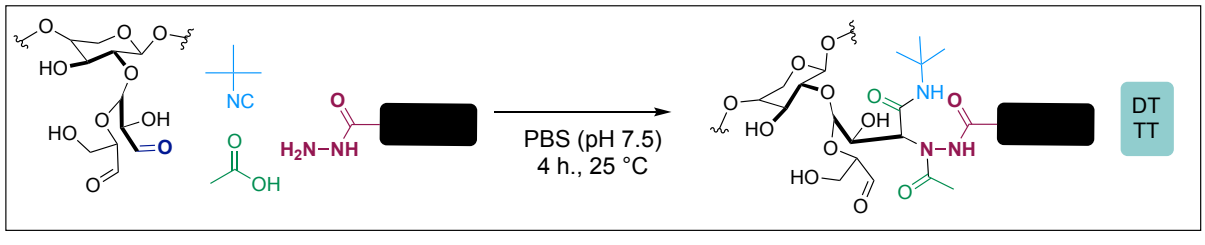

Figure 39: Linkage of two biomolecules using the Ugi MCR.

To summarize, there are two MCRs that have been applied to bioconjugation: Mannich (and Mannich like) 3-CR and the Ugi 4-CR. Protocol transfer to bioconjugation often requires to use large excess of conjugation reagent in combination with extended reaction time. The four-component version of the Ugi reaction (U-4CR) was used for the labeling of amine — lysines and *N*-ter residues — or carboxylic acids — aspartate and glutamate. Most notably, all the developed strategies tend to require large excess of reagents and long reaction times. More problematically, absence of thorough analytical investigation prevented the confirmation that the Ugi reaction was responsible for the observed conjugation and not another competition mechanism such as Passerini reaction for example.

The conducted studies on the Mannich reactions are more recent and, for instance deeper analysis of the selectivity of the reaction was performed. Upon targeting lysines, high degree of site-selectivity was reached on several proteins. Hence, we decided to investigate the potential use of the mechanistically related Robinson-Schöpf synthesis for the labeling of lysines.

II. Exploration of the Robinson-Schöpf MCR for the conjugation of trastuzumab

Trastuzumab is a therapeutic monoclonal antibody (mAb) that can selectively bind to the extra-cellular domain of the human epidermal growth factor receptor 2 (HER-2). This receptor is implicated in the growth and survival of its host cell and is over-expressed in some types of breast cancer. For instance, trastuzumab is used on a routine basis as blocker of those receptor for cancer therapy but it is also used as drug carrier in the context of ADCantibody drug (Figure 40).[119] ADCs consist in three components: the antibody also called immunoglobulin (Ig) that targets a surface receptor of the cancer cell with great selectivity, and that can elicit a biological response. The linker, that determines the conjugation site and prevents early delivery of the payload. Finally, the payload displays a cytotoxic activity toward the target cancer cell, mainly when released from the antibody. Most importantly, generation of ADC requires high control and selectivity of the bioconjugation method as it might impact the pharmacokinetics and pharmacodynamics of the construct. Among the many applications of bioconjugation, the generation of ADC is the most popular and thus many tests and comparison points are available for those constructs making mAb good model protein for the development of new bioconjugation methods.

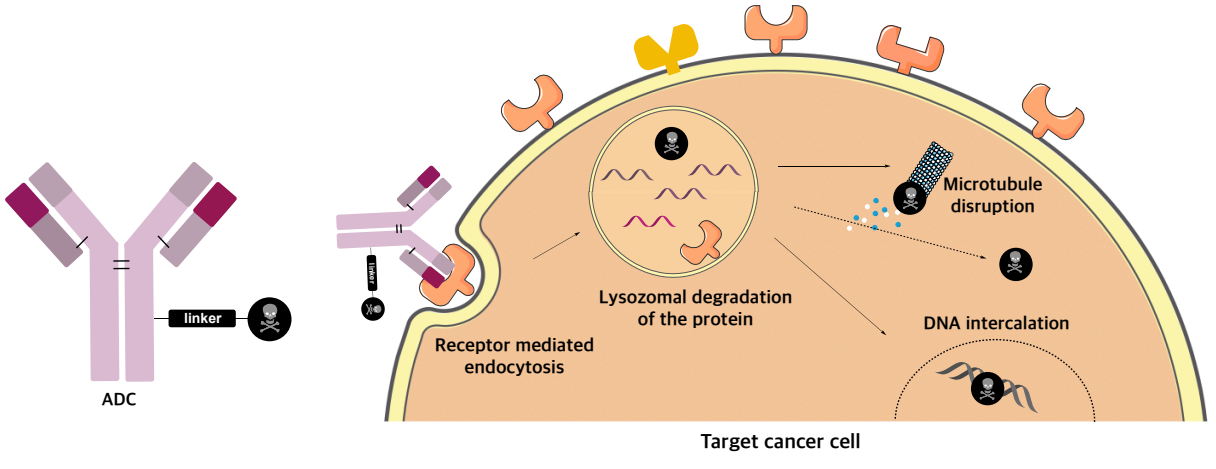

Figure 40: General structure and mechanism of an ADC

Mannich reactions are three component reactions, between an aldehyde an amine and malonate-based nucleophile. Good transferability of Mannich reaction and mechanistically related reaction was observed for the labelling of proteins with good degree of selectivity. We could not help but notice the absence of investigation of the Robison-Schöpf reaction among the Mannich like developed strategies. This one-pot reaction happens between methyl amine **R150**, 3-oxoglutaric acid **R151** and a succinaldehyde **R149** hence we hypothesized that it could be used for lysine labelling by reacting a protein with the two carbonyl components following the mechanism presented (Figure 31).

As this reaction was shown to necessitate acidic medium (pH = 5) and mild temperature (40 °C) for the key double decarboxylation to happen, we first evaluated whether these conditions might affect the structural integrity of our model protein, trastuzumab.[170] To do so, native trastuzumab was buffer exchanged to PBS (1X, pH 5.0) and incubated at 45 °C overnight; native MS analysis of the mAb did not show any structural alteration. In addition, we evaluated if such harsh conditions could have a detrimental effect on the affinity of the mAb for its target. Thus, we selected the HER-2 positive cell line SKBR-3 as positive control and the HER-2-negative cell line MDA-MB-231 as negative control (Figure 41). We evaluated the binding of a FITC-labelled trastuzumab on both cell lines by real-time affinity measurement using a Ligand Tracer Green apparatus (Ridgeview instruments) and compared it with an FITC-labelled native trastuzumab. The similar k_{on}, k_{off} and K_D obtained — 2.38 10^4 $M^{-1}.s^{-1}$, 1.07 10^{-5} s^{-1}, 0.48 nM for trastuzumab and 2.41 10^4 $M^{-1}.s^{-1}$, 0.56 10^{-5} s^{-1}, 0.24 nM for the heated trastuzumab, respectively — allowed us to conclude that those conditions did not impair the antibody recognition for its target.

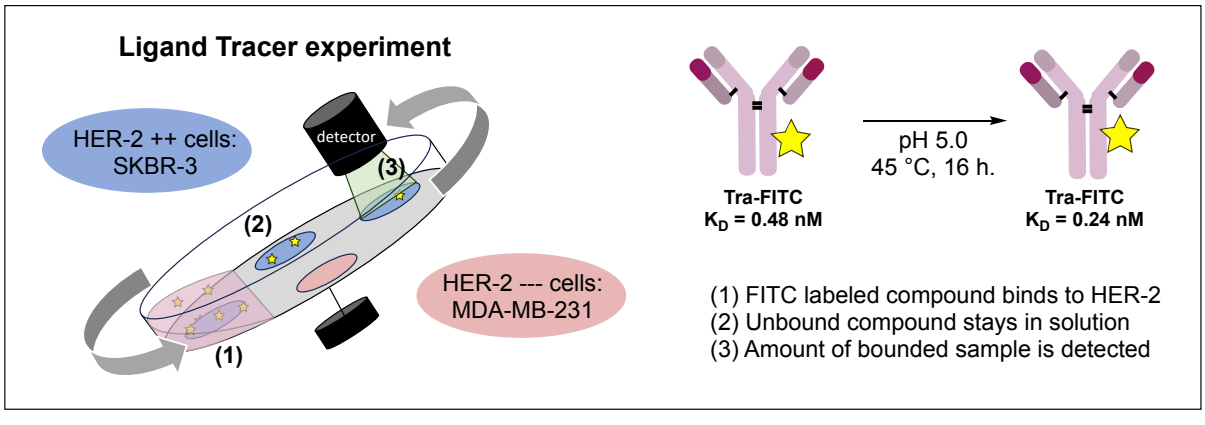

Figure 41: Principle of Ligand tracer experiment. Affinity measure for tra-FITC and heated tra-FITC.

Having those results in hands, direct application of the conditions described by Burks *et al.* was conducted on trastuzumab, with the sole exception of an increased amount of reagents and reaction time.

In more details, succinaldehyde **1** was freshly generated by reacting 2,5-dimethoxytetrahydrofuran **2** in water at pH 1, acidified using concentrated HCl, at 70 °C for 30 minutes. The resulting dialdehyde **1** (10 equiv.) was then added to a solution of trastuzumab (PBS 1X, pH 5.0) containing 12 equiv. of 3-oxoglutaric acid **3**, 14 equiv. of HCl and 40 equiv. NaOAc and the mixture was stirred at 37 °C for 3 hours (Figure 42). Because PBS buffering ability is based on the couple dihydrogen phosphate/ hydrogen phosphate (pK_A = 7.2) we assumed that adjusting PBS pH to 5.0 might lead to lower buffering ability. Thus, we measured the pH after addition of the reagents to the mAb mixture and were glad to find it did not vary from 5.0. Because the mass of the expected payload is only 108 Da, resulting in suboptimal resolution in MS analyses, we decided to functionalize the resulting carbonyl as an oxime, using aminooxy-(2,4,6-trimethoxyphenyl)phosphonium bromide (TMPP) reagent **4**, a method inspired from the late-stage functionalization of cyclohexanone-modified proteins described by the team of Vishal Rai.[171]

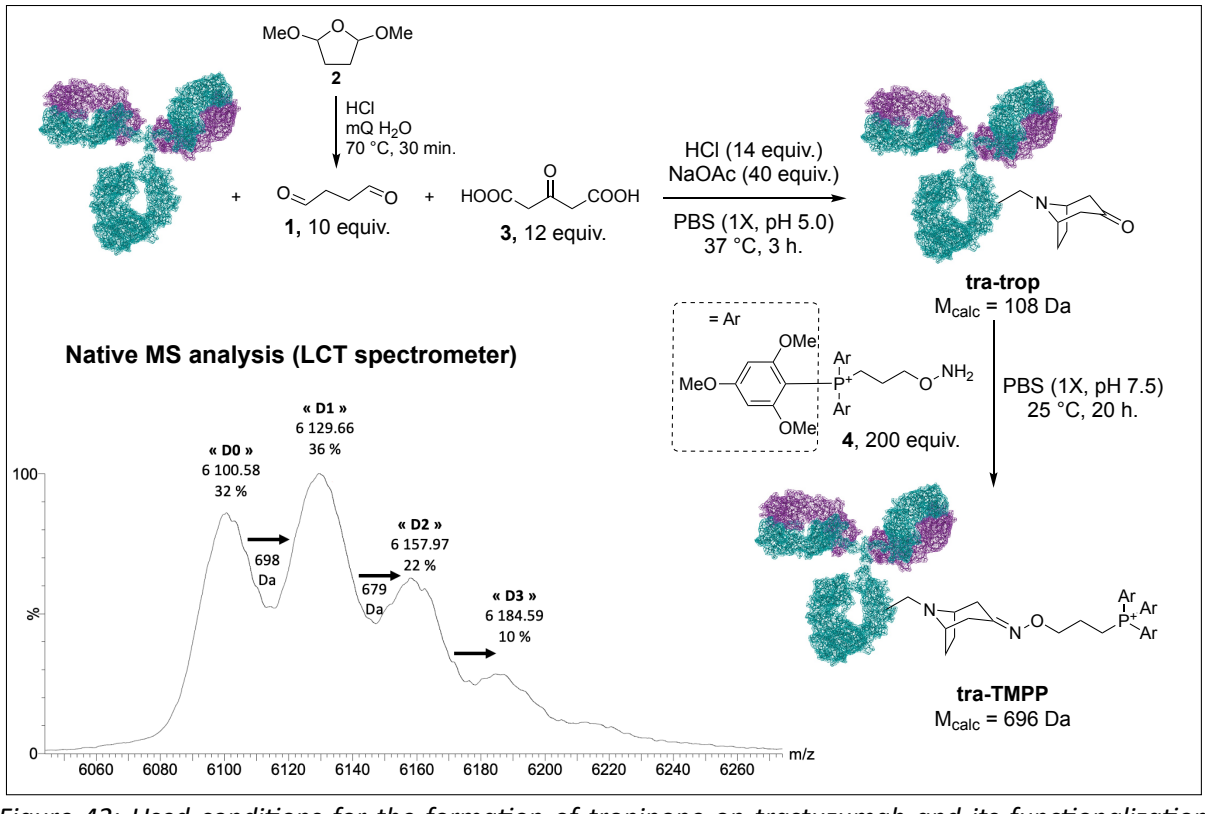

Figure 42: Used conditions for the formation of tropinone on trastuzumab and its functionalization using aminooxy-TMPP. Zoom on the + 24 charge state of the Native MS spectra obtained from using the LCT spectrometer is presented.

Native MS analysis of the obtained conjugate on the LCT spectrometer presented several oddities: first a + 531 Da mass shift was observed for the first peak — coined “D0”, Figure 42 — in comparison with the mass of native trastuzumab (M = 145 883 Da) suggesting full conversion of the native mAb but with ‘unexpected’ adducts as this shift does not correspond to a full payload — M_{calc} = 696 Da. Moreover, if a distribution of payloads is observed, only the increment between “D0” and “D1” matches that of the expected oxyme conjugate (M_{obs} = 698 Da), the others presenting lower molecular weights.

Altogether, those result show that the formation of **tra-TMPP** adduct is possible; however, the reaction might be in competition with several others that we tried to elucidate in following experiments. As those competitive mechanisms might involve low molecular weight adducts, we decided to use a more resolutive spectrometer: the Exactive plus EMR spectrometer from Thermo Fisher allowing to detect payloads ≥ 50 Da. Analysis of **tra-trop** and **tra-TMPP** with this spectrometer allowed the identification of various low molecular weight adducts from one peak to the other — e.g. Δ (a) = M peak b – M peak a — presented in Figure 43. We hypothesized that the different adducts might come from incomplete formation of tropinone — i.e., **tra-I1**, **tra-I2**, **tra-I3** —, from the reaction of 3-oxoglutaric acid **3** with a primary amine — **tra-acid** — or from the cross-linking of trastuzumab with succinaldehyde — cross-linked tra. The obtained spectra presented too much heterogeneity for correct attribution of the observed adducts however presence of **tra-I1** resulting from mono-dehydration of succinaldehyde (M_1 = 69 Da, M_2 = 65 Da, M_3 = 67 Da, M_4 = 70 Da) seemed to be present in the two analysed samples.

Surprisingly, the analysis of **tra-trop** conjugate, obtained prior to TMPP functionalization, led to the observation of only one tropinone adduct — between peak h and peak g —in comparison with the distribution obtained in the case of **tra-TMPP** which might indicate a stabilization of the tropinone adduct upon oxime formation. The other observed adducts could not be attributed to any of the reaction intermediate which might come from protein degradation or instability of the tropinone adduct.

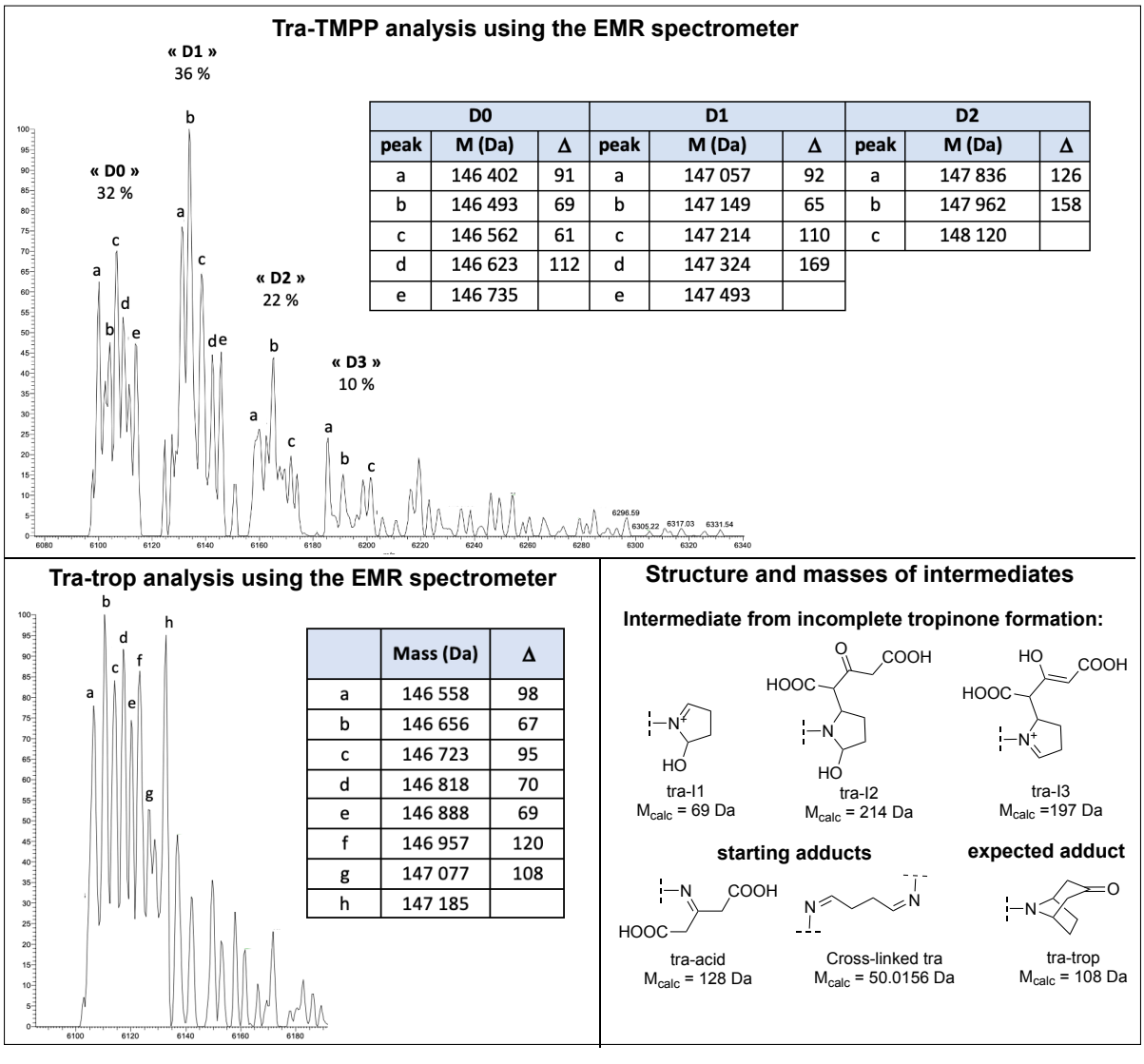

D0			D1			D2		
peak	M (Da)	Δ	peak	M (Da)	Δ	peak	M (Da)	Δ
a	146 402	91	a	147 057	92	a	147 836	126
b	146 493	69	b	147 149	65	b	147 962	158
c	146 562	61	c	147 214	110	c	148 120	
d	146 623	112	d	147 324	169			
e	146 735		e	147 493				

	Mass (Da)	Δ
a	146 558	98
b	146 656	67
c	146 723	95
d	146 818	70
e	146 888	69
f	146 957	120
g	147 077	108
h	147 185	

Figure 43: Analysis of tra-TMPP and tra-trop on the EMR spectrometer. Structure and masses of potential adducts are presented.

Because incomplete adducts were observed, we tried to vary the different reaction's parameter in order to favour exclusively tropinone formation and prevent degradation (Table 2). Our first observation was that any increased amount of reagent led to complete degradation of the mAb. Total removal of HCl and NaOAc from the reaction medium resulted in unconjugated mAb containing various adducts, each presenting a different mass and thus indicating the probable degradation of the mAb. Sole removal of HCl led to a distribution, similar to that obtained under the first conditions presented above, suggesting that its presence is not required for the reaction to happen. Removal of NaOAc from the reaction mixture led to a larger distribution

(up to D5), implying higher conversion to the desired adduct in this condition. Even though the broad peaks observed might be a sign of degradation.

Finally, reduction of the reaction temperature – a key parameter of the Robinson Schöpf reaction – led to the formation of even broader peaks (that might contain carboxylated adducts) and "poor" TMPP functionalization was observed. Finally, control experiments showed that 3-oxoglutaric acid alone does not react with the mAb, contrary to succinaldehyde, which probably leads to cross-linked adducts (56 Da).

Table 2: Optimization of the conditions for the tropinone functionalization of trastuzumab.

Equiv.				**pH**	**T (°C)**	**t (h.)**	**"D0" %**	**M_{obs} (Da)**	**Aspect**
CHO, 1	**COOH, 3**	**HCl**	**NaOAc**						
20	24	28	80	5	37	3	Degradation of the mAb		
10	0	14	40	5	37	3	100	56	Broad peak
0	12	14	40	5	37	3	100	/	Native mAb
10	12	0	0	5	37	3	100	/	Broad peak
10	12	0	40	5	37	3	26	684	Distribution Max: D3
10	12	14	0	5	37	3	16	681	distribution Max: D5
10	12	14	40	7.5	37	3	48	672	Distribution Max: D3
10	12	14	40	5	25	3	42	680	Distribution Max: D1
10	12	14	40	5	37	1	100	51	Broad peak
5	50	0	0	5	37	0.5	100	51	4 adducts
5	0	0	0	5	37	0.5	100	50	4 adducts

Considering this conserved heterogeneity, we decided to use simpler model before pursuing this optimization, first by using smaller proteins. In the case of ubiquitin, myoglobin and cytochrome-c, very low amount of unmodified protein was recovered, probably linked to stability issues under the used conditions, while BSA led to the exclusive formation of + 50 Da adducts, suggesting cross-linking of the protein's surface by succinaldehyde.

At this point we were still unable to validate that the observed conjugation resulted from the formation of tropinone on the protein or from another, yet unidentified, side reaction. In order to validate that lysine could indeed replace methyl amine in Robinson-Schöpf reactions we

incubated Ac-Lys-NHMe **5** in mQ H_2O with 1 equiv. of succinaldehyde **1**, 1 equiv. of 3-oxoglutaric acid **3**, 1.4 equiv. HCl and 40 equiv. NaOAc and at 40 °C for 1 hour, according to Burks's procedure (Figure 44).[170] ^{1}H and ^{13}C NMR analyses of the solid obtained after work-up allowed the identification of two products in a 9:1 ratio. The main product was identified to be the desired lysine-tropinone adduct (**Lys-trop**) and we attributed the side product to a pyrrole-functionalized lysine. This hypothesis is supported by the chemical shifts observed — two triplets at 6.70 and 5.95 ppm (predicted 7.31 ppm and 6.14 ppm) with same coupling constants (2.1 Hz) linked to two ^{13}C signals around 120.9 and 107.8 ppm (predicted 120.9 ppm and 108.7 ppm) — indicating an aromatic ring.

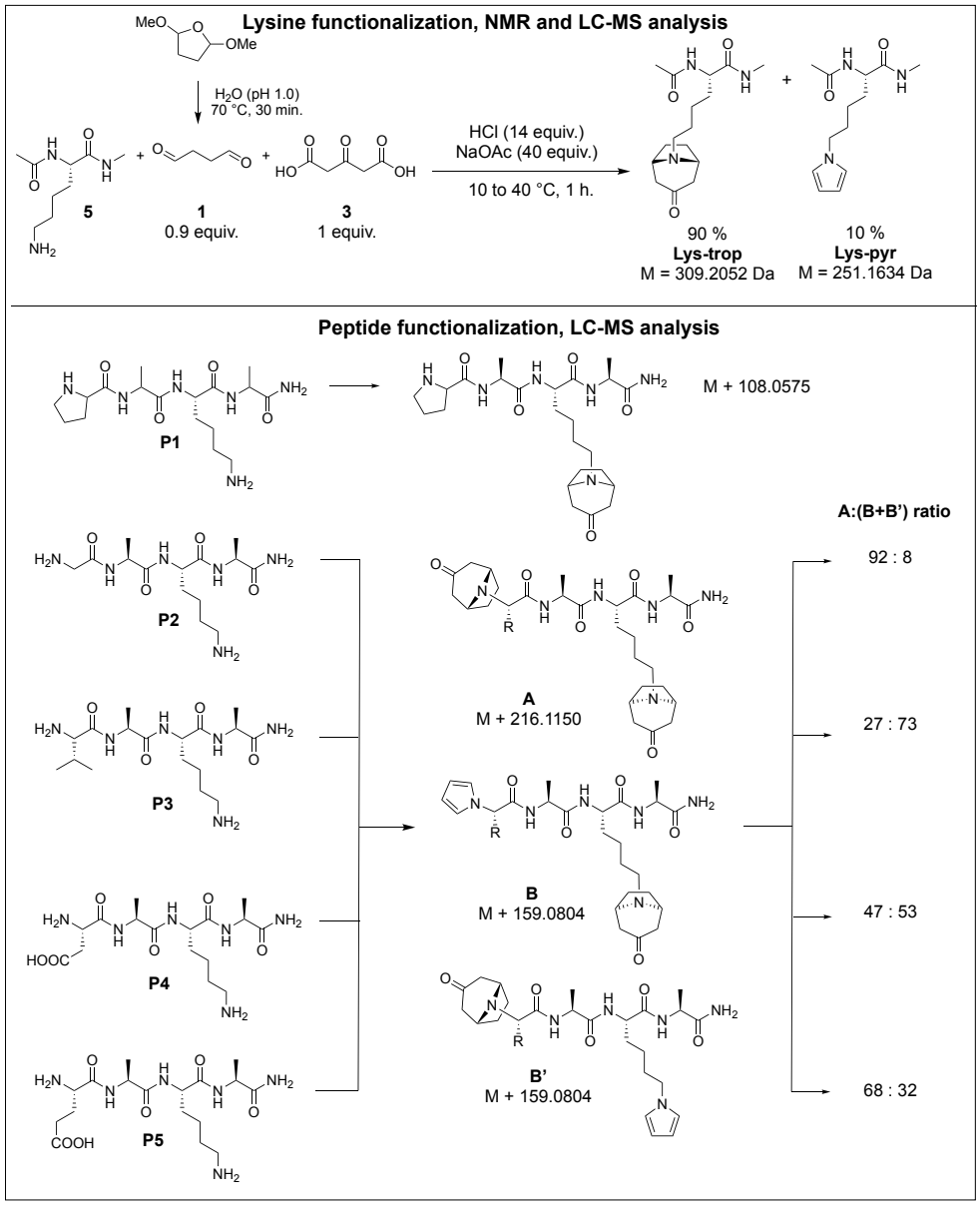

Figure 44: Ac-Lys-NHMe and small lysine containing peptide labeling using Robinson-Schöpf conditions. Masses were obtained by LC-MS analysis and structure of Lys-trop and Lys-pyr adducts were determined by NMR analysis.

More interestingly, variation of the reaction conditions showed that the integration of those two signals — and thus the amount of aromatic compound — was inversely correlated with that

of the signals of the tropinone but not with the ones of lysine, validating the presence of different lysine products in the mixture. Dillution of the reaction medium led to increased amounts of pyrrole signals.

Moreover, LC-MS analysis of the crude mixture led to the identification of the **Lys-trop** adduct (M = 310 Da) and of 252 Da adduct that fits with the lysine-pyrrole (**Lys-pyr**) adduct. The separation of the two products by column chromatography could not be performed due to poor separation in normal phase and degradation of the products after isolation by reverse phase, probably due to the used acidic conditions. Functionalization of small lysine-containing peptides was then considered, as separation of the different adducts might be facilitated. Using the same conditions as the ones used for the reaction with of Ac-Lys-NHMe, functionalization of the different peptides was found to reach completion in just 15 minutes, based on LC-MS analysis. Peptide **P1**, containing a *N*-ter proline and thus a single modification site was found to be fully converted to a peptide-tropinone adduct (Figure 44). The other peptides containing two free primary amines (*N*-ter and lysine) were found to be labelled with two tropinones (adducts **A**) or with one tropinone and one pyrrole (adducts **B** and **B'**) with different ratios estimated based on the area below the curve of the obtained UV chromatogram. We observed that the amount of pyrrole adducts did increase upon dilution of the reaction medium from 0.1 M to 0.05 M, which, in addition with the hindrance of the primary amine, might be the key parameter guiding tropinone formation. Separation of the two adducts was not possible as systematic degradation of the peptide was observed after preparative HPLC separation. Analysis of the crude reaction mixture could not be performed due to the use of NaOAc buffer, leading to interferences in the obtained complex spectra.

Based on those observations, we hypothesized that the + 50 Da adducts observed upon protein's functionalization might not result from cross-linking but more likely from pyrrole functionalization of the protein. Hence the observed tra-I1 adduct (Figure 43) might preferentially undergo a dehydration leading to its aromatization rather than the addition of 3-oxoglutaric acid. We thus evaluated if the addition of a 10-fold excess of 3-oxoglutaric acid in comparison with succinaldehyde might lead to a favoured formation of tropinone, but only the formation of the + 50 Da adduct was observed (Table 2). We then developed conditions leading to a controlled distribution of those adducts on native trastuzumab (Figure 45). For instance, we found that trastuzumab's incubation with 5 equiv. of succinaldehyde **1** in

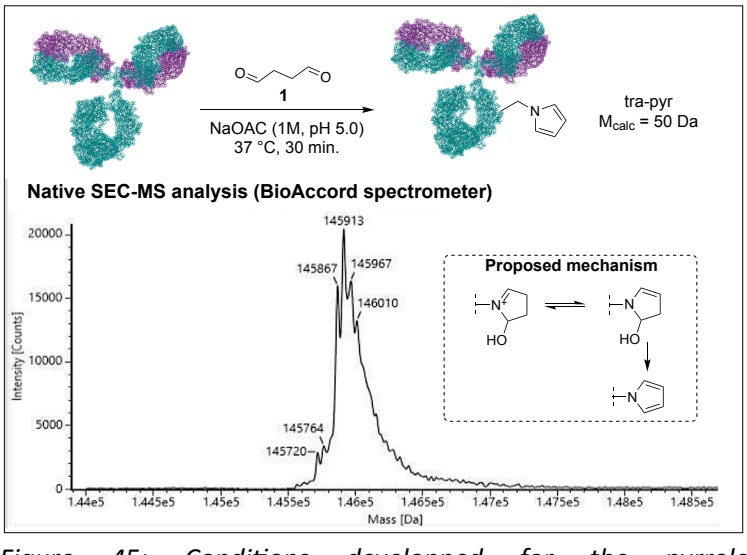

Figure 45: Conditions developped for the pyrrole functionalization of trastuzumab.

NaOAc buffer pH 5.0 for 30 minutes led to homogeneous pyrrole distribution. The formation of such pyrrole lysine adducts in presence of succinaldehyde was reported in 2014 as a naturally occurring modification involved in the production of DNA mimic proteins triggering an autoimmune response, making them interesting for therapeutic application.[172]

In summary, we evaluated whether the Robinson-Schöpf reaction could be used for the labelling of proteins. We found that, in the tested conditions, many adducts were formed on the protein without clear understanding of their formation mechanism. In an optimization attempt we found that, even on simpler models such as isolated amino acids or small peptide the reaction is in competition with the formation of a pyrrole adduct. Deeper mechanistic study might allow better comprehension and thus the development of conditions allowing to favour the MCR conjugation. As Ugi 4-CR were largely described for the conjugation of proteins we decided to turn back to this reaction and more precisely to the Ugi-4C-3CR variant of the reaction.

III. Ugi 4C-3CR for site-selective conjugation of native proteins

III.1. Preliminary results

Our team proposed in 2020 that the Ugi reaction could be used to modify trastuzumab.[119] The idea was to use trastuzumab as the source of both the carboxylic acid and the amine components, in the form of its constitutive aspartate/glutamate and lysine residues, respectively. It was thus hypothesized that the addition of an aldehyde and an isocyanide to the antibody solution would lead to an "inter-residue" conjugation through a U-4C-3CR, whose mechanism is described in Figure 34. As solvent accessibility and close spatial proximity between the two reactive residues should be key parameters for a successful reaction, the number of potential reactive sites should be limited, thus maximizing our chances of developing a site-selective reaction.

Over the course of the optimization procedure spearheaded by Dr Charlotte Sornay, our team determined some key parameters influencing the modification of trastuzumab using the Ugi reaction. For instance, optimal results were obtained with 45 equivalents of reagents and equimolar quantities of isocyanide and aldehyde – the latter being the preferred source of carbonyls over ketones. The reagents' structure also had a great impact on both the conversion and the observed av. DoC, especially the aldehyde, with conversions ranging from 0 to 97% (av. DoC = 4.0). Slight influence of the temperature was also observed, as heating up to 37 °C largely increased the conversion, whereas little or no reaction was observed at 4 °C. On the other hand, pH and buffer composition seemed to have no impact on the protein's conjugation. Overall, the resulting conjugates were found to be stable to pH variations in PBS and in human plasma, underlining the potential of the method.

Based on those results, optimal conditions — 45 equivalents of carbonyl **6** and isocyanide **a** in PBS (1x, pH 7.5) at 25 °C for 16 hours — leading to an average degree of conjugation (av. DoC) around 0.9 with a medium conversion of 57 % were developed following a "plug-and-play" strategy. The Ugi reaction (the "plug" step) would be used to label the antibody with an azide group – borne by the carbonyl component **6** (Figure 46) – that could be selectively modified in a second step (the "play" step) with virtually any payload bearing a strained alkyne, via a reaction coined strain-promoted azide-alkyne cycloaddition (SPAAC). Fluorophores (sulfo-cyanine-5 (Cy5) and TAMRA), affinity tags (iminobiotin), other biomolecules (oligonucleotides) and a cytotoxic agent (MMAE) were thus successfully introduced on the mAb following this strategy. In the latter case, the IC_{50} of the resulting ADC was found to be comparable to that of the benchmark Kadcyla.

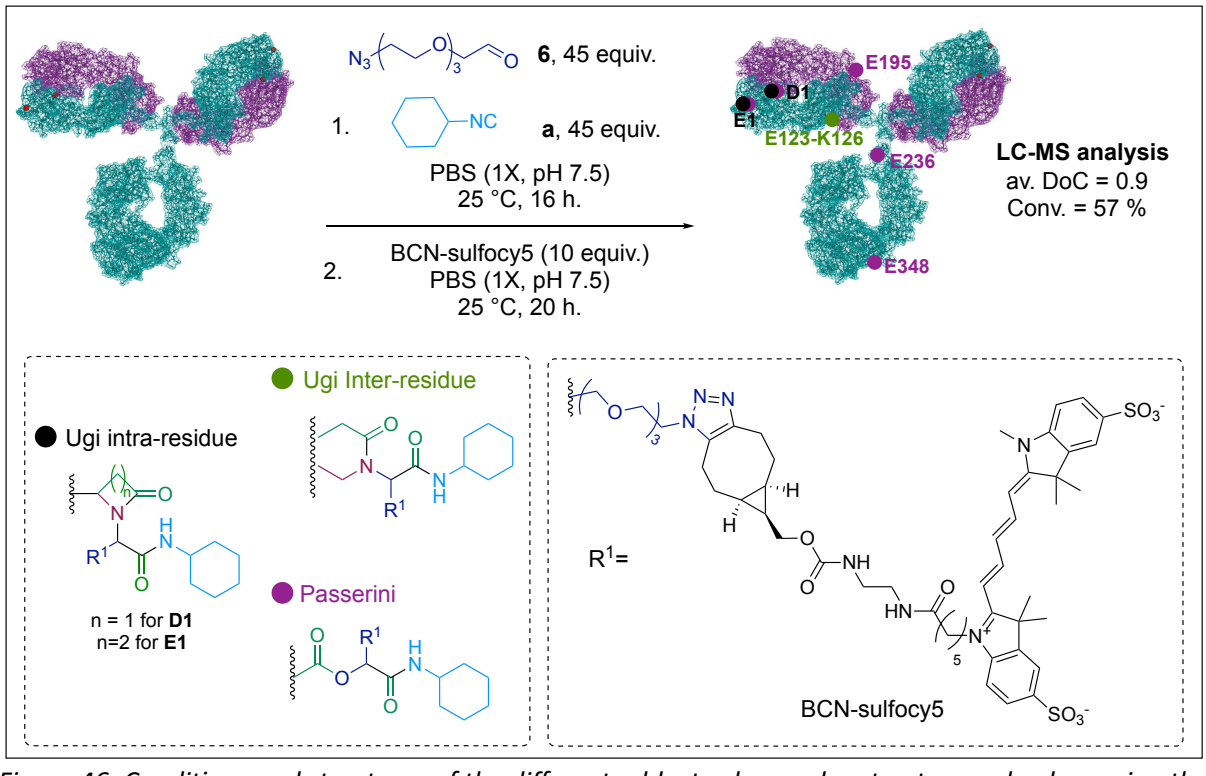

Figure 46: Conditions and structures of the different adducts observed on trastuzumab when using the "optimal" Ugi conditions published in 2020. Conv. and av. DoC were determined by LC-MS analysis and modification sites as well as the modification mechanism were determined by LC-MS/MS.

To gain further insights into the mechanism responsible for the observed conjugation, a handful of conjugates were analysed by LC-MS/MS in order to determine the identity of the modification sites. They found that only one site had been modified via the expected Ugi "inter-residue" mechanism (K126 and E123), in competition with an "intra-residue" Ugi modification, occurring on the *N*-terminal aspartate and glutamate residues (E1 and D1). In this latter case, the amine source corresponds to the α-amine group instead of the ε-amine of a lysine residue, leading to β- and γ-lactams adducts, respectively. These Ugi conjugates were accompanied with the modification of three glutamate residues – E195, E236, and E348 – via a side Passerini reaction (Figure 46). Building on these positive results, we next engaged in an in-depth LC/MS-MS mechanistic study of this transformation, to try to decipher the rules governing the reactivity at the surface of the protein, with the final intent of developing conditions that would favour a single multicomponent reaction conjugation over the three detected.

III.2. Variation of the carbonyl electrophile

We first wondered whether a mechanistic control could be possible by playing on the carbonyl source. We had previously identified that aldehydes were better substrates than ketones, but we wondered whether pre-formed imines could tame the carbonyl reactivity and diminish the number of potential reactive sites. However, considering the poor stability of imines in aqueous media, we decided to investigate instead the use of the more stable α-chlorooximes and hydrazones.

III.2.a. α-Chlorooximes

α-Chlorooximes are known to generate highly electrophilic nitrile *N*-oxide species in aqueous media, which are known to react with carboxylic acid and isocyanides via a Passerini-like mechanism yielding *syn*-α-oxiaminoamides adducts **R183** (Figure 47).[173] Still in the presence of isocyanides, they were also reported to react with other nucleophilic species, such as primary and secondary amines — yielding *C*-oximinoamidines **R184** —, phenols — yielding aryloxyimino amides **R185** — and even water in the absence of a more reactive nucleophile – yielding α-oxiaminoamides **R186**.[174–177]

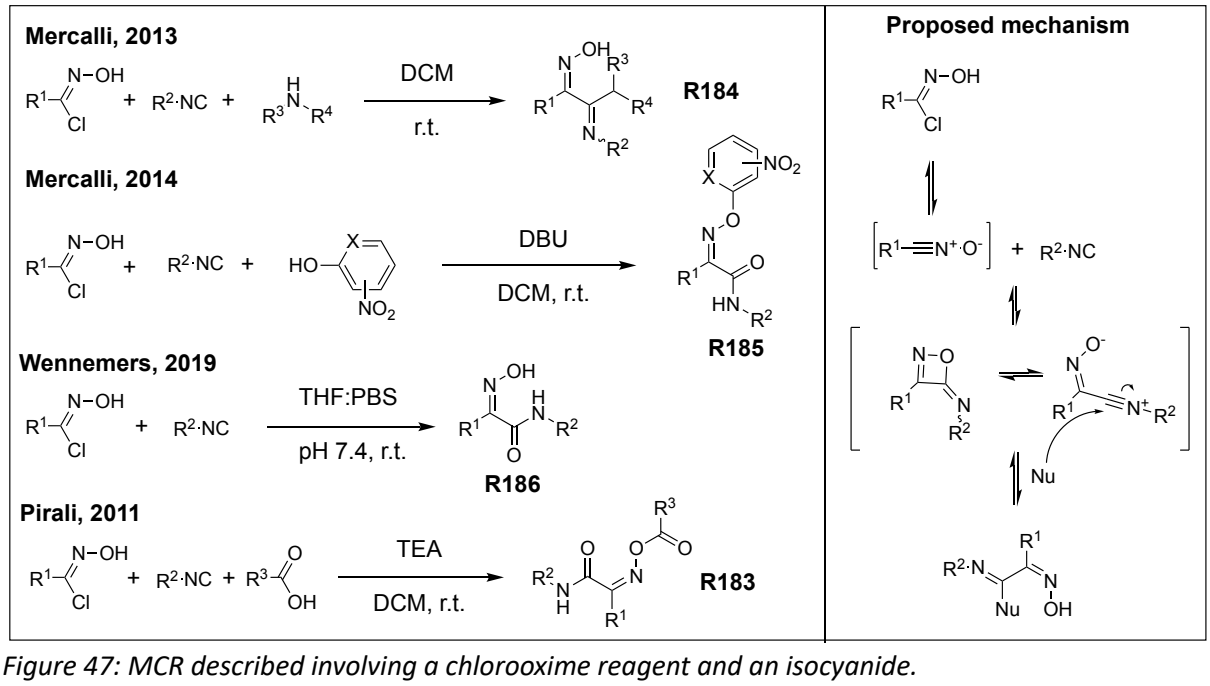

Figure 47: MCR described involving a chlorooxime reagent and an isocyanide.

Because we had observed the formation of Passerini adducts on trastuzumab, we reasoned that the use of α-chlorooxime in the presence of an isocyanide and trastuzumab might favour a similar single-residue conjugation, following the reactivity described by Pirali *et al*. in 2011 (Figure 47).[173]

We started this project with the synthesis of α-chlorooxime **8** from aldehyde **6** in two steps, following reported procedures and we evaluated its reactivity towards trastuzumab under the "optimal" Ugi conditions previously reported in the group (Table 3).[119,177] This led to a highly

heterogeneous profile and poorly resolved peaks by native LC-MS analysis, suggesting multiple modifications. Interestingly, a control experiment showed that the conjugation did not require the isocyanide to happen, thus indicating another mechanism than the ones reported in figure 20. Interestingly, acceptable av. DoC and conversion (av. DoC = 0.9 and conv. = 59%) were obtained after only 2 hours of reaction, using 5 equivalents of reagent **8** at 4 °C and followed by a SPAAC reaction with BCN-Cy5 (Table 3). Native LC-MS analysis of the protein suggested that a simple addition-elimination between **8** and trastuzumab had happened, consistent with the detected mass of the payload (i.e. 1089 Da), leading to conjugate **C1** (table 3).

*Table 3: Synthesis of oxime **7** and α-chlorooxime **8**. Reaction condition for the labeling of trastuzumab. Conv. and av. DoC were determined by LC-MS analysis on the LCT spectrometer.*

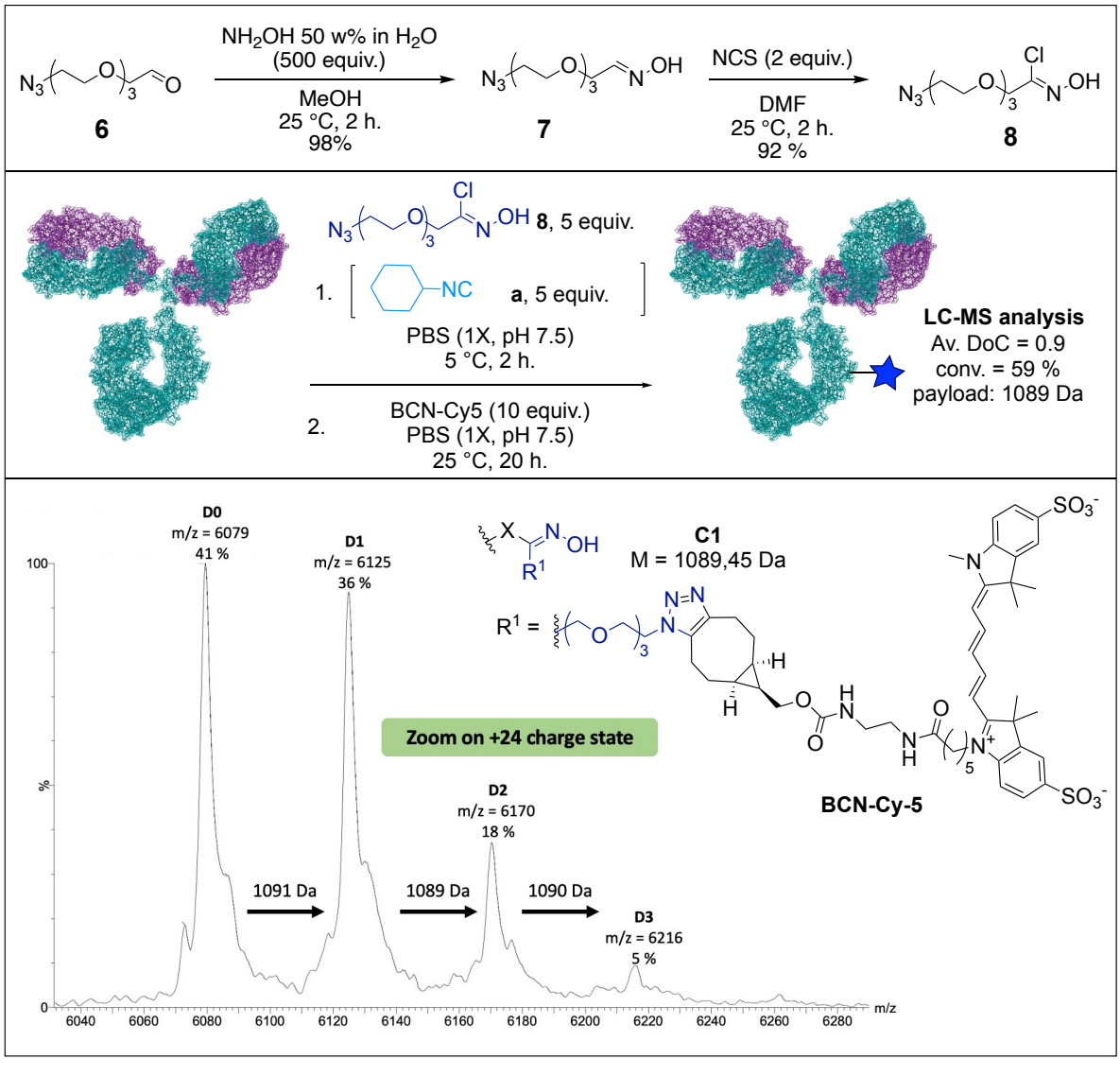

.

In order to identify the modified residues, competition experiments were set up with the addition of different *N*-terminally and *C*-terminally protected amino acids—Ac-aa-NHMe — to the reaction mixture, to evaluate if they might be responsible for the modification of trastuzumab.

An excess (50 equiv.) of the chosen amino acids — i.e., lysine (Lys), tyrosine (Tyr), histidine (His), glycine (Gly), aspartate (Asp) and glutamate (Glu) — was introduced in the reaction medium at the same time as the α-chlorooxime **8**, and the reaction was carried out under the same conditions as mentioned before (Table 3). The av. DoC was then estimated by absorbance measurement after introduction of the Cy5 dye and compared to the ones obtained without competitor (Figure 48). It was expected that if the added amino acid's side chain reacted with the α-chlorooxime reagent, the fluorescent DoC post purification would be lower than that of the control experiment; on the contrary, if the added amino acid was unreactive toward the α-chlorooxime, the fluorescent DoC should not be impaired. The results presented in Figure 48 indicate that among the tested amino acids, Asp, Glu and His seemed to react preferentially with the α-chlorooxime but not Lys or Tyr. This suggests that, in our conjugation conditions, the modified residues are mostly Asp, Glu or His residues. In order to confirm this reactivity profile, a UV-visible analogue of α-chlorooxime **8** was synthesized using CuAAC reaction with ethynylbenzene and the resulting α-chlorooxime **9** was reacted with the same protected amino acids in water (Figure 49). LC/MS analysis led to systematic observation of nitril oxide **10**, and absence of chlorooxime 9 suggesting it is form very quickly**.** The results were analysed by LC/MS and we were surprised to see that only Ac-Lys-NHMe and Ac-His-NHMe — yielding structure **11** and **12**, respectively — reacted and neither Ac-Asp-NHMe nor Ac-Glu-NHMe, even after a 24-hour incubation at 25 °C, in apparent contradiction with what had been observed previously on trastuzumab. Given the absence of buffering salt in the reaction medium, this result might however be due to an acidification of the mixture preventing the carboxylic acid to behave as nucleophiles. The reactivity observed with His fits with the results of the competition experiment (Figure 48). The

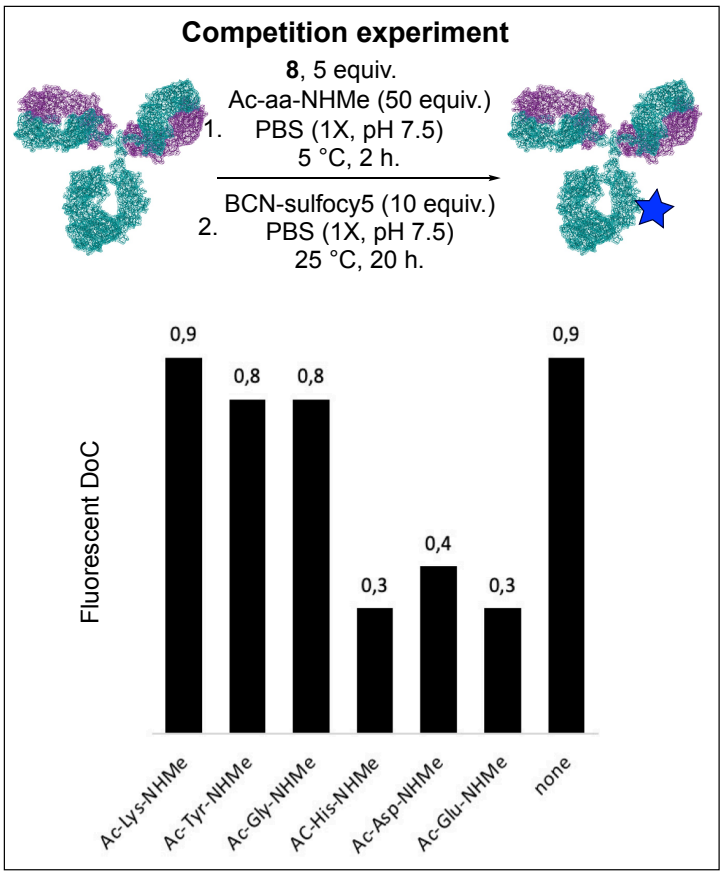

Figure 48: Competition experiment for identification of 8 preferential modification residue.

observed Lysine reactivity might come from the high concentration in amino acid used for this experiment which is differs from the diluted conditions used for the competition experiment.

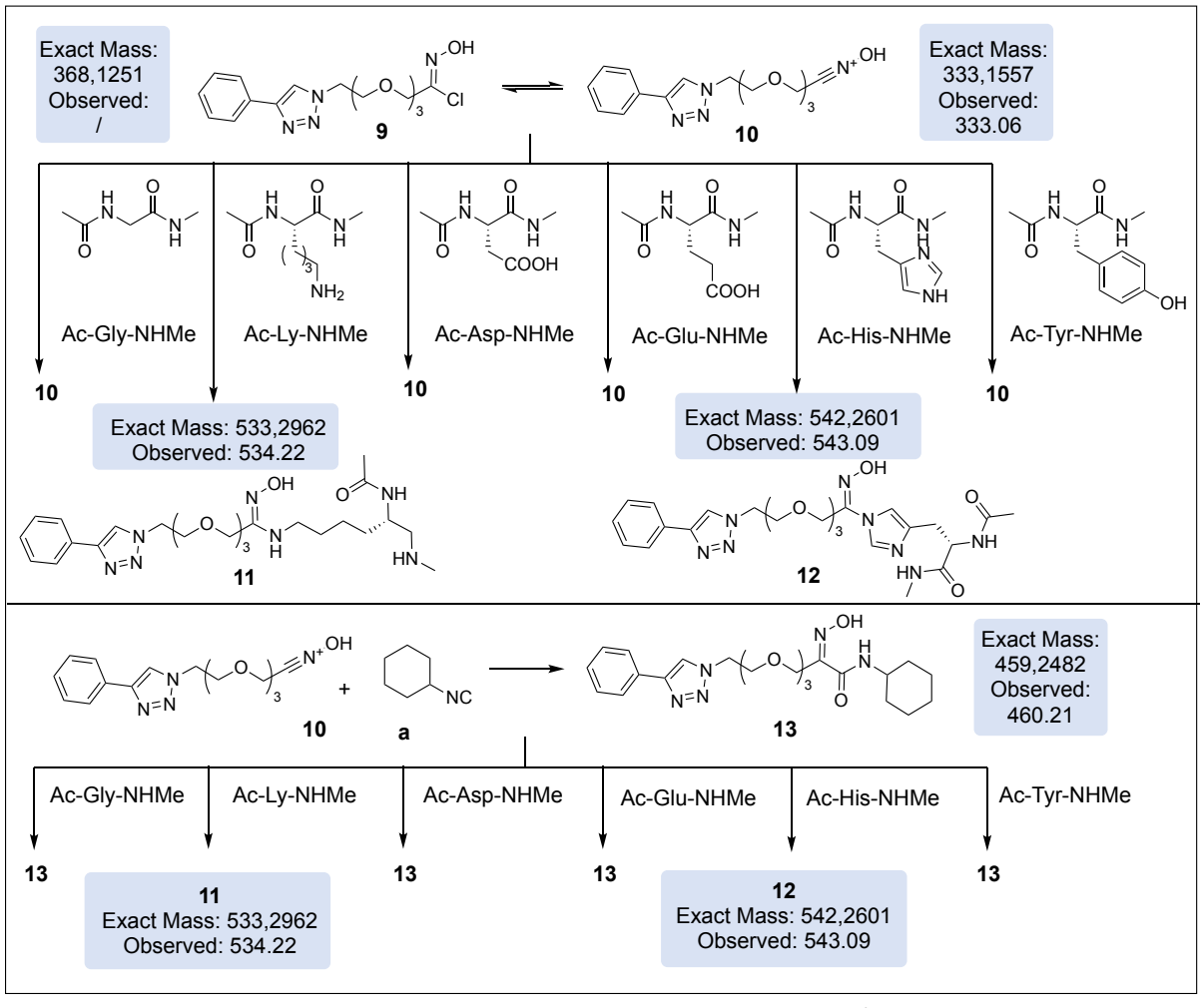

*Figure 49: LC-MS analysis of chlorooxime **8** reactivity with different N-ter/C-ter protected amino acids.*

Given this disparity in reactivity between isolated amino acids and protein, we conducted the same experiment in the presence of cyclohexyl isocyanide **a** to evaluate if the reactivity presented Figure 47 could happen with isolated amino acids (Figure 49). The same adducts **11** and **12** resulting from nucleophilic addition of Ac-Lys-NHMe and Ac-His-NHMe on **10** were observed as the sole products by LC-MS analysis suggesting full conversions. For all the other amino acids — i.e., Asp, Glu, Tyr, and Gly —, isocyanide **a** addition to nitrile oxide **10** leading exclusively to the adduct **13** was observed, as reported by Wennemers.[177] This suggests that the nucleophilic addition of Ac-Lys-NHMe and Ac-His-NHMe on α-chlorooxime **9** is faster than the addition of the isocyanide at 25 °C ($k > 0.74\ M^{-1}s^{-1}$), but also that the reaction between isocyanides and α-chlorooximes is technically not bioorthogonal.

To conclude, we evaluated the use of α-chlorooxime as potential Passerini partners for the labelling of aspartate and glutamates of trastuzumab. We found that another faster reaction — which does not necessitate the presence of an isocyanide to happen — was happening stably, leading to good conv. of 59 % and av. DoC of 0.9. The mass of the obtained products suggests the nucleophilic addition of a residues directly on the chlorooxime (vide supra). Competition

experiment showed that this amino acid might be either a histidine residue or an aspartate or glutamate residue. Reactivity on isolated amino acids was evaluated and we found that the nucleophilic addition of His and Lys on **9** was faster than the previously reported addition of isocyanide and water (vide supra). Considering the acidity of the media, no conclusion could made concerning the reactivity of Asp and Glu in those conditions. In depth mechanistic study will be conducted in order to validate thus assumption.

Considering the high reactivity observed for α-chlorooxime, we decided to turn toward less reactive species for the labelling of trastuzumab through Passerini-like mechanism.

We thus replaced the aldehyde **6** by the oxime **7** (Table 3) in the Ugi "optimal" conditions but no labelling of the mAb could be observed suggesting a lack of reactivity of **7**. Hence, we turned our attention to structurally related hydrazone derivatives.

III.2.b. Hydrazones

We decided to generate a different imine-like compound by reacting aldehyde **6** with methyl hydrazine, yielding hydrazone **14** (Scheme 7). Given that no MCR reports the use of hydrazones, we wondered through which mechanism the reaction could proceed – if ever it did. Among the possibilities, an Ugi-like mechanism was considered with one of the two nitrogens of the hydrazone being involved in the irreversible Mumm rearrangement step, leading to compound **C1** (M = 1213,6 Da).

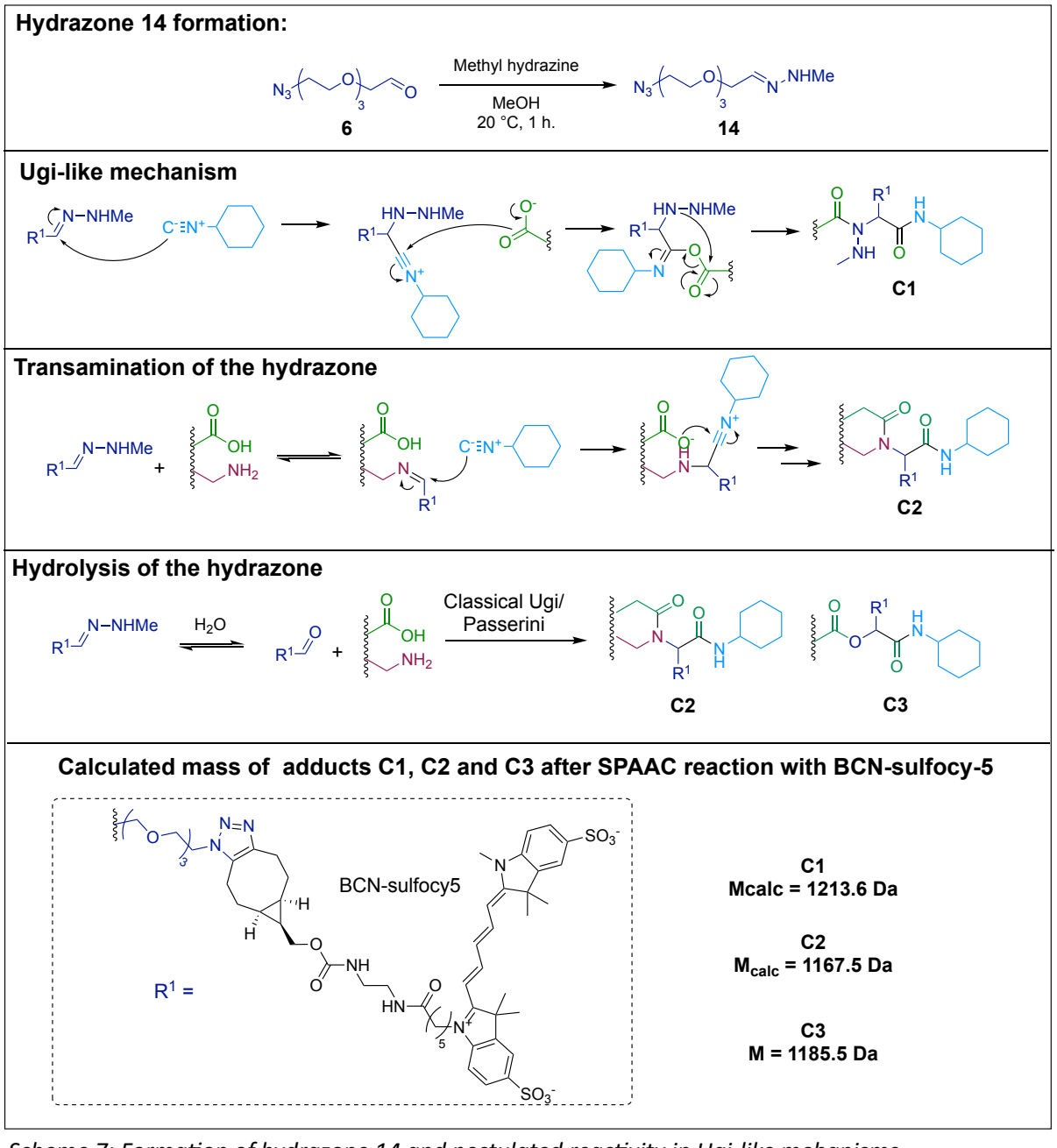

Scheme 7: Formation of hydrazone 14 and postulated reactivity in Ugi-like mehanisms.

A second potential mechanism could be the transamination of hydrazone **14** with either α- or ε-amines from trastuzumab, followed by a Ugi mechanism leading to payload **C2** (M = 1167.5 Da) or a hydrolysis, liberating the parent aldehyde in the medium. A third and final hypothesis implied the hydrolysis of the hydrazine and the in-situ formation of the parent

aldehyde prior to its conjugation leading to Ugi/Passerini reactions with a mixture of compound **C2** and **C3** (M = 1167,5 Da and M = 1185,5 Da respectively) (Scheme 7).

Surprisingly, considering the structural similarities with oxime **7**, partial labelling of trastuzumab was obtained using hydrazone **14** instead of aldehyde **6** under our classical Ugi conditions (43% conv., av. DoC 0.5) (Table 4). More importantly, we validated that the isocyanide was essential for the reaction to happen, thus confirming the multicomponent character of the reaction. Considering the limited efficiency of the transformation, a small optimization was conducted. We found that by increasing the quantity of used reagent (from 45 to 100 equivalents) and prolonging the reaction time from 16 h to 20 h, similar av. DoC as the ones observed with our classical Ugi conditions were obtained (i.e., av. DoC 0.9); those conditions, coined 'hydrazone conditions' were then used for the rest of the study (Table 4). The mass of the obtained payloads seems to validate the transamination mechanism; however, considering the resolution of the used spectrometer and the low difference in molecular weights between payloads, deeper mechanistic study was performed.

Table 4: Hydrazone conditions developed for the labeling of native trastuzumab. Conv. and av. DoC were measured by LC-MS analysis. Zoom on z = 24 spectra are presented.

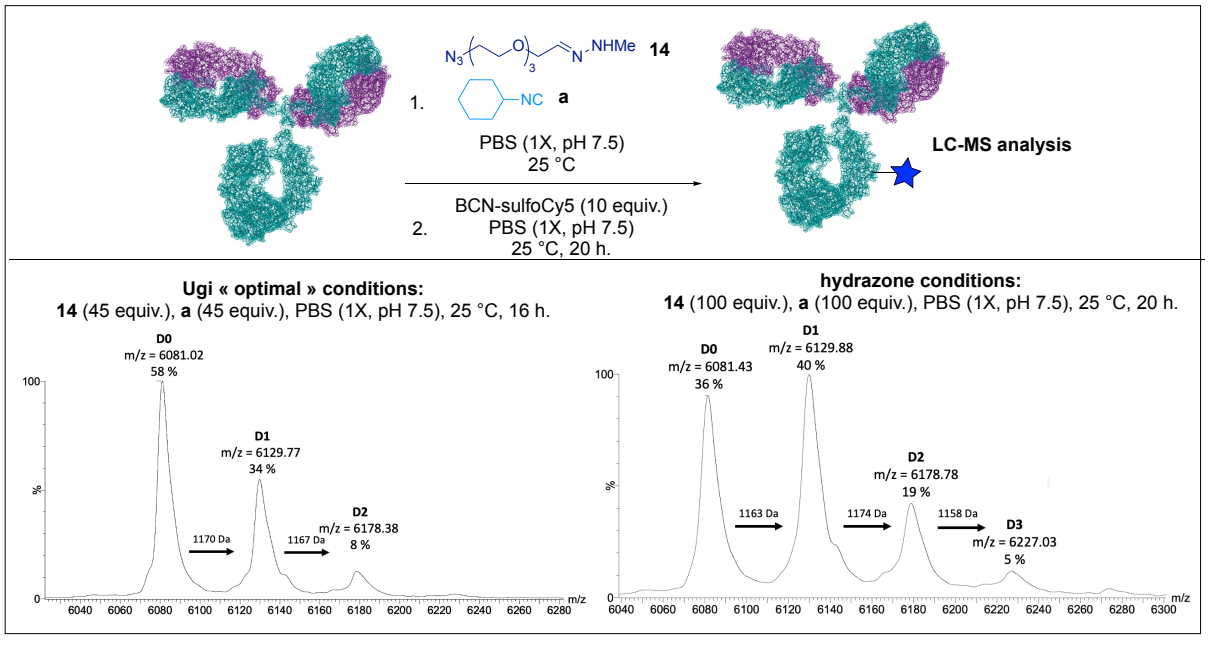

We continued the investigation by exploring the influence of the isocyanide and hydrazone side chains. First hydrazones **15**, **16** and **17** were synthesized and their reactivity in our hydrazone conditions was evaluated (Table 5). In the case of **15**, similar reactivity as **14** was observed — conv. = 69 %, av. DoC = 1, $M_{payload}$ = 1 175 Da). The use of **16** and **17** led to an absence of conjugation, supporting the transamination hypothesis. Indeed, the hydrophobic substituent of **16** and **17** might prevent spatial proximity between the hydrazone and the surface of the protein but should not prevent hydrolysis.

Influence of the isocyanide's side chain was also evaluated using isocyanides **b**, **c** and **d** (Table 5). Those isocyanides were already screened during the development of the Ugi optimal conditions and low to no variations in the reactions' conv. and av. DoC were observed in this case. In our case, replacement of **a** by **b** and **c** led to low obtained conversions and av. DoC suggesting this lack of reactivity is strongly linked to the replacement of aldehyde **6** with hydrazone **14**. This result shows that the transamination mechanism must be the main conjugation mechanism as, in the case of hydrazone's hydrolysis similar results as the one obtained using aldehyde **6** should be reached. The low observed reactivity might come from the presence of a small portion of hydrolysed hydrazone in the reaction medium but it also points out that maybe, those two isocyanides favour a Passerini mechanism over an Ugi one. Indeed, if they had no influence the transamination mechanism should not impact their conjugation.

Table 5: Influence of the variation of the hydrazone's and isocyanide's side chain on the conjugation efficiency.

Hydrazone	isocyanide	Conv. (%)	Av. DoC	M_{obs} (Da)	M_{calc} (Da)
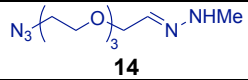 **14**	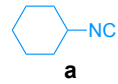 **a**	69	0.9	1165	1167.5
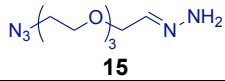 **15**		61	1.0	1174	1167.5
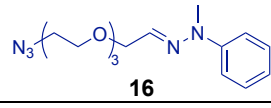 **16**		/	/	/	1167.5
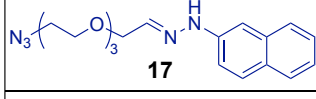 **17**		/	/	/	1167.5
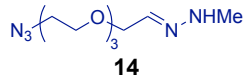 **14**	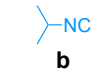 **b**	19	0.2	1131	1127.5
	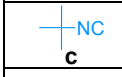 **c**	20	0.2	1143	1141.5
	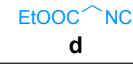 **d**	47	0.6	1154	1171.5

On a different note, considering the yields obtained after the SPAAC reaction (60% on average) due to the precipitation of high DoC species functionalized with the highly hydrophobic BCN-Cy5, we analyzed an unclicked sample and a clicked one from the same batch. In the case of the unclicked sample, conversion was found to be 72% with an av. DoC of 1.3 versus 57% and 0.8 for the clicked sample.

In summary, we showed that hydrazones can be used as carbonyl source for the labelling of trastuzumab through a Ugi 4C-3CR reaction. The introduced hydrazone seems to undergo a transamination step with available ε- or α-amines from the protein leading to the formation of desired Ugi adducts however this reaction might be in competition with hydrolysis of the hydrazone. Overall, peptide mapping experiment should be performed in order to validate the

exact structure of the adducts as well as precise determination of the modification sites. This should be performed using 45 and 100 equivalents of reagent to validate if the observed decrease in conversion and av. DoC is due to a gain in selectivity and if this selectivity is conserved upon "stronger" reaction conditions. The reaction displayed low observed DoCs and conv. upon variation of the side chain of the used isocyanide in comparison with the Ugi conditions developed in the preliminary results. This might also be related to a favoured Passerini mechanism influenced by the isocyanide's side chain in the case of isocyanide **b** and **c**. Such influence of the side chain of the used reagent on the modification mechanism was not studied in the preliminary results as it requires nontrivial peptide mapping analysis. We thus decided to conduct an in-depth mechanistic study of the Ugi 4C-3CR for the labelling of trastuzumab, because of all the knowledge accumulated during the development of the Ugi 'optimal' conditions we first decided to go back to those original conditions, using an aldehyde as carbonyl source.

III.3. Variation of the reagents' side chains

The two Ugi mechanisms — i.e., intra- and inter- residue — result in the same mass of the payload and only differ in the modification site, and because the Passerini mechanism only leads to a difference of +18 Da in the mass of the final payload, native LC-MS analysis of the conjugated proteins often gives a mass in between the two theorical masses, due to a coexistence of the two modifications, combined to a lack of sensitivity of the used spectrometer thus preventing us to distinguish between the three mechanisms. In order to differentiate them, peptide mapping analysis of the conjugates was performed. This technique relies on the digestion of the protein into small peptides using trypsin and their subsequent analysis by LC-MS/MS. Masses of the fragmented peptides are then compared to those obtained after digestion of the unconjugated protein allowing to identify the localization and structure of the modification.

III.3.a. Mechanistic comprehension of the "optimal" Ugi conditions

First, we decided to switch the SPAAC reagent from BCN-Cy5 to BCN-iminobiotin to minimize precipitation, as observed in the case of hydrazones (*vide supra*). We thus incubated 45 equivalents of aldehyde **6** and isocyanide **a** in the Ugi optimal conditions — i.e., 16 hours at 25 °C in PBS (1X, pH 7.5) — the resulting azido-labelled trastuzumab (**tra-N_3**) was then functionalized by SPAAC using 30 equiv. of BCN-imminibiotin to yield **tra-biot**. Moreover, we seized the opportunity of this large peptide mapping campaign to evaluate the reproducibility and repeatability of the method. In order to do so, three experimenters — Dr. Charlotte Sornay (CS), Ilias Koutsopetras (IK) and Valentine Vaur (VV) — conducted the same experiments (N = number of analysed samples) and the obtained results were compared.

Results, summed up in table 6, showed indeed a variation in observed conv. and DoCs depending on the used strained alkyne — 59% and av. DoC 0.9 for BCN-Cy5 (CS, N = 1) versus 72% and av. DoC 1.3 for BCN-iminobiotin (CS: N = 1, IK: N = 3 and VV: N = 2). Among the six samples, one (CS) really stood out from the others, presenting higher conv. and av. DoC — 86% and 1.8 — while the others (IK and VV) presented low variations in obtained conv. and av. DoC with standard deviation (σ) of 5.3 and 0.2, respectively. If those results tend to indicate good reproducibility of the reaction, we really wanted to evaluate the regio-selectivity of the method, hence focus was made on the modification sites.

Table 6: Peptide mapping analysis of the Ugi "optimal" conditions used for the labeling of trastuzumab. Conv. and av. DoC were determined by LC-MS analysis and modification sites and mechanism were determined by LC-MS/MS.

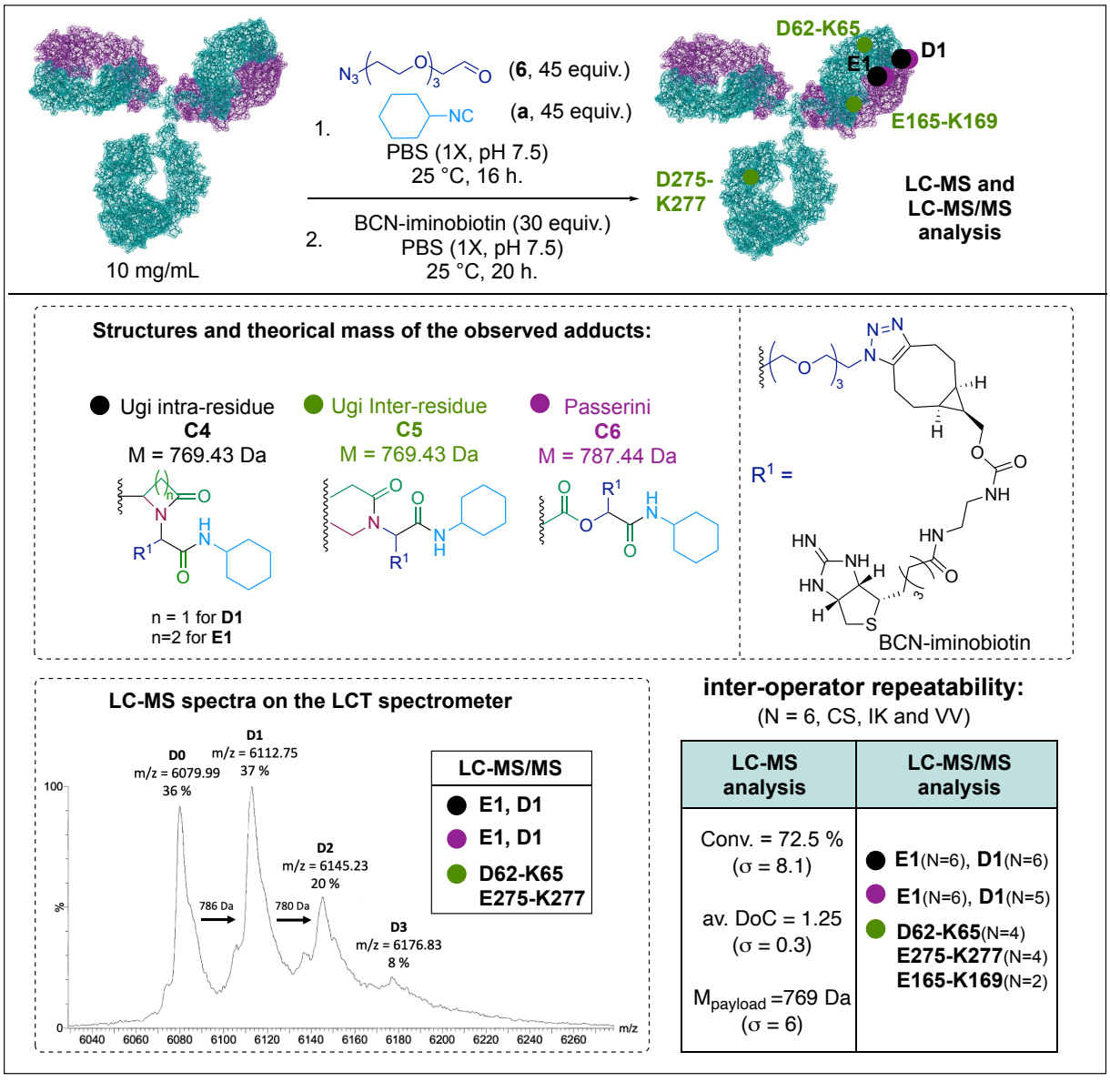

The intra-residue Ugi modification **C4** of E1 and D1 residues — i.e., *N*-terminal modifications — was observed in all samples (N = 6), along with the inter-residue Ugi modification **C5** between D62-K65 (N = 4), E275-K277 (N = 4) and E165-K169 (N = 2) among the different batches (Table 6).

The Passerini modification **C6** of E1 was observed in all analysed samples (N = 6), along with D1 modification (N = 5). This indicates that the preferred modification sites, observed in all the samples, are E1 and D1 residues — modified through intra-residue Ugi and Passerini mechanisms — and that inter-residue modifications are less represented, with an apparent preference for D62-K65 and E275-K277 over E165-K169 .

In order to understand if those preferred sites could be selected based on kinetic control of the reaction — or if they are just less abundant, resulting in low detection during LC-MS/MS analysis —, a time course study was conducted (Table 7). [1] Variation of the reaction time from 1 h to 16 h indicated rapid progression of the reaction during the first 4 hours (with variations of conv. and av. DoC) and slower progression afterwards, with a plateau observed after 8 hours. Interestingly, during the fast progression phase, exclusive *N*-terminal modification is observed and it is only after the plateau is reached — that can be correlated with an observed av. DoC ≥ 1 — that other modification sites are detected, in good agreement with the previously presented results. Regarding the modification mechanism, both intra-residue Ugi and Passerini mechanisms seems to happen at the same time, thus preventing a kinetic control of the reaction mechanism.

Table 7: Time course study of the Ugi reaction in the optimal conditions.

Time (h.)	1	2	4	8	16
conv. (%)	11	28	62	78	86
av. DoC	0.1	0.3	0.9	1.4	1.8
Modification sites	● **E1/D1** ● **E1**	● **E1/D1** ● **E1**	● **E1/D1** ● **E1/D1**	● **E1/D1** ● **E1/D1** ● **E275-K277** **E165-K169**	● **E1/D1** ● **E1/D1/E236** ● **E165-K169**

a (45 equiv.), **6** (45 equiv.), PBS (1X, pH 7.5), 25 °C

Because the pK_a of ε-amines differs from that of α-amines — i.e., 10.5 and 7.7,[178] respectively — we expected that varying the pH could orient the selectivity toward *N*-termini conjugation or inter-residue conjugation (Table 8).[2] No influence of the pH variation — from 5.5 to 8.5 — was

Table 8: Influence of the variation of the pH for the labelling of trastuzumab in the Ugi optimal

PBS pH	5.5	6.5	7.5	8.5
conv. (%)	65	58	65	66
av. DoC	1.0	0.9	1.0	1.0
Modification sites	● **E1/D1** ● **E1**	● **E1/D1** ● **E1**	● **E1/D1** ● **E1**	● **E1/D1** ● **E1**

a (45 equiv.), **6** (45 equiv.), PBS (1X), 25 °C, 16 h.

[1] Conducted by Dr Charlotte Sornay
[2] Conducted by Ilias Koutsopetras

observed on either the conversion or the av. DoC, with only *N*-terminal conjugation being detected. However, those results tend to confirm our assumption that *N*-terminal selectivity is observed when av. DoC □ 1 are obtained. While site-selective in essence, this modification was still the consequence of two competing MCRs, the Ugi and the Passerini reactions, and we decided to explore the mechanism further by an in-depth study of the influence of the reagent's structure on the mechanism of the reaction.

III.3.b. Reagents variation

Based on the initial results reported in 2020, we knew that the greatest variations in conv. and av. DoC were observed upon variation of the aldehyde and isocyanide reagents and assumed these could be directly linked to variations in conjugation sites and mechanisms. Hence, we evaluated the influence of several aldehydes and isocyanides' side chains on the modification site (Table 9).

Table 9: Peptide mapping analysis of the influence of the variation of the aldehyde and of the isocyanide side chains on the labeling of trastuzumab. Conv. and av. DoC were determined by LC-MS analysis and modification sites and mechanism were determined

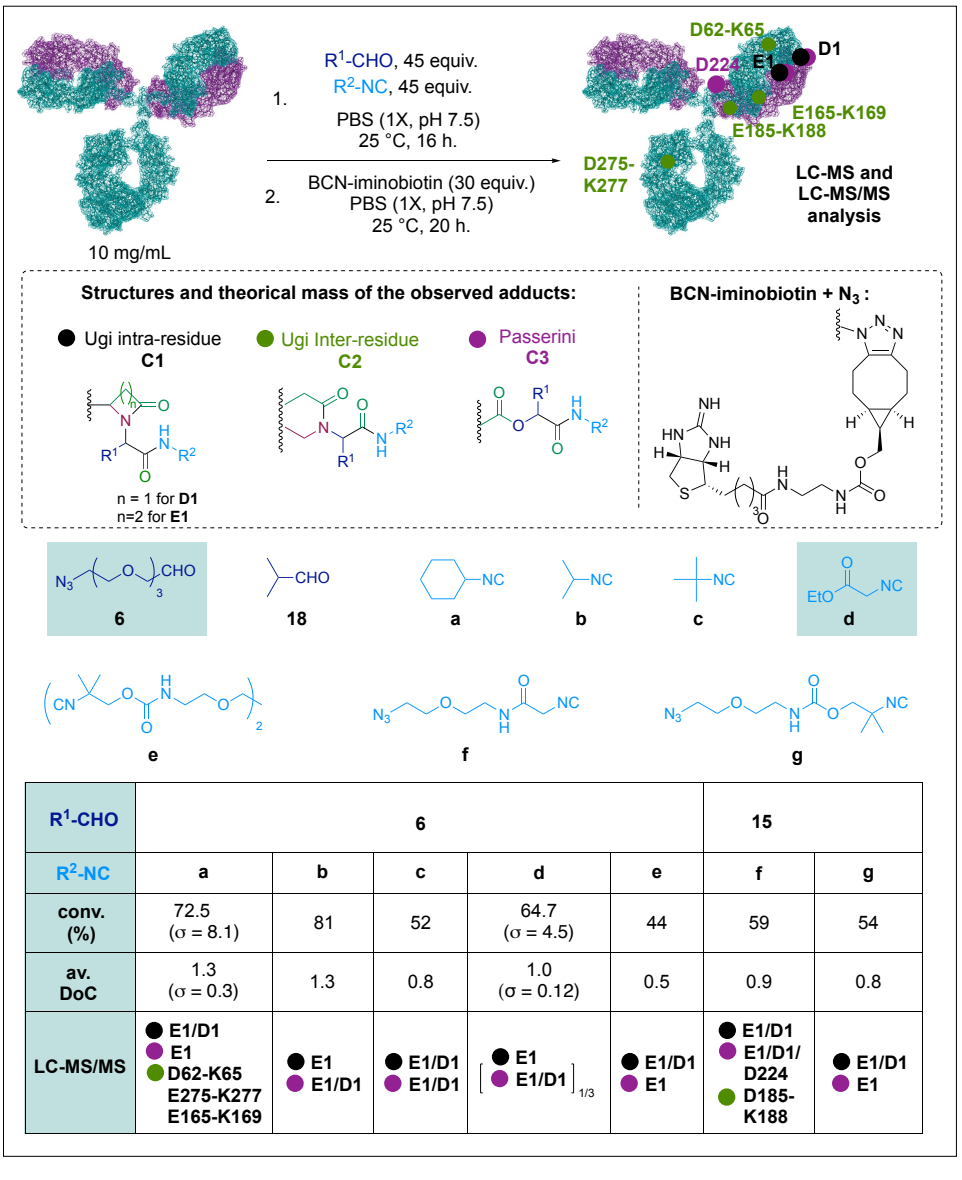

R1-CHO	6					15	
R2-NC	a	b	c	d	e	f	g
conv. (%)	72.5 (σ = 8.1)	81	52	64.7 (σ = 4.5)	44	59	54
av. DoC	1.3 (σ = 0.3)	1.3	0.8	1.0 (σ = 0.12)	0.5	0.9	0.8
LC-MS/MS	● E1/D1 ● E1 ● D62-K65 E275-K277 E165-K169	● E1 ● E1/D1	● E1/D1 ● E1/D1	● E1 ● E1/D1 1/3	● E1/D1 ● E1	● E1/D1 ● E1/D1/ D224 ● D185-K188	● E1/D1 ● E1

When choosing the reagents, we took special care to keep not only the plug and play approach possible, meaning that either the aldehyde or the isocyanide had to bear an azide group, but also a facile access to the reagents, either purchased or obtained after few synthetic steps. LC-MS/MS analysis of the different obtained conjugates, summarized in table 9, confirmed the trend observed earlier with E1 and D1 being the most detected modification sites through both intra-residue Ugi and Passerini mechanisms. Interestingly, in the case of aldehyde **18** and isocyanide **f**, unprecedented inter-residue Ugi sites were detected, confirming that modification sites can indeed be affected by the reagents' structures.

The combination of aldehyde **6** and ethyl-isocyanoacetate **d** under our optimal conditions — 45 equiv., PBS (1X, pH 5.0), 25 °C, 16 h. — held our attention, as single residue (E1) modification was reached in half of the samples analysed by LC-MS/MS, thus narrowing down the number of reactive sites to only two (Table 10). Even more remarkably those samples presented an absence of Passerini modification allowing to coin the method 'mechanism selective'. We noted that such degree of selectivity seemed linkd to av. DoC ≤ 1 suggesting similar behaviour as the one observed for the couple **6**+**a**. In the other samples (IK1 and IK2), the modification of E1 and D1 through Passerini mechanism was also detected suggesting that, even when the plateau is reached, *N*-ter selectivity is conserved.

Table 10: Peptide mapping analysis of the influence of the variation of the concentration, time and temperature on the labeling trastuzumab using "E1-selective" conditions. Conv. and av. DoC were determined by LC-MS analysis and modification sites and mechanism were determined by LC-MS/MS.

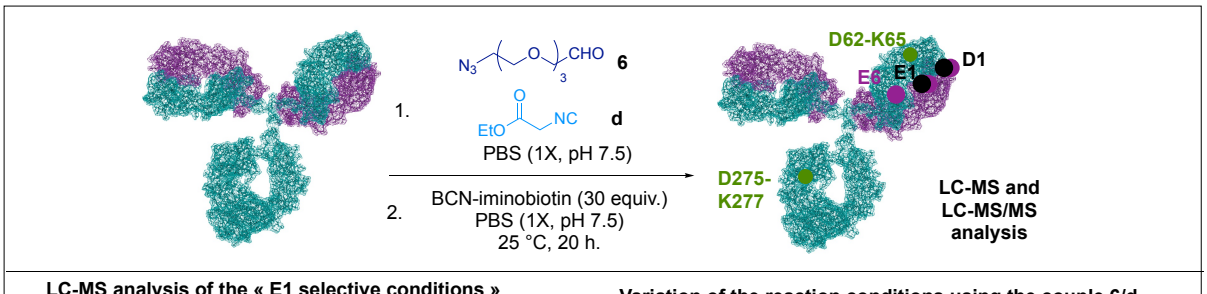

LC-MS analysis of the « E1 selective conditions »
6 (45 equiv.), **d** (45 equiv.), PBS (1X, pH 7.5), 25 °C, 16 h.

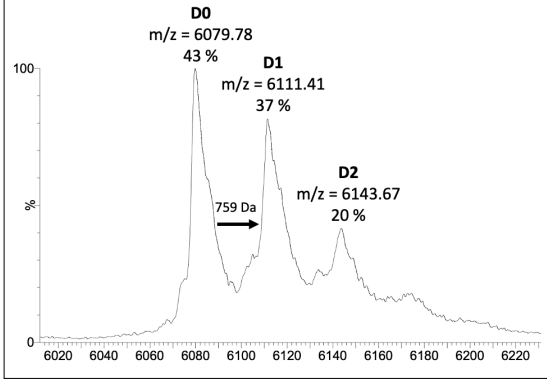

Variation of the reaction conditions using the couple 6/d

[mAb] (mg/mL)	equiv. CHO:NC	T (°C)	t (h.)	conv. (%)	av. DoC	LC-MS/MS
10	45 : 45	25	16	60	0.9	● E1 [● E1/D1] DoC > 1
10	75 : 75	25	16	91	2.5	● E1 ● E1/E6/D1 ● D62-K65 E275-K277
10	100 : 100	37	2	79	1.6	● E1/D1 ● E1/E6/D1
15	45 : 45	25	16	83	1.8	● E1/D1 ● D1

The reproducibility and repeatability of those E1-selective conditions were then evaluated by four experimenters (N = 14, CS, IK, VV and Léa Rochet - LR) and narrow variations were obtained leading to an average conv. 60% and av. DoC = 0.9. In most cases (N = 11), av. DoC < 1 were

observed suggesting a major E1-selectivity for those conditions. While the reaction never reached full conversion under these conditions, any attempt at pushing it further (e.g., increasing concentration in reagents, temperature, reaction time) resulted in an erosion in site-selectivity (Table 10). Interestingly, increasing the concentration in trastuzumab to 15 mg/mL instead of 10 mg/mL led to the expected increase in conversion and av. DoC whilst maintaining a certain degree of selectivity – only *N*-terminal modifications of E1 and D1 were detected, through both Ugi and Passerini reactions.

While the complementary determining regions (CDR) of trastuzumab, responsible for HER-2 recognition, does not contain the highly conserved E1/D1 residues,[179] we still wanted to validate that their conjugation did not impair the protein's affinity for its target. In order to do so, we selected the HER-2 positive cell line, SKBR-3, as positive control and the HER-2-negative cell line, MDA-MB-231, as negative control. We evaluated the binding of a FITC-labelled trastuzumab on both cell lines by real-time affinity measurement using a Ligand Tracer Green apparatus (Ridgeview instruments) and compared it with a FITC-labelled Ugi sample. The similar k_{on}, k_{off} and K_D obtained — 2 10^4 $M^{-1}.s^{-1}$, 1.37 10^{-5} s^{-1}, 0.65 nM for trastuzumab and 2.4 10^4 $M^{-1}.s^{-1}$, 1 10^{-5} s^{-1}, 0.45 pM for the Ugi-modified trastuzumab, respectively — allowed us to conclude that the Ugi modification did not impair trastuzumab HER-2 recognition ability (Figure 50).

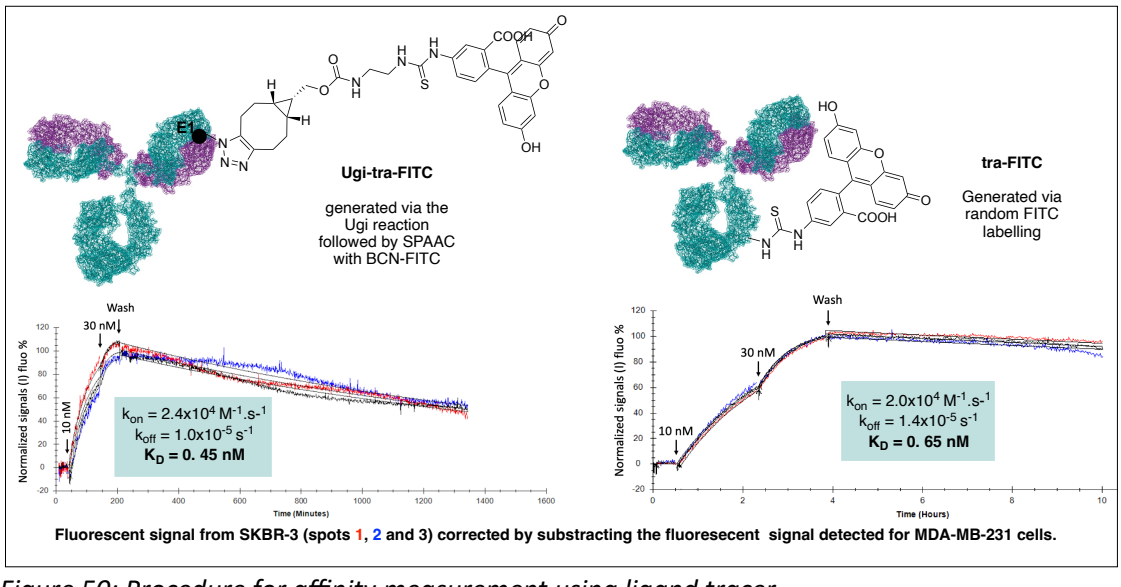

Figure 50: Procedure for affinity measurement using ligand tracer.

Considering the excellent level of regioselectivity observed, we next decided to evaluate these conditions on other mAbs and proteins (Table 11). We selected the humanised antibody bevacizumab and the human antibody ramucirumab to assess the applicability of our method to other immunoglobulins G (IgGs) containing *N*-terminal D1 and E1. We were glad to observe that, when subjected to our E1-selective conditions, selectivity for this residue was maintained, even though side Passerini reaction competed for the conjugation of this residue with ramucirumab. In both cases, slightly lower conv. and av. DoC — 52 % and av. DoC 0.8 for ramucirumab and 44 % and av. DoC 0.6 for bevacizumab — were observed in comparison with trastuzumab. We then decided to extend the scope of the reaction to IgGs deprived of *N*-

terminal aspartate and glutamate residues, by using the chimeric murine/human mAb rituximab, which bears N1 and Q1 residues instead. When subjected to the E1-selective Ugi conditions, native LC-MS analysis of rituximab showed similar behaviour as the other mAbs with conv. 55% and av. Doc 0.8. However, no labelling site could be detected by LC-MS/MS analysis, probably due to an incomplete sequence coverage or low abundance of modified peptides which could suggest the presence of several reactive sites.

Table 11: mAb transferability of the E1 selective conditions.

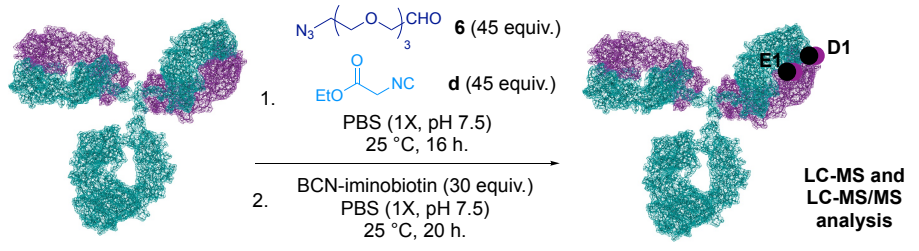

mAb	[mAb] (mg/mL)	equiv. CHO:NC	T (°C)	t (h.)	conv. (%)	av. DoC	LC-MS/MS
rituximab	10	45 : 45	25	16	45	1.5	/
ramucirumab	10	45 : 45	25	16	52	0.8	● E1 ● E1/D1
bevacizumab	10	45 : 45	25	16	44	0.6	● E1

While partially inconclusive, this result still underlines the protein dependence of the selectivity of our method. However, the presence of several reactive sites on rituximab that are "ignored" in the presence of *N*-ter E1 and D1 showcases the applicability of MCRs to the conjugation of different families of IgGs.

III.4. Conclusion on the Ugi MCR

In conclusion to this methodology work, we varied all conjugation parameters of our previously developed Ugi conjugation reaction in order to study their impact on the selectivity of our approach. We proved that mAbs responded well to this approach, with a handful of key reactive sites being systematically detected. Importantly, we managed to refine some conditions to allow the selective *N*-terminal conjugation of aspartate and glutamate, culminating in the precise modification of a single site through an intra-residue U-4C-3CR when commercial ethyl isocyanoacetate was used. This selectivity seems to be driven by matters of accessibility of the targeted site by the reagents and spatial proximities between the two reactive functions provided from the protein, but more elaborated studies might be necessary to evaluate the panel of Ugi-reactive proteins – the "Ugiome".

IV. Conclusion and perspectives

MCRs are powerful reactions for organic synthesis with few to no side reactivity that can lead to the formation of complex structure with good tolerance for various side chains among the components of the reaction. With the aim of exploring their use for the site-selective labeling of native proteins, we conducted mechanistic studies on three main strategies.

Because good selectivity was observed by other teams using Mannich-like MCRs we evaluated if the Robinson-Schöpf 3-CR could lead to selective labelling of primary amines. However, a side reaction, presumably leading to the formation of a pyrrole adduct, was observed, seemingly triggered by concentration effects. If we failed to develop conditions selective only for the Robinson-Schöpf reaction, we were able to favour only the side reaction by reducing the reaction time. Further investigation for the functionalization of those pyrrole adduct would be highly interesting, using Diels-Alder reaction for example.

Based on our previously published results concerning the investigation of the Ugi/Passerini MCR for the site-selective labelling of native trastuzumab, we engaged in a large campaign to understand better the factors governing its efficiency and selectivity, with the intent to develop conditions favouring one mechanism over the other. We first hypothesized that replacing the aldehyde with carbonyl surrogates could promote modification of aspartate / glutamate residues, following a Passerini-like reaction. As imines are poorly stable in aqueous media, the use of the more robust oximes, chlorooximes and hydrazones was evaluated. This study highlighted the difficult balance between stability and reactivity one has to address when developing a new bioconjugation reaction, oximes being unreactive whilst chlorooximes and hydrazones being too sensitive to nucleophilic substitution leading to heterogenous labelling in the case of the chlorooxime and to transamination in the case of the hydrazone.

Turning to classical Ugi conditions, an in-depth mechanistic study based on LC-MS/MS analysis was conducted. We observed that the variation of the isocyanide's and aldehyde's side chains was key to favouring certain modification sites on the protein, with one notable case where single-residue — E1 — labelling of trastuzumab was observed through a Ugi intra-residue mechanism. Even more interestingly, we were able to evaluate the parameters influencing the selectivity of this method — increasing the concentration for instance led to retained selectivity for *N*-terminal residues, while any temperature increase led to complete loss of selectivity. Finally, our method was shown to be transferable to other human and humanized IgGs with a conserved *N*-ter selectivity, however in the chimeric mAb rituximab, which does not present E1 and D1, loss of selectivity was observed. We highlighted in this study that their adaptation in complex biological environment — implying among other constraints diluted aqueous reaction media and short temperature range — can result in side-reactions, resulting in heterogeneous

mixture of labelled proteins, but that fine tuning of the reaction's conditions can lead to selective labeling of proteins.

The high tolerance of the Ugi reaction for variations in the side chains of the used reagents allowed to maintain a plug and play approach while developing site-selective condition thus allowing us to explore various applications of the obtained conjugate from the classical formation of an ADC to the more challenging formation of proteins dimers.

Formation of bsAb based on the *N*-ter selective U-4C-3CR conditions

I. Introduction

I.1. Presentation of bsAbs

The term bispecific antibody (bsAb) describes a large family of molecules designed to recognize two different epitopes or antigens. The global idea of combining two antibody-based molecules — through mild cysteine re-oxidation of two different rabbit Fab fragments — was proposed by Nisonoff and co-workers in 1960.[180] In this context, specificity consists in the ability of the antibody to discriminate between various antigens. Demonstration of the dual specificity — hence the ability to discriminate two antigens among many others — of such construct was demonstrated four years later through observation of the agglutination of two different cell types mediated by the construct.[181]

The linkage of the two mAbs specificities in a single compound can be used as a surrogate to the combination of two therapeutic mAbs in so-called combinatorial bsAbs. In that case, they can lead to the simultaneous inhibition of two cell surface receptors, two ligands, or to the cross-linking of two receptors (Figure 51).[182,183] Such combinatorial therapies are used in the treatment of multifactorial disorders such as tumours, inflammatory disorders and diabetes.

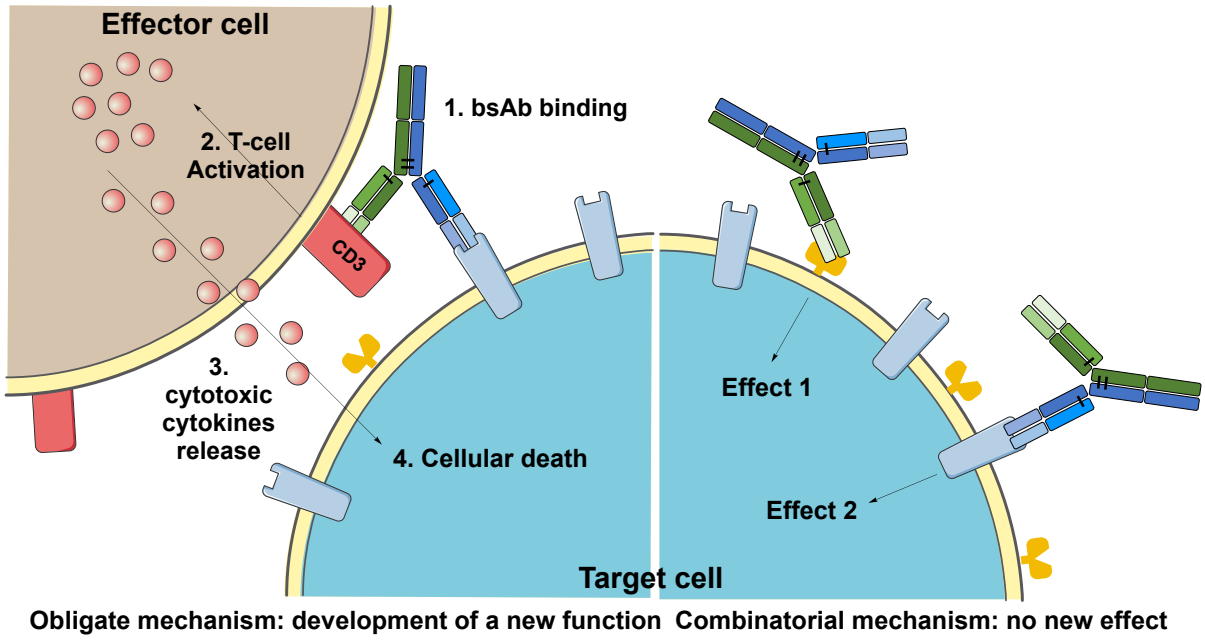

Figure 51: Chosen example for the illustration of obligate bsAbs (left) and combinatorial bsAb (right). For obligate bsAbs, bispecific T-cell engager example was chosen, target cell death is triggered by cytokines produced by a nearby T-cell brought to spatial proximity of the target by binding of the bsAb. The example for combinatorial bsAb is the case where the bsAb can recognize two surface receptors of the target cell.

However such bispecific construct can display a new functionality, not present by simple combination of the two parent mAbs, resulting in obligate bsAbs. The best example of obligate bsAbs is bispecific T-cell engager (BiTE), which combines the specificity of a mAb that can recognize an undesirable cell in the host and a specificity that can trigger immune response from the host.[184–186] The linkage of the two specificities results in liberation of cytotoxic cytokines in the direct environment of the undesirable cell resulting in its death (Figure 51).[187] Other mechanisms of action for obligate bsAbs is co-factor mimicry for the precise orientation of an enzyme with its cofactor.

Among the nine bsAbs approved by the EMA presented in table 12, seven of them follow an obligate mechanism and six target the T lymphocyte antigen CD3 and a cancer antigen well exemplifying the trend in bsAb's application. While the classification of bsAbs into obligate and combinatorial provides interesting insights into their mode of action, it does not reflect the diversity in formats bsAbs can take on.

Table 12: List of the different bsAbs approved by the EMA and their associated characteristics.

bsAb	Target 1	Target 2	Indication	Format	Year of approval
catumaxomab	CD3	EpCAM	lung cancer	IgG like	2009
blinatumomab	CD3	CD19	leukemia	Tandem scFv	2015
tebentafusp	CD3	gp 100 HLA peptide	melanoma	scFv-TCR	2022
mosunetuzumab	CD3	CD20	lymphoma	IgG like	2022
teclistamab	CD3	B-cell maturation antigen	myeloma	IgG like	2022
glofitamab	CD3	CD20	lymphoma	IgG+Fab	2023
emicizumab	coagulation factor IXa	coagulation factor X	Haemophilia	IgG like	2018
amivantamab	MET	EGFR	lung cancer	IgG like	2021
faricimab	VEGF	angiopoietin 2	Macular degeneration Macular edema	IgG like	2022

Considering that any biomolecule combining two variable fragments (Fv) – usually composed of a heavy chain variable domain (V_H) and a light chain variable domain (V_L) – can be considered bispecific, a large panel of structurally diverse bsAbs exists.

I.2. Genetic engineering for the production of bsAbs

The many formats bsAbs can have are mostly related from their production method.For instance, bsAbs can be produced by the hybrid hybridoma — or quadroma — technique developed in 1983,[185,188] derivatized from the hybridoma technology proposed by Kölher and Milstein in 1975 (Figure 52).[189] The hybridoma technique is based on the fusion of a chosen B lymphocyte, the cells responsible for the production of mAbs, with immortal myeloma cells, leading to mAb-producing hybrid cells with high longevity – the two pivotal features of their individual parent cell lines.[189,190] The quadroma technique is based on the fusion of two hybridoma cell lines, resulting in the random assembly of light chains (LC) and heavy chains (HC) in 16 possible combinations and ten different antibody variants (due to their symmetrical nature), among which only one is a bsAb of the size of a classical mAb (Figure 52).[188] Depending on the origin of the combined B-cells, mixing 2 HC from different origins can trigger unwanted toxicity or affect pairing, in which cases F(ab')$_2$ fragments, obtained from pepsin digestion, can be preferred over whole mAbs (Figure 53). Thanks to progresses in genetic engineering, it eventually became possible to address these pairing issues by "forcing" correct HC pairing using knobs-into-holes technology (KiH) by introducing for example a bulky tryptophan residue in one HC and a corresponding cavity on the other fragment that can accommodate it.[191–193] More recently, alternatives to this steric approach were developed such as charge interaction-based pairing techniques.[194] As mispairing of Fab were also encountered

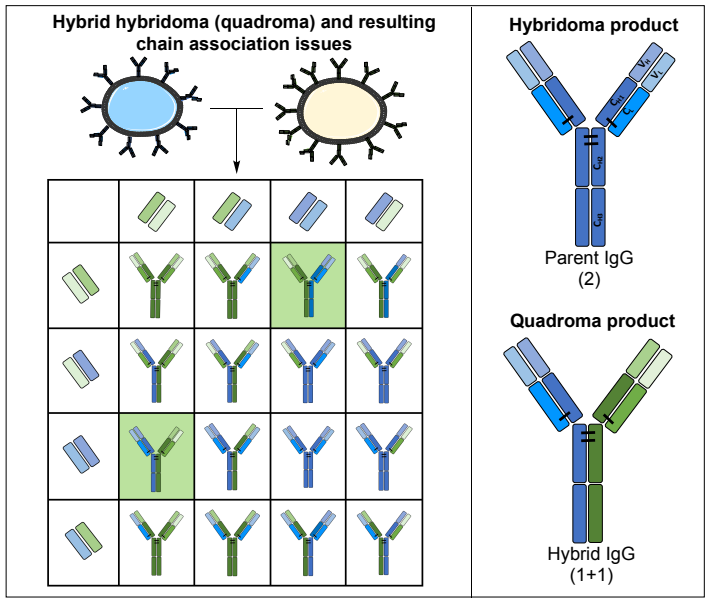

Figure 52: General quadroma technique and resulting products.

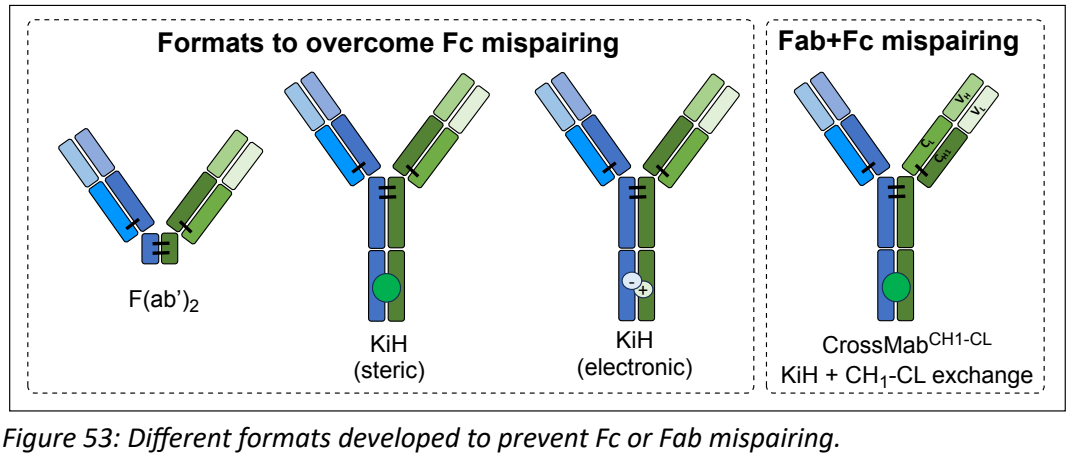

Figure 53: Different formats developed to prevent Fc or Fab mispairing.

for the reconstitution of bsAbs, CrossMab technologies was developed by Roche. This approach consists in the exchange of domains between light and heavy chains by directed mutagenesis — for example CH1 and CL, (Figure 53) —and was found to be highly efficient.[195] While the formats described here present a 1+1 valency — i.e., one binding site for each targeting molecule —, the emergence of genetic and protein engineering allowed the formation of more diverse formats, with various sizes and valences.

For instance, fragment-based formats, consisting in two Fvs, can be expressed in lower eukaryotic and prokaryotic expression systems such as Chinese hamster ovary (CHO) cells resulting in high yield and low production costs (Figure 54).[196] Those recombinant formats are highly customisable in terms of valency (1+1, 1+2, 2+2), but their fully artificial nature and reduced size were shown to result sometimes in stability issues as well as impaired pharmacokinetics and physicochemical properties.[197] Among the different strategies evaluated to overcome this issue, the development of Fc fusion proteins ($(scFV)_4$-Fc, Figure 54) helped to prevent protein's catabolism — i.e. prevent enzymatic degradation of the construct. Building on those models, the fusion of V_H and V_L sequences of interest on the *N*-termini of existing mAbs was widely explored, resulting in higher molecular-weight species with 2+2 (DVD iG) or 2+1 (CrossMab $^{F(ab')3}$) valences (Figure 54).

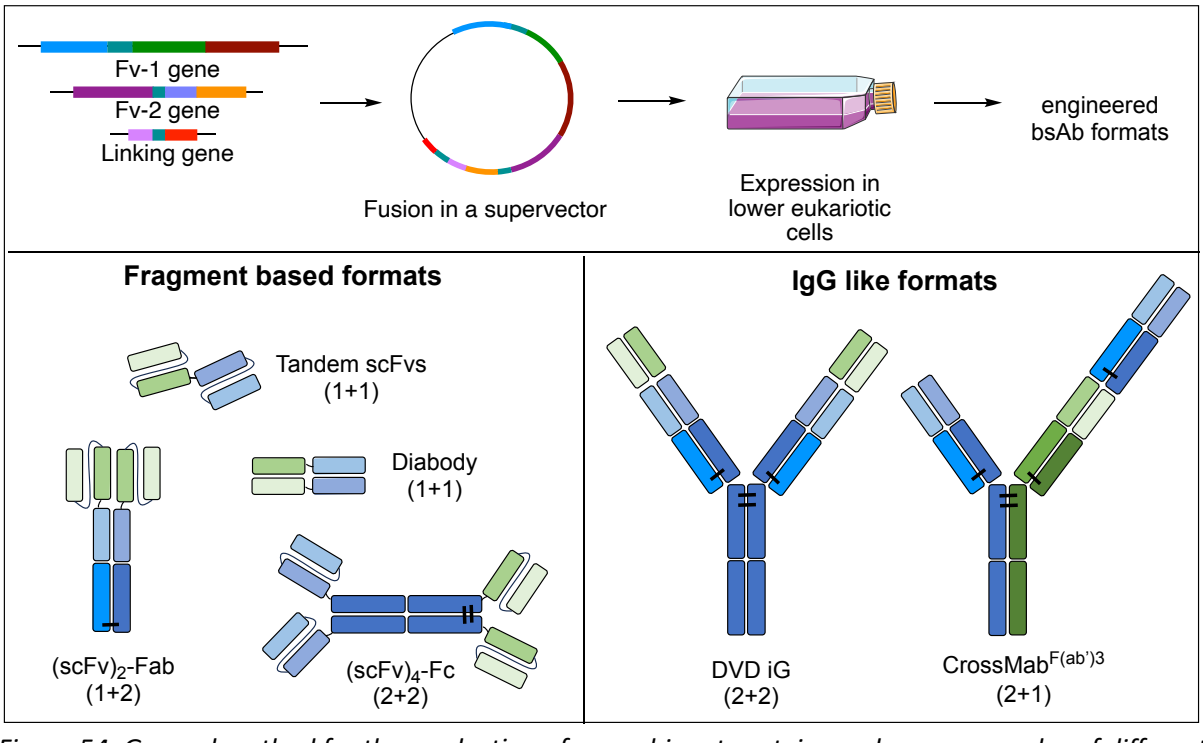

Figure 54: General method for the production of recombinant proteins and some examples of different resulting formats.

Genetic engineering also allows the introduction of unnatural amino acids in the sequence of mAbs or mAbs fragments which can later be assemble by chemical coupling. Those techniques emerged with the recent advances in bioorthogonal chemistry.

For instance in 2012, Schultz and co-workers developed a bsAbs based on the incorporation of p-acetylphenylalanine residue in defined sites of Fab fragments.[198] Using bifunctional aminooxy-azide linker **R187** on one Fab and aminooxy-BCN **R188** on the other they were able to stably form bispecific construct through SPAAC reaction (Figure 55).

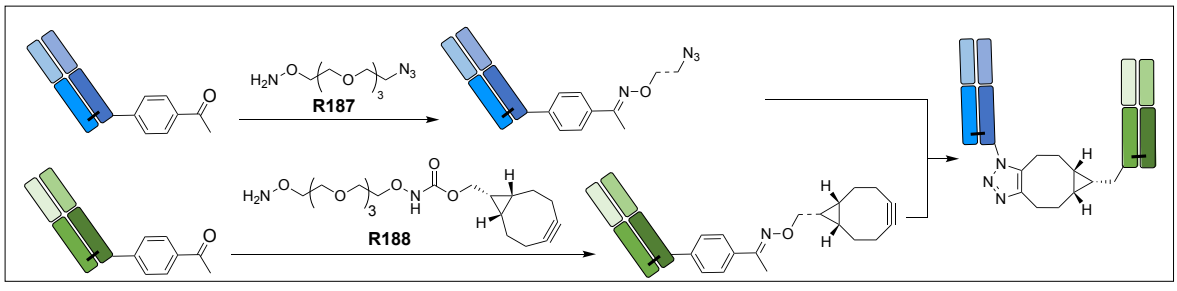

Figure 55: Chemical formation of bsAbs using engineered Fab fragments.

Similar technique using a CHO-tag instead of an engineered mAb was proposed by Rabuka and co-workers the same year allowing to rupurpose existing antibodies with known pharmacokinetic and pharmacodynamic profiles.[199,200] However, the production of bsAbs by genetic engineering and expression in lower eukariotic cell is the most widely used method nowadays, the advances in bioorthogonal chemistry along with the development of site-selective conjugation methods, renewed the interest for chemical formation of bsAbs.

I.3. Chemical formation of bsAbs

The first chemical method described by Nisonnof in 1960 consists in the digestion of the Fc fragment of an intact Rabbit IgG using pepsin to yield a $F(ab')_2$ fragment, followed by mild reduction using 2-mercaptiethylamine (**R189**) — according to them allowing the exclusive reduction of the hinge disulfides — in order to obtain two reduced Fab' fragments (Figure 56).

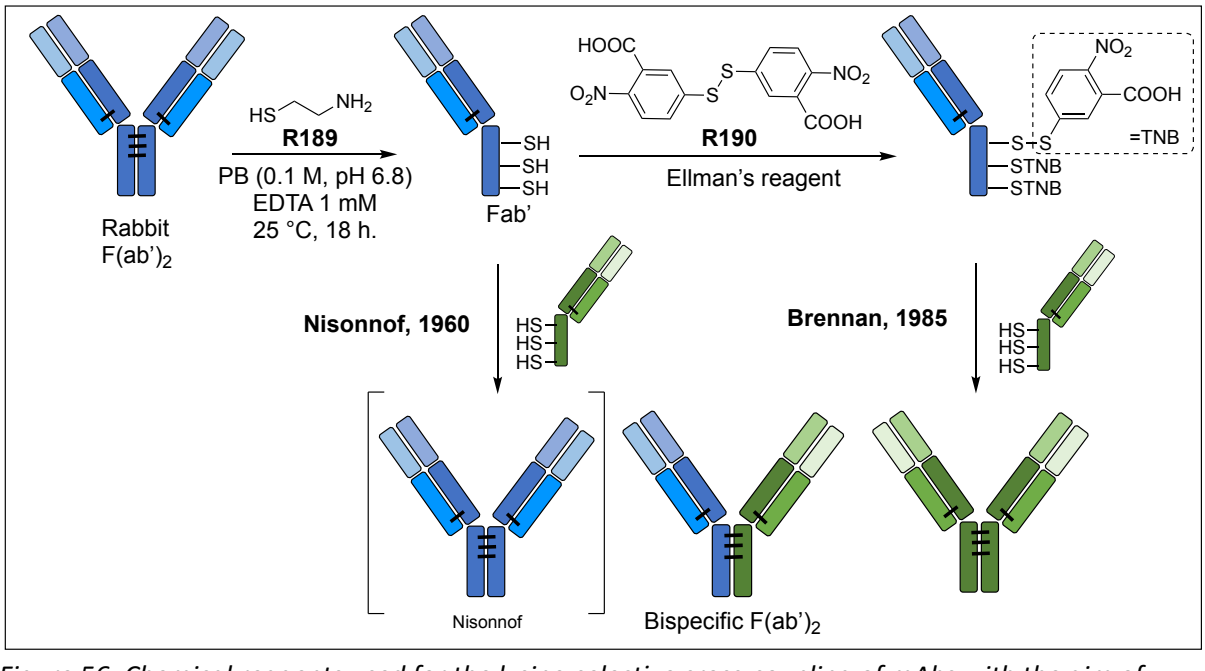

Figure 56: Chemical reagents used for the lysine-selective cross-coupling of mAbs with the aim of producing bispecific constructs.

Fab' fragments from two different rabbit IgGs were then mixed, allowing reoxidation of the previously reduced disulfide bonds in open air, yielding a statistical mixture of three products among which one is a bispecific F(ab')$_2$.[180] Brennan *et al.* proposed an improved version of this method in 1985, in which they stabilized one of the obtained Fab' fragment from murine IgG using Ellman's reagent **R190,** reducing the number of products formed to just two (Figure 56). It was not before 2011 that this approach was successfully applied to full mAbs, necessitating the use of acidic conditions that were shown to favour the separation of the half mAbs thus increasing the yields of the obtained bsAb.[201,202]

As an alternative platform, the formation of covalently bonded antibody heteroaggregates using dimethyl suberimidate (DMS, **R191**) or *N*-succinimidyle 3-(2-pyridyldithio)propionate (SPDP, **R192**) cross linkers was reported as early as 1984 (Figure 57). However, while the activity of the bispecific hetero-aggregate was demonstrated, no indication concerning the valency of the formed complexes was mentioned besides the loose "heavy and lighter fractions" mentioned by Karpovsky *et al*. in 1984 and the "heterodimer, trimer and tetramer" mentioned by Ring *et al.* in 1994 (Figure 57).[203–205] Other cross-linking techniques were developed in order to increase the yield in bsAb and reduce the amount of inactive side products.

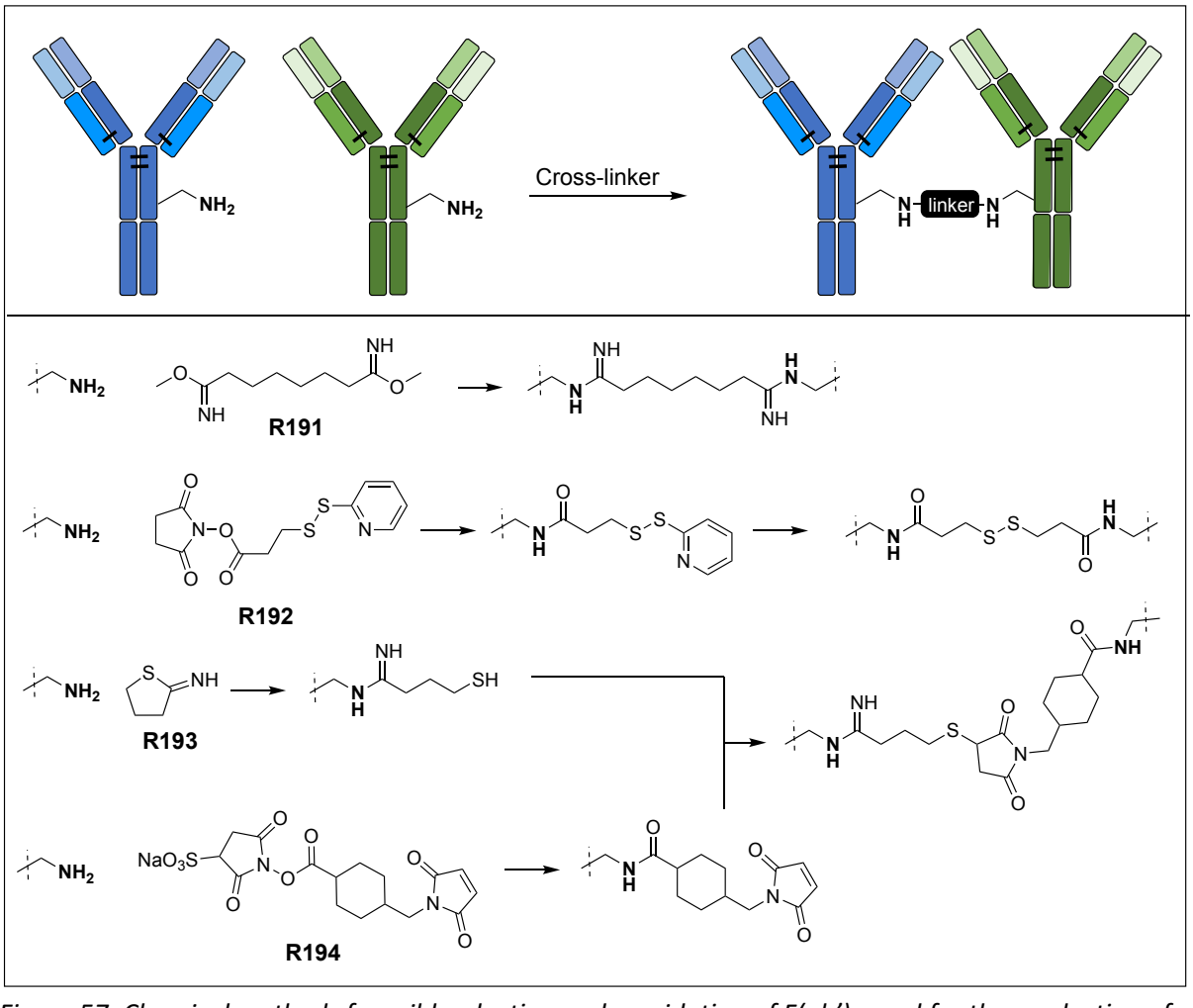

Figure 57: Chemical methods for mild reduction and reoxidation of F(ab')$_2$ used for the production of bsAbs.

For instance, Anderson *et al.* proposed the functionalization of one mAb with Traut's reagent **R193** thus generating thiol-functionalized mAb (formation of dimers at this step was not discussed), which was then chemoselectively assembled to a second sulfo-SMCC **R194** functionalized mAb. This method developed in 1992, was still applied in 2006 by Reusch *et al*.[206,207]

While lysine-selective crosslinkers allowed the formation of functional bsAbs, the heterogeneity of the products can lead to variable efficacy, pharmacodynamics and toxicity. Along with the progress in site selective conjugation of native proteins, the development of more precise cross-linking reagent, mostly based on cysteine selectivity, were developed.
Glennie *et al.* developed in 1987 a di-maleimide reagent **R195**, setting bases for rebridging reagents, that allowed artificial reconstruction of disulfide bridges by sequential reaction on two reduced Fab' fragments (Figure 58).[208]

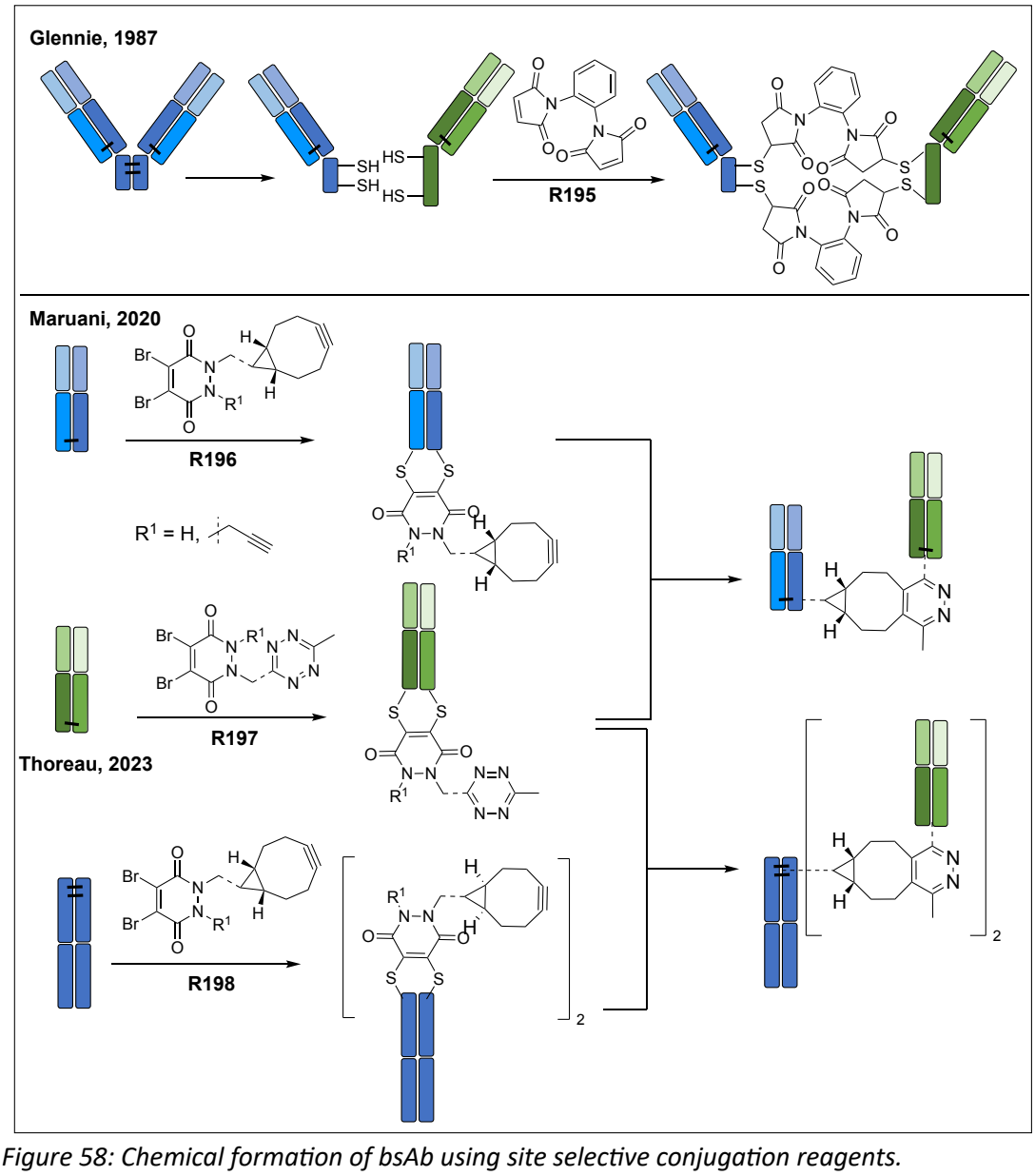

Figure 58: Chemical formation of bsAb using site selective conjugation reagents.

Chudasama and co-workers used their own developed family of rebridging reagents, dibromopyridazinediones (PDs), allowing the mono-functionalization of IgG-Fab fragment and bi-functionalization of IgG-Fc fragments using two bioorthogonal handles — i.e., a BCN **R196** and a tetrazine **R197**.[102,104] The functionalized protein fragments were then reacted together in order to perform strain-promoted inverse electron demand Diels-Alder cycloaddition (SPIEDAC) allowing the formation of various bsAbs formats. In addition, the use of PD reagents facilitated the further functionalization of the constructs, depending on the derivatization of the second nitrogen borne by the reagent (R^1, Figure 58). Those results show the key advantages of the chemical formation of bsAbs in comparison with other production methods, as it allows fast generation of molecularly defined bsAbs libraries with great flexibility and few side products.

I.4. Conclusion

BsAbs exists since 1960 and, if such constructs seem promising in comparison with therapeutic mAbs, it took 50 years of development before some eventually reached the market. This can be explained by the wide variety of formats they can have, each presenting different pharmacodynamic and pharmacokinetic properties. In addition to the choice of the adequate format, the production method can also be challenging, often resulting in low yields and hard separation from side products. Of the three main methods developed to produce bsAbs – i.e., the hybrid hybridoma technology, the production of recombinant or fusion proteins, and the chemical conjugation of mAbs —, protein engineering is the most widely used to date because it is the most cost- and time-effective. However, new artificial proteins might present stability issues or even systemic toxicity, urging to focus on strategies using proteins with known properties. This is one of the reasons behind the success of chemical methods, employing site-selectively conjugated mAbs, whose reactivity was already described and analysed. Having this in mind and our site-selective Ugi conjugation reactions in hands, we thus decided to take advantage of its ‘plug-and-play’ character to functionalize the resulting azide-containing conjugates with a BCN-functionalized protein allowing fast and easy access to protein dimers using SPAAC reaction.

II. Chemical formation of bsAbs using the Ugi 4C-3CR reaction

II.1. Design of linkers for bsAb formation

II.2.a. Azido-functionalized IgG

We showed in part I of this manuscript that the Ugi reaction can be used for the selective labelling of human and humanized IgGs with an azido-moiety. Because chemical formation of protein dimers can be accompanied with low yields and hard separation of the different formed species, we decided to exploit our trastuzumab E1-selective conditions — i.e., trastuzumab 10 mg/mL using 45 equiv. of aldehyde **6** and isocyanide **d** — that were shown to retain a certain degree of site-selectivity when applied to the human or humanized IgGs ramucirumab and bevacizumab. As these conjugates were shown to partake efficiently in a further SPAAC functionalization step using various BCN derivatives — e.g., BCN-TAMRA, BCN-Cy5, BCN-FITC, BCN-iminobiotin, BCN-DM1 —, we hypothesized that using BCN-functionalized protein or fragment of protein should lead to molecularly defined protein dimers. More interestingly, the addition of such large species onto the IgG should allow the separation by SEC of the obtained regioisomers — i.e., 43 % D0, 37 % D1 and 20 % D2 —, leading to the formation of pure and homogeneous constructs. Moreover, having shown that the affinity of the Ugi-modified trastuzumab was not impaired in comparison with native IgG, we were confident that our strategy should lead to the formation of active bispecific antibodies (bsAbs) with (2+1) and/or (2+2) valences upon coupling with appropriate BCN-functionalized Fv.

II.2.b. BCN-functionalization reagent

In order to generate those BCN-Fv, we chose to modify Fab fragments. These are accessible from full mAbs through pepsin and/or papain digestion and they have the advantage of presenting a single inter-chain disulfide bond, easily accessible for reduction and thus, site-selective functionalization. This characteristic is essential because the Ugi-reaction permits the introduction of a single azido motif per modification site, hence the introduction of a single BCN motif per Fv — in our case, per Fab — is necessary in order to obtain molecularly defined bsAbs. Our attention turned to dibromomaleimides (DBM, **R199**) reagents — also coined next generation maleimides (NGM) — as, in comparison with classical maleimides, those reagents lead to a rapid and complete rebridging of disulfide moieties.[209] The formed thioalkenyl bonds were described to be sensitive to thiol exchange in presence of free thiol groups — as in glutathione (GSH), for example — suggesting plasmatic stability issues.[210] Hydrolysis of the maleimide ring **R200** into maleamic acid **R201** under slightly alkaline conditions (pH 8.5) was shown to prevent this thiol-exchange side reaction, yielding highly stable conjugates (Figure 59).[211] Lyon *et al*. showed that such hydrolysis was accelerated when electron-withdrawing groups were added to the maleimide ring's nitrogen and Morais *et al.* showed that,

on full mAb, DBM-C_2 (**R202**) and DBM-ph (**R203**)reagents displayed higher hydrolysis rates than DBM-C_6 (**R204**)— $t_{1/2}$ = 19.3 min, 16.3 min and 48.1 h, respectively (Figure 59).[212]

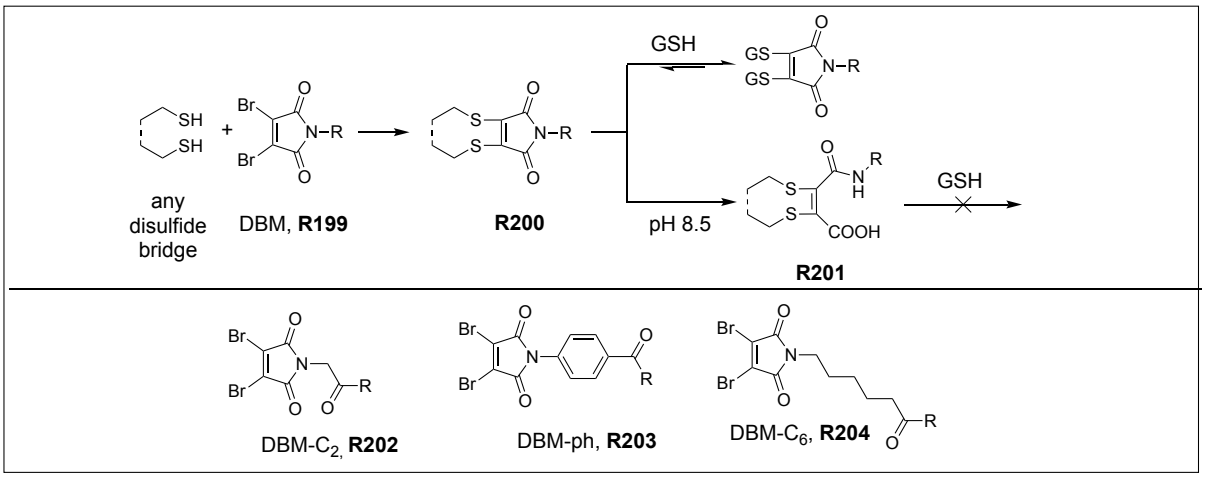

Figure 59: Structure of the adducts formed upon rebridging with DBMs. Example of different reagents studied by Morais et al.

Having this in mind, we opted for a strategy inspired by the work of Castañeda *et al*., activating dibromomaleimides **19** into *N*-methoxycarbonyldibromomaleide **20** that can be functionalized through formal *trans*-carbamatation in presence of a primary amine-containing reagent (Scheme 8).[213] Two different BCN-NH_2 were synthesized, starting with the *endo* isomer of BCN alcohol **21** according to reported literature.[214] First, the alcohol derivative **21** was activated as an electrophilic *p*-nitrophenol (PNP) carbonate **22**. Nucleophilic addition of 1,3-propylene-diamine on **22** under diluted controlled conditions led to the formation of DBM-NH_2 **23**. Finally, the addition of **23** onto DBM **20** led to **DBM-1** with 70% yield (Scheme 8).

As protein dimer formation might be prone to steric hindrance between the two proteins, we synthesized an analogous DBM functionalized with a PEG_4 spacer allowing greater flexibility between the DBM core and BCN moiety of the reagent. BCN-PNP **22** was thus functionalized via the nucleophilic addition of amino-PEG_4-*tert*-butyl ester **24**, yielding compound **25**. The latter was saponified into the corresponding carboxylic acid **26** using LiOH and further activated as a PNP-ester **27** to yield BCN-NH_2 **28** upon addition of 1,3-propylenediamine under carefully controlled conditions. Coupling between BCN-NH_2 **28** and our previously synthesized DBM **20** led to the formation of **DBM-2** with good yield of 71%. (Scheme 8).

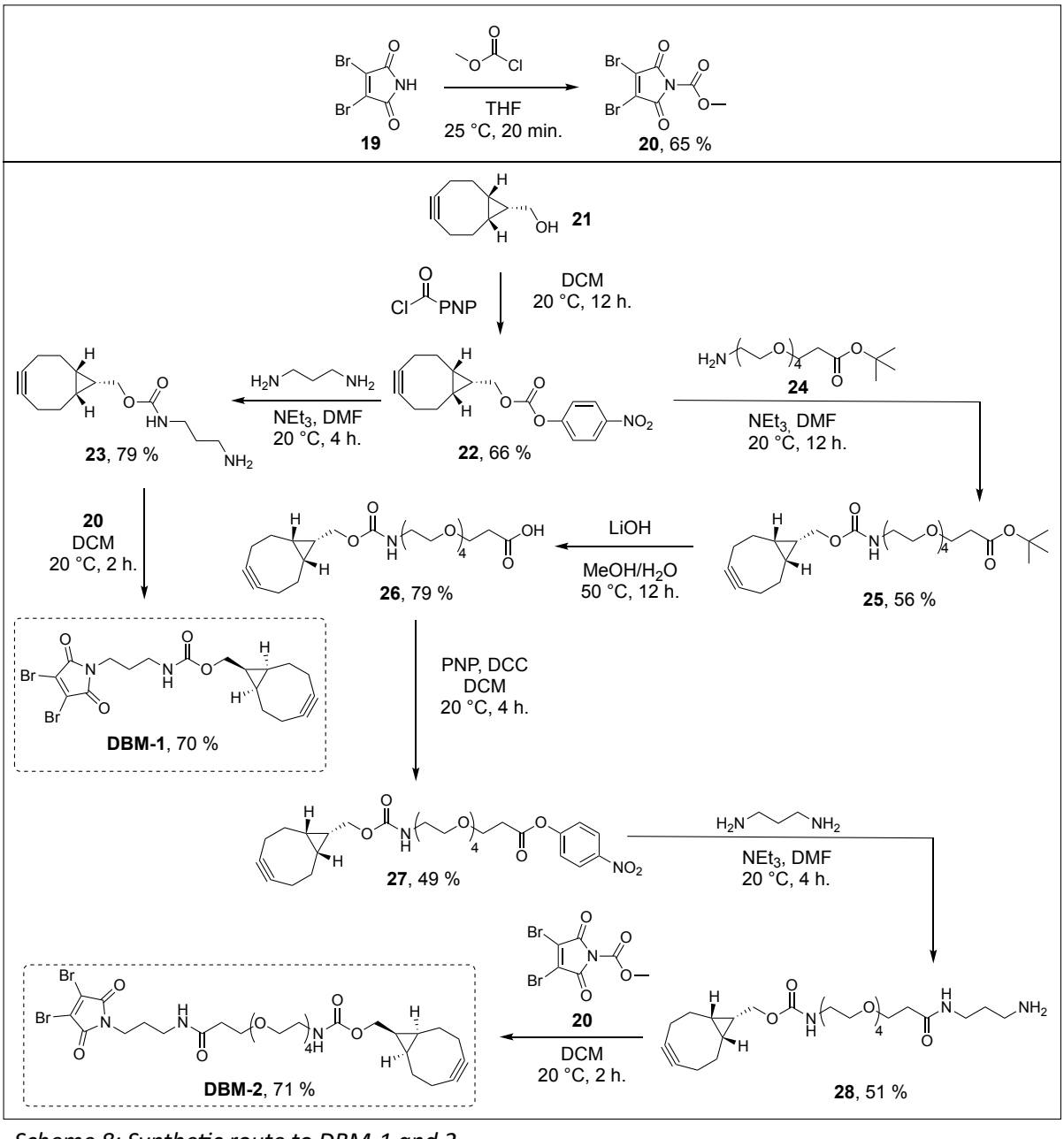

Scheme 8: Synthetic route to DBM-1 and 2.

DBM-1 and **2** contain a carbamate linkage that can present some in-cellulo instability hence we turn toward the use of bicyclo[6.1.0]nonyne carboxylic acid **29** as a way to produce more stable BCN derivatives.[215] Home-made **29** was activated as PNP ester **30** and functionalized with propylene diamine to yield BCN-NH_2 **31**, with good yield. The addition of **31** on DBM **20** allowed the formation of **DBM-3** with excellent yield of 95% (Scheme 9).

If **20** is structurally related to DBM-C_2 developed by Morais *et al.*, we still wanted to make sure the reactivity of those two DBMs was comparable. Thus, we synthesized DBM-C2 **34** from dribromomaleic acid **32** and glycine **33**.[209] Coupling between **34** and **31** was performed through classical amide bond formation conditions, using 2-ethoxy-1-ethoxycarbonyl-1,2-dihydroquinoline (EEDQ) as the coupling reagent. However, surprisingly low yields of **DBM-4**

were observed, systematically below 30%, probably due to the low reactivity of the coupling agent (Scheme 9).[209]

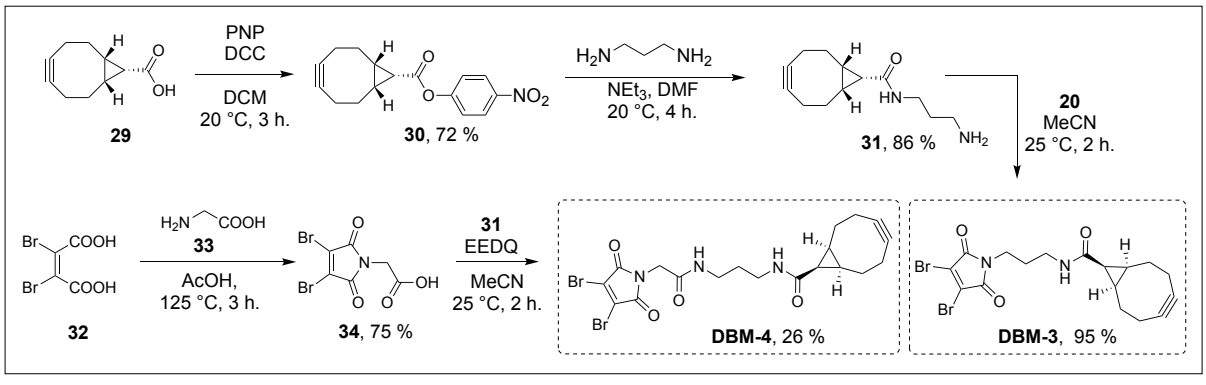

Scheme 9: Synthetic path to DBM-3 and 4.

With those reagents in hands, we next turned our attention toward the rebridging and functionalization of disulfide-containing proteins, such as Fab fragments.

II.2. Fab-BCN generation

II.2.a. Fab production

Having produced our heterobifunctional reagents, we then turned to the production of the Fab fragments, selected from various mAbs classically used in oncology, following an appropriate combination of immobilized pepsin and papain. Pepsin digestion, under controlled conditions, leads to the proteolysis of the mAb's Fc portion, yielding a $F(ab')_2$ fragment as the sole product (Figure 60). $F(ab')_2$ can also be further trimmed using papain, a non-selective sulfhydryl protease cleaving IgGs between an histidine and a threonine residue in the highly conserved motif CDKTH/TC above the hinge region but below the HC-LC interchain disulfide, resulting in two identical Fab fragments.[216,217] We then selected different IgGs — i.e., trastuzumab, rituximab, avelumab, durvalumab and muromonab — whose characteristics are summed up in**Erreur ! Source du renvoi introuvable.** 13.

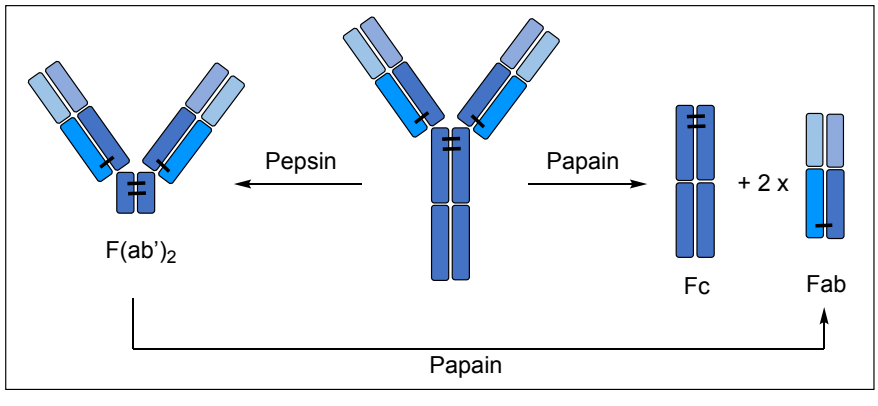

Figure 60: The different fragments obtained upon IgG digestion with pepsin and/or papain.

With the precious help from Ms Léa Rochet, a PhD student working under the supervision of Professor Vijay Chudasama at University College London, bespoke conditions were developed for the digestion of each IgG, using analytical SEC to follow its progress.

Avelumab, durvalumab and muromonab were digested with papain under optimised conditions — i.e., using cysteine hydrochloride as reducing agent in order to reduce all accessible disulfide bonds of the IgG and the active sulfhydryl of the papain in PB (pH 7.0, 10 mM EDTA) at 37 °C for 3 h — yielding the desired solutions of Fab and Fc fragments. In the case of durvalumab, the separation of these two fragments could be performed by SEC with high yields and purity.

For avelumab and muromonab, the size difference was too small to allow efficient separation of the two fragments by SEC, and affinity chromatography was performed instead, using protein A. Protein A presents a high affinity for the Fc region of various IgGs (i.e., K_a around 10^8 M^{-1}) at neutral pH, allowing the isolation of pure Fab fragment, while Fc fragments can be recovered after acidic treatment of the protein A column if needed.[218] As over-digestion of rituximab was observed under those conditions, leading to protein species with lower molecular weights, papain was pre-activated using dithiothreitol (DTT) in order to free its active sulfhydryl group before the reducing agent was removed by gel filtration prior to digestion of the whole, unreduced mAb in PB (pH 6.8, 1 mM EDTA) for 16 hours at 37 °C. Under those conditions, a mixture of Fc and Fab was obtained, easily separated by affinity chromatography.

For trastuzumab, effective digestion was observed using papain under our optimal conditions but separation by affinity chromatography could not be performed, due to the binding of both Fab and Fc to the protein A column. Instead, trastuzumab's Fc was digested using pepsin, generating $F(ab')_2$ trastuzumab, whose hinge region was further digested using pre-activated papain in PB (pH 6.8, 1 mM EDTA) for 24 hours at 37 °C.

Table 13: Characteristics and methods used for the digestion of different mAbs into Fab fragments. The given molecular weights were observed by native SEC-MS analysis.

mAb	type	Target	digestion	Purification	Fab MW (Da)
avelumab	Human IgG1λ	PD-L1	papain	Protein A	46 855
muromonab	Murine IgG2a	CD3	papain	Protein A	47 446
durvalumab	Human IgG1κ	PD-L1	papain	SEC	48 047
rituximab	murine/human IgG1κ	CD20	Mild Papain	Protein A	47 180
trastuzumab	Humanized IgG1κ	HER-2	Pepsin then mild papain	SEC	47 637

We thus developed custom digestion conditions for the production of five Fab originating from diverse IgGs with acceptable to good yields (54 to 85%). With those Fab fragments in hands, rebridging conditions using the previously synthesized DBM-BCN were finally explored.

II.2.b. Fab rebridging

In order to evaluate the rebridging efficacy of our DBM-BCN reagents, and more importantly their hydrolysis into maleamic acid, rituximab Fab (**F_{Rit}**) was chosen as model Fab for the study. The disulfide bridge of **F_{Rit}** was reduced using two equivalents of *tris*(2-carboxyethyl)phosphine (TCEP) in PBS (pH 7.5, 5 mM EDTA) after incubation at 37 °C for 60 minutes, to free the two sulfhydryl groups (Figure 61).[213,209, 93] Reduced **F_{Rit}** was then incubated with 2 equiv. of **DBM** in PBS (pH 7.5) at 25 °C for 20 minutes. The resulting **F_{Rit}-BCN** conjugates were then incubated with 5 equiv. of **Cy5-azide** in PBS (pH 7.5) at 25 °C for 16 h. This last step has two purposes: to evaluate the SPAAC efficacy of the used reagent and promote the hydrolysis of the maleimide into its maleamic acid form. Resulting conjugates were analysed by native SEC-MS. The results summed up in figure 61 show that **F_{Rit}** was rebridged efficiently with all the tested DBM; however, slightly lower conversions were observed using carbamate-based **DBM-1** and **2**. With single modification being observed in all cases and hydrolysis to maleamic acid for the four tested DBM thus validating they are all suitable for Fab-rebridging.

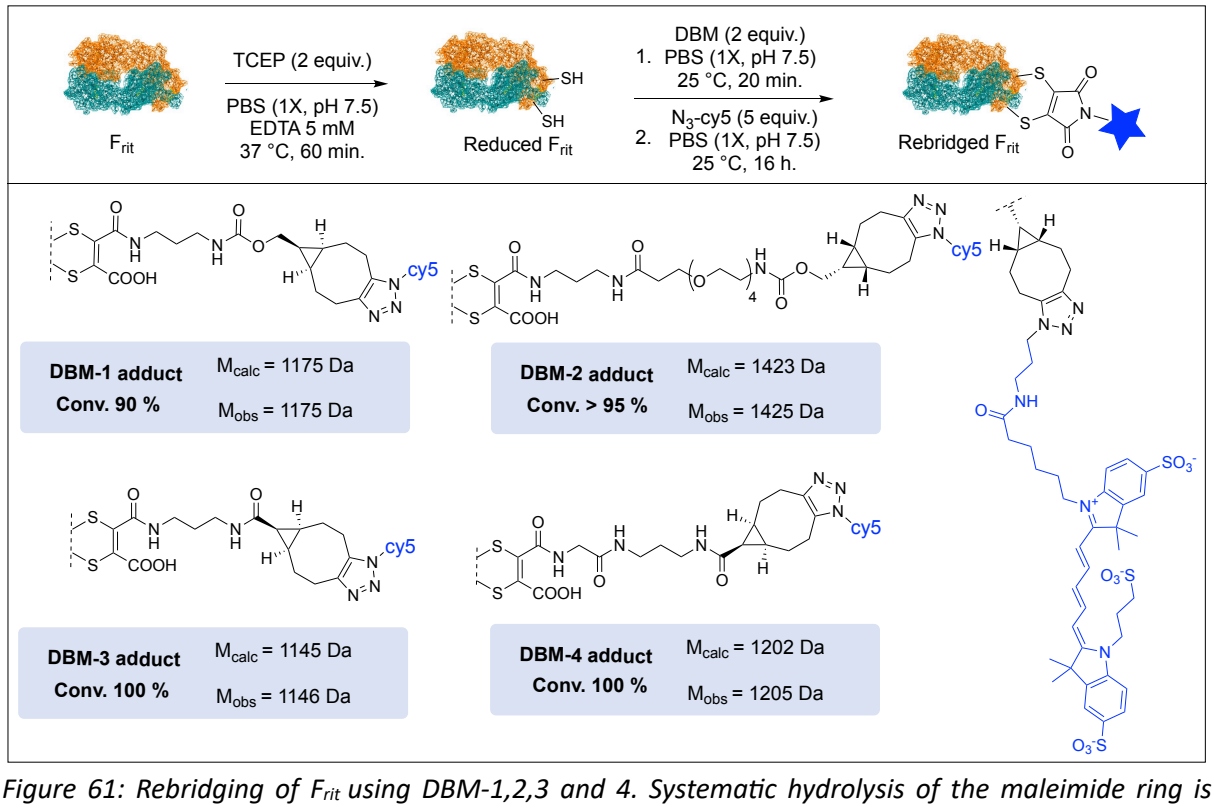

Figure 61: Rebridging of F_{rit} using DBM-1,2,3 and 4. Systematic hydrolysis of the maleimide ring is observed after 16 hours incubation at 25 °C in PBS (pH 7.5).

Because Morais *et al.* reported the optimal maleimide to be the DBM-C2, we pursued this optimization study with **DBM-4**. Control experiments showed that incubation of **F_{Rit}** with **DBM-4** without prior reduction of the inter-chain disulfide bonds led to an absence of fluorescence, thus validating the chemo-selectivity of the method. Since simultaneous reduction and

rebridging of Fab fragments using PDs was reported to be efficient in some cases, we evaluated whether **DBM-4** could be used under similar conditions. However, any attempt at conducting these two steps simultaneously led to decreased conversion, and we therefore decided to pursue with our two-step process.

Finally, the same reaction conditions were applied to the other Fab fragments — i.e., Fab avelumab (**F_{ave}**), Fab muromonab (**F_{muro}**), Fab durvalumab (**F_{durva}**) and Fab trastuzumab (**F_{tra}**) — and the resulting conjugates were analysed by native SEC-MS. Excellent results were obtained with these other Fabs, except for F_{muro} for which low rebridging (40%) was observed.

Muromonab being an IgG2a, it presents an exceptional disulfide geometry with the heavy chain sulfhydryl implicated in the Fab interchain disulfide bridge being located not in the hinge region but at the fusion of the V_H and CH1 domains making the disulfide bridge more prone to post-translational modification (Figure 62).[219,220] Post-translational trisulfide bond formation between the two cysteine residues that normally form the inter light chain-heavy chain disulfide bond and dissolved cysteine or hydrogen sulfide (H_2S) under its nucleophilic sulfhydryl (HS^-) form was considered.[221] Analysis by native SEC-MS of the unmodified Fab disproved the presence of such adducts with single peak being observed, leading us to suspect that reduction with TCEP might be more difficult for this disulfide geometry. Thus, we evaluated the influence of an increased amount of reducing agent on the overall rebridging conversion and were pleased to observe that using a large excess of TCEP (50 equiv.) led to complete reduction of **F_{muro}**, allowing its complete rebridging with good yield.

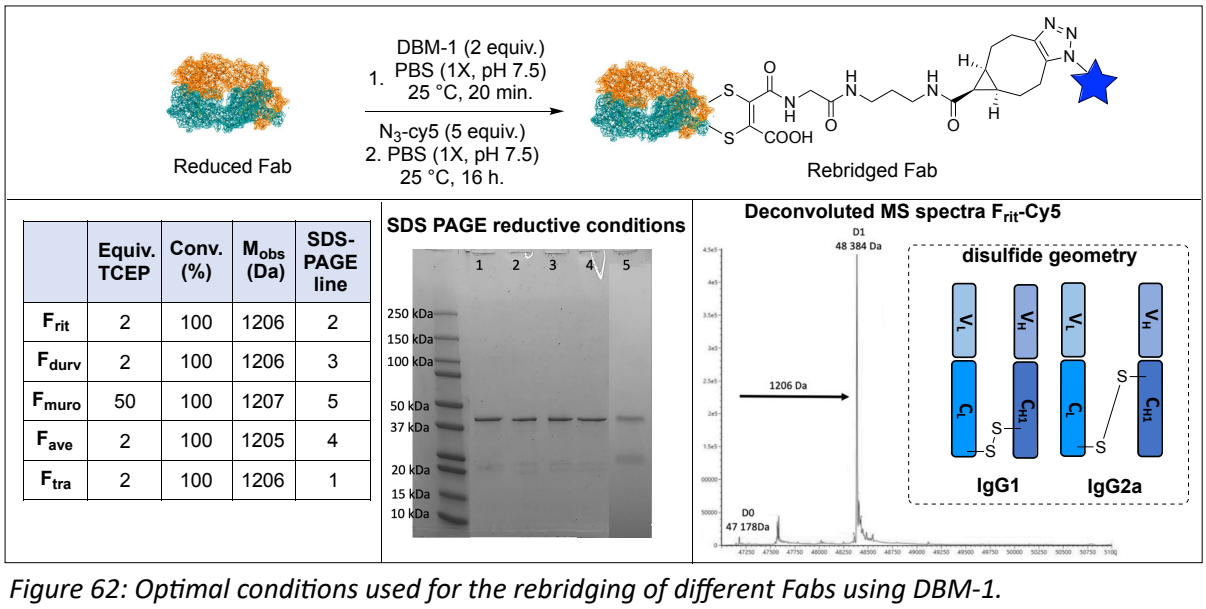

	Equiv. TCEP	Conv. (%)	M_{obs} (Da)	SDS-PAGE line
F_{rit}	2	100	1206	2
F_{durv}	2	100	1206	3
F_{muro}	50	100	1207	5
F_{ave}	2	100	1205	4
F_{tra}	2	100	1206	1

Figure 62: Optimal conditions used for the rebridging of different Fabs using DBM-1.

The efficacy of the rebridging was controlled and confirmed by SDS-PAGE under reducing conditions. If the rebridging is efficient, reductive conditions associated with denaturing conditions will lead to the formation of LC and a Fd fragment of heavy chain of around 25 kDa each, easily observable by SDS-PAGE. The gel presented in figure 62 shows that the rebridging is efficient with very low amount of species at 25 kDa. With those results in hands, we finally

evaluated the SPAAC between our rebridged Fab / BCN fragment and our site-selectively Ugi-conjugated mAb / azide fragment.

II.3. BsAb production

In order to first assess the formation of bsAbs, we used a model system composed of Ugi-modified trastuzumab (**Tra-N_3**) and F_{rit} rebridged with **DBM-4** (**F_{rit}-BCN**). The SPAAC reaction was monitored by SEC and SDS-PAGE, focusing on the formation of high-molecular weight species. In order to limit the amount of side products such as IgG aggregates, **Tra-N_3** was purified by SEC prior to SPAAC and mixed with **F_{rit}-BCN** in a 1:1 molar ratio in order to obtain a 67 □M final concentration of **tra-N_3** in PBS (1X, pH 7.5). The solution was then incubated at 25 °C for 24 hours but low amounts of high molecular weight species was observed in this case (Figure 63). Because the production of Fab by enzymatic digestion is time and cost-consuming, we decided to use another model protein instead, and elected bovine serum albumin (BSA) as our Fab surrogate to optimize SPAAC conditions between two proteins.

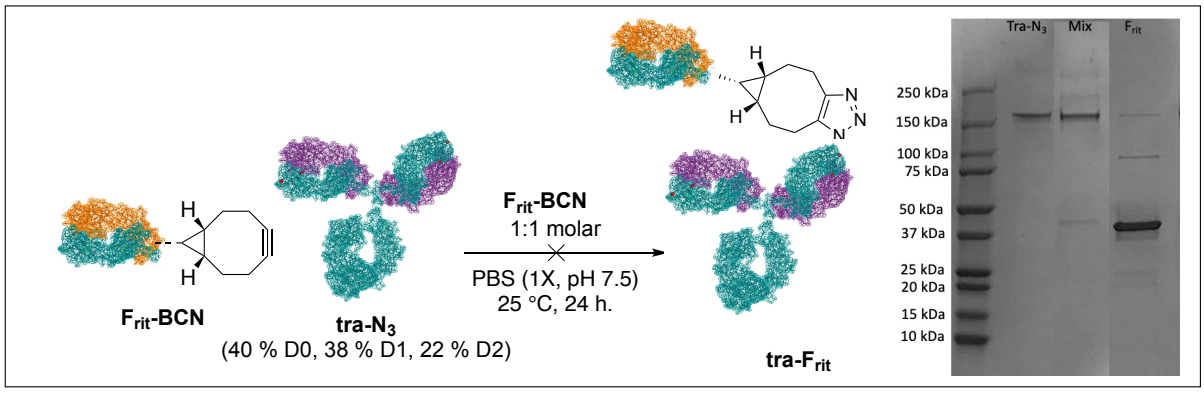

Figure 63: Analysis of the first attempted formation of tra-Frit.

II.3.a. BSA-BCN formation

Albumins are 65-kDa proteins that are highly abundant in blood plasma and play important roles in the maintenance of osmotic pressure as well as carriers of nutrients — fatty acids, mineral — or hormones to cells.[222] Serum albumins present great stability from pH 4.0 to 9.0 and can be heated up to 60 °C for 40 hours without deleterious effect on their structure and physicochemical properties.[223] Moreover, because of their great biocompatibility and easy preparation, they have been extensively used as drug vehicles for therapeutic applications.[224–228] Interestingly, albumins possess one unpaired cysteine residue, poised for chemo- and regio-selective reaction with our previously developed DBMs through single bromine substitution.

BSA was purchased from ACROS scientific, and it was found to be only 79% pure after analysis by SEC, 16% of those impurities being a BSA-dimer. Moreover, native MS analysis of a pre-purified BSA sample — using preparative SEC — showed some intrinsic heterogeneity: if a main peak at 66 429 Da corresponding to native BSA could be observed, it was accompanied by three other small peaks (Figure 64). The first one, with a mass of 66 549 Da, corresponds to a cysteinylation adduct, with the free cysteine of native BSA forming a disulfide bond with a cysteine amino acid (M = 121.15 Da).[229] The second peak, with a mass of 66 597 Da, was

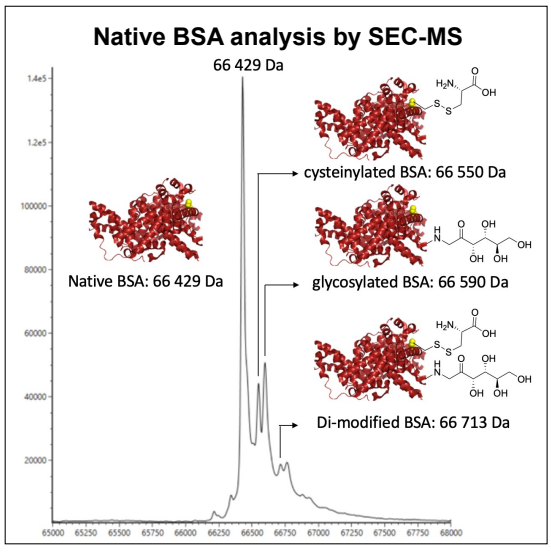

Figure 65: Structure of the different adducts identified after native MS analysis of BSA.

assigned as a fructoselysine glycosylation adduct (M = 163.00 Da), resulting from the Amadori rearrangement of an imine adduct between glucose and a BSA's lysine residue, resulting from the production mode of BSA.[230] Finally, the third peak presents a mass of 66 763 Da, matching that of a doubly cysteinylated/glycosylated adduct.

In addition, we also observed a fourth side species upon reacting BSA with a DBM reagent, with an increment in mass of 30 Da, probably hidden in the shoulder peak of the main BSA peak in native BSA analysis. This is presumably a *S*-nitrosocysteine adduct, resulting from the reaction of the cysteine's free thiol with nitric oxide.[231] As none of these cysteine adducts could partake in reactions with DBM, this must be taken into account when calculating the yields and conversion of the reaction. Based on the conditions developed for the rebridging of Fab fragments (*vide supra*), BSA was incubated in PBS (1X, pH 7.5) with 2 equiv. of **DBM-1** for 20 minutes at 25 °C (Figure 65). Interestingly, good conversion (> 90%) of thiol-free BSA – that is, native BSA and glycosylated BSA – was easily obtained. Unexpectedly, we observed the systematic loss of the second bromide of the DBM reagent as well as addition of a second equivalent of DBM on BSA (D2 species), albeit to a lesser extent. While this points toward a lack of chemo-selectivity of the DBM reagent, we have not been able to identify the competing residues yet.

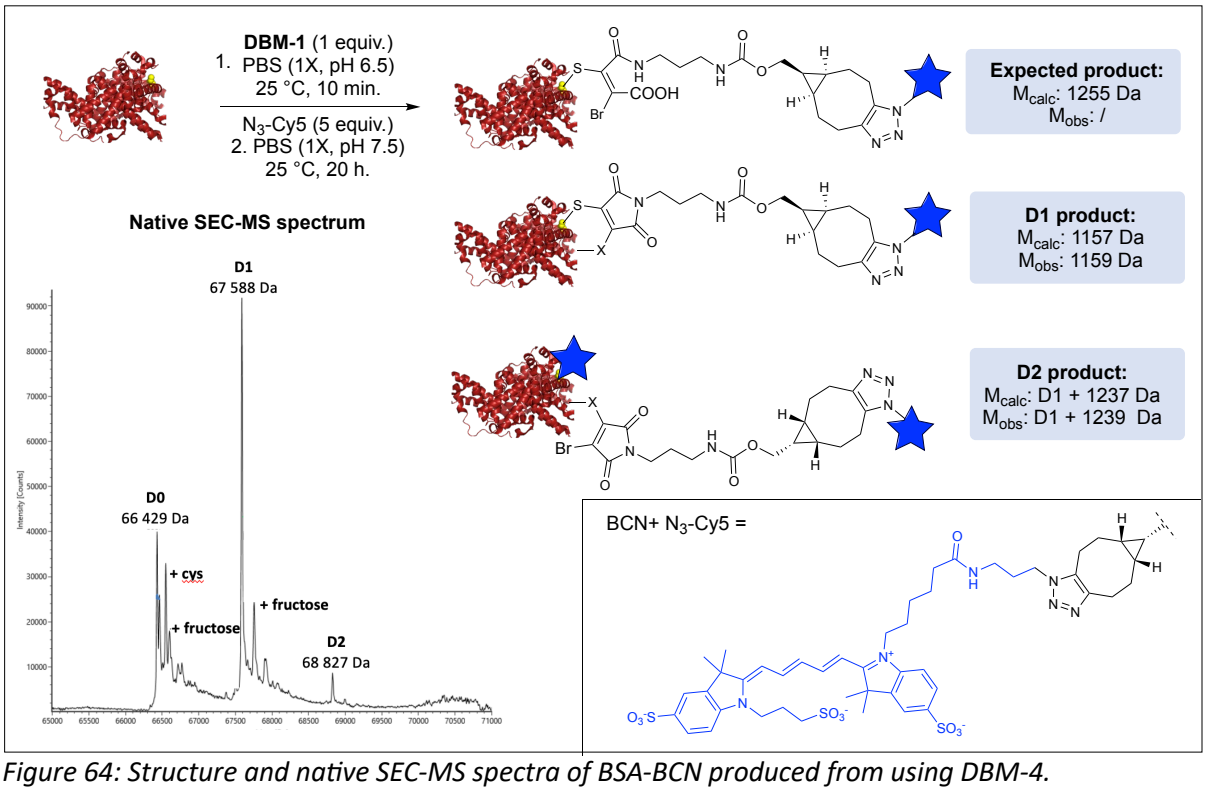

Figure 64: Structure and native SEC-MS spectra of BSA-BCN produced from using DBM-4.

Nevertheless, we managed to minimize this second addition to limit it to < 5% by using only 1 equiv. of **DBM-1** in PBS (1X, pH 6.5) and reducing the incubation time to 10 minutes. Any increase in reaction time, temperature or number of DBM equivalent was found to lead to an increase of the D2 species; surprisingly, varying the pH (from 6.5 to 8.5), usually crucial to prove competition between lysine and cysteine, did not seem to have a significant influence on the formation of the D2. SPAAC of the resulting BSA conjugates with **Cy5-azide** was found to reach completion under standard conditions – small excess in reagent (5 equiv.) in PBS (1X, pH 7.5) for 20 hours at 25 °C –; however, no hydrolysis of the maleimide ring was observed. Similar reactivity was observed when using other DBMs, with systematic loss of the two bromides on D1, small D2 species and no hydrolysis of the maleimide ring. Having developed conditions for the production of BCN-functionalized BSA, we decided to evaluate the feasibility of its SPAAC with tra-N_3 produced by our Ugi E1-selective conditions.

II.3.b. Tra-BSA dimers

As previously discussed, the chemical formation of protein dimers is a non-trivial process as it can result in complex mixture of compounds that can be hard to separate. Having our selective Ugi-E1 conditions in hands for the generation of tra-N_3 and a selective BSA-BCN production method, we assumed that the generation of homogeneous antibody-BSA dimers should be readily possible.

The structures of the different adducts that might be formed by such reaction are summed up in figure 66. Even if our E1 conditions are highly selective, the produced **tra-N_3** contains a mixture of three compounds, namely unmodified trastuzumab (**tra D0**), trastuzumab modified with one Ugi reaction (**tra-N_3 D1**) and trastuzumab modified with two Ugi reactions (**tra-N_3 D2**). The respective amount of each species is given by the native SEC-MS spectrum of the Ugi-E1 presented in figure 66, indicating that only 60% of all antibody species present in the medium bear an azide group and are thus able to react with a strained alkyne. Among these 60%, around 65% of the azido-functionalized trastuzumab possess a single azido handle (**tra-N_3 D1**) free to react with BSA-BCN to form tra-BSA (M = 212 940 Da), while the remaining 35% bear two azide groups (**tra-N_3 D2**) and can then lead to the formation of a trimer species composed of a trastuzumab functionalized with two BSA (**tra-BSA_2**, M = 280 007 Da). However, it is also possible that the **tra-N_3 D2** species reacts only once with BSA-BCN, leading to **Tra-N_3-BSA** (M = 213 252 Da), due to the steric hindrance caused by the first addition.

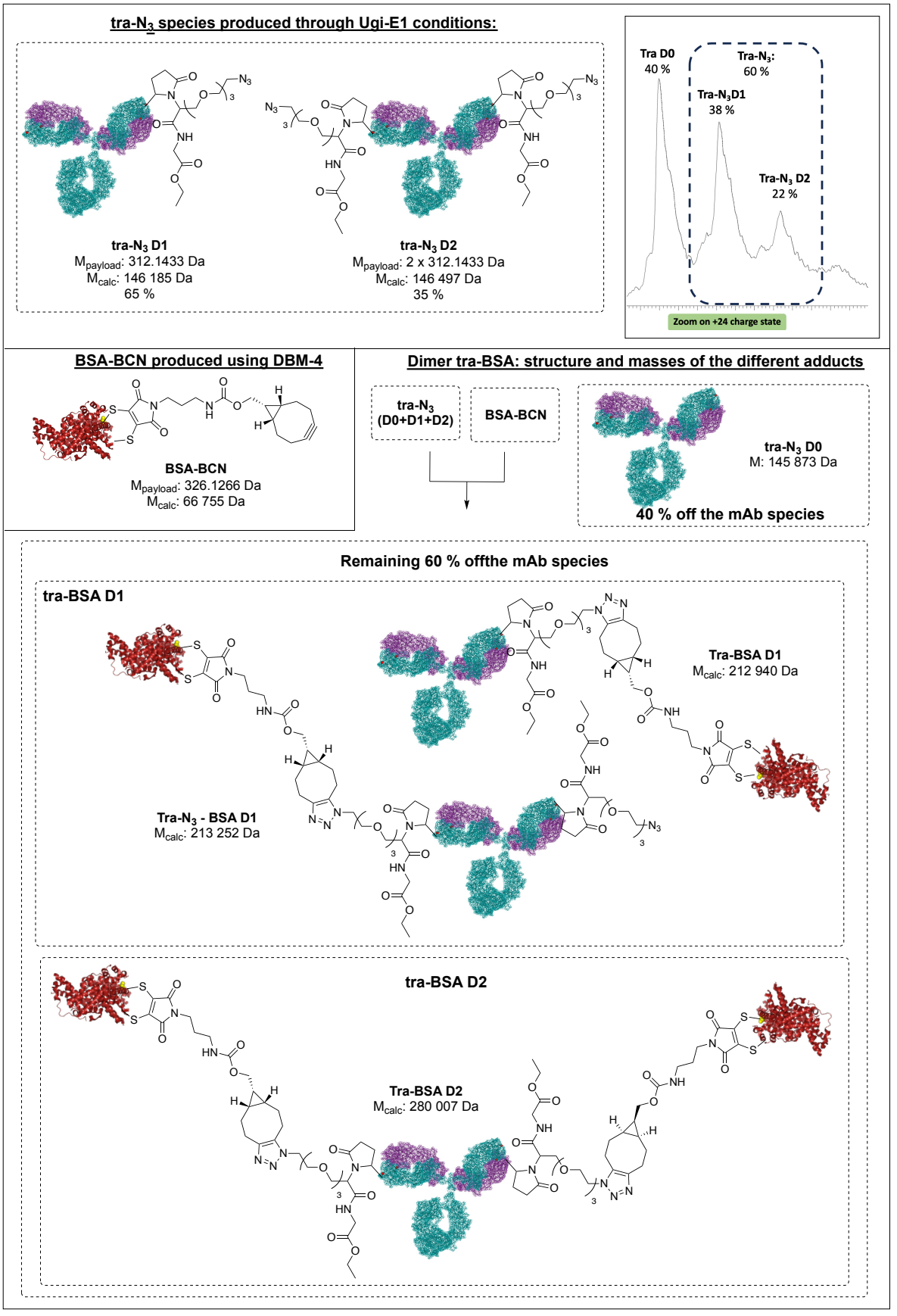

Figure 66: Structures and masses of the theoretical adducts resulting from the reaction of tra-N_3 and BSA-BCN.

In a first attempt to develop effective SPAAC conditions, we incubated 2 nmol of a 67 □M **tra-N_3** solution with 3 equivalents of **BSA-BCN** produced using **DBM-1**. This mixture was incubated at 37 °C for 24 hours before it was analysed by native SEC-MS (Figure 67). Four species, which could be quantified based on their absorbance at 280 nm, were separated by SEC (peak 1 to 4) and analysed by MS, allowing us to determine the composition of the reaction mixture. Peak 1 (24% of the formed species, elution time = 9.12 min.) was found to contain the excess of **BSA-BCN** introduced in the reaction mixture (M_{obs} = 66 758 Da; M_{calc} = 66 755 Da). The second peak (33% of the formed species, elution time = 8.68 min.) was found to contain a mixture of **BSA-BCN** — probably resulting from a poor separation from peak 1 by SEC — and of **tra-D0** (M_{obs} = 145 872 Da; M_{calc} = 145 873 Da). This indicates that the SPAAC reaction is complete under those conditions, as azido-functionalized trastuzumab species are no longer detected in the mixture. The third peak (29% of the formed species, elution time = 7.10 min.) was found to contain a mixture of two compounds: the first one — M_1 = 133 596 Da — was assigned as a **BSA-BCN** dimer, an artefact resulting from the analysis (M_{calc} = 133 510 Da), while the second one — M_2 = 213 052 Da — could be attributed either to the expected **tra-BSA** — with a shift in mass (Δ) of 112 Da in comparison with the expected 212 940 Da. Such shift can be linked to the presence of fructoselysine modification of BSA or to the co-elution of **tra-BSA** and **tra-N_3-BSA** resulting in average observed molecular weights. Peak 4 (14% of the formed species, elution

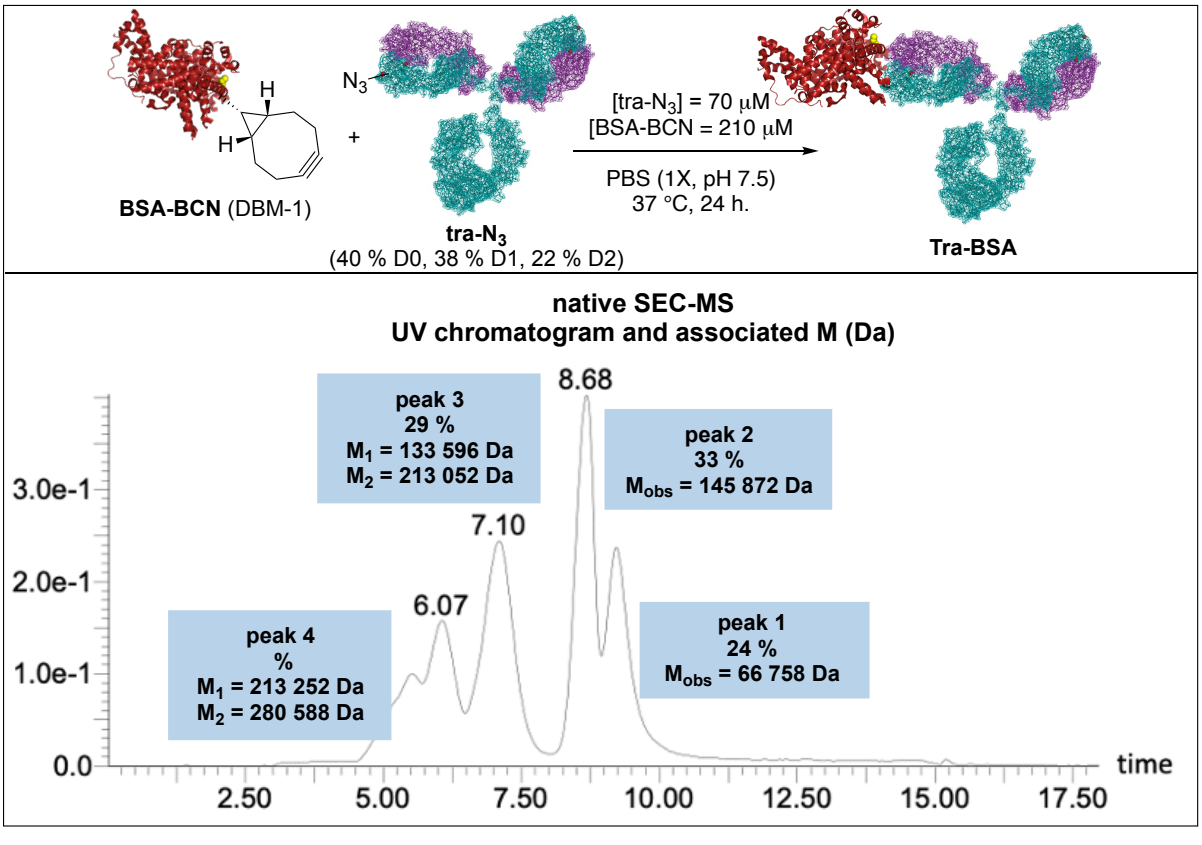

Figure 67: SDS-PAGE and native SEC-MS analysis of the reaction of tra-N_3 (70 □M) with 3 equiv. of BSA-BCN (from DBM-1) incubated a 37 °C for 24 hours.

time = 6.07 min) was found to contain a mixture of two high molecular-weight species (M_1 = 213 252 Da and 280 588 Da) which do not match the expected **D2** species (M_{calc} = 280 007 Da), urging us to hypothesize that those species might come from mAb aggregation due to the high concentration and temperature used for the reaction.

To validate this hypothesis, tra-N_3 was incubated in the presence of native BSA under the same reaction conditions. If the formation of BSA dimer was still observed (M_{calc} = 132 858 Da; M_{obs} = 132 863 Da), other high molecular weight species were also detected, which could not be identified (M_{obs} = 199 613 Da and 285 855 Da). Incubation of native trastuzumab with **BSA-BCN** did not lead to the detection of high molecular weight species suggesting the high molecular weight species are linked to the presence of a free thiol in BSA and that the high concentration and long incubation do not lead to trastuzumab's aggregation. Hence, we hypothesized that peak 4 species might present a mixture of the high molecular weight species observed upon incubation of **tra-N_3** and native BSA.

Variations in the reaction conditions was performed in order to minimize the formation of these aggregates, while conserving a full conversion of the azido species. For instance, we conducted an optimization campaign relying on analytical SEC quantification of the different formed species (Figure 68). We found that, in order to reach full conversion, the addition of an excess of **BSA-BCN** ($\geq$ 2 equiv.) was required as well as 48 hours of incubation time. Variation in the temperature and concentration of the solution showed low impact on the conversion and quantity of aggregates. On the other hand, large excess of **BSA-BCN** (4 equiv.) did lead to higher conversions, but no increased amounts of D1 species was observed to the profit of the

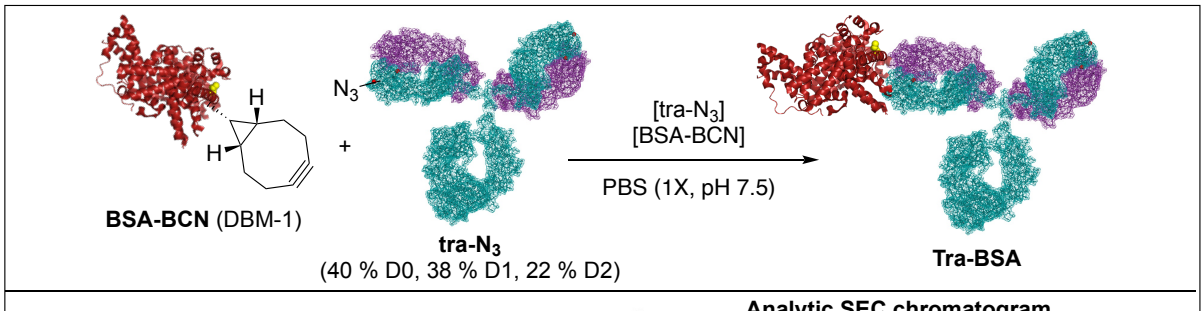

[tra-N_3] (μM)	[BSA-BCN] (μM)	T (°C)	t (h.)	Conv. (%)	% aggregates
100	100	25	48	29	6
100	100	37	48	51	18
100	200	25	24	51	13
100	200	25	48	63	26
100	200	37	24	53	13
100	200	37	48	62	24
50	100	37	48	55	18
100	400	37	24	71	32

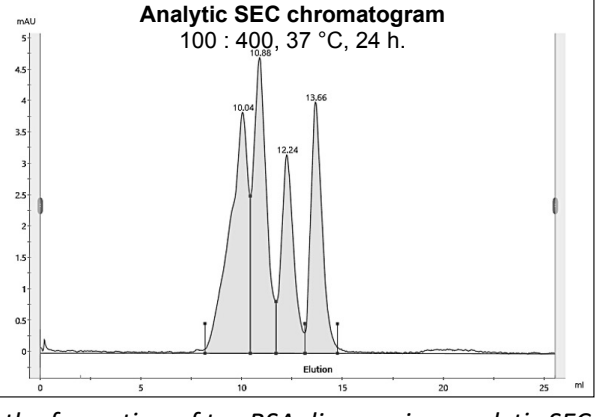

Figure 68: Optimization of the SPAAC conditions for the formation of tra-BSA dimer using analytic SEC.

aggregates peak. However this might come from the formation of D2 species, no separation from the previously observed aggregates was observed (Figure 68).

Having validated and optimised the formation of the expected protein dimer, we next engaged in its purification. Isolation of peak 3 by preparative SEC was attempted using an isocratic 0.5 mL/min flow of PBS (1X, pH 7.5) as eluent. The separation between all species was found to be challenging, as overlapping between peaks 3 and 4 was observed (Figure 68). Gratifyingly, better resolution was observed when concentrating the injected sample to at least 2 mg/mL. Our D1 species was isolated (purity ≥ 90%) with a 28% yield, calculated from the amount of tra-N_3 initially used — a corrected 47% yield is obtained if we consider that only 60% of the introduced tra-N_3 can actually form dimers (Figure 69). The detected mass (M = 213 216 Da) was in good agreement with either tra-BSA or with a mixture of tra-BSA and tra-N_3-BSA thus validating the formation of the desired dimer. Peak 4 was also isolated, albeit in too low concentration to be analysed by native SEC-MS, suggesting it contains some aggregates that might precipitate.

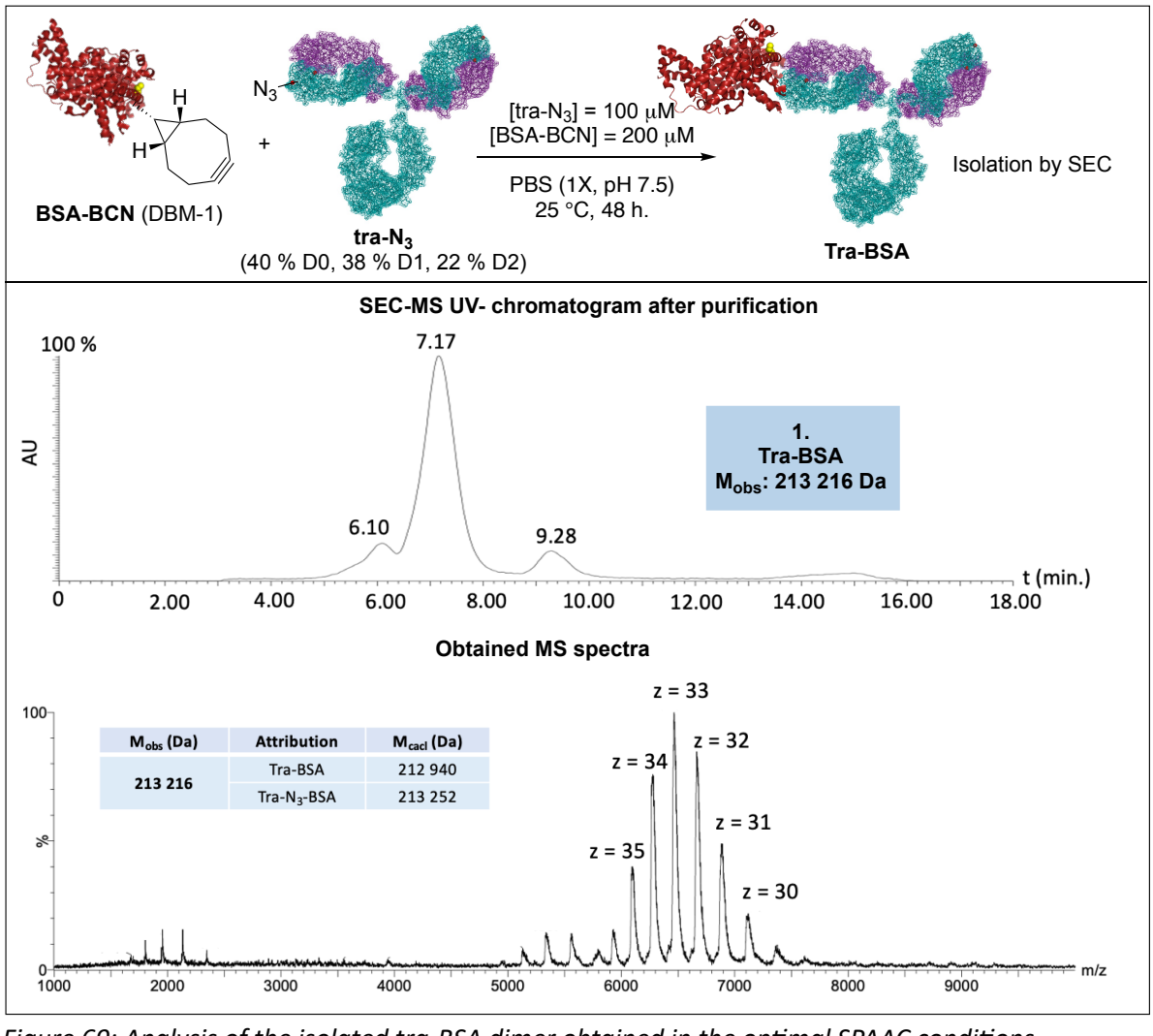

Figure 69: Analysis of the isolated tra-BSA dimer obtained in the optimal SPAAC conditions.

As a summary, we managed to develop conditions for the SPAAC reaction between **tra-N_3**, produced by Ugi reaction, and BSA-BCN, produced using a thiol-selective rebridging agent. We noticed that concentrated solutions were mandatory for the SPAAC to happen, along with elevated reaction times; however, the impact of the temperature was shown to be negligible. Due to the inherent heterogeneity of our BSA sample, presenting several by-species and adducts, the isolated dimers could not be linked to a precise species and are more likely to correspond to a mixture of four different compounds, *viz.* **tra-BSA**, **tra-BSA-fructoselysine**, **tra-N_3-BSA** and **tra-N_3-BSA-fructoselysine** (av. M = 213 200 Da, M_{obs} = 213 216 Da). While we selected BSA as a model protein to develop our SPAAC conditions, such antibody-BSA dimers could still be interesting for different applications, notably to generate drug conjugates with less systemic toxicity, which we will investigate in a near future. Having validated our approach and developed optimal conditions, we now needed to apply them to the production of our desired bsAbs.

II.3.c. bsAb formation

Following our successful production of **tra-BSA** dimers, we turned back to our previously developed **F_{rit}-BCN** coupling partner and applied our optimised conditions. We thus incubated 100 □M of **tra-N_3** with 200 □M of **F_{rit}-BCN** at 25 °C (Figure 70) and monitored the progress of the SPAAC by native SEC-MS after 24, 48 and 120 hours, to evaluate the time needed to reach completion. SEC allowed the separation of three different peaks (peak 1-3): peak 1 — elution

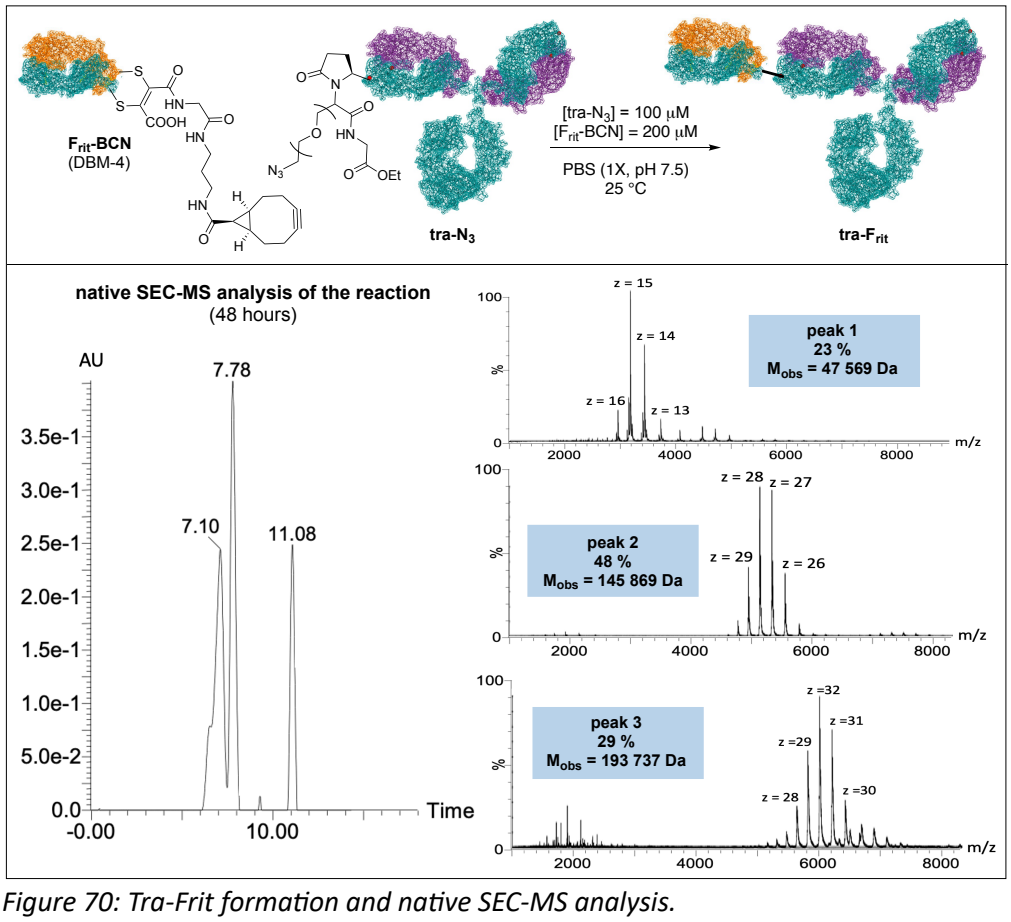

Figure 70: Tra-Frit formation and native SEC-MS analysis.

time = 11.08 min. — was found to contain **F_{rit}-BCN** (M_{obs} = 47 569 Da, M_{calc} = 47 551 Da); peak 2 — elution time = 7.78 min. — was found to contain **tra-N_3** (D0 + D1) after 24 hours (M_1 = 145 870 Da, M_2 = 146 173 Da, respectively) but only tra D0 after 48 hours (M_{obs} = 145 869 Da), suggesting that 48 hours were necessary for complete SPAAC to happen. Peak 3 — elution time = 7.10 mL— was found to contain a single compound, whose mass (M_{obs} = 193 737 Da) matched perfectly that of our expected **bsAb** (M_{calc} = 193 736 Da). Similar results were obtained after 120 h. and no higher molecular weight species were observed suggesting selective formation of tra-F_{rit} with neither aggregation nor formation of D2 species under those conditions.

Purification and isolation of the bsAb was then performed by preparative SEC. Because of the lower molecular weight of the Fab in comparison with BSA, the separation was found to be challenging, with overlapping of peaks 2 and 3 observed by preparative SEC (Figure 71). Any attempt in varying the eluent to increase the resolution was met with failure, while increasing the concentration of the loaded sample was found to be beneficial only to a certain extent. We suspect that the conjugated Fab might stack onto the full mAb resulting in a clear separation of the species under denaturing conditions, such as SDS-PAGE, but in a poor increase of the hydrodynamic radius, resulting in mediocre separation under native conditions (Figure 71). For these reasons, two consecutive purification runs were necessary to fully separate the bsAb from its parent mAb, delivering pure **Tra-F_{rit}** with a 48% yield (**tra-N_3** based). Analysis by native SEC-MS confirmed the isolation of the desired product and, in this case, mixture of **tra-F_{rit}**

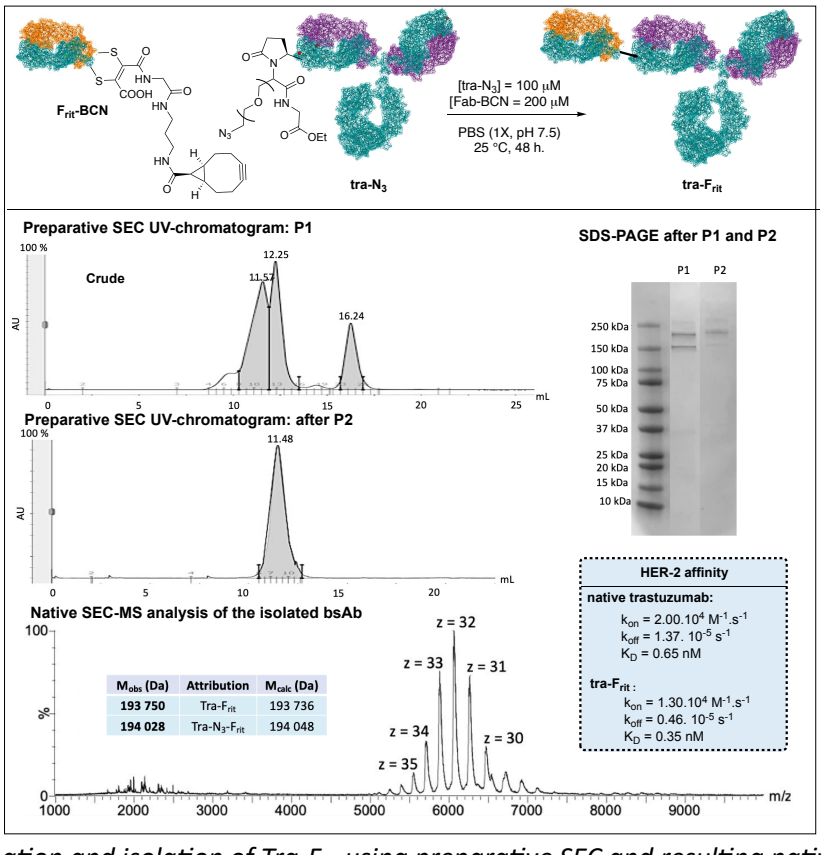

Figure 71: Formation and isolation of Tra-F_{rit} using preparative SEC and resulting nativeSEC-MS spectra.

(M_{obs} = 193 750 Da, M_{calc} = 193 736 Da) and **tra-N_3-F_{rit}** (M_{obs} = 194 028 Da, M_{calc} = 194 048 Da) was observed. Interestingly, pure unreacted **F_{rit}-BCN** could also be recovered and be recycled for bsAb production. A mixture of **tra-F_{rit}** and **tra-N_3-F_{rit}** was obtained which confirms that all the azido-functionalized forms of the introduced tra-N_3 were indeed functionalized however no more than one Fab was added to the full mAb, probably for steric reasons.

Having validated the formation of the bsAb, we then evaluated if the attachment of **F_{rit}** on the E1 residue of trastuzumab had an impact on its affinity for HER-2. Tra-F_{rit} was labelled with FITC and HER-2 affinity was measured using SKBR-3 cells as positive control and MDA-MB-231 cells as negative control using the LigandTracer technology. Intact affinity for HER-2 (K_D = 0.35 nM) was observed, comparable to the affinity of native trastuzumab (K_D = 0.65 nM) thus validating that the attachment of F_{rit} did not impair the recognition of the mAb (Figure 71).

Any variation in the used rebridging reagent (**DBM-1** and **DBM-2**) led to similar profiles with complete SPAAC being observed in all the cases. In the case of **DBM-2**, we hypothesized that the longer linker — PEG_4 — would provide greater flexibility and might lead to a bigger hydrodynamic radius, however no improved separation was observed (see experimental part).

Building on those positive results, other bsAbs were produced by varying the Fab-BCN produced using **DBM-4** — i.e., **F_{tra}**, **F_{durva}**, **F_{ave}** and **F_{muro}** – but also by using another Ugi-functionalized mAb – i.e., ramucirumab (**Ram-N_3**) –, as well as the pepsin-digested fragment of trastuzumab **F(ab')$_2$-tra-N_3**. Pleasingly, our method proved to be well applicable to these other proteins, allowing access to seven different bsAbs, albeit with lower yields than those observed for Tra.F_{rit} formation (Table 14). Interestingly, all the bsAbs produced from Ugi-functionalized trastuzumab showed excellent affinity for HER-2, comparable with that of native trastuzumab, and proving that the addition of a large biomolecule fragment has no impact on this key biological property of antibodies. In a similar way, Ram-F_{tra}, built around another whole IgG scaffold — ramucirumab —, showed only a slightly decreased affinity towards HER-2 receptor compared to native trastuzumab. As this construct is the only one for which the HER-2 recognition motif

Table 14: Key characteristics of the bsAb formed through SPAAC reaction.

bsAb	target 1	target 2	M_{obs} (Da)	M_{calc} (Da)	yield (%)	K_D (nM)
tra.F_{rit}	HER-2	CD20	193 750	193 736	48	0.35
			194 028	194 048		
tra.F_{tra}	HER-2	HER-2	194 209	194 193	22	0.50
			194 491	194 505		
tra-F_{durva}	HER-2	PD-L1	194 615	194 603	23	0.39
tra.F_{ave}	HER-2	PD-L1	193 410	193 411	24	0.49
			193 702	193 723		
tra.F_{muro}	HER-2	CD3	194 001	194 002	20	0.44
			194 290	194 314		
F(ab')$_2$tra.F_{muro}	HER-2	CD3	145 408	145 425	33	0.42
			146 052	146 049		
Ram.F_{tra}	VEGFR-2	HER-2	192 565	192 564	20	2.9
			192 861	192 876		

comes solely from the added Fab-fragment, it shows that the formation of the bsAb does not impair the recognition of the Fab fragment either.

Having validated our strategy and demonstrated that the site-selective Ugi reaction is a powerful conjugation method to access bsAbs, we wanted to engage in an in-depth pharmacological study of certain of our dimers, namely **tra-F$_{muro}$** and **F(ab')$_2$tra-F$_{muro}$**, as they possess a CD3-targeting Fab fragment capable of binding and activating T-cells, making them potential bispecific T-cell engagers (BiTE, see introduction). For those two BiTE formats, the CD3 and HER-2 occupancy as well as the T-cell-dependent cellular cytotoxicity (TDCC) was evaluated by the group of Professor Chris Scott, our collaborators at the Queen's University Belfast.

The binding of the **tra-F$_{muro}$** and **F(ab')$_2$tra-F$_{muro}$** constructs to human breast cancer HER2-expressing HCC1954 cells and human T lymphocyte CD3-expressing Jurkat cells was evaluated by flow cytometry. For this purpose, HCC1954 cells (HER2$^+$ CD3$^-$) and Jurkat cells (CD3$^+$ HER2$^-$) were incubated with the bsAb at 4 °C to prevent any premature receptor internalization. Following incubation, samples were washed to remove any unbound bsAb and stained with either phycoerythrin (PE)-conjugated anti-human IgG Fc secondary antibody or allophycocyanin (APC)-conjugated anti-CD3 secondary antibody. The results of the receptor occupancy studies showed clear binding of both bispecific constructs to CD3, indicated by a significant reduction in fluorescence of the bsAb-incubated samples in comparison with the untreated, APC-stained controls in Jurkat cells (Figure 72). This means that less CD3 receptor is available when the bsAb is added to the Jurkat cells thus validating its occupancy by the bsAb.

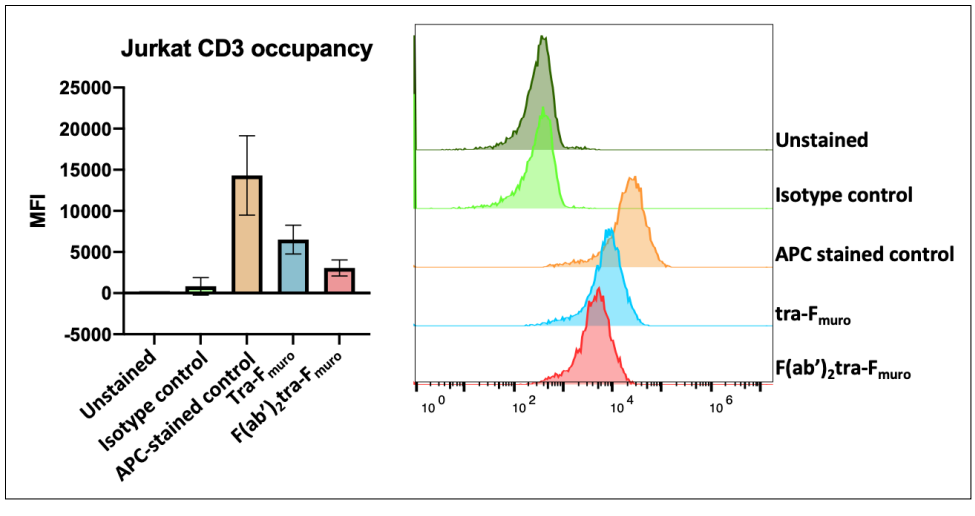

Figure 72: CD3 occupancy of tra-F$_{muro}$ and F(ab')$_2$tra-F$_{muro}$ evaluated on Jurkat cells.

Furthermore, binding of **tra-F_{muro}** to HER-2 was confirmed by a clear increase in fluorescence of the HCC1954 samples incubated with the bsAb (Figure 73) compared with untreated, PE-stained control, suggesting that the functionality of trastuzumab and paratopes of **tra-F_{muro}** was not hindered. Because of its intrinsic mechanism, validation of the HER-2 occupancy of **F(ab')$_2$-tra-F_{muro}** could not be evaluated using the same method (PE labelled anti-human IgG Fc secondary antibody) as this format does not comprise a Fc. However, our LigandTracer experiment showed that HER-2 recognition was not impaired on this format. The flow cytometry evaluation of the HER-2 occupancy of the **F(ab')$_2$tra-F_{muro}** will still be evaluated in the coming weeks, by using an appropriate APC-labelled anti human IgG Fab secondary antibody.

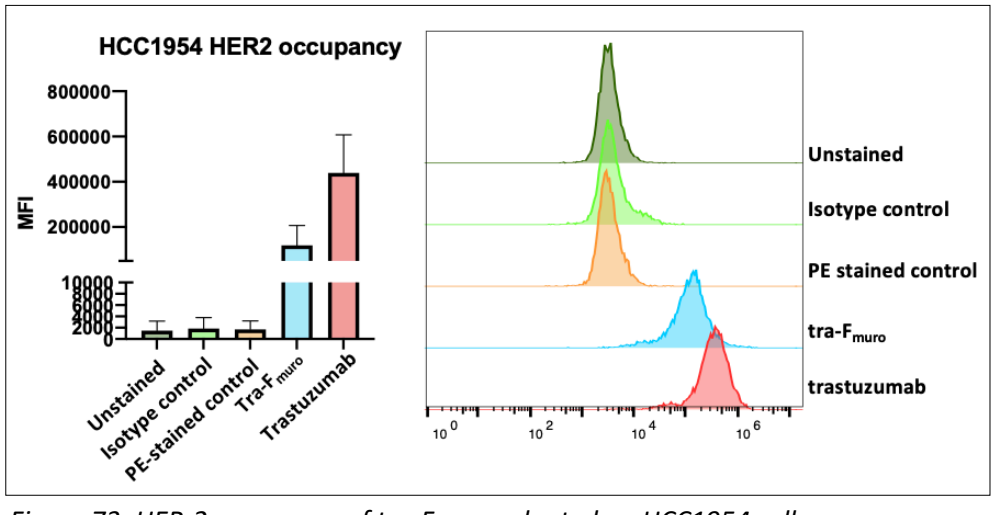

Figure 73: HER-2 occupancy of tra-F_{muro} evaluated on HCC1954 cells.

Following the confirmation that bsAbs maintain the antigen-binding properties of their parent mAb and Fab, their capability to induce TDCC upon tumour cell/T cell antigen engagement was evaluated *via* a 72 h dose response study. Briefly, HCC1954 cells were cultured with primary T cells isolated from buffy coats of healthy donors at an effector to target (E:T) ratio of 10:1 and treated with increasing concentrations of tra-F_{muro} or F(ab')$_2$tra-F_{muro} (9.9 pM – 2.53 nM and 13.7 pM – 3.5 nM, respectively). Following 72 h treatment, tumour cell viability was measured using CellTiter-Glo® assay (Promega) following the manufacturer's instructions. Both bsAbs showed to induce T cell-mediated cancer cell death in a dose-dependent manner, with the IC_{50} of tra-F_{muro} falling at 77 pM, and the IC_{50} of F(ab')$_2$tra-F_{muro} equating 83 pM (Figure 74). Control experiment showed that the addition of 500 □g/mL of pure trastuzumab in the co-culture did not lead to any toxicity thus validating the observed toxicity is only linked to the T-cell activation mediated by the used bsAb.

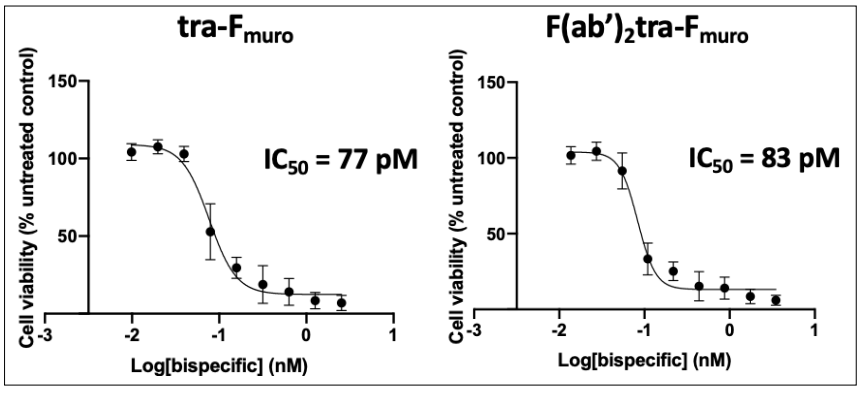

Figure 74: 72 hours dose response study in T cell - HCC1954 coculture (E:T, 10:1). Treating concentration of bsAbs: 500 □g/mL (tra-F_{muro} = 2.53 nM and F(ab')$_2$tra-F_{muro} = 3.5 nM). Each graph presents datas representative of three independent experiments performed using three different donors.

Those result show that our Ugi-based bsAbs indeed combine the affinities of the two parent mAbs for their respective targets. Moreover, in the case of HER-2xCD3 recognition, we were also able to show that our bsAbs did present good toxicity toward HCC1954 cells in presence of T-cells from three different donors.

If our format presents an asymmetric structure, resulting in a 2+1 valency, which is not common for the bsAbs produced by chemical conjugation, we showed that it does not impair neither the affinity nor the activity of the formed construct. Moreover, smaller and more compact formats were efficiently produced, showing similar properties.

V. Conclusion

Bispecific antibodies (bsAbs) are widely used for the treatment of complex multifactorial diseases such as cancer. The most widely described application of such construct is the combination of an anti-cancer specificity with an anti-T cell specificity leading to a construct, called bispecific T-cell engager (BiTE), that can trigger cancer cell death through re-orientation of the immune system. Nowadays, most of the bsAb are produced via genetic engineering but, this production method comes with necessity of new development for each desired combination of specificity resulting in high production costs and time. For this reason, employing site-selectively conjugated mAbs, whose reactivity was already described and analysed, as started to emerge as promising strategy for bsAb production allowing to simplify and thus accelerate the process.

We decided to evaluate the efficacy of our *N*-terminal selective Ugi 4C-3CR conditions, generating homogeneously azido-functionalized human mAbs, to produce bsAbs. We chose to introduce the second specificity by SPAAC reaction with a Fab fragment of a different mAb, through bioorthogonal chemistry, and developed efficient digestion methods for the generation

of Fab from five different off-the-shelf mAbs. Using the widely described DBM reagents, functionalized with a strained alkyne, we were able to site-selectively label them. However, the reaction between two proteins being impaired by steric hindrance between the two proteins, 48 hours of incubation at 25 °C, using two equivalents of BCN-functionalized Fab, were needed to lead to the full consumption of the azido functionalized mAb. Addition of a single Fab was observed in all cases, allowing the isolation and characterization of six different bsAbs presenting a 2+1 valency with yields varying from 20 to 48%.

Using the LigandTracer technology, we were able to validate that their affinity was not impaired whether the paratope came from the mAb or from the Fab. Among the formed bsAbs, two were T-cell engager formats — through recognition of CD3 from T cells and HER-2 from breast cancer — and, thanks to collaborators from the Queen's University of Belfast, we were able to validate both their CD3 and HER-2 occupancy as well as good T-cell dependent cellular cytotoxicity with IC_{50} around 80 pM in both cases.

In addition, this method could also be applied to the formation and isolation of other protein dimers such as trastuzumab-BSA dimers. As our protein dimers present intact disulfide bonds, they could allow their further homogeneous functionalization using widely described rebdirging methods and pave the way toward the formation of bsAb-drug conjugates.

General conclusion and perspectives

During this thesis, different aspects of the site-selective chemical conjugation of native proteins were studied. The first aspect concerned the development of site-selective methods, based on the use of multicomponent reactions for the labelling of either a single chemical function of the protein or two spatially close chemical functions of the protein borne by a single residue or two different residues. The second aspect concerned the exploration of the applications of such selective method, in our case for the formation of protein dimers and more precisely bispecific antibodies.

In a first part, we evaluated the use of the Robinson-Schöpf 3-CR for the selective labelling of lysine residues of native trastuzumab — a therapeutic monoclonal antibody used in the treatment of HER-2 positive breast cancer. This reaction between a primary amine, succinaldehyde **1** and 3-oxoglutaric acid **3** was described to lead to the formation of tropinone under acidic conditions (pH 5.0) and medium heating to 40 °C. On proteins, the reaction was found to compete with many other side reactions that could not be all identified resulting in highly heterogeneous labelling (Figure 75). Any variation in the reaction conditions did not lead to the desired, full tropinone functionalization, suggesting this reaction is not yet suitable for the labelling of proteins. However, during the investigation, we managed to develop conditions which seemed to lead to selective pyrrole functionalization of trastuzumab with good conversion (> 60%) and av. DoC > 1.3 (Figure 75). Because pyrroles can react as diene in Diels-Alder reactions, we can imagine further functionalization of such functionalized mAb using the appropriate dienophile.

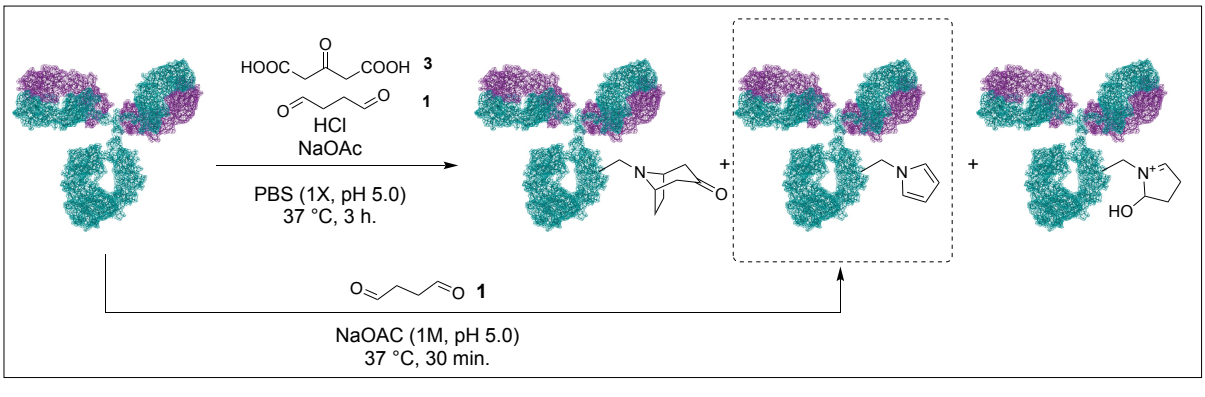

Figure 75: Outcome of the investigation of the Robinson-Schöpf reaction for the labelling of trastuzumab.

Parallel to this study, we explored the Ugi-4C-3CR for the labelling of trastuzumab. This four-component reaction between a primary amine, a carboxylic acid, an isocyanide and a carbonyl was reported by our team to efficiently label trastuzumab through both Ugi and Passerini mechanism. In this case, trastuzumab is either source of both amine and carboxylic acid, in the case of an Ugi mechanism, or source of only carboxylic acid in the case of a Passerini reaction. First, we evaluated if the variation of the used carbonyl from aldehyde **6** to a preformed imine

— under the form of α-chlorooxime **8** or hydrazone **14** — might lead, in presence of isocyanide **a**, to selective labelling of Asp and Glu of the protein through an Ugi-like mechanism.

The highly electrophilic α-chlorooxime **8** was found to react in a very fast manner with trastuzumab, as good conversions and av. DoC — i.e., 59 % and 0.9 — were observed after only 2 h incubation at 4 °C. However, a control experiment showed that the reaction does not follow the expected Ugi-like mechanism, as the isocyanide had no influence on the reaction. A competition experiment suggested that the nucleophilic amino acids responsible for the conjugation are either Asp, Glu or His residues (Figure 76). This peculiar reactivity contrasts with previously reported chlorooxime-isocyanide based MCR, necessitating deeper mechanistic studies to be conducted in order to better understand it. However the great observed homogeneity of the conjugation makes it interesting for further investigation.

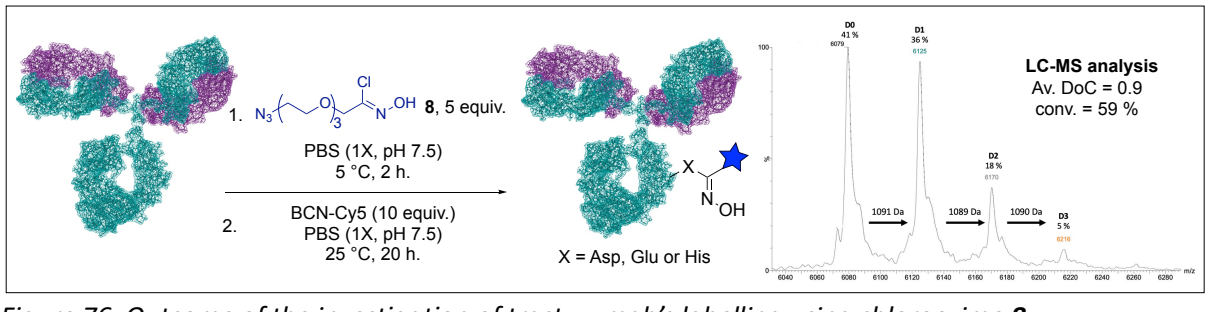

*Figure 76: Outcome of the investigation of trastuzumab's labelling using chlorooxime **8**.*

Reaction of hydrazone **14**, in presence of isocyanide **a** led to the labelling of trastuzumab with medium conv. and av. DoC — i.e., 43% and 0.5. Because no MCR involving a hydrazone was reported, we engaged in a study to understand the mechanism of the modification (Figure 77). It appeared that the hydrazone is likely to undergo a transamination step with a primary amine borne by the protein, before it reacts with an isocyanide and a carboxylic acid following the classical Ugi mechanism. It is also possible that a small fraction of the introduced hydrazone is hydrolyzed, albeit to a lesser extent. Such reactivity is of great interest because, if the transamination process is validated then we will have selected a Ugi mechanism as, in this case no Passerini reaction should happen. Interestingly, those conditions showed poor tolerance for isocyanide's side chain variation which raised our attention toward the influence of the reagent's side chain on the selectivity of the reaction. Considering the low obtained conv. and DoC values, we decided to go back to the use of an aldehyde **6** as carbonyl electrophile to study deeper the influence of the isocyanide's side chain variation on the selectivity of the reaction.

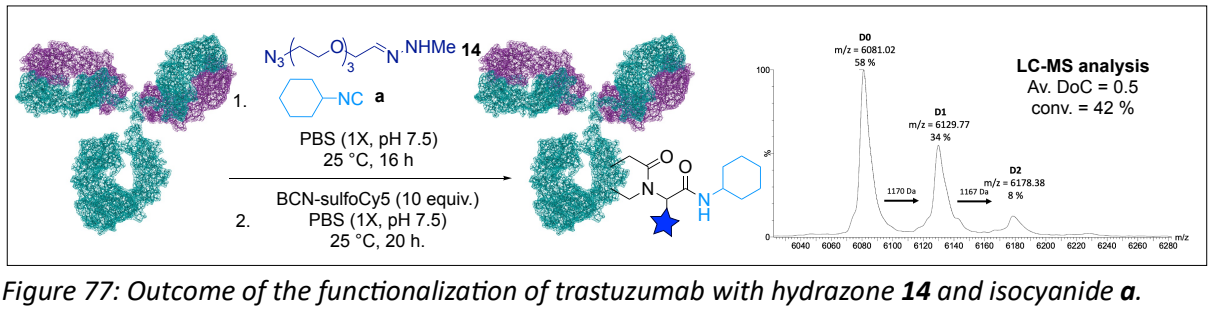

*Figure 77: Outcome of the functionalization of trastuzumab with hydrazone **14** and isocyanide **a**.*

We found that the association of isocyanide **d** and aldehyde **6** led to the selective Ugi 4C-3CR labelling of *N*-terminal glutamic acid (E1) residue via an intra-residue mechanism with good conv. and av. DoC — i.e., 60% and 0.9 (Figure 78). We were able to show *N*-terminal selectivity was conserved when increasing the protein concentration or using a different human or humanized mAb, even though this was at the expense of selectivity. The high tolerance of the Ugi reaction for variations in the side chains of the used reagents allowed us to maintain a plug and play approach while developing our *N*-terminal selective condition. This means that virtually any payload can be introduced on the azido functionalized mAb.

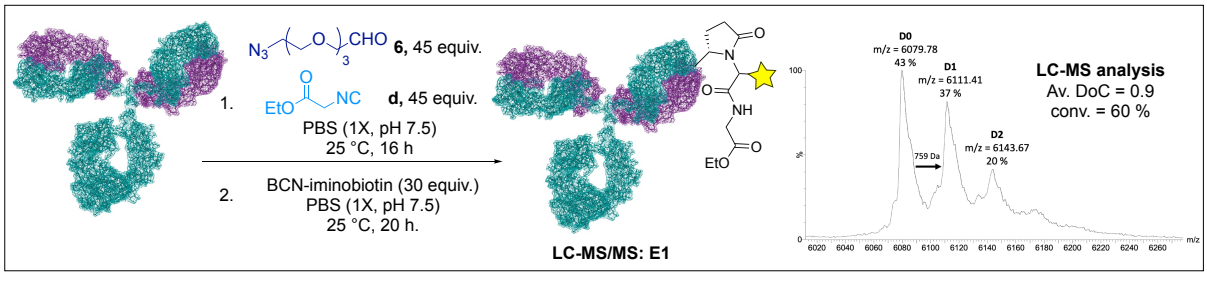

*Figure 78: N-ter selective U-4C-3CR using aldehyde **6** and isocyanide **d**.*

With the aim of developing a highly tuneable method for the formation of bsAbs via SPAAC reaction, we turned toward the introduction of Fab fragments functionalized with strained alkyne in order to add them to our Ugi-modified mAb. Hence, we developed conditions for the digestion of various off the shelf mAbs into Fab fragments — through either pepsin and/or papain digestion — and we used the widely described DBM reagents for their site-selective functionalization with a BCN strained alkyne, yielding Fab-BCN compounds with good yields. After a quick optimization monitored by analytic SEC, we found that incubation of azido functionalized protein (100 □M) with 2 equiv. of BCN-functionalized protein in PBS (1X, pH 7.5) at 25 °C for 48 hours led to complete SPAAC and to the formation of the desired bsAb (Figure 79). Isolation of the obtained bsAb was performed by SEC with yields varying from 20 to 48% and we were able to show that their affinity toward HER-2 receptors was retained in all of

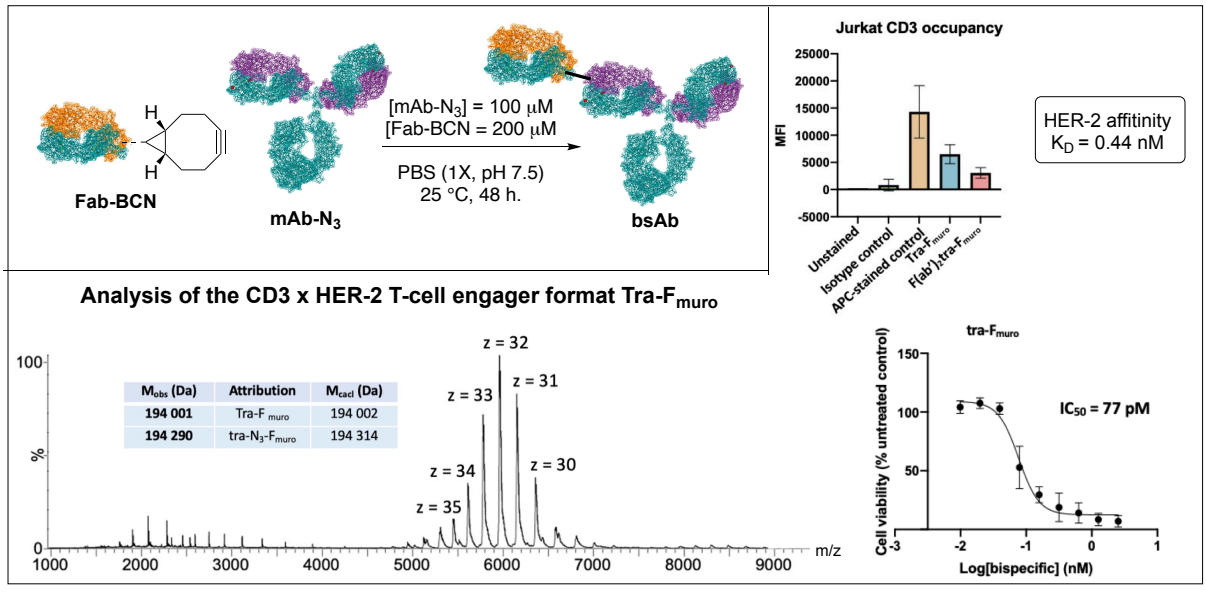

Figure 79: Example of the formation of a bispecific T-cell engager based on the use of the U-4C-3CR.

the formed bsAbs using the LigandTracer technology. We even managed to produce two bispecific T-cell engager formats, targeting both CD3 and HER-2, which showed excellent CD3 and HER-2 occupancy as well as T-cell dependant cellular cytotoxicity with IC_{50} around 80 pM (Figure 79).

We have shown that the selectivity provided by our *N*-ter selective Ugi 4C-3CR conditions allows the formation of virtually any human and humanized mAb-based bsAb with conserved affinity from both the parent mAbs and even good activity in the case of bispecific T cell engager. Because our bsAb production method is based on *N*-terminal selectivity, the further functionalization of the formed bsAb through rebridging of the full mAbs's disulfide bridge can be considered thus leading to the homogeneous formation of bsAb drug conjugate.

Experimental part

I. Materials and methods

I.1. Synthetic chemistry

All reagents were obtained from commercial sources and used without any further purifications. Dry solvents were obtained from Sigma-Aldrich. Column chromatography was carried out using silica gel G-25 (40-63 µm) from Macherey-Nagel. Thin layer chromatography (TLC) was performed using plates cut in aluminum sheets (ALUGRAM Xtra SIL G/UV254) purchased from Macherey-Nagel. Visualization was achieved under a 254 or 365 nm UV light and by using an appropriate TLC stain.

I.2. Spectroscopy and spectrometry

^{1}H and ^{13}C NMR: NMR spectra were recorded at 23 °C on Bruker Avance III - 400 MHz / 500 MHz spectrometers. Recorded shifts (δ) are reported in parts per million (ppm) and calibrated using residual non-deuterated solvent. Data are represented as follows: chemical shift, multiplicity (s = singlet, d = doublet, t = triplet, q = quartet, m = multiplet, br = broad, app = apparent), coupling constant (*J*, Hz), integration and assignment in case of ^{1}H NMR data.

High-resolution mass spectra (HRMS): HRMS spectra were obtained using an Agilent Q-TOF 6520.

IR spectra: Spectra were recorded in a Thermo-Nicolet FT/IR-380 spectrometer. Spectra were interpreted with OMNIC 9 software and are reported in cm^{-1}. The abbreviations used are: w (weak), m (medium), s (strong) and br (broad).

Melting points: Melting points were determined on a melting point apparatus SMP3 from Stuart Scientific.

LC/MS of native proteins: The spectrometer was coupled to an automated chip-based nanoESI infusion source (Triversa Nanomate, Advion, Ithaca, NY) both operating in positive ion mode. Electrospray ionization was conducted at a capillary voltage of 1.75 kV and nitrogen nanoflow of 0.75 psi. Samples were directly infused after manual desalting step at a concentration of 10 µM. Average DoC values were calculated using the following equation:

$$DoC = \frac{\sum_{k=0}^{8} k\ x\ intensity\ DoC\ k}{\sum_{k=0}^{8} intensity\ DoC\ k}$$

These results were derived from the relative peak intensities measured from deconvoluted mass spectra, following a method developed and validated by the Sarah Cianférani group.

LCT spectrometer (Waters, Manchester, UK): The extraction cone value was set to 5 V or 50 V and the cone voltage was set to 120 V or 180 V for cysteine-conjugates and lysine-conjugates, respectively. The pressure in the interface region was fixed at 6 mbar. Acquisitions were performed in the m/z range 1,000–10,000 with a 4 s. scan time. External calibration was performed using singly charged ions produced by a 2 g/L solution of cesium iodide in 2-propanol/water (50/50 v/v). MS data interpretations were performed using Mass Lynx V4.1 (Waters, Manchester, UK).

Exactive Plus EMR (Thermo Fisher, Bremen, Germany): The spectrometer was coupled to an automated chip-based nanoESI infusion source (Triversa Nanomate, Advion, Ithaca, NY) both operating in positive ion mode. Electrospray ionization was conducted at a capillary voltage of 1.75 kV and nitrogen nanoflow of 0.75 psi. Samples were directly infused after manual desalting step at a concentration of 10 µM. The in-source collision- induced dissociation (CID) was set to 75 eV for cysteine-conjugates and optimized between 75 - 150 eV for lysine-conjugates. The higher-energy collisional dissociation (HCD) cell was set to 10 eV for each analysis to improve the desolvation. The trapping gas pressure was set to 7 a.u. (which corresponds to an Ultra High Vacuum of 1.10^{-9} mbar). To improve the transmission of the high mass species, the voltages on the injection-, inter-, and bent-flatapoles were fixed to 8, 7, and 6 V, respectively. Acquisitions were performed in the m/z range 1,000– 10,000 with a 3 s scan time and a resolution of 17,500 at 200 m/z with an automatic gain control (AGC target) fixed to 1.10^{6} and a maximum injection time set to 100 ms. External calibration was performed using singly charged ions produced by a 2 g/L solution of cesium iodide in 2-propanol/water (50/50 v/v). Orbitrap MS data interpretation was performed using BioPharmaFinder 2.0 (Thermo Fisher Scientific, Bremen, Germany).

Native SEC- MS of native proteins:

Synapt G2 HDMS (Waters, Manchester, UK): An ACQUITY UPLC H-class system (Waters, Manchester, UK) comprising a quaternary solvent manager, a sample manager cooled at 10 °C, a column oven maintained at room temperature and an UV detector operating at 280 nm and 214 nm hyphenated to a Synapt G2 HDMS mass spectrometer (Waters, Manchester, UK) was used for the online native SEC-MS instrumentation. Forty micrograms of mAb were loaded on the ACQUITY UPLC Protein BEH SEC column (4.6 x 150 mm, 1.7 µm particle size, 200 Å pore size) from Waters (Manchester, UK) using an isocratic elution of 100 mM ammonium acetate (NH_4OAc) at pH 6.9 with the following flow rate gradient: 0.250 mL/min over 3.0 min, then 0.100 mL/min from 3.1 to 15.0 min, and finally 0.250 mL/min from 15.1 to 18.0 min. The Synapt G2 HDMS was operated in positive mode with a capillary voltage of 3.0 kV while sample cone and pressure in the interface region were set to 180 V and 6 mbar, respectively. Acquisitions were performed in 1,000–10,000 m/z range with a 1.5 s scan time. The mass spectrometer was

calibrated using singly charged ions produced by a 2 g/L solution of cesium iodide (Acros organics, Thermo Fisher Scientific, Waltham, MA USA) in 2-propanol/water (50/50 v/v). Native MS data interpretations were performed using Mass Lynx V4.1 (Waters, Manchester, UK).

BioAccord system (Waters, Manchester, UK): Comprising a binary solvent manager, a sample manager cooled at 8 °C, a column oven maintained at room temperature and an UV detector operating at 280 nm and 214 nm hyphenated to the ACQUITY RDa detector was used for the online SEC-native MS instrumentation. Around twenty micrograms of antibody were loaded on the ACQUITY UPLC Protein BEH SEC column (2.1 x 150 mm, 1.7 µm particle size, 200 Å pore size) from Waters (Manchester, UK) using 0.100 mL/min flow rate and isocratic elution of 100 mM ammonium acetate (NH4OAc) at pH 6.9 for a 6 min total run.
The ACQUITY RDa detector (TOF analyzer) was operated in positive mode with a capillary voltage of 1.5 kV while sample cone and desolvation temperature were set to 120 or 160 V (cystein or lysine conjugate) and 250 °C, respectively. Acquisitions were performed under full scan mode and high mass range (400–7,000 m/z) with 2 Hz scan rate. The mass spectrometer was calibrated using the ACQUITY RDa Detector Calibrant and Wash Kit (Waters, Manchester, UK, ref. 186009013). The ACQUITY RDa Waters connect LockMass Kit (Waters, Manchester, UK, ref. 186009298) was used before and after each injection in order to compensate for mass variations due to temperature changes in the laboratory. UNIFI Scientific Information System (Waters, Manchester, UK) was used as a single solution to encompass data acquisition and processing.

Peptide mapping analysis:

Trypsin digestion

20 µg of sample were solubilized in 150 mM NH_4HCO_3, 0.1% RapiGest (Waters) at pH 7.8, to obtain a final volume of 24 µL. Disulfide reduction was performed by incubating the solution with 5 mM DTT for 30 min at 57 °C. Alkylation of cysteines was performed in 10 mM IAM in the dark at room temperature for 40 min The enzyme was prepared by suspending 20 µg of trypsin in 100 µL of H_2O. Digestion was performed by adding 1 µL of trypsin (Promega, V5111), which corresponds to a 1:100 enzyme:substrate ratio. Samples were incubated overnight at 37°C. The reaction was stopped by 1% of TFA. RapiGest was eliminated by incubation at 37°C for 30 min and centrifugation at 10,000 g for 5 min.

nanoLC-MS/MS

The analysis were performed using a nanoACQUITY Ultra-Performance-LC (Waters) coupled to a Q Exactive HF-X Hybrid Quadrupole-Orbitrap Mass Spectrometer (ThermoFisher). A volume equivalent to 140 ng of digest were trapped on a Symmetry C18 pre-column (180 µm x 20 mm, 5 µm particle size, Waters) and the peptides were separated on an ACQUITY UPLC® BEH130 C18 separation column (75 µm × 250 mm, 1.7 µm particle size, Waters). The solvent system consisted of 0.1% FA in water (solvent A) and 0.1% FA in acetonitrile (solvent B). Peptide trapping was performed during 3 min at a flow rate of 5 µL/min with 99% A and 1% B and elution was performed at 60 °C at a flow rate of 350 nL/min from 6% to 40% of B in 43 min. MS and

MS/MS acquisition were performed in positive mode, with the following settings: spray voltage 1800 V and capillary temperature 250°C. The MS scan had a resolution of 70000, the AGC target was $3x10^6$ and the maximum IT was 50 ms on m/z [300-1800] range. The MS/MS scans were acquired at a resolution of 17500, the AGC target was $1x10^5$ and the maximum IT was 100 ms with fixed first mass of 100 m/z and Isolation window of 2 m/z. Top 10 HCD was selected with intensity threshold of $5x10^4$ and dynamic exclusion of 3 s. The normalized collision energy was fixed at 27 V. The complete system was fully controlled by Thermo Scientific™ Xcalibur™ software. Raw data collected were processed and converted with MSConvert into .mgf peak list format.

Peptide identification

Identification of peptides was performed by using the search engine MASCOT 2.6.2 algorithm (Matrix Science). The search was performed against the amino acid sequence of the protein. Spectra were searched with a mass tolerance of 10 ppm for MS and 0.05 Da for MS/MS data. The search was made without enzyme specified, in order to allow the identification of any non-specific peptide cleavage. Variable modifications were specified: carbamidomethylation of cysteine residues, oxidation of methionine residues and adduct of Ugi (see table) payload on lysine, aspartate and glutamate residues. Peptide identifications were validated with a minimal Mascot ion score of 25. Peptides containing Ugi or Passerini payload were validated with the following criteria: be a tryptic peptide (without unspecific cleavage), the retention time higher than that of the unmodified peptide, identification of signature fragment ions (characteristic of payload fragmentation in the spectrum).

Couple aldehyde /isocyanide	**Mass of Ugi adduct**	**Mass of Passerini adduct**	**m/z of signature fragment ions**
6/a	769.4309	787.4415	286.172 – 637.343
6/d	773.3894	791.4000	286.172 – 637.343
6/c	743.4153	761.4258	286.172 – 637.343
18/g	770.4262	788.7257	286.172 – 637.343
18/f	712.3843	730.3949	292.187
18/e	1058.5583	1076.5688	286.172 – 637.343

II. General procedures

Protein concentration: 1 □L of sample was used for concentration measurement by absorbance spectrometry at 280 nm using a NanoDrop spectrophotometer (Thermo Fisher Scientific, Illkirch, France). In case of impaired absorbance at 280 nm or unknown extinction coefficient of a protein or conjugate, BCA assay was performed.

SDS-PAGE: Gel electrophoresis was performed on 4 – 15% Mini-PROTEAN® TGXTM gel (Bio-Rad, Hercules, U.S.A) following standard lab procedures. To the samples containing protein conjugates (24 µL, 0.1 mg/mL solution in H_2O) was added 8 µL of loading buffer 120 (Laemmli SDS sample buffer, reducing or not) and heated at 95 °C for 3 min. The gel was run at constant voltage (200 V) for 35 min using TRIS 0.25 M – Glycine 1.92 M – SDS 1% as a running buffer. The fluorescence was visualized on GeneGenius bio-imaging system prior to staining with Coomassie blue.

BCA assay: In certain cases, protein concentration was assessed using BCA Protein Assay kit (Ref. 23224, Thermo Fisher Scientific, Illkirch, France) using BSA diluted in PBS (1X, pH 7.5) as ladder concentration.

Deglycosylation: Prior to native MS analysis the mAb's glycans were removed using 10 nL/µg mAb of Remove-iT® Endo S (New England Biolabs, Ipswich, U.S.A)

Manual desalting: The deglycosylated mAb were then desalted against 150 mM ammonium acetate solution buffered at pH 7.5 using ten cycles of concentration/dilution on Vivaspin centrifugal concentrators (500 µL, 50 kDa).

Preparative size exclusion chromatography: The volume of the protein's containing sample was adjusted to 100 □L using PBS (1X, pH 7.5). It was then directly injected in a 500-□L loop plugged on an AKTA pure system, loaded on a Superdex^{TM} 200 Increase 10/300 GL column and eluted using an isocratic 0.5 mL/min flow of PBS (1X, pH 7.5) for two column volumes. Fractions were collected according to their absorption at 280 nm (collection started Abs > 0.5 UA).

Analytical size exclusion chromatography: Protein containing solution (20 □g) was diluted to 100 □L using PBS (1X, pH 7.5) before it was injected in a 500 □L loop plugged on an AKTA pure system. It was then loaded on a Superdex^{TM} 200 Increase 10/300 GL column and eluted using an isocratic 0.5 mL/min flow of PBS (1X, pH 7.5) for 1.5 column volum.

III. Organic synthesis and characterization

2-Acetamido-*N*-methyl-6-(3-oxo-8-azabicyclo[3.2.1]octan-8-yl)hexanamide (Lys-trop):

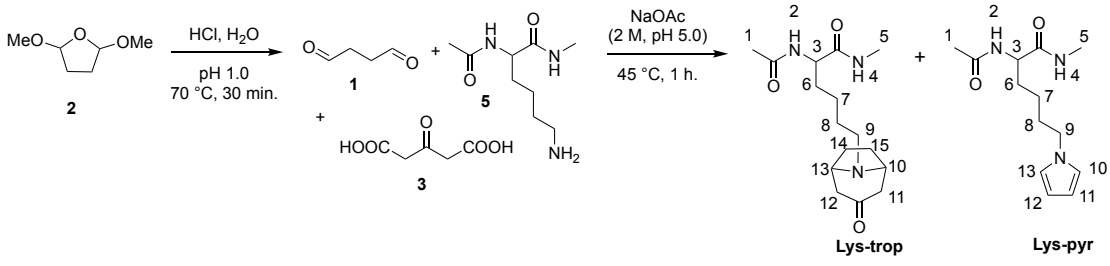

To 1 L of mQ H_2O, 164 g of NaOAc were added. Once all the salt was solubilized pH was adjusted to 5 using a 1 M HCl aqueous solution to give a 2 M NaOAc buffer (stored at room temperature(r.t.) in a glass bottle). In a 1.5 mL Eppendorf, 2,5-dimethoxytetrahydrofuran **2** (100 µL, 0.76 mmol, 1 equiv.) was added to 254 µL of mQ H_2O and HCl, (10 µL from a 38% solution in H_2O, 0.12 mmol, 0.16 equiv.) was added. pH was measured using pH paper and adjusted to 1 if required. Eppendorf was then shaken at 600 rpm and heated at 70 °C using a bioshaker for 30 min leading to a solution of 1,4-butanedial **1**. In a microwave tube, Ac-Lys-NHMe **5** (168 mg, 0.84 mmol, 1.1 equiv.) and 3-oxoglutaric acid **3** (123 mg, 0.84 mmol, 1.1 equiv.) were solved in 3 mL of NaOAc buffer (2 M, pH 5) and the mixture was cooled to 0 °C using an ice bath. The butanedial solution was also cooled to 0 °C before it was added to the amino acid containing solution. The microwave tube was then heated to 45 °C for 1 h using a sand bath before it was cooled to room temperature and alkalanized to pH 10 using a 1 M NaOH aqueous solution and excess of NaCl was added. Resulting aqueous layer was extracted with five times with DCM (10 mL) and combined organic layers were dried over Na_2SO_4, filtered and concentrated under reduced pressure to give desired compound as a white solid in a mixture of lysine-pyrrole (9:1) (106 mg).

Lysine-tropinone adduct:

^{1}H NMR (400 MHz, DMSO-d_6) δ 7.96 (d, *J* = 8.2 Hz, 1H, H2), 7.84 (q, *J* = 4.5 Hz, 1H, H4), 4.15 (td, *J* = 8.4, 5.5 Hz, 1H, H3), 3.81 (m, 2H, H13, H10), 2.64 – 2.41 (m, 7H, H5, H9, H11'-12'), 2.05 – 1.95 (m, 2H, H11''-H12''), 1.89 (m, 2H, H14'-15'), 1.83 (s, 3H, H1), 1.68 – 1.20 (m, 8H, H14''-15'', H6-8)

^{13}C NMR (101 MHz, DMSO-d_6) δ 209.9, 172.8, 169.8, 58.3 (2C), 52.9, 49.3, 47.1 (2C), 32.5 (2C), 28.5, 28.1, 26.0, 23.8, 23.0.

BRMS (ESI+) calcd for $C_{16}H_{28}N_3O_3^+$ $[M+H]^+$ 310.2125, found: 310.1775.

Lysine-pyrrole adduct:

^{1}H NMR (400 MHz, DMSO-d_6) δ 7.96 (d, *J* = 8.2 Hz, 1H, H2), 7.84 (q, *J* = 4.5 Hz, 1H, H4), 6.69 (t, *J* = 2.1 Hz, 2H, H10,H13), 5.94 (t, *J* = 2.1 Hz, 2H, H11-12), 4.15 (td, *J* = 8.4, 5.5 Hz, 1H, H3), 2.64 – 2.41 (m, 5H, H5, H9), 1.83 (s, 3H, H1), 1.68 – 1.20 (m, 6H, H6-8).

^{13}C NMR (101 MHz, DMSO-d_6) δ 172.8, 169.8, 120.9 (2C), 107.8 (2C), 52.9, 49.3, 32.5 (2C), 26.0, 23.8, 23.0.

BRMS (ESI+) calcd for $C_{13}H_{22}N_3O_2^+$ $[M+H]^+$ 252.1707, found: 252. 1712.

Tropinone functionalization with aminoxy-TMPP:

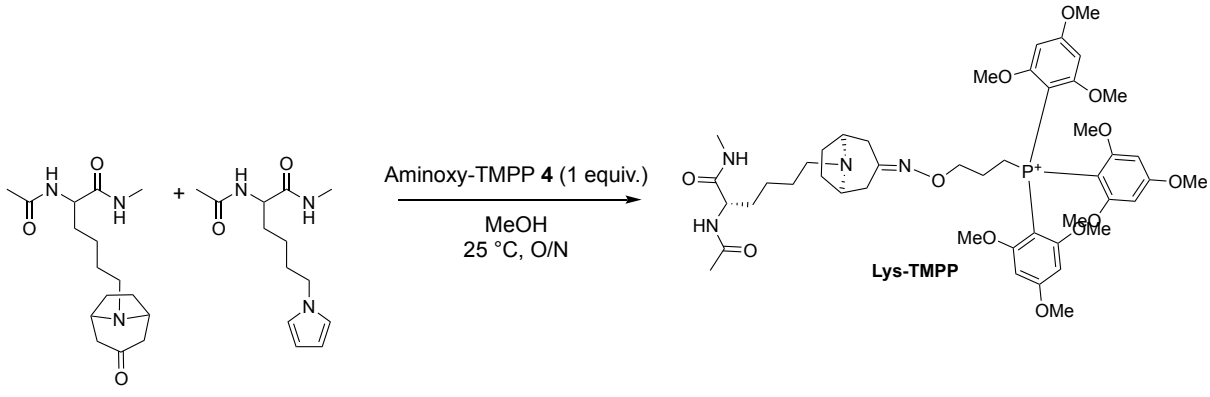

The white solid containing a mixture of Lys-trop and Lys-pyrrole (1 mg, approx. 3 mmol) was dissolved in MeOH (10 mL) to obtain a 0.1 mg/mL solution of functionalized lysine. To 500 □L of this solution, 1.0 equiv. of aminoxy-TMPP (3 □L from a 0.05 M stock solution in DMSO) were added. Mixture was stirred at 25 °C overnight before it was analysed by HRMS.
HRMS (ESI+) calcd for $C_{46}H_{66}N_4O_{12}P^+$ $[M]^+$ 897.4409, found: 897.4417.

2-(2-(2-(2-Azidoethoxy)ethoxy)ethoxy)acetaldehyde (6):

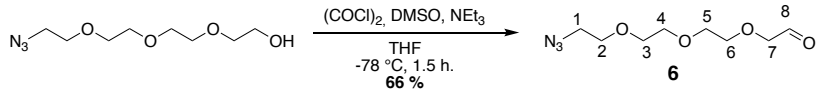

Oxalyl chloride (80 µL, 0.92 mmol, 2.0 equiv.) was added dropwise to a solution of DMSO (100 µL, 1.37 mmol, 3.0 equiv.) in dry THF (3 mL) at -78 °C under inert atmosphere. The mixture was stirred for 15 min before N_3-PEG_4-OH (100 mg, 0.46 mmol, 1.0 equiv.) in dry THF (3 mL) was added dropwise to the reaction mixture which was stirred for 30 min at -78 °C. Triethylamine (0.40 mL, 2.74 mmol, 6.0 equiv.) was then added dropwise, and the reaction mixture was stirred for 15 min at -78 °C before being warmed to room temperature. The formed precipitate was removed by filtration and the filtrate was concentrated under reduced pressure. Crude yellow solid was dissolved in DCM (5 mL) and washed three times with water (5 mL). The aqueous layer was finally extracted three times with DCM (10 mL). The organic layer was dried over Na_2SO_4, filtered and concentrated under reduced pressure. The crude product was purified by column chromatography (eluent: cyclohexane (cHex) 3/7 ethyl acetate (EtOAc)) and the desired compound was obtained as a yellowish oil with 66% yield (65 mg, 0.30 mmol).
Rf: 0.20 (eluent: cHex 30/70 EtOAc; stained with phosphomolybdic acid (PMA))
^{1}H NMR (400 MHz, $CDCl_3$) δ 9.73 (brs, 1H, H8), 4.16 (d, *J* = 0.9 Hz, 2H, H7), 3.76 – 3.65 (m, 10H, H2-6), 3.39 (t, *J* = 5.1 Hz, 2H, H1).
^{13}C NMR (100 MHz, $CDCl_3$) δ 201.1, 77.0, 71.4, 71.0, 70.9, 70.8, 70.2, 50.8.
HRMS (ESI+) calcd for $C_8H_{15}N_3O_4Na^+$ $[M+Na]^+$ 240.0955; found 240.0956.

(*E*)/(*Z*)-*N*-(2-{2-[2-(2-Azidoethoxy)ethoxy]ethoxy}ethylidene)hydroxylamine (7):

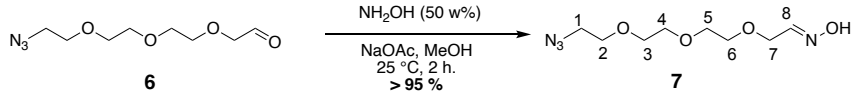

6 **7**

2-{2-[2-(2-Azidoethoxy)ethoxy]ethoxy}acetaldehyde **6** (170 mg, 0.78 mmol, 1.0 equiv.) was dissolved in MeOH (5 mL). A solution of hydroxylamine (0.06 mL, 0.79 mmol, 1.1 equiv.; 50 wt% in water) and sodium acetate (128.4 mg, 1.57 mmol, 2.0 equiv.) was then added to the mixture, which was stirred at room temperature for 2 h The crude mixture was diluted in EtOAc (5 mL) and water (5 mL). The aqueous layer was extracted three times with EtOAc (10 mL) and the combined organic layers were dried over Na_2SO_4, filtered and concentrated under reduced pressure to give the desired compound as a light yellow oil with 95% yield (181 mg, 0.78 mmol).
Rf: 0.20 (eluent: cHex 60/40 EtOAc; stained with PMA)
^{1}H NMR (400 MHz, $CDCl_3$) δ 9.53 (brs, 1H, H8), 4.22 (d, *J* = 0.9 Hz, 2H, H7), 3.76 – 3.65 (m, 10H, H2-6), 3.39 (t, *J* = 5.1 Hz, 2H, H1).
^{13}C NMR (100 MHz, $CDCl_3$) δ 152, 77.0, 71.4, 71.0, 70.9, 70.8, 70.2, 50.8.

(*Z*)-2-{2-[2-(2-Azidoethoxy)ethoxy]ethoxy}-*N*-hydroxyethanecarbonimidoyl chloride (8):

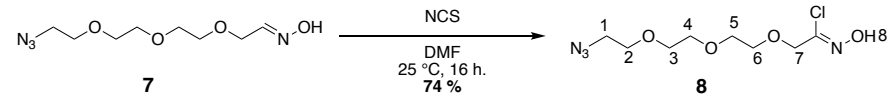

7 **8**

2-{2-[2-(2-Azidoethoxy)ethoxy]ethoxy}ethylidene)hydroxylamine **7** (170 mg, 0.73 mmol, 1.0 equiv.) was dissolved in DMF (5 mL). *N*-Chlorosuccinimide (352 mg, 2.64 mmol, 3.6 equiv.) was added portion wise to the reaction mixture which was stirred at room temperature 16 h. Then, the mixture was diluted with Et_2O (5 mL) and washed 5 times with a saturated NaCl aqueous solution (30 mL). The organic layer was dried over Na_2SO_4, filtered and concentrated under reduced pressure to give the desired compound as a white oil with 74% yield (145 mg, 0.54 mmol) that was used without further purification.
Rf: not stable on silica
^{1}H NMR (400 MHz, $CDCl_3$) δ 9.31 (s, 1H, H8), 4.28 (s, 2H, H7), 3.70 – 3.64 (m, 10H, H2-6), 3.41 – 3.37 (m, 2H, H1).
^{13}C NMR (101 MHz, $CDCl_3$) δ 138.0, 72.0, 70.8, 70.7, 70.6, 70.1, 69.9, 50.8.
*ν*max (thin film) /cm-1 3285 (br), 2915 (m), 20998 (s), 1631 (w), 1441 (m), 1347 (w), 1284 (m), 1081 (s), 950 (m), 848 (w), 688 (w).
HRMS (ESI+) calcd for $C_8H_{15}ClN_4O_4K^+$ $[M+K]^+$ 305.0413; found 305.0431.

2-(2-{2-[2-(4-Phenyl-1*H*-1,2,3-triazol-1-yl)ethoxy]ethoxy}ethoxy)acetaldehyde (6'):

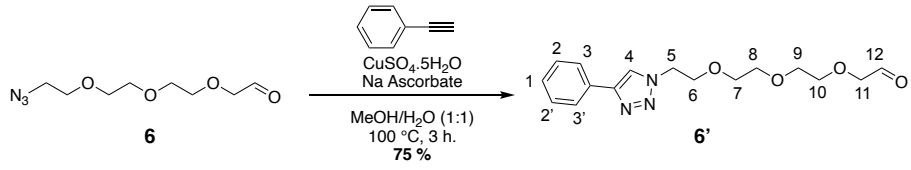

2-{2-[2-(2-Azidoethoxy)ethoxy]ethoxy}acetaldehyde **6** (100 mg, 0.46 mmol, 1.0 equiv.) was dissolved in a previously degassed MeOH/H_2O (1:1) mixture (20 mL). Phenylacetylene (0.1 mL, 0.91 mmol, 2.0 equiv.) was slowly added to the mixture followed by sodium ascorbate (36.3 mg, 0.18 mmol, 0.4 equiv.) and $CuSO_4.5H_2O$ (7.3 mg, 0.05 mmol, 0.1 equiv.) and the mixture was heated to reflux (100 °C) for 3 h. The reaction was quenched using a saturated aqueous solution of NH_4Cl (30 mL) and the aqueous layer was extracted four times with DCM (20 mL). The combined organic layers were dried over Na_2SO_4, filtered and concentrated under reduced pressure. The crude was purified by column chromatography using a slow gradient from DCM/MeOH (99:1) to DCM/MeOH (98:2) as eluent mixture. 2-(2-{2-[2-(4-phenyl-1H-1,2,3-triazol-1-yl)ethoxy]ethoxy}ethoxy)acetaldehyde was obtained as a yellow oil with 75% yield (112 mg, 0.35 mmol).

Rf: 0.34 (eluent: DCM 98/2 MeOH)

^{1}H NMR (400 MHz, $CDCl_3$) δ 9.65 (s, 1H, H12), 8.16 – 8.01 (m, 1H, H4), 7.89 – 7.82 (m, 2H, H3-3'), 7.42 (t, *J* = 6.9 Hz, 2H,H2-2'), 7.32 (t, *J* = 7.4 Hz, 1H, H1), 4.60 (t, *J* = 4.9 Hz, 2H, H5), 4.07 (s, 2H), 3.91 (t, *J* = 4.9 Hz, 2H, H6), 3.80 – 3.19 (m, 8H, H7-10).

^{13}C NMR (101 MHz, $CDCl_3$) δ 200.4, 130.7, 128.6, 127.9, 125.5, 76.6, 71.0, 70.5, 70.4, 70.3, 69.3, 50.3.

HRMS (ESI+) calcd for $C_{16}H_{22}N_5O_4^+$ $[M+H]^+$ 320.1610 ; found : 320.1613.

2-(2-(2-(2-(4-Phenyl-1H-1,2,3-triazol-1-yl)ethoxy)ethoxy)ethoxy)acetaldehyde oxime (6''):

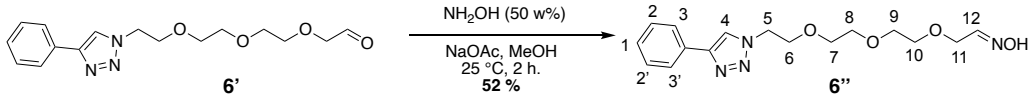

2-(2-{2-[2-(4-Phenyl-1H-1,2,3-triazol-1-yl)ethoxy]ethoxy}ethoxy)acetaldehyde **6'** (25 mg, 0.08 mmol, 1.0 equiv.) was dissolved in MeOH (5 mL). A solution of hydroxylamine 50 w% in water (0.1 mL, 3.28 mmol, 39 equiv.) and sodium acetate (25.7 mg, 0.31 mmol, 4.0 equiv.) were then added to the mixture which was stirred at room temperature for 4 h. The mixture was then diluted with EtOAc (5 mL) and water (5 mL). The aqueous layer was extracted three times with EtOAc (5 mL) and the combined organic layers were dried over Na_2SO_4, filtered and concentrated under reduced pressure to give *N*-[2-(2-{2-[2-(4-phenyl-1H-1,2,3-triazol-1-yl)ethoxy]ethoxy}ethoxy)ethylidene]hydroxylamine **6''** as yellow oil with 52% yield (13.6 mg, 0.04 mmol).

Rf: 0.28 (eluent: DCM 98/2 MeOH)

^{1}H NMR (400 MHz, $CDCl_3$) δ 7.99 (s, 1H, H4), 7.96 (t, *J* = 5.6 Hz, 1H, H12), 7.85 – 7.78 (m, 2H, H3-3'), 7.40 (dd, *J* = 8.4, 6.9 Hz, 2H, H2-2'), 7.35 – 7.28 (m, 1H, H1), 4.57 (t, *J* = 5.0 Hz, 2H, H5), 4.07 (d, *J* = 5.6 Hz, 2H, H11), 3.89 (t, *J* = 5.0 Hz, 2H, H6), 3.64 – 3.54 (m, 8H, H7-10).

^{13}C NMR (101 MHz, $CDCl_3$) δ 128.9, 128.2, 125.8 (d), 121.2, 70.6 – 68.9 (m), 68.0, 50.5.
HRMS (ESI^+) calcd for $C_{16}H_{23}N_4O_4$ $[M+H]^+$ 335.1719, found 335.1727

(Z)-N-Hydroxy-2-(2-(2-(2-(4-phenyl-1H-1,2,3-triazol-1-yl)ethoxy)ethoxy)ethoxy)acetimidoyl chloride (9):

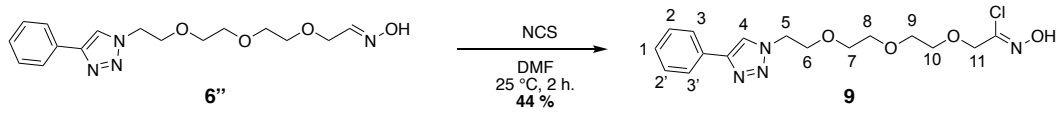

6" 9

2-(2-(2-(2-(4-Phenyl-1H-1,2,3-triazol-1-yl)ethoxy)ethoxy)ethoxy)acetaldehyde oxime **6''** (25.6 mg, 0.08 mmol, 1.0 equiv.) was dissolved in DMF (2 mL). N-chlorosuccinimide (21 mg, 0.15 mmol, 2.0 equiv.) was added portion wise to the mixture which was stirred at room temperature for 2 h. The mixture was diluted in Et_2O (5 mL) and washed five times with a saturated NaCl aqueous solution (25 mL), the organic layer was then dried over Na_2SO_4, filtered and concentrated under reduced pressure to give the desired compound as a transparent oil with 44% yield that was used without further purification (12.5 mg, 0.03 mmol).
Rf: not stable on silica
^{1}H NMR (400 MHz, $CDCl_3$) δ 7.99 (s, 1H, H4), 7.85 – 7.80 (m, 2H, H3-3'), 7.45 – 7.39 (m, 2H, H2-2'), 7.36 – 7.30 (m, 1H, H1), 4.62 – 4.55 (m, 2H, H5), 4.23 (s, 2H, H11), 3.95 – 3.90 (m, 2H, H6), 3.67 – 3.60 (m, 8H, H9-10).
^{13}C NMR (101 MHz, $CDCl_3$) δ 129.1, 126.0, 74.2 – 67.8 (m), 50.9, 29.8.
HRMS (ESI^+) calcd for $C_{16}H_{21}N_4O_4^+$ $[M-Cl]^+$ 333.1557, found 333.1522.

14-Azido-6,9,12-trioxa-2,3-diazatetradec-3-ene (14):

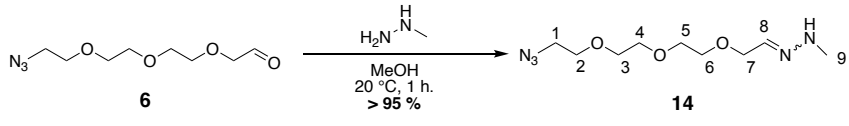

6 14

2-{2-[2-(2-Azidoethoxy)ethoxy]ethoxy}acetaldehyde (53 mg, 0.24 mmol, 1.0 equiv.) was dissolved in MeOH (5 mL). Methylhydrazine (0.5 mL, 9.15 mmol, 37 equiv.) was added to the mixture which was stirred at room temperature for 2 h. The solution was diluted with DCM (10 mL) and poured on mQ water (10 mL). The organic layer was washed three times with water (10 mL) and once with a saturated NaCl solution (10 mL), dried over Na_2SO_4, filtered and concentrated under reduced pressure to give to give the title compound as a mixture of isomers (Z/E 6:4) as a brown oil (59 mg, 0.24 mmol) which was used without further purification.
Rf: 0.20 (eluent: cHex 20/80 EtOAc; stained by PMA)
^{1}H NMR (400 MHz, $CDCl_3$) δ 6.85 (t, *J* = 5.2 Hz, 1H, H8), 4.10 (t, *J* = 5.2 Hz, 2H, H2), 3.69 – 3.57 (m, 8H, H3-6), 3.40 – 3.35 (m, 2H, H1), 2.80 (s, 3H, H9).
^{13}C NMR (101 MHz, $CDCl_3$) δ 134.2, 72.3 – 68.3 (m), 51.1, 34.8.
HRMS (ESI^+) calcd for $C_{17}H_{33}N_8O_6^+$ [transaminated dimer]$^+$ 445.2518, found: 445.2504.

13-Azido-5,8,11-trioxa-1,2-diazatridec-2-ene (15):

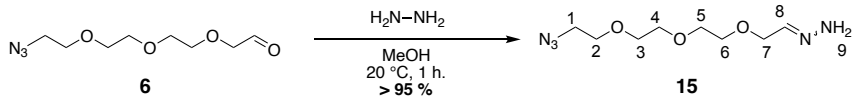

2-{2-[2-(2-Azidoethoxy)ethoxy]ethoxy}acetaldehyde **6** (40 mg, 0.18 mmol, 1.0 equiv.) was dissolved in MeOH (5 mL). Hydrazine as a 1 M solution in THF (0.5 mL, 0.50 mmol, 2.8 equiv.) was added to the mixture which was stirred at room temperature for 2 h. The solution was diluted with DCM (10 mL) and poured on distilled water (10 mL). The organic layer was washed three times with water (10 mL) and once with a saturated NaCl solution (10 mL), dried over Na_2SO_4, filtered and concentrated under reduced pressure to give the title compound as a mixture of isomers (Z/E 8:2) as a brown oil (43 mg, 0.18 mmol) which was used without further purification.

Rf: 0.19 (eluent: cHex 20/80 EtOAc, stained by PMA)

Z isomer:

^{1}H NMR (400 MHz, $CDCl_3$) δ 7.09 (t, *J* = 5.3 Hz, 1H, H8), 4.08 – 3.98 (m, 2H, H1), 3.71 – 3.51 (m, 10H, H2-6), 3.34 (m, 2H, H7).

E isomer:

^{1}H NMR (400 MHz, $CDCl_3$) δ 6.60 (t, *J* = 4.0 Hz, 1H, H8), 4.13 (d, *J* = 4.0 Hz, 2H, H1), 3.71 – 3.51 (m, 10H, H2-6), 3.34 (m, 2H, H7).

^{13}C NMR (101 MHz, $CDCl_3$) δ 141.6, 71.7 – 68.9 (m), 50.7.

HRMS (ESI+) calcd for $C_{16}H_{30}N_8NaO_6$ [transaminated dimer+Na]$^+$ 453.2186, found 453.2163.

14-Azido-2-phenyl-6,9,12-trioxa-2,3-diazatetradec-3-ene (16):

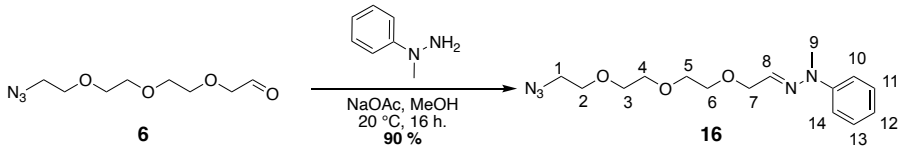

2-{2-[2-(2-Azidoethoxy)ethoxy]ethoxy}acetaldehyde **6** (25 mg, 0.12 mmol, 1.0 equiv.) was dissolved in MeOH (2 mL). NaOAc (10.39 mg, 0.13 mmol, 1.1 equiv.) and 1-methyl-1-phenylhydrazine (0.014 mL, 0.12 mmol, 1.0 equiv.) were successively added to the flask and the mixture was stirred at room temperature overnight. The solution was then concentrated under reduced pressure and the salts were removed by filtration (washed with DCM). The filtrate was concentrated under reduced pressure to give 14-azido-2-phenyl-6,9,12-trioxa-2,3-diazatetradec-3-ene as a brown oil with 90% yield (33 mg, 0.10 mmol).

Rf: 0.32 (eluent cHex 70/30 EtOAc)

^{1}H NMR (400 MHz, $CDCl_3$) δ 7.31 – 7.18 (m, 4H, H10-11, H13-14), 6.88 (tt, *J* = 6.8, 1.6 Hz, 1H, H12), 6.82 (t, *J* = 5.3 Hz, 1H, H2), 4.29 (d, *J* = 5.3 Hz, 2H, H7), 3.72 – 3.60 (m, 8H, H3-6), 3.36 (t, *J* = 5.1 Hz, 2H, H1), 3.24 (d, *J* = 0.8 Hz, 3H, H9).

^{13}C NMR (101 MHz, $CDCl_3$) δ 147.5, 130.4, 128.7 (d), 120.3, 115.0 (d), 71.4 – 69.2 (m), 70.5, 70.4, 69.8, 69.2, 50.5, 32.9.

HRMS (ESI+) calcd for $C_{15}H_{23}N_5NaO_3^+$ $[M+Na]^+$ 344.1693, found : 344.1695.

13-Azido-1-(naphthalen-2-yl)-5,8,11-trioxa-1,2-diazatridec-2-ene (17):

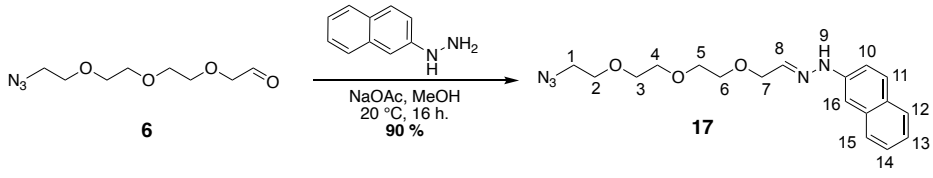

6 **17**

2-{2-[2-(2-azidoethoxy)ethoxy]ethoxy}acetaldehyde **6** (25 mg, 0.12 mmol, 1.0 equiv.) was dissolved in MeOH (2 mL). NaOAc (10.39 mg, 0.13 mmol, 1.1 equiv.) and (naphtalen-2-yl)hydrazine (22.40 mg, 0.12 mmol, 1.0 equiv.) were successively added to the flask. The mixture was stirred at room temperature overnight. The solution was then concentrated under reduced pressure and the salts were removed by filtration (washed with DCM). The filtrate was concentrated under reduced pressure to give the title compound as a mixture of isomers (Z/E 86:14) as an orange oil with 90% yield (37 mg, 0.10 mmol) which was used without further purification.

Rf: 0.22 (eluent: cHex 70/30 EtOAc)

^{1}H NMR (500 MHz, $CDCl_3$) δ 7.62 (t, *J* = 8.2 Hz, 1H, H8), 7.33 – 7.28 (m, 2H, H10, H12), 7.26-7.07 (m, 5H, H11, H13-16), 4.17 (d, *J* = 5.4 Hz, 2H, H1), 3.66 – 3.49 (m, 10H, H3-6), 3.31 – 3.27 (m, 2H, H2)

^{13}C NMR (126 MHz, $CDCl_3$) δ 136.7, 129.2, 127.7, 126.5, 123.0, 115.4, 106.9, 71.6 – 68.0, 67.3, 61.8, 50.7.

HRMS (ESI+) calcd for $C_{18}H_{23}N_5NaO_3^+$ $[M+Na]^+$ 380.1693, found : 380.1701.

***N*-(2-(2-azidoethoxy)ethyl)-2-isocyanoacetamide (f):**

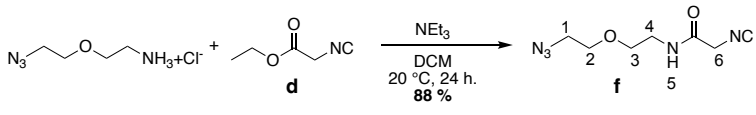

d **f**

2-(2-Azidoethoxy)ethan-1-aminium chloride (40 mg, 0.24 mmol, 1.0 equiv.) was solved in DCM (1 mL) and triethylamine (48.6 µL, 0.36 mmol, 1.5 equiv.) was added. The mixture was stirred at room temperature for 30 min before ethyl 2-isocyanoacetate **d** (39.3 µL, 0.36 mmol, 1.5 equiv.) was added. The mixture was stirred at room temperature for 24 h before it was dried under reduced pressure. The crude brown oil was solubilized in EtOAc (5 mL) and washed twice with 1 M NaH_2PO_4 aqueous solution (5 mL) and saturated NaCl aqueous solution (10 mL) before it was dried over Na_2SO_4, filtered and concentrated under reduced pressure to give a black oil which was purified by column chromatography (eluent: DCM 98/2 MeOH), the desired compound was obtained as a black oil with 88% yield (42 mg, 0.21 mmol)

Rf: 0.31 (eluent: DCM 98/2 MeOH; stained with vaniline)

^{1}H NMR (400 MHz, $CDCl_3$) δ 6.74 (s, 1H, H5), 4.17 (s, 2H, H6), 3.73 – 3.52 (m, 6H, H2-4), 3.40 (t, *J* = 4.9 Hz, 2H, H1).

^{13}C NMR (101 MHz, $CDCl_3$) δ 163.9, 114.8, 70.2, 69.2, 60.4, 50.6, 39.7.

HRMS (ESI+) calcd for $C_7H_{12}N_5O_2^+$ $[M+H]^+$ 198.0986; found 198.0987.

2-Isocyano-2-methylpropyl (2-(2-azidoethoxy)ethyl)carbamate (g):

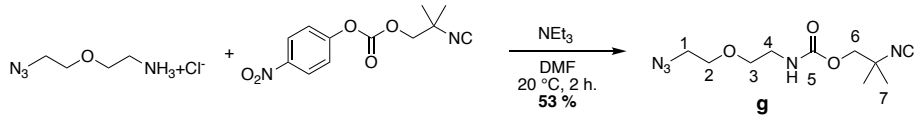

2-(2-Azidoethoxy)ethan-1-aminium chloride (49.5 mg, 0.30 mmol, 1.5 equiv.) was solved in DMF (1 mL) and triethylamine (55 µL, 0.38 mmol, 2 equiv.) was added. The mixture was stirred at room temperature for 30 min before 2-isocyano-2-methylpropyl (4-nitrophenyl) carbonate (50 mg, 0.19 mmol, 1 equiv.) was added as a solution in DMF (1 mL). The mixture was stirred at room temperature for 2 h before it was poured on a saturated NH_4Cl aqueous solution (12 mL) the organic layer was washed twice with NH_4Cl aqueous solution (12 mL) followed by a saturated NaCl solution (12 mL) before it was dried over Na_2SO_4, filtered and concentrated under reduced pressure. The crude yellow oil was then purified by column chromatography (eluent: cHex 50/50 EtOAc) and the desired compound was obtained as a yellow oil with 53% yield (25.8 mg, 0.10 mmol).

Rf: 0.38 (eluent: cHex 50/50 EtOAc stained with ninhydrin)

^{1}H NMR (400 MHz, $CDCl_3$) δ 5.26 (s, 1H, H5), 4.07 – 4.01 (m, 2H, H6), 3.67 (t, *J* = 4.9 Hz, 2H, H4), 3.58 (t, *J* = 5.1 Hz, 2H, H1), 3.41 (dt, *J* = 14.6, 5.1 Hz, 4H, H2-3), 1.46 – 1.41 (m, 6H, H7).

^{13}C NMR (101 MHz, $CDCl_3$) δ 155.8, 126.1, 115.2, 70.1, 69.9, 56.7, 56.7, 50.6, 41.0, 25.8.

HRMS (ESI+): calcd for $C_{10}H_{18}N_5O_3$ $(M+H)^+$ 256.1404; found 256.1412.

Methyl 3,4-dibromo-2,5-dioxo-2,5-dihydro-1H-pyrrole-1-carboxylate (20):[213]

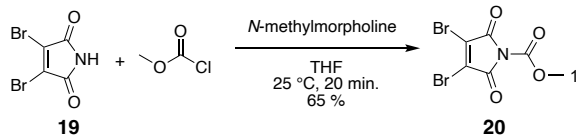

Dibromomaleimide **19** (2 g., 7.85 mmol, 1.0 equiv.) and *N*-methylmorpholine (0.86 mL, 7.85 mmol, 1.0 equiv.) were solved in THF (40 mL). Mixture was cooled to 0 °C using an ice bath and methylchloroformate (0.61 mL, 7.85 mmol, 1.0 equiv.) was slowly added. Mixture was stirred at room temperature for 20 min before it was diluted with DCM (100 mL) and washed twice with mQ H_2O (50 mL) and a saturated NaCl aqueous solution (50 mL). The organic layer was dried over Na_2SO_4, filtered and concentrated under reduced pressure to give a black oil. It was then purified by column chromatography (eluent: cHex 70/30 EtOAc) to afford *N*-methoxycarbonyl dibromomaleimide **20** as a white powder with 65% yield (1.6 g, 5.1 mmol).

Rf: 0.24 (eluent: cHex 80/20 EtoAC)

^{1}H NMR (400 MHz, DMSO) δ 3.87 (s, 3H, H1).

^{13}C NMR (101 MHz, DMSO) δ 160.6 (2C), 147.5, 131.8 (2H), 54.6.

HRMS (ESI+) calcd for $C_6H_4Br_2NO_4^+$ $[M+H]^+$ 311.8502 found 311.8504.

((1R,8S,9S)-Bicyclo[6.1.0]non-4-yn-9-yl)methyl (4-nitrophenyl) carbonate (22):

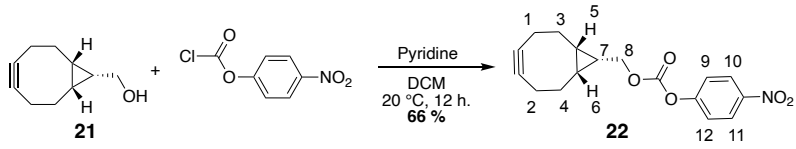

21 22

To a solution of (1R,8S,9S)-bicyclo[6.1.0]non-4-yn-9-ylmethanol **21** (500 mg, 3.33 mmol, 1.0 equiv.) in dichloromethane (12.5 mL) was added p-nitrophenol chloroformate (805,43 mg, 3.99 mmol, 1.2 equiv.) and pyridine (2.63 g, 2.58 mL, 33.3 mmol, 10 equiv.). The reaction was stirred at room temperature overnight. After concentration, the mixture was quenched by saturated NH_4Cl aqueous solution (75 mL) and extracted three times with EtOAc (75 mL). The combined organic layers were washed with a saturated NaCl aqueous solution (75 mL), dried over Na_2SO_4, filtered and concentrated under reduced pressure. The obtained yellow solid was purified by column chromatography (cHex 100% to cHex90/10 EtOAc) to afford the title compound as a colourless oil with 66% yield (0.697 g, 2.21 mmol).

Rf: 0.32 (eluent: cyclohexane 70/30 EtOAc; stained with vanillin)

^{1}H NMR (400 MHz, $CDCl_3$) δ 8.31 – 8.25 (m, 2H, H10-11), 7.42 – 7.35 (m, 2H, H9,H12), 4.40 (d, *J* = 8.2 Hz, 2H, H8), 2.33-2.25 (m, 5H, H1-2, H7), 1.65 – 1.56 (m, 2H, H5-6), 1.60 – 1.45 (m, 2H, H3-4), 1.12 – 1.01 (m, 2H, H3''-4'').

^{13}C NMR (101 MHz, Chloroform-*d*) δ 155.6, 152.6, 145.3, 125.3(2C), 121.8(2C), 98.7 (2C), 68.0, 29.1, 21.4(2C), 20.5 (2C), 17.3 (2C).

((1*R*,8*S*,9*S*)-Bicyclo[6.1.0]non-4-yn-9-yl)methyl (3-aminopropyl)carbamate (23)*:*

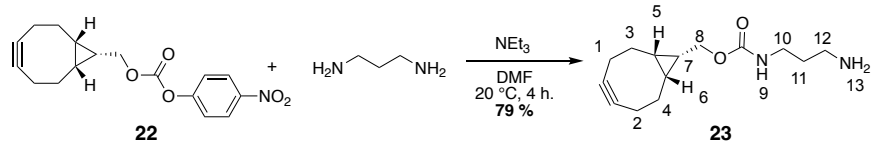

22 23

To a solution of triethylamine (0.66 mL, 4.75 mmol, 10 equiv.) and propane-1,3-diamine (0.4 mL, 4.75 mmol, 10 equiv.) in DMF (1 mL) was slowly added a solution of (1*R*,8*S*,9*s*)-*N*-(3-aminopropyl)bicyclo[6.1.0]non-4-yne-9-carboxamide **22** (150 mg, 0.475 mmol, 1 equiv.) in DMF (1 mL). The reaction was stirred at room temperature for 4 h. Mixture was poured on mQ H_2O (30 mL) and the aqueous layer was extracted three times with DCM (10 mL). Combined organic layers were washed 5 times with a saturated NaCl aqueous solution (30 mL), dried over Na_2SO_4 filtered and concentrated under reduced pressure to afford the tile compound as a yellow oil with 79% yield (92 mg, 0.37 mmol).

Rf: 0.33 (eluent: DCM 90/10 MeOH, 1% NEt_3; stained with vanillin)

^{1}H NMR (500 MHz, MeOD) δ 4.14 (d, *J* = 8.1 Hz, 2H, H8), 3.17 (t, *J* = 6.7 Hz, 2H, H12), 2.69 (t, *J* = 7.1 Hz, 2H, H10), 2.30 – 2.13 (m, 5H, H1-2, H7), 1.64-1.54(m, 4H, H11, H5-6), 1.52 – 1.37 (m, 2H, H3'-4'), 1.0 – 0.92 (dt, *J* = 16.3, 8.6 Hz, 2H, H3''-4'').

^{13}C NMR (126 MHz, MeOD) δ 162.2, 98.1 (2C), 62.3, 38.1, 37.5, 31.9, 28.7, 20.5(2C), 20.0 (2C), 17.5 (2C).

((1R,8S,9s)-Bicyclo[6.1.0]non-4-yn-9-yl)methyl (3-(3,4-dibromo-2,5-dioxo-2,5-dihydro-1H-pyrrol-1-yl)propyl)carbamate (DBM-1):

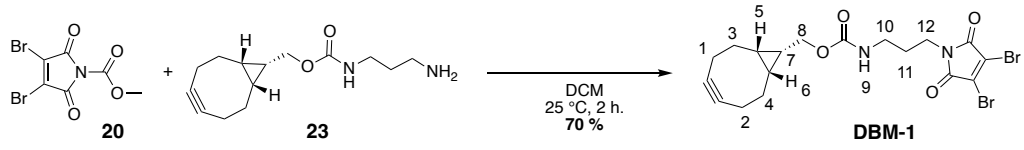

20 **23** **DBM-1**

To a solution of methyl 3,4-dibromo-2,5-dioxo-2,5-dihydro-1H-pyrrole-1-carboxylate (50 mg, 0.16 mmol, 1.0 equiv.) in DCM (5 mL) was slowly added ((1R,8S,9s)-bicyclo[6.1.0]non-4-yn-9-yl)methyl (3-aminopropyl)carbamate (60 mg, 0.24 mmol, 1.5 equiv.) solved in DCM (5 mL) and mixture was stirred at 25 °C for 2 h before it was concentrated under reduced pressure. The crude mixture was then diluted in EtOAc (5 mL) and poured over a saturated solution of NH_4Cl (5mL). The aqueous layer was extracted twice with EtOAc (5mL) and the combined organic layers were dried over Na_2SO_4, filtered and concentrated under reduced pressure. Crude mixture was purified by column chromatography (eluent: cHex 70/30 EtOAc) and the title compound was isolated as a white solid with 70% yield (54.1 mg, 0.11 mmol).

Rf: 0.26 (eluent cHex 80/20 EtOAc; stained with vanilin)

^{1}H NMR (400 MHz, DMSO) δ 4.02 (d, *J* = 8.0 Hz, 2H, H8), 3.47 (t, *J* = 7.2 Hz, 2H, H12), 2.97 (q, *J* = 6.5 Hz, 2H, H10), 2.26 – 2.07 (m, 5H, H1-2, H7), 1.67 (p, *J* = 7.0 Hz, 2H, H11), 1.64-1.54 (m, 2H, H5-6), 1.53 – 1.20 (m, 2H, H3'-4'), 0.95 – 0.85 (m, 2H, H3"-H4").

^{13}C NMR (101 MHz, DMSO) δ 164.7, 129.6, 129.4, 128.7, 125.8, 99.5, 61.8, 38.3, 37.6, 29.1, 28.5, 21.5, 21.3, 20.0, 18.1.

HRMS (ESI+) calcd for $C_{18}H_{21}Br_2N_2O_4^+$ [M+H]$^+$: 486.9863 found: 486.9850.

***Tert*-butyl-1-((1*R*,8*S*,9*S*)-bicyclo[6.1.0]non-4-yn-9-yl)-3-oxo-2,7,10,13,16-pentaoxa-4-azanonadecan-19-oate (25):**

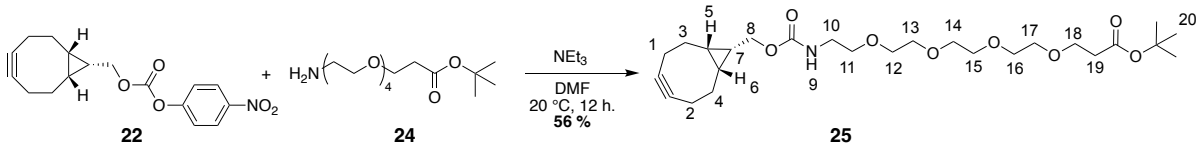

22 **24** **25**

A solution of (1R,8S,9S)-bicyclo[6.1.0]non-4-yn-9-ylmethyl (4-nitrophenyl) carbonate **22** (100 mg, 0.32 mmol, 1.0 equiv.) in DMF (1 mL) was added to a solution of tert-butyl 1-amino-3,6,9,12,15,18-hexaoxahenicosan-21-oate **24** (112.1 mg, 0.35 mmol, 1.1 equiv.) and triethylamine (0.13 mL, 3.33 mmol, 3.0 equiv.) in DMF (1 mL). The mixture was stirred overnight at r.t. before it was diluted with mQ H_2O (10 mL) and extracted three times with DCM (30 mL) combined organic layers were then washed with saturated NaCl aqueous solution (30 mL). The organic layer was dried over Na_2SO_4, filtered and concentrated under reduced pressure to afford the tile compound as a colourless oil with 56% yield (89 mg, 0.18 mmol).

Rf: 0.32 (eluent: cHex 80/20 EtOAc; stained with $KMnO_4$)

^{1}H NMR (500 MHz, MeOD) δ 4.18 (d, *J* = 8.1 Hz, 2H, H8), 3.74 (t, *J* = 6.2 Hz, 2H, H18), 3.67 – 3.57 (m, 12H,H12-17), 3.57 (t, *J* = 5.5 Hz, 2H, H10), 3.34 (d, *J* = 1.7 Hz, 1H, H7), 3.32 (t, *J* = 5.5 Hz, 2H, H11), 2.51 (t, *J* = 6.2 Hz, 2H, H19), 2.34 – 2.17 (m, 4H, H1-2, H7), 1.73 – 1.58 (m, 2H, H5-6), 1.49 (s, 9H, H20), 1.47 – 1.25 (m, 2H, H3'-4'), 1.04 – 0.91 (m, 2H, H3''-4'').
^{13}C NMR (126 MHz, MeOD) δ 171.4, 157.9, 98.1 (2C), 80.3, 70.3 – 70.0 (m,5C), 69.9, 69.6, 66.5, 62.3, 40.3, 35.9, 28.8, 27.0 (3C), 20.5 (2C), 20.0 (2C), 17.6 (2C).

1-((1*R*,8*S*,9S)-Bicyclo[6.1.0]non-4-yn-9-yl)-3-oxo-2,7,10,13,16-pentaoxa-4-azanonadecan-19-oic acid (26):

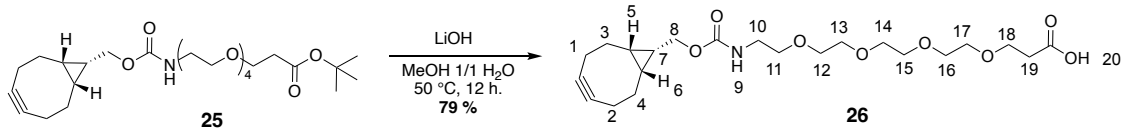

To a solution of tert-butyl-1-((1R,8S,9s)-bicyclo[6.1.0]non-4-yn-9-yl)-3-oxo-2,7,10,13,16-pentaoxa-4-azanonadecan-19-oate **25** (120 mg, 0.24 mmol, 1.0 equiv.) in MeOH 1/1 H_2O (2 mL) was added LiOH (57.7 mg, 2.41 mmol, 10 equiv.). The reaction was stirred at 50 °C overnight under argon atmosphere. MeOH was evaporated under reduced pressure and the resulting solution was poured on a 1 M NaH_2PO_4 aqueous solution (10 mL) which was extracted four times with DCM (15 mL). The combined organic layers were washed with a saturated NaCl solution (30 mL), dried over Na_2SO_4, filtered and concentrated under reduced pressure to afford the title compound as a yellowish oil with 79% yield (84 mg, 0.19 mmol).

Rf: 0.33 (eluent: DCM 90/10 MeOH; stained with vanillin, bromocresol green)
^{1}H NMR (400 MHz, MeOD) δ 4.18 (d, *J* = 8.1 Hz, 2H, H8), 3.77 (t, *J* = 6.4 Hz, 2H, H18), 3.68 – 3.64 (m, 12H, H12-17), 3.58 (t, *J* = 5.5 Hz, 2H, H10), 3.39 (s, 1H, H7), 3.36 – 3.30 (m, 2H, H11), 2.56 (t, *J* = 6.4 Hz, 2H, H19), 2.34 – 2.15 (m, 4H, H1-2), 1.71 – 1.57 (m, 2H, H5-6), 1.45 – 1.23 (q, *J* = 8.6 Hz, 2H, H3'-H4'), 1.03 – 0.90 (m, 2H, H3''-4'').
^{13}C NMR (101 MHz, MeOD) δ 174.5, 159.4, 98.1 (2C), 70.2 – 70.0 (m, 5C), 69.9, 69.7, 66.4, 62.4, 40.2, 35.4, 28.8, 20.5 (2C), 20.0 (2C), 17.5 (2C).

4-Nitrophenyl 1-((1*R*,8*S*,9*s*)-bicyclo[6.1.0]non-4-yn-9-yl)-3-oxo-2,7,10,13,16-pentaoxa-4-azanonadecan-19-oate (27):

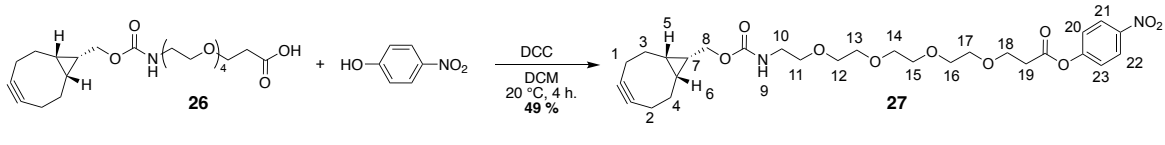

1-((1R,8S,9s)-bicyclo[6.1.0]non-4-yn-9-yl)-3-oxo-2,7,10,13,16-pentaoxa-4-azanonadecan-19-oic acid **26** (84 mg, 0.19 mmol, 1 equiv.) and 4-nitrophenol (31.7 mg, 0.23 mmol, 1.2 equiv.) were dissolved in DCM (4 mL). Then DCC (47 mg, 0.23 mmol, 1.2 equiv.) was added to the reaction mixture. The reaction was stirred at room temperature for 4 h under argon atmosphere before it was filtered. The filtrate was concentrated under reduced pressure. Crude mixture was diluted in a saturated NH_4Cl aqueous solution (15 mL) and DCM, the aqueous layer was then extracted three times with DCM (30 mL). Combined organic layers were washed three times with a saturated NaCl aqueous solution (40 mL). The organic layer was

dried over Na_2SO_4, filtered and concentrated under reduced pressure before mixture was purified by column chromatography (eluent: cyclohexane 100% to cHex 70/30 EtOAC, then EtOAc 100%) to afford the title compound as a yellowish oil with 49% yield (52 mg, 0.09 mmol).

Rf: 0.32 (eluent: cHex70/30 EtOAc; stained with vanillin)
^{1}H NMR (400 MHz, MeOD) δ 8.35 – 8.26 (m, 2H, H21-22), 7.43 – 7.35 (m, 2H, H20,H23), 4.13 (d, *J* = 8.1 Hz, 2H, H8), 3.87 (t, *J* = 6.0 Hz, 2H, H18), 3.68 – 3.57 (m, 12H, H12-17), 3.51 (t, *J* = 5.5 Hz, 2H, H10), 3.31 (s, 1H, H7), 3.26 (t, *J* = 5.5 Hz, 2H, H11), 2.89 (t, *J* = 6.0 Hz, 2H, H19), 2.34 – 2.11 (m, 4H, H1-2), 1.89 – 1.80 (m, 2H), 1.71 – 1.60 (m, 2H, H5-6), 1.43 – 1.06 (m, 2H, H3'-4'), 0.92 (t, *J* = 9.8 Hz, 2H, H3''-4'').
^{13}C NMR (101 MHz, MeOD) δ 172.1, 159.3 (2C), 125.9, 124.7, 122.6, 115.2, 106.3, 98.1 (2C), 70.2 – 69.7(m, 7C), 66.4, 62.4, 40.1, 33.4, 29.1, 20.5 (2C), 20.0 (2C), 17.4 (2C).

((1*R*,8*S*,9*s*)-Bicyclo[6.1.0]non-4-yn-9-yl)methyl (19-amino-15-oxo-3,6,9,12-tetraoxa-16-azanonadecyl)carbamate (28):

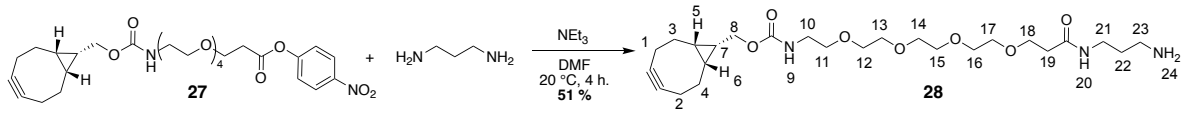

To a solution of triethylamine (0.12 mL, 0.83 mmol, 10 equiv.) and propane-1,3-diamine (0.07 mL, 0.83 mmol, 10 equiv.) was added a solution of 4-nitrophenyl 1-((1*R*,8*S*,9*s*)-bicyclo[6.1.0]non-4-yn-9-yl)-3-oxo-2,7,10,13,16-pentaoxa-4-azanonadecan-19-oate **27** (47 mg, 0.08 mmol, 1 equiv.). The reaction was stirred at room temperature for 4 h. After the reaction was completed, the product was diluted in H_2O (10 mL) and extracted four times with DCM (20 mL). The combined organic layers were washed three times with a saturated NaCl solution (20 mL), dried over Na_2SO_4, filtered and concentrated under reduced pressure to give the title compound as a yellow oil with 51% yield (21 mg, 0.04 mmol).

Rf: 0.33 (eluent: 90/10 MeOH, 1% NEt_3; stained with Ninhydrin, vanillin)
^{1}H NMR (400 MHz, MeOD) δ 4.15 (d, *J* = 8.1 Hz, 2H, H8), 3.65 (t, *J* = 6.1 Hz, 2H, H18), 3.67 – 3.57 (m, 12H, H12-H17), 3.53 (t, *J* = 5.5 Hz, 2H, H11), 3.27 (t, *J* = 5.5 Hz, 2H, H10), 2.75 (t, *J* = 7.0 Hz, 2H, H21), 2.44 (t, *J* = 6.0 Hz, 2H,), 2.30 – 2.08 (m, 6H, H1-2, H3'-4'), 1.70 (p, *J* = 6.8 Hz, 2H, H22), 1.62 – 1.60 (m, 2H, H5-6), 1.38 (p, *J* = 8.6 Hz, 1H, H7), 1.01 – 0.82 (m, 2H, H3''-H4'').
^{13}C NMR (101 MHz, MeOD) δ 182.7, 133.1, 98.1 (2C), 70.1 – 69.9 (m, 7C), 66.9, 62.4, 38.5, 36.3, 28.8, 25.4 (2C), 24.7, 20.5 (2C), 20.0 (2C), 17.5 (2C).

((1R,8S,9s)-Bicyclo[6.1.0]non-4-yn-9-yl)methyl (19-(3,4-dibromo-2,5-dioxo-2,5-dihydro-1H-pyrrol-1-yl)-15-oxo-3,6,9,12-tetraoxa-16-azanonadecyl)carbamate (DBM-2):

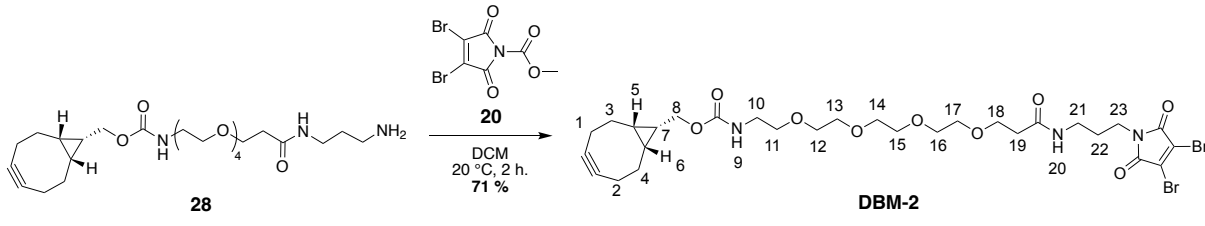

To a solution of methyl 3,4-dibromo-2,5-dioxo-2,5-dihydro-1H-pyrrole-1-carboxylate **20** (8.76 mg, 0.03 mmol, 1.0 equiv.) in DCM (2 mL) was added a solution of **28** (21 mg, 0.04 mmol, 1.5 equiv.) in DCM (2 mL). The reaction was stirred at room temperature for 2 h. After the

reaction was completed, the product was diluted in NH_4Cl (10 mL) and the resulting aqueous layer was extracted four times with DCM (20 mL). The combined organic layers were washed three times with a saturated NaCl aqueous solution (20 mL), dried over Na_2SO_4, filtered and concentrated under reduced pressure. The crude mixture was purified by column chromatography (cHex 50/50 EtOAc to DCM 80/20 MeOH) to afford the title compound as a yellow oil with 71% yield (14 mg, 0.02 mmol).

Rf = 0.31 (eluent: cHex 70/30 EtOAc; stained with vanillin)
^{1}H NMR (500 MHz, MeOD-d_4) δ 4.14 (d, *J* = 8.1 Hz, 2H, H8), 3.72 (t, *J* = 6.1 Hz, 2H, H18), 3.68 – 3.58 (m, 12H, H12-H17), 3.53 (t, *J* = 5.5 Hz, 2H, H11), 3.27 (d, *J* = 5.5 Hz, 2H, H10), 3.20 (t, *J* = 6.9 Hz, 2H, H21), 2.67 (t, *J* = 7.0 Hz, 2H, H23), 2.44 (t, *J* = 6.1 Hz, 2H, H19), 2.31 – 2.12 (m, 6H, H1-2, H3'-4'), 1.82 (p, *J* = 6.9 Hz, 2H, H22), 1.61 (d, *J* = 11.2 Hz, 3H, H5-H7), 0.94 – 0.73 (m, 2H, H3"-4").
^{13}C NMR (126 MHz MeOD-d_4) δ 174.5, 165.9, 159.6 (2C), 130.7 (2C), 99.9 (2C), 72.1 – 71.4 (m, 7C), 68.6, 64.1 (C12), 38.6, 38.1, 29.5, 22.3 (2C), 21.7, 19.8.3 (2C), 19.3 (2C), 17.5 (2C).
HRMS (ESI+) calcd for $C_{29}H_{41}Br_2N_3O_9^+$ $[M+Na]^+$: 756.1102 found: 756.1106.

4-Nitrophenyl (1*R*,8*S*,9*s*)-bicyclo[6.1.0]non-4-yne-9-carboxylate (30):

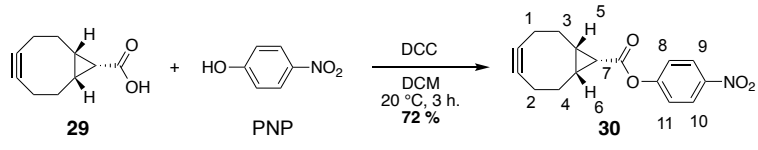

(1*R*,8*S*,9*s*)-bicyclo[6.1.0]non-4-yne-9-carboxylic acid **29** (406 mg, 2.5 mmol, 1.0 equiv.) — freshly produced by Michel Mosser —, and 4-nitrophenol (413 mg, 3 mmol, 1.2 equiv.) were solved in DCM (15 mL) and DCC (619 mg, 3 mmol, 1.2 equiv.) was added. The mixture was stirred at room temperature for 3 h before it was filtrated. The filtrate was concentrated under reduced pressure and the resulting yellow oil was diluted in a saturated NH_4Cl aqueous solution (15 mL) and EtOAc (20 mL). The organic layer was washed three times with a saturated NH_4Cl aqueous solution (15 mL) and three times with a saturated NaCl aqueous solution (20 mL) before it was dried over Na_2SO_4, filtered and concentrated under reduced pressure. Crude mixture was then purified by column chromatography (eluent: cyclohexane 90/10 EtOAc) to afford the title compound as a white solid with 72% yield (504 mg, 1.8 mmol).

Rf: 0.32 (eluent: cHex 70/30 EtOAc; stained with vanillin)
^{1}H NMR (400 MHz, DMSO-d_6) δ 8.35 – 8.24 (m, 2H, H9-10), 7.52 – 7.32 (m, 2H, H8, H11), 2.38 – 2.03 (m, 7H, H1-2, H5-7), 1.63 – 1.49 (m, 2H, H3-4).
^{13}C NMR (101 MHz, DMSO) δ 169.4, 155.3, 144.9, 125.2 (2C), 123.3 (2C), 98.6 (2C), 27.2, 25.8 (2C), 20.9 (2C), 20.2 (2C).
HRMS (ESI+): calcd for $C_{16}H_{16}NO_4^+$ $[M+H]^+$ 286.1074; found 286.1080.

(1*R*,8*S*,9*S*)-*N*-(3-aminopropyl)bicyclo[6.1.0]non-4-yne-9-carboxamide (31):

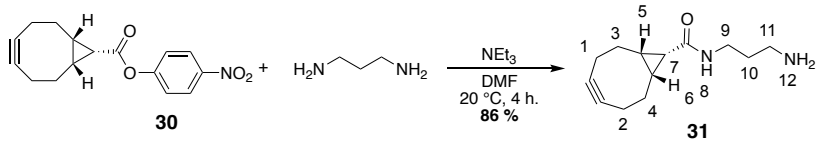

30 31

1,3-Propanediamine (1.17 mL, 14 mmol, 10 equiv.) was solved in DMF (3 mL) and triethylamine (2 mL, 14 mmol, 10 equiv.) was added. The mixture was stirred at room temperature for 5 min before 4-nitrophenyl (1*R*,8*S*,9*s*)-bicyclo[6.1.0]non-4-yne-9-carboxylate **30** (400 mg, 1.4 mmol, 1 equiv.) solved in DMF (3 mL) was slowly added to the amine containing solution. Reaction mixture was stirred at room temperature for 4 h before it was diluted in mQ H_2O (60 mL) and extracted four times with DCM (60 mL). Combined organic layers were washed three times with a saturated NaCl aqueous solution (60 mL), dried over Na_2SO_4, filtered and concentrated under reduced pressure to give the desired product as sticky yellow oil with 86% yield (256 mg, 1.2 mmol).

Rf: 0.33 (eluent: DCM 80/20 MeOH, 1% NEt_3; stained with ninhydrin)
^{1}H NMR (400 MHz, DMSO-d_6) δ 7.90 (t, *J* = 5.6 Hz, 1H, H8), 3.32 (m, 2H, H9), 3.07 (td, *J* = 6.8, 5.6 Hz, 2H, H11), 2.59 – 2.51 (m, 2H, H10), 2.33 – 2.07 (m, 6H, H1-2, H5-6), 1.95 – 1.85 (m, 2H,H12), 1.69 (t, *J* = 9.0 Hz, 1H, H7), 1.45 (p, *J* = 6.8 Hz, 2H, H3'-4'), 1.18 – 1.03 (m, 2H, H3''-4'').
^{13}C NMR (101 MHz, DMSO) δ 170.9, 99.3 (2C), 36.5 (2C), 33.6, 27.9, 23.5 (2C), 22.4 (2C), 21.1 (2C).
HRMS (ESI+) calcd for $C_{13}H_{21}N_2O^+$ $[M+H]^+$: 221.1648; found: 221.1657.

(1R,8S,9S)-*N*-(3-(3,4-Dibromo-2,5-dioxo-2,5-dihydro-1H-pyrrol-1-yl)propyl)bicyclo[6.1.0]non-4-yne-9-carboxamide (DBM-3):

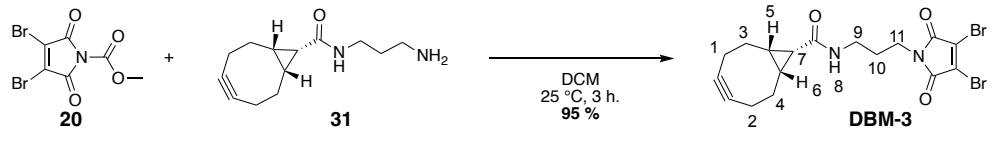

20 31 DBM-3

To a solution of methyl 3,4-dibromo-2,5-dioxo-2,5-dihydro-1H-pyrrole-1-carboxylate **20** (28 mg, 0.09 mmol, 1.0 equiv.) in DCM (2.5 mL) was added a solution of **31** (30 mg, 0.136 mmol, 1.5 equiv.) in DCM (2.5 mL). The reaction was stirred at room temperature for 3 h. After completion, the product was diluted in NH_4Cl (10 mL) and extracted four times with DCM (20 mL). The combined organic layers were washed three times with a saturated NaCl aqueous solution (20 mL). Combined organic layers were dried over Na_2SO_4, filtered and concentrated under reduced pressure. Crude mixture was purified by column chromatography (cHex 100% to cHex 70/30 EtOAc) to afford the title compound as a white solid with 95% yield (39 mg, 0.09 mmol).

Rf = 0.31 (eluent: cHex 70/30 EtOAc ; stained with vanillin)

^{1}H NMR (500 MHz, DMSO) δ 3.46 (m, 2H, H11), 3.03 (q, *J* = 6.6 Hz, 2H, H9), 2.32 – 2.10 (m, 6H, H1-2, H10), 1.91 (m, 2H, H5-6), 1.72 – 1.61 (m, 3H, H3'-4', H7), 1.09 (m, 2H, H3"-4").
^{13}C NMR (126 MHz, DMSO) δ 170.7, 164.4 (2C), 129.3 (2C), 99.0 (2C), 37.4, 36.2, 28.2, 27.6, 23.2 (2C), 22.1 (2C), 20.8 (2C).
HRMS (ESI+) calcd for $C_{17}H_{19}Br_2N_2O_3^+$ [M+H]$^+$: 456.9757 ; found: 456.9765.

2-(3,4-Dibromo-2,5-dioxo-2,5-dihydro-1*H*-pyrrol-1-yl)acetic acid (34):[209]

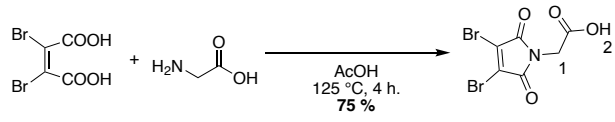

32 **33** **34**

3,4-dibromomaleic acid (250 mg, 0.91 mmol, 1.0 equiv.) was stirred at refluxed (125 °C) in acetic acid (5 mL) for 1 h before mixture was cooled down to room temperature. Then glycine (75 mg., 1 mmol, 1.1 equiv.) was added and mixture was refluxed for another 3 h before acetic acid was removed under reduced pressure, acetic acid traces were removed by co-evaporation three times with toluene (10 mL) and crude mixture was purified by column chromatography using slow gradient from DCM 99/1 AcOH to DCM 80/19 MeOH AcOH 1%) as eluting mixture. Product was isolated as a white powder with 78% yield (220 mg, 0.71 mmol).
Rf: 0.26 (eluent: $CHCl_3$ 90/10 MeOH)
^{1}H NMR (400 MHz, DMSO-d_6) δ 13.38 (s, 1H, H2), 4.26 (s, 2H, H1).
^{13}C NMR (101 MHz, DMSO-d_6) δ 168.4, 163.7 (2C), 129.6 (2C), 40.1.
HRMS (ESI+) calcd for $C_6H_4Br_2NO_4^+$ [M+H]$^+$: 311.8502 found: 311.8504.

(1R,8S,9S)-*N*-(3-(2-(3,4-Dibromo-2,5-dioxo-2,5-dihydro-1H-pyrrol-1-yl)acetamido)propyl)bicyclo[6.1.0]non-4-yne-9-carboxamide (DBM-4):

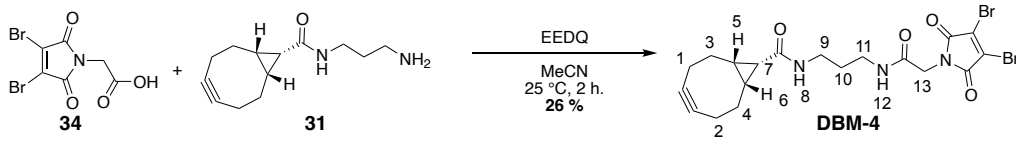

34 **31** **DBM-4**

2-(3,4-Dibromo-2,5-dioxo-2,5-dihydro-1H-pyrrol-1-yl)acetic acid **34** (31.3 mg, 0.10 nmol, 1.2 equiv.) was solved in MeCN (2 mL) and 2-ethoxy-1-ethoxycarbonyl-1,2-dihydroquinoline (EEDQ) (26.7 mg, 0.11 nmol, 1.2 equiv.) was added. The resulting pink mixture was stirred at room temperature for 1 h before (1*R*,8*S*,9*s*)-*N*-(3-aminopropyl)bicyclo[6.1.0]non-4-yne-9-carboxamide **31** (20 mg, 0.09 nmol, 1.0 equiv.) was added as a solution in MeCN (1 mL). Mixture was stirred at room temperature for an extra hour and MeCN was removed under reduced pressure. Crude orange solid was purified by column chromatography (eluent cHex 50/50 EtOAc) to afford the title compound as a white foamy solid with 26% yield (12 mg, 0.02 mmol).
Rf = 0.3 in cHex/EtOAc (30:70), UV visible + stained by vaniline.
^{1}H NMR (400 MHz, DMSO-d_6) δ 8.15 (t, *J* = 5.7 Hz, 1H, H8), 7.92 (t, *J* = 5.7 Hz, 1H, H12), 4.08 (s, 2H, H13), 3.09 – 2.95 (m, 4H, H9-H11), 2.32 – 2.04 (m, 4H, H1-2), 1.94 – 1.85 (m, 2H, H3'-4'), 1.68 (t, *J* = 9.1 Hz, 1H, H7), 1.49 (q, *J* = 6.9 Hz, 2H, H10), 1.14 – 1.05 (m, 2H, H3"-4").
^{13}C NMR (101 MHz, DMSO-d_6) δ 171.0, 168.4, 163.2 (2C), 130.0 (2C), 99.3 (2C), 62.3, 36.7 (2C), 29.8, 27.9, 23.6 (2C), 22.4 (2C), 21.1 (2C).
HRMS (ESI+) calcd for $C_{19}H_{22}Br_2N_3O_4^+$ [M+H]$^+$ 513.9972; found 513.9965.

IV. Bioconjugation

IV.1. Multicomponent reactions for labelling of native proteins

IV.1.a. Robinson-Schöpf MCR

Reaction mechanism and calculated masses of the different adducts

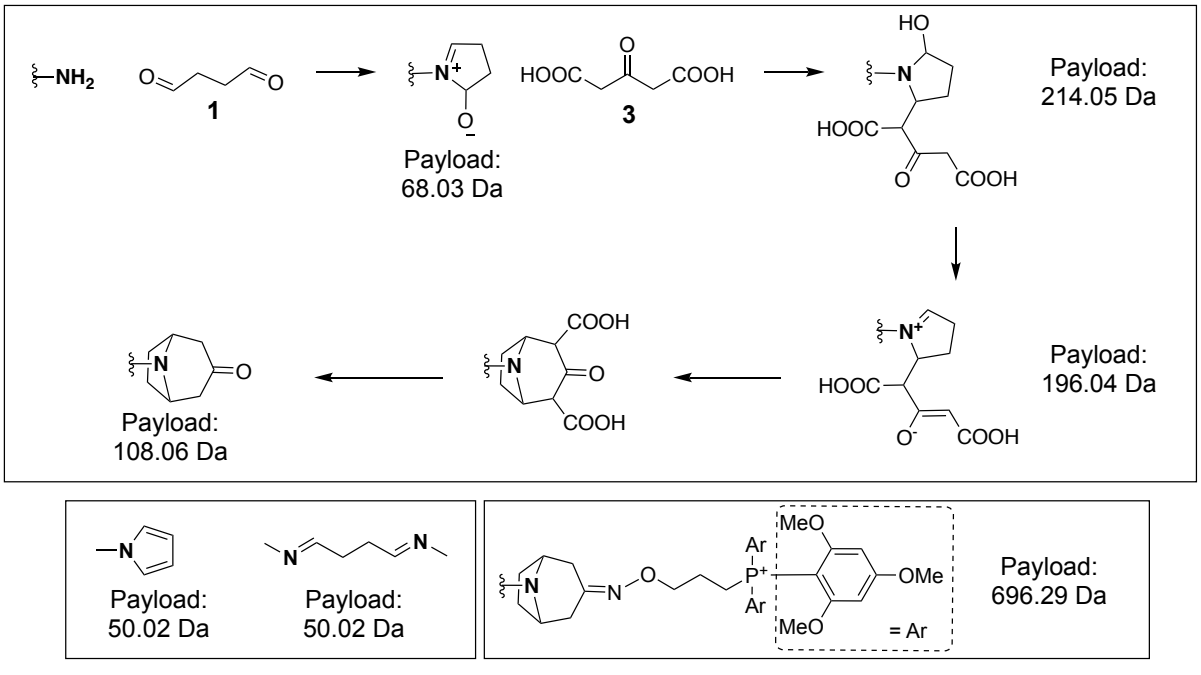

Procedures

Dialdehyde formation: To a 100 µL solution of 2,5-dimethoxytetrahydrofuran **2** (0.1 M in H_2O) was added HCl (as a 0.1 M solution in H_2O, 16 µL). The reaction mixture was then heated at 70 °C for 30 min after which, the reaction mixture was cooled to room temperature.

Tropinone formation: To a solution of trastuzumab (10 mg/mL in PBS (1X, pH 5.0), 50 µL, 1.0 equiv.) was added 3-oxoglutaric acid **3** (as a 0.01 M solution in H_2O, 4.11 µL, 12 equiv.), HCl (as a 0.01 M solution in H_2O, 4.38 µL, 12.8 equiv.) and NaOAc (as 0.1 M solution in H_2O, 1.37 µL, 40 equiv.). Then, the dialdehyde **1** (as a 0.01 M solution (diluted from the 0.1 M solution with H_2O), 3.42 µL, 10 equiv.) was added and the reaction mixture was incubated at 37 °C for 3 h before the excess of reagent was removed by gel filtration chromatography using biospins P-30 columns pre-equilibrated with PBS (1X, pH 7.5) to give a solution of tra-trop.

Tropinone functionalization: To the purified solution of tra-trop was added TMPP-ONH_2 (as 0.05 M solution in H_2O (or DMSO), 5 µL, 200 equiv.) and the reaction was incubated for 16 h at

25 °C before the excess of reagent was removed by gel filtration chromatography using biospins P-30 columns pre-equilibrated with PBS (1X, pH 7.5) to give a solution of tra-TMPP. Samples was then deglycosylated and buffer exchanged to NH_4OAc (150 mM, pH 7.5) buffer before it was analysed on the LCT spectrometer and the EMR spectrometer.

Pyrrole formation: To a solution of trastuzumab (5 mg/mL in NaOAc buffer (1M, pH 5), 50 µL, 1.0 equiv.) was added succinaldehyde **1** (as a 0.01 M solution in H_2O, 0.8 µL, 5 equiv.). The reaction mixture was incubated at 37 °C for 30 min before the excess of reagent was removed by gel filtration chromatography using biospins P-30 columns pre-equilibrated with PBS (1X, pH 7.5) to give a solution of tra-pyr.

Variation of different reaction's parameters

Variation of the pH, equivalent of reagent and temperature were evaluated on the conjugation efficiency, after TMPP functionalization.

Equiv.				pH	T (°C)	t (h)	"D0" %	$M_{payload}$ (Da)	Aspect
CHO, 1	COOH, 3	HCl	NaOAc						
20	24	28	80	5	37	3	Degradation of the mAb		
10	0	14	40	5	37	3	100	56	Broad peak
0	12	14	40	5	37	3	100	/	Native mAb
10	12	0	0	5	37	3	100	/	Broad peak
10	12	0	40	5	37	3	26	684	3 adducts
10	12	14	0	5	37	3	16	681	5 adducts
10	12	14	40	7.5	37	3	48	672	3 adducts
10	12	14	40	5	25	3	42	680	1 adduct
10	12	14	40	5	37	1	100	51	Broad peak
5	50	0	0	5	37	0.5	100	51	4 adducts
5	0	0	0	5	37	0.5	100	50	4 adducts

Analysis of tra-TMPP:

LCT analysis:

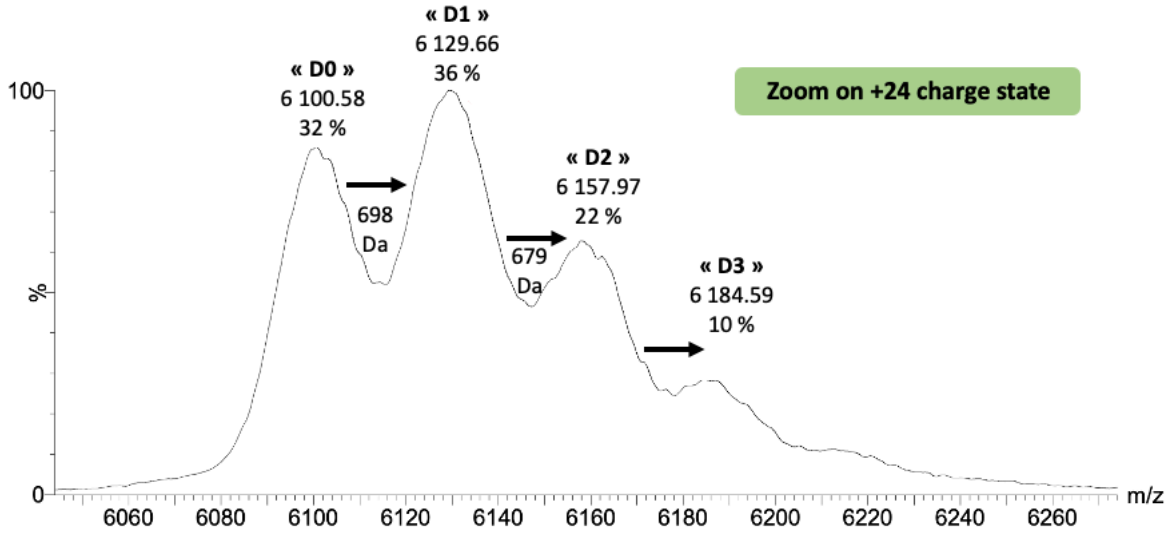

EMR analysis:

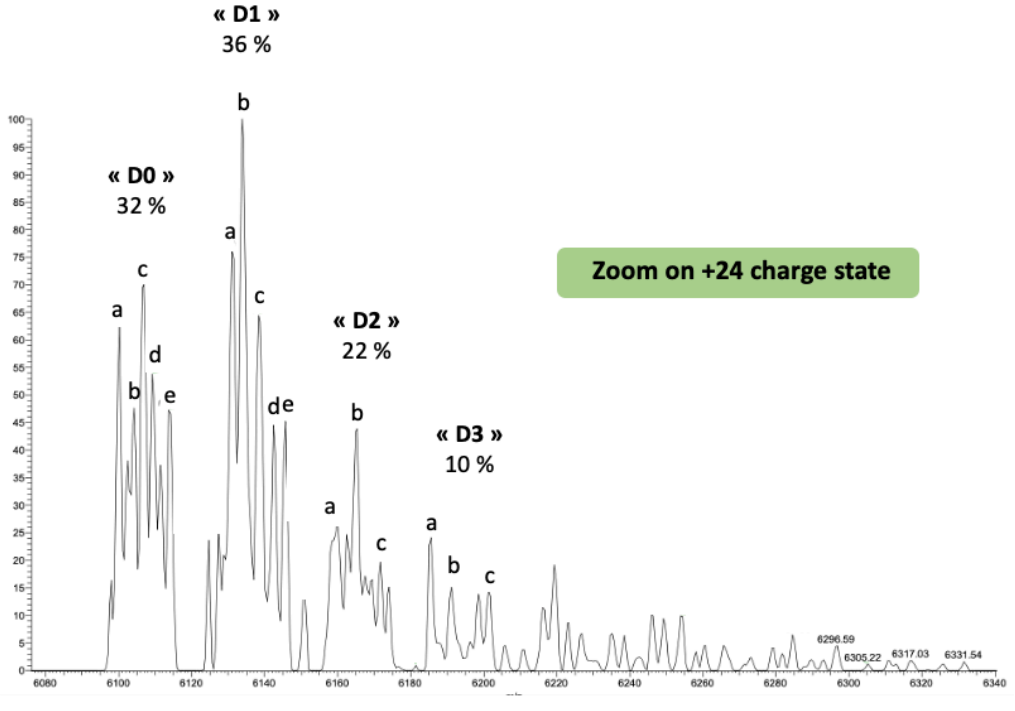

D0		
peak	M (Da)	Δ
a	146 402	91
b	146 493	69
c	146 562	61
d	146 623	112
e	146 735	

D1		
peak	M (Da)	Δ
a	147 057	92
b	147 149	65
c	147 214	110
d	147 324	169
e	147 493	

D2		
peak	M (Da)	Δ
a	147 836	126
b	147 962	158
c	148 120	

Δ = mass difference between peak n and n+1.

Analysis of tra-trop:

LCT analysis:

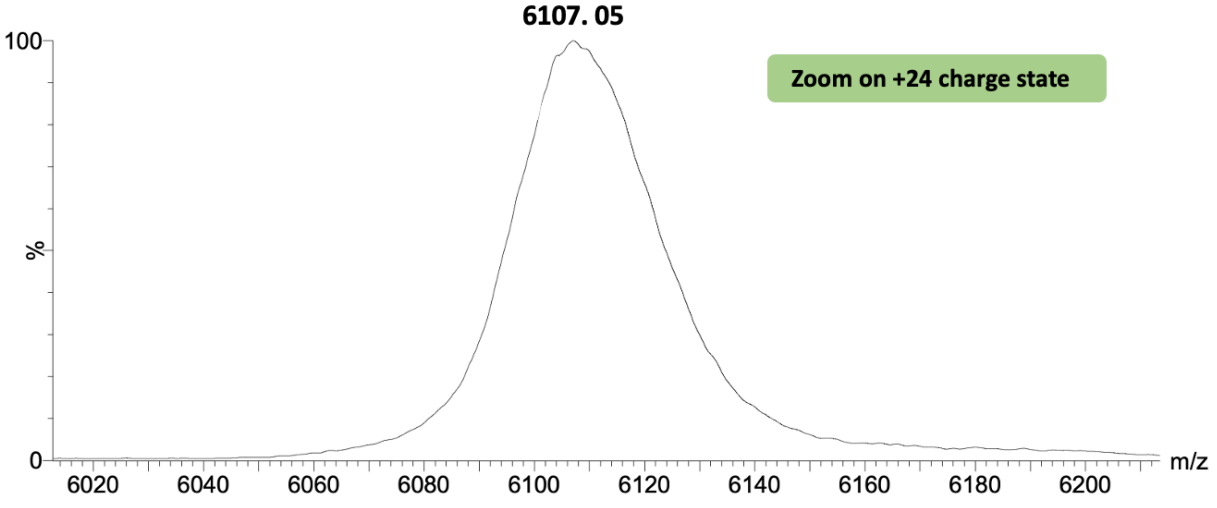

EMR analysis:

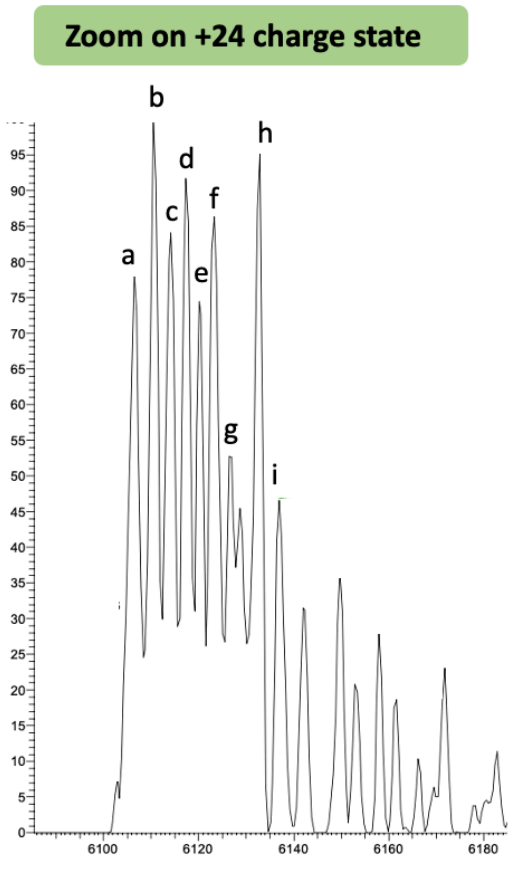

peak	M (Da)	Δ
a	146 558	
		98
b	146 656	
		67
c	146 723	
		95
d	146 818	
		70
e	146 888	
		69
f	146 957	
		120
g	147 077	
		108
h	147 185	

Analysis of tra-pyr:

Native SEC-MS analysis on the BioAccord:

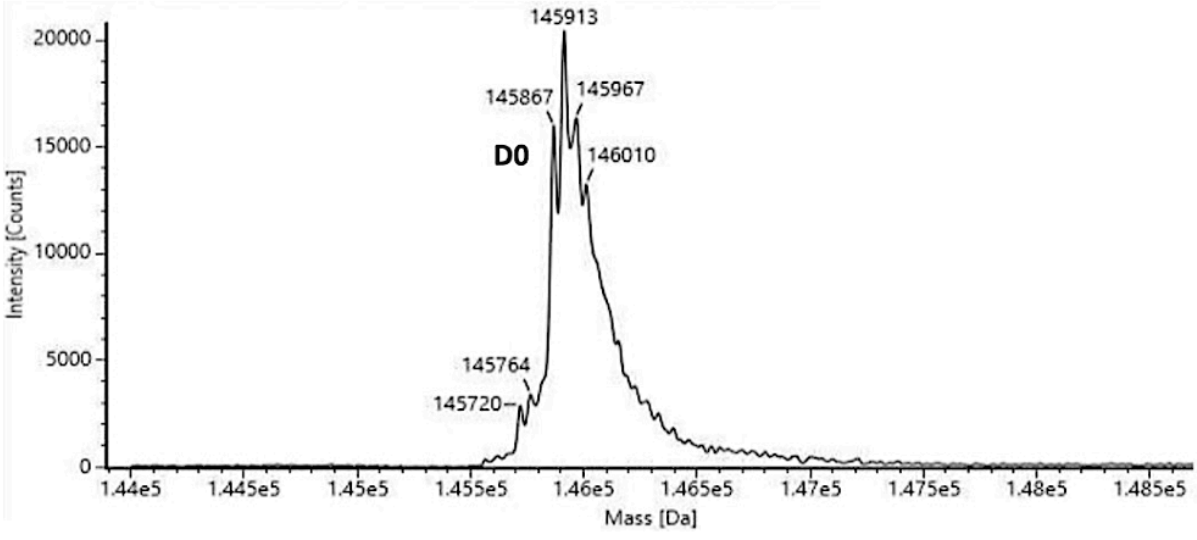

IV.1.b. Chlorooxime conjugation for the Ugi 4C-3CR:

Structure of the conjugates:

Carbonyl	Isocyanide	Conjugate	M (Da)
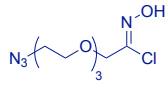		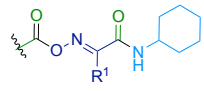	1198.53
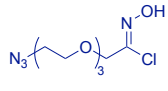	/	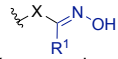 X: any nucleophilic amino acid	1089.45

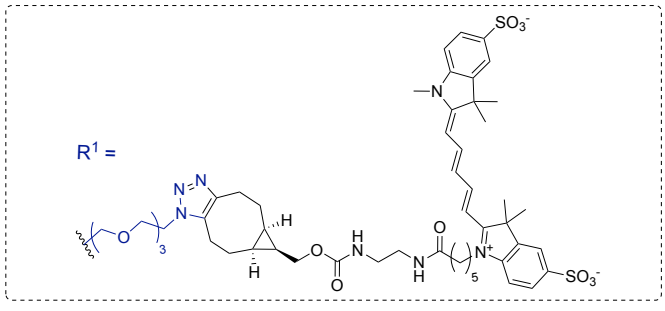

Procedure:

Chlorooxime conjugation: To a solution of trastuzumab (1 equiv., 10 mg/mL, 50 µL in PBS (1X, pH 7.5), 3.33 nmol) was added α-chlorooxime **8** (5 equiv., 1.71 µL from a 10 mM stock solution in DMSO). The reaction mixture was incubated for 2 h at 5 °C before the excess of reagent was removed by gel filtration chromatography using biospins P-30 columns pre-equilibrated with PBS (1X, pH 7.5) to give a solution of tra-N_3.

SPAAC functionalization: To this solution of tra-N_3 was added BCN-Cy5 (10 equiv. from a 10 mM stock solution in DMSO) and the solution was incubated at 25 °C for 20 h before the excess of reagent was removed by gel filtration chromatography using biospins P-30 columns pre-equilibrated with PBS (1X, pH 7.5) to give a solution of mAb-Cy5.

Preparation for analysis: Samples were then deglycosylated and buffer exchanged to NH_4OAc (150 mM, pH 7.5) buffer before they were analysed on the LCT spectrometer.

Time course study:

To evaluate the influence of the time on the conjugation of **8**, time variation studies were conducted in the chlorooxime's conjugation conditions mentioned above. Optimal conditions are highlighted in green.

time (h)	Conv. (%)	Av. DoC	M payload (Da)
2	59	0.86	1091.09
4	67	0.98	1088.48
2	59	1.00	1088.00
0.25	0	0	/
0.5	5	0.05	1086.32
1	20	0.20	1097.00
2	60	0.82	1088.90
8	72	1.12	1089.00

Competition experiment:

To a solution of trastuzumab (1 equiv., 10 mg/mL, 50 µL in PBS (1X, pH 7.5), 3.33 nmol) was added α-chlorooxime **8** (5 equiv., 1.71 µL from a 10 mM stock solution in DMSO) and the appropriate Ac-aa-NHMe (50 equiv., 1.71 □L from a 0.1 M stock solution in H_2O). The reaction mixture was incubated for 2 h at 5 °C before the excess of reagent was removed by gel filtration chromatography using biospins P-30 columns pre-equilibrated with PBS (1X, pH 7.5) to give a solution of mAb-N_3. To this solution of mAb-N_3 was added BCN-Cy5 (10 equiv. from a 10 mM stock solution in DMSO) and the solution was incubated at 25 °C for 20 h before the excess of reagent was removed by gel filtration chromatography using biospins P-30 columns pre-equilibrated with PBS (1X, pH 7.5) to give a solution of mAb-Cy5. Concentration in protein and dye were analysed by absorbance at 280 nm using LigandTracer mode "protein and Label.

Ac-aa-NHMe	DoC (Fluo)
Lys	0.9
Tyr	0.8
Gly	0.8
His	0.3
Asp	0.4
Glu	0.3
Ø	0.9

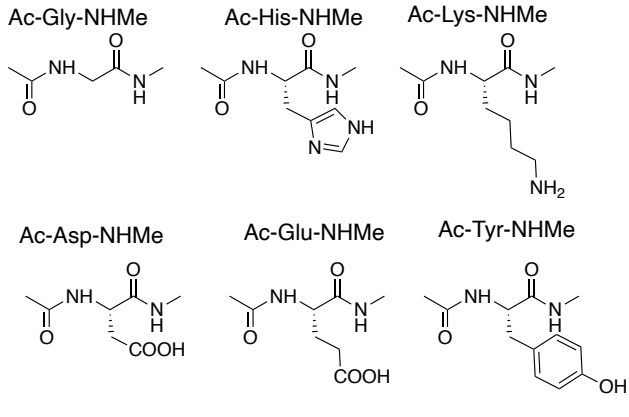

Analysis on the LCT spectrometer:

Tra-Cy5 produced using 5 equiv. of chlorooxime **8** incubated at 4 °C for 2 h followed by SPAAC using BCN-Cy5.

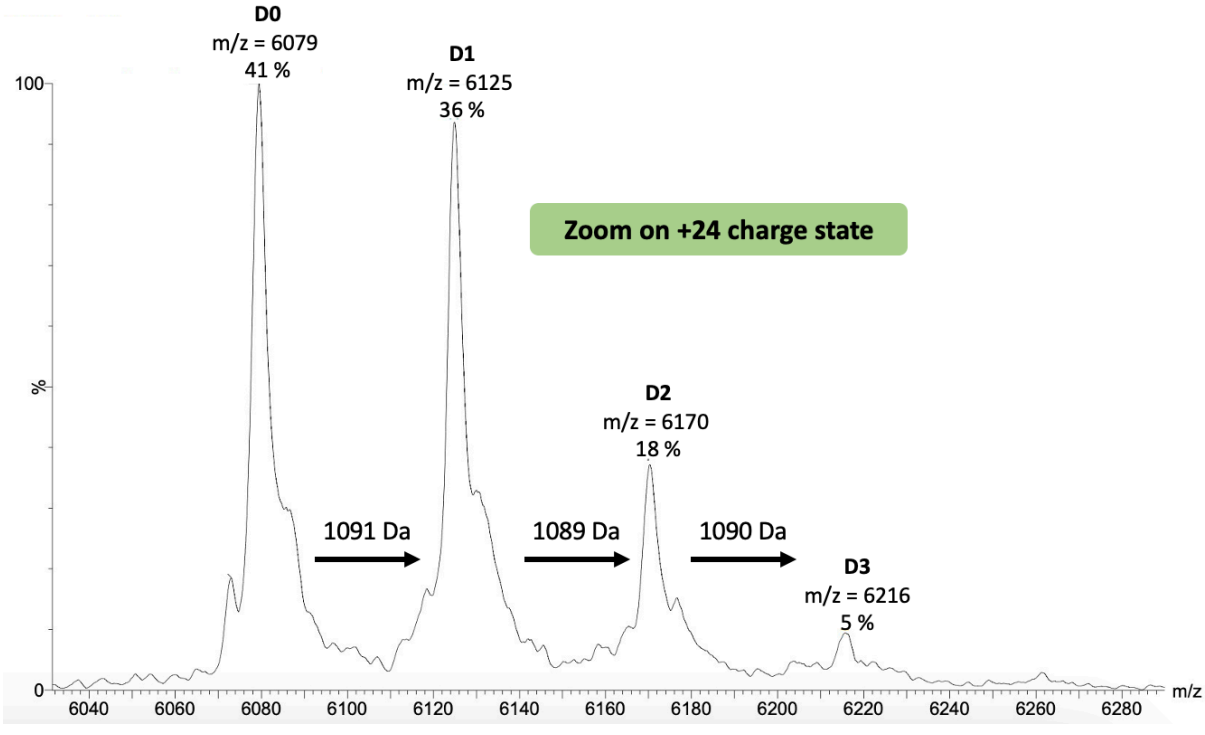

IV.1.c. Hydrazone conjugation

Structure of the conjugates:

Hydrazone	isocyanide	C1 (Da)	C2 (Da)	C3 (Da)
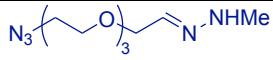 **14**	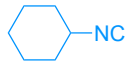 **a**	1213.6	1167.5	1185.5
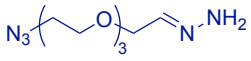 **15**		1199.6	1167.5	1185.5
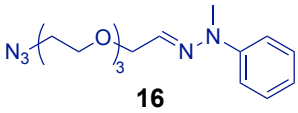 **16**		/	1167.5	1185.5
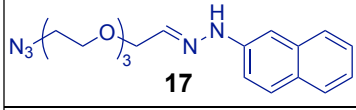 **17**		1325.6	1167.5	1185.5
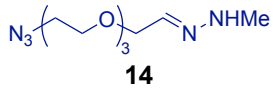 **14**	 **b**	1173.5	1127.5	1145.5
	 **c**	1187.6	1141.5	1159.5
	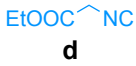 **d**	1125.4	1171.5	1189.5

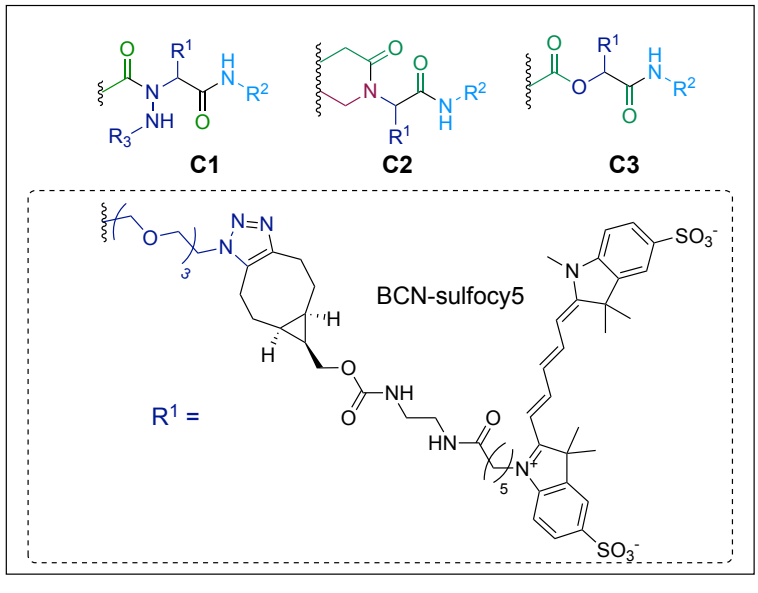

Procedures:

Hydrazone conjugation: To a solution of trastuzumab (10 mg/mL, 50 µL in PBS (1X, pH 7.5), 3.33 nmol, 1.0 equiv.) was added isocyanide **a** (from a 0.3 M stock solution in DMSO) followed by hydrazone **14** (from a 0.3 M stock solution in DMSO). The reaction mixture was incubated for the 20 h at 25 °C before NH_2OH (1 v% of a 50 w% solution in water) was added. Sample was incubated an extra hour at 25 °C before the excess of reagent was removed by gel filtration chromatography using biospins P-30 columns pre-equilibrated with PBS (1X, pH 7.5) to give a solution of tra-N_3.

SPAAC functionalization: To this solution of tra-N_3 was added BCN-Cy5 (10 equiv. from a 10 mM stock solution in DMSO), the solution was then incubated at 25 °C for 20 h. The excess of reagent was removed by gel filtration chromatography using biospins P-30 columns pre-equilibrated with PBS (1X, pH 7.5) to give a solution of tra-Cy5.

Native MS preparation: Samples were then deglycosylated and buffer exchanged to NH_4OAc (150 mM, pH 7.5) buffer before it was analysed on the LCT spectrometer.

Optimization of the conditions:

The influence on the variation in the reaction time, temperature and reagents quantity on the hydrazone conjugation was evaluated using isocyanide **a** and hydrazone **14**. Selected optimal conditions are highlighted in green.

Equiv. hydrazone:NC	t (h)	T (°C)	pH	Conv. (%)	Av. DoC	M payload (Da)
45:45	16	25	7.5	47	0.56	1168.75
75:75	16	25	7.5	58	0.83	1172.16
100:100	16	25	7.5	57	0.75	1169.04
100:100	24	25	7.5	84	1.70	1169.13
100:100	24	37	7.5	77	1.43	1244.81
100:0	24	37	7.5	0	0	/
25:25	24	25	7.5	17	0.17	1181.75
50:50	24	25	7.5	42	0.50	1168.75
60:60	24	25	7.5	48	0.50	1167.5
75:75	24	25	7.5	58	0.80	1169
90:90	24	25	7.5	58	0.80	1174.67
100:100	24	25	7.5	66	1.00	1164.33
100:100	24	25	6.5	70	0.98	1172.58
100:100	24	25	7.5	75	1.23	1162.62
100:100	24	25	8.5	75	1.22	1170.66
100:100	24	5	7.5	13	0.13	1165
100:100	24	25	7.5	60	0.90	1191,12

100:100	24	37	7.5	75	1.22	1170.00

Variation of the hydrazone component:

The influence of the hydrazone's substituent was then evaluated, using isocyanide **a** in the optimal conditions mention above. Results seems to indicate a clear impact of this parameter on the bioconjugation efficiency.

hydrazone	Conv. (%)	Av. DoC	M payload (Da)
15	69	1	1123.84
16	0	0	0
17	0	0	0

Variation of the isocyanide:

The influence of the isocyanide's side chain was then evaluated, using hydrazone **14** in the optimal conditions mention above. Results seems to indicate a clear impact of this parameter on the bioconjugation efficiency.

Used NC	Conv. (%)	Av. DoC	M payload (Da)
b	19	0.19	1131
c	20	0.20	1143
a	62	0.90	1170
d	47	0.59	1154

Analysis on the LCT spectrometer:

Tra-Cy5 produced using 100 equiv. of isocyanide **a**, 100 equiv. of hydrazone **14**, incubated at 25 °C for 20 h followed by SPAAC using BCN-Cy5.

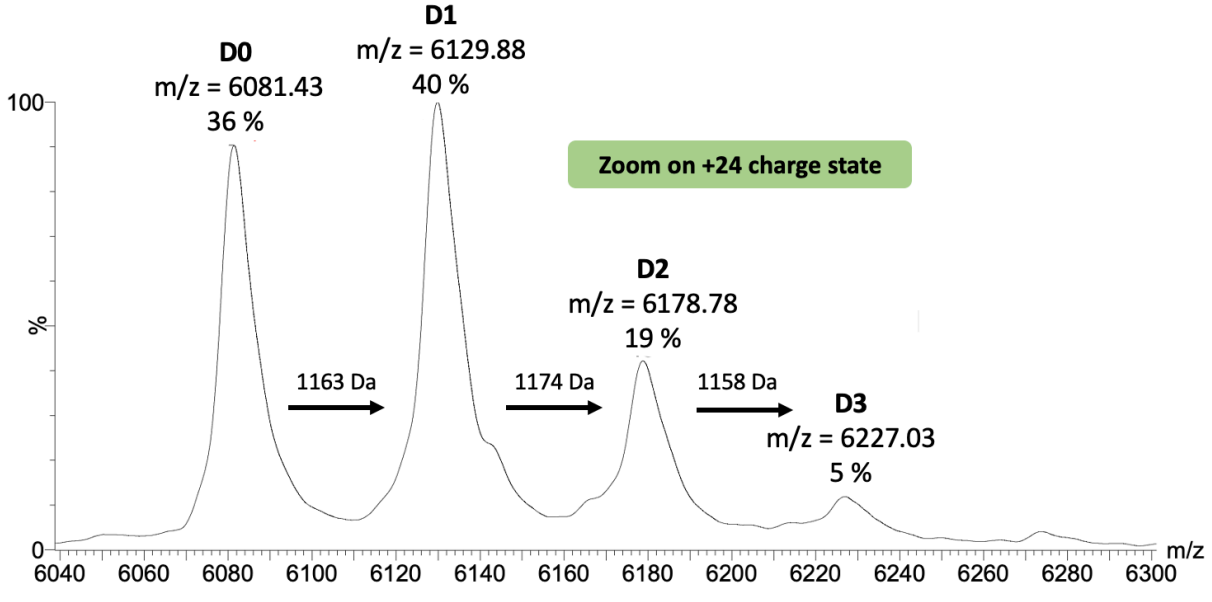

Tra-Cy5 produced using 45 equiv. of isocyanide **a**, 45 equiv. of hydrazone **14**, incubated at 25 °C for 16 h followed by SPAAC using BCN-Cy5.

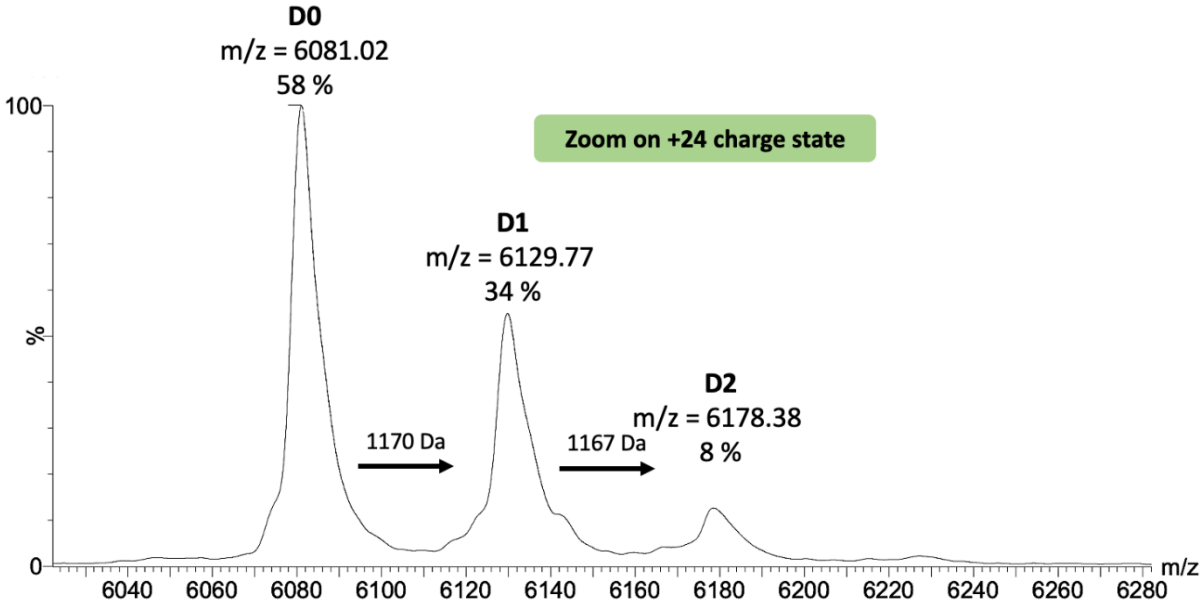

IV.1.d. In depth mechanistic study of the Ugi 4C-3CR

Structure of the conjugates:

R^1-CHO	R^2-NC	Passerini payload (Da)	Ugi payload (Da)
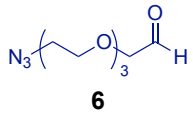 **6**	 **a**	787	769
	 **b**	747	729
	 **c**	761	743
	 **d**	791	773
	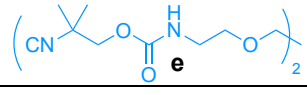 **e**	1077	1059
 **18**	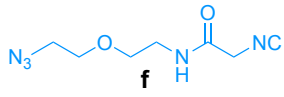 **f**	730	712
	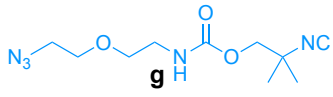 **g**	788	770

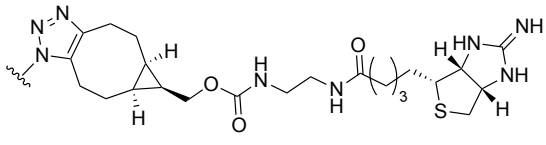

N_3 + BCN-iminobiotin

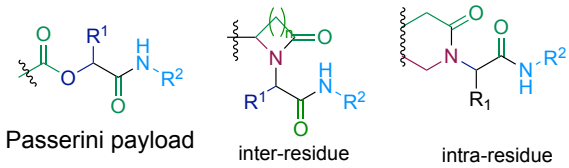

Procedures:

Ugi reaction: To a solution of trastuzumab (3.3 nmol in PBS (1X, pH 7.5), 1.0 equiv.) was added the isocyanide (from a 0.1 M stock in DMSO) followed by the aldehyde (from a 0.1 M stock in DMSO). The solution was incubated at 25 °C for 16 h before NH_2OH (1 v% of a 50 w% solution in water) was added. Sample was incubated an extra hour at 25 °C before the excess of reagent was removed by gel filtration chromatography using biospins P-30 columns pre-equilibrated with PBS (1X, pH 7.5) to give a solution of tra-N_3.

SPAAC functionalization: To a solution of tra-N_3 solution was added BCN-iminobiotin (30 equiv. from a 10 mM stock solution in DMSO) and the solution was incubated at 25 °C for 20 h. The excess of reagent was removed by gel filtration chromatography using biospins P-30 columns pre-equilibrated with PBS (1X, pH 7.5) to give a solution of tra-biotin.

Native MS preparation: Samples were then deglycosylated and buffer exchanged to NH_4OAc (150 mM, pH 7.5) buffer before it was analysed on the LCT spectrometer. Remaining samples were then analysed by LC-MS/MS and modification sites and structures were determined.

Reproducibility of the method:

In order to validate the reproducibility of this bioconjugation method, three operators conducted the same experiment in the Ugi "optimal" conditions — i.e. trastuzumab (10 mg/mL in PBS 1X, pH 7.5) incubated with 45 equiv. of isocyanide **a** and aldehyde **6** at 25 °C for 16 h followed by SPAAC reaction with BCN-iminobiotin — several times and the resulting samples were analyzed by LC-MS and LC-MS/MS analysis.

exp	Conv. (%)	Av. DoC	Payload (Da)	Chain	Peptide	AA	Ugi	Passerini
CS	86	1.8	771.63	HC	1-19	E1	X	X
				LC	1-18	D1	X	X
				LC	150-183	E165-K169	X	
VV	64	1	774.67	HC	1-19	E1	X	X
				HC	60-87	D62-K65	X	
				HC	259-291	E275-K277	X	
				LC	1-18	D1	X	X
VV	74	1.3	772.00	HC	1-19	E1	X	X
				HC	60-87	D62-K65	X	
				HC	259-291	E275-K277	X	
				LC	1-18	D1	X	X
IK	70	1.1	765.67	HC	1-19	E1	X	X
				HC	60-87	D62-K65	X	
				HC	259-291	E275-K277	X	
				LC	1-18	D1	X	X
IK	76	1.3	757.33	HC	1-19	E1	X	X
				HC	60-87	D62-K65	X	
				HC	259-291	E275-K277	X	
				LC	1-18	D1	X	X
				LC	150-183	D165-K169	X	
IK	65	1.0	770.00	HC	1-19	E1	X	X
				LC	1-18	D1	X	

pH variation (IK):

Influence of the pH on the modification sites and mechanism was evaluated in the "optimal" reaction conditions i.e. trastuzumab (10 mg/mL in PBS 1X) incubated with 45 equiv. of isocyanide **a** and aldehyde **6** at 25 °C for 16 h.

pH	Conv. (%)	Av. DoC	Payload (Da)	Chain	Peptide	AA	Ugi	Passerini
5.5	67	1.0	760.33	HC	1-19	E1	X	X
				LC	1-18	D1	X	
6.5	58	0.9	771.33	HC	1-19	E1	X	X
				LC	1-18	D1	X	
7.5	65	1.0	770.00	HC	1-19	E1	X	X
				LC	1-18	D1	X	
8.5	66	1.0	775.00	HC	1-19	E1	X	X
				LC	1-18	D1	X	

Time course experiment (CS):

Influence of the reaction time on the modification sites and mechanism was evaluated in the "optimal" conditions i.e. trastuzumab (10 mg/mL in PBS 1X, pH 7.5) incubated with 45 equiv. of isocyanide **a** and aldehyde **6** at 25 °C followed by a SPAAC reaction with BCN-iminobiotin.

t (h)	Conv. (%)	Av. DoC	Payload (Da)	Chain	Peptide	AA	Ugi	Passerini
1	11	0.1	775.00	HC	1-19	E1	X	X
				LC	1-18	D1	X	
2	28	0.3	775.00	HC	1-19	E1	X	X
				LC	1-18	D1	X	
4	62	0.9	775.00	HC	1-19	E1	X	X
				LC	1-18	D1	X	
8	78	1.4	766.67	HC	1-19	E1	X	X
				LC	1-18	D1	X	
16	86	1.8	771.63	HC	1-19	E1	X	X
				LC	1-18	D1	X	X
				LC	150-183	E165-K169	X	

Variation of the isocyanide's side chains:

Influence of the variation of the isocyanide's side chains on the modification sites and mechanism was evaluated in the Ugi "optimal" conditions i.e. trastuzumab (10 mg/mL in PBS 1X, pH 7.5) incubated with 45 equiv. of isocyanide and aldehyde **6** at 25 °C for 16 h followed by a SPAAC reaction with BCN-iminobiotin.

Exp	NC	Conv. (%)	Av. DoC	Payload (Da)	Chain	Peptide	AA	Ugi	Passerini
CS	**b**	81	1.3	725.0	HC	1-19	E1	X	X
					LC	1-18	D1		X
IK	**c**	52	0.8	732.0	HC	1-19	E1	X	X
					LC	1-18	D1	X	X
CS	**d**	65	1.0	750.0	HC	1-19	E1	X	
IK	**d**	69	1.2	719.3	HC	1-19	E1	X	
					LC	1-18	D1	X	X
VV	**d**	60	0.5	755.7	HC	1-19	E1	X	
VV	**e**	44	0.5	1063.0	HC	1-19	E1	X	X
					LC	1-18	D1		X

Variation of both isocyanide and aldehyde's side chain:

Influence of the replacement of aldehyde **6** by aldehyde **18** was then studied. In order to maintain the Plug-and-Play character of the reaction, azido functionalized isocyanides were used in the optimal Ugi conditions i.e. trastuzumab (10 mg/mL in PBS 1X, pH 7.5) incubated with 45 equiv. of isocyanide and aldehyde **18** at 25 °C for 16 h followed by a SPAAC reaction with BCN-iminobiotin.

Exp	NC	Conv. (%)	Av. DoC	Payload (Da)	Chain	Peptide	AA	Ugi	Passerini
IK	**g**	54	0.8	766	HC	1-19	E1	X	X
					LC	1-18	D1	X	X
VV	**f**	59	0.9	733	HC	1-19	E1	X	X
					HC	222-251	D224		X
					LC	1-18	D1	X	X
					LC	184-207	D185-K188	X	

Exploration of the E1-selective conditions:

Based on the E1-selectivity observed in the Ugi "optimal" conditions — i.e. trastuzumab (10 mg/mL in PBS 1X, pH 7.5) incubated with 45 equiv. of isocyanide **d** and aldehyde **6** at 25 °C for 16 h followed by SPAAC reaction with BCN-iminobiotin —, variation of the conditions of reaction as well as inter-experimenter reproducibility was studied to evaluate their influence on the observed selectivity.

C (mg /mL)	Equiv. CHO:NC	t (h)	T (°C)	Conv. (%)	Av. DoC	Chain	Peptide	AA	Ugi	Passerini
10	45:45	16	25	60	0.9	HC	1-19	E1	X	
10	45:45	16	25	65	1.0	HC	1-19	E1	X	
10	45:45	16	25	69	1.2	HC	1-19	E1	X	
						LC	1-18	D1	X	X
15	45	16	25	83	1.8	HC	1-19	E1	X	
						LC	1-18	D1	X	X
15	100	2	25	61	0.5	HC	1-19	E1	X	X
						HC	60-87	D62-K65	X	
						HC	259-291	E275-K277	X	
						LC	1-18	D1		X
15	100	4	25	73	1.2	HC	1-19	E1	X	X
						HC	4-19	E6		X
						HC	60-87	D62-K65	X	
						HC	259-291	E275K-277	X	
						LC	1-18	D1		X
10	75	16	25	91	2.5	HC	1-19	E1	X	X
						HC	4-19	E6		X
						HC	60-87	D62-K65	X	
						HC	259-291	E275-K277	X	
						LC	1-18	D1		X
10	100	2	37	79	1.6	HC	1-19	E1	X	X
						HC	4-19	E6		X
						LC	1-18	D1	X	X

Protein transfer:

We next evaluated the transferability of the both the Ugi ”optimal” conditions — i.e. mAb (10 mg/mL in PBS 1X, pH 7.5) incubated with 45 equiv. of isocyanide **a** and aldehyde **6** at 25 °C for 16 h followed by SPAAC with BCN-iminobiotin and the E1-selective conditions — i.e. mAb (10 mg/mL in PBS 1X, pH 7.5) incubated with 45 equiv. of isocyanide **d** and aldehyde **6** at 25 °C for 16 h followed by SPAAC with BCN-iminobiotin — to other IgGs and the influence it might have on the conjugation efficiency and the modification sites.

Isocyanide a /aldehyde 6:

mAb	Conv. (%)	Av. DoC	Chain	Peptide	AA	Ugi	Passerini
rituximab	85	1.7	HC	260-292	E276-K278	X	
			LC	149-182	E165-K169	X	
bevacizumab	77	1.4	HC	1-19	E1	X	X
			LC	1-18	D1	X	
			LC	149-182	E164-K168	X	
ramucirumab	39	0.5	HC	1-19	E1	X	X
			LC	1-18	D1	X	

Isocyanide d/aldehyde 6:

mAb	Conv. (%)	Av. DoC	Chain	Peptide	AA	Ugi	Passerini
rituximab	45	1.5	/	/	/		
bevacizumab	44	0.6	HC	1-19	E1	X	
ramucirumab	52	0.8	HC	1-19	E1	X	X

Analysis on the LCT spectrometer:

Tra-biotin produced using 45 equiv. of isocyanide **a**, 45 equiv. of aldehyde **a**, incubated at 25 °C for 20 h followed by SPAAC using BCN-iminobiotin.

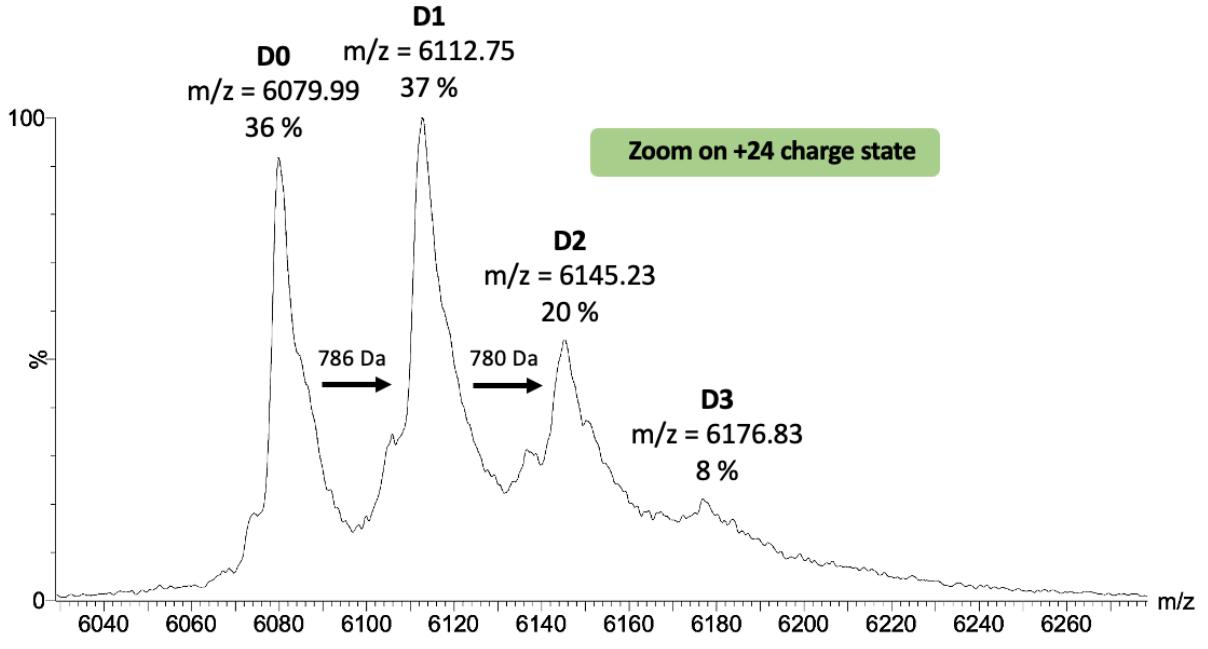

Tra-biotin produced using 45 equiv. of isocyanide **d**, 45 equiv. of aldehyde **a**, incubated at 25 °C for 20 h followed by SPAAC using BCN-iminobiotin.

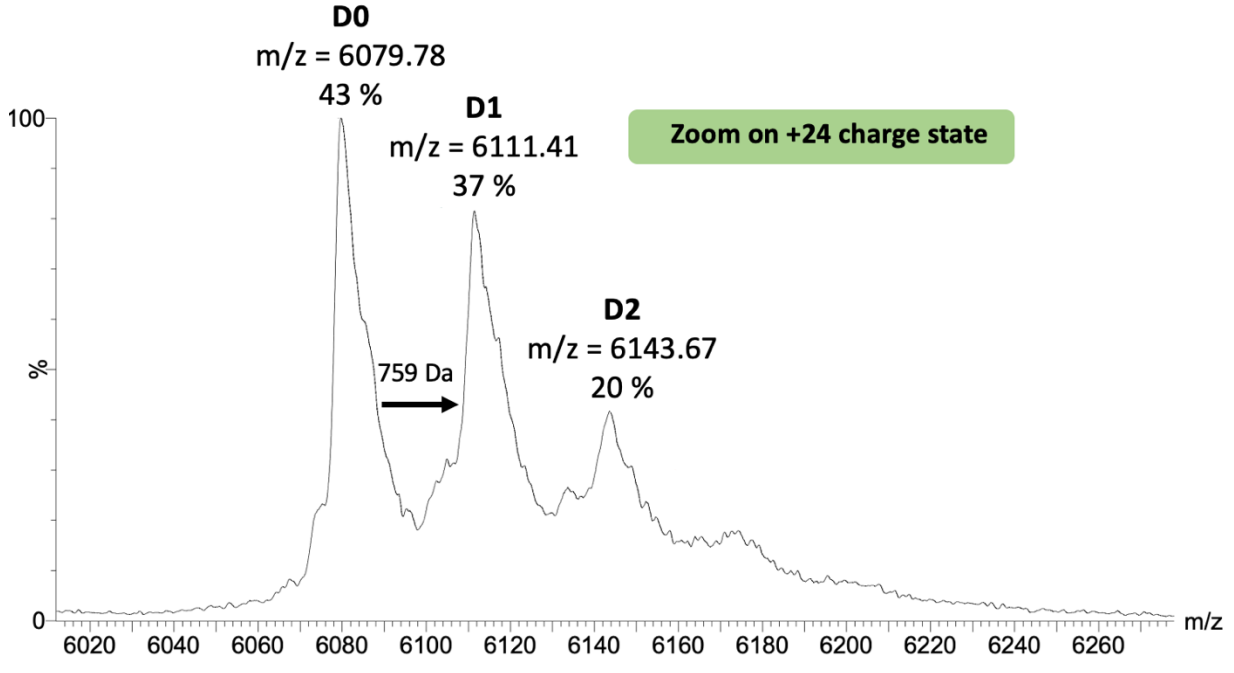

IV.2. Chemical formation of protein dimers

IV.2.a. Fab production

Procedures:

Pepsin digestion: Full mAb (1 equiv., 16 mg/mL, 500 µL) was buffer exchanged to pepsin digestion buffer (20 mM sodium acetate, pH 3.1) using Pierce Protein concentrator MWCO 30 kDa through three concentration/dilution cycles and the final volume of the sample was adjusted to 500 µL. Immobilized pepsin (350 µL) was charged on Pierce columns and storage solution was removed by centrifugation before the resin was washed with three times with 500 µL of digestion buffer. Sample was charged on the column and mixture was incubated at 37 °C under strong agitation (1100 rpm) for 6 h. Resin was then dried and washed with 3 x 500 µL PBS (1X, pH 7.5). Combined flush and washes were concentrated using Pierce Protein concentrator MWCO 10 kDa to give a solution of $F(ab')_2$ in PBS (1X, pH 7.5) with 60% yield.
Rq: After 6 h, some Fab (10%) and full mAb (16%) are observed by SEC using a Superdex^{TM} 200 Increase 10/300 GL column with 0.5 mL/min flow of PBS 1X, pH 7.5. The $F(ab')_2$ is eluted after 13.47 mL.

$F(ab')_2$ digestion: Immobilized papain (1 mL/mg mAb, 0.5 µL) was charged on a Pierce column, storage solution was removed by centrifugation and replaced with 500 µL of papain digest buffer (26 mM NaH_2PO_4, 77 mM Na_2HPO_4, 150 mM NaCl, 1 mM EDTA pH 6.8) supplemented with 10 mM DTT. Resin was incubated at 37 °C under strong agitation (1100 rpm) for 90 min. The resin was then washed with 6 x 500 µL of papain digestion buffer and the Fab_2 previously buffer exchanged to digest buffer was charged on the resin. Mixture was incubated at 37 °C under strong agitation (1100 rpm) for 24 h before the resin was flushed and washed with 3 x 500 µL of PBS. The digestat and washes were combined and concentrated using Pierce Protein concentrator MWCO 10 kDa to give a solution of Fab and Fc in PBS (1X, pH 7.5).

Papain digestion, method 1 (M1): Full mAb (5 mg) was buffer exchanged into digest buffer (20 mM NaH_2PO_4, 10 mM EDTA, 80 mM L-cysteine.HCl, pH 7.0) using Pierce Protein concentrator MWCO 30 kDa through three concentration/dilution cycles and the final volume of the sample was adjusted to 500 µL. Immobilized papain (0.1 mL/mg mAb, 0.5 mL) was charged on a pierce column, storage solution was removed and the resin was washed with 3 x 500 µL digest buffer before the mAb was charged on the column. Mixture was incubated at 37 °C, under strong agitation (1100 rpm) for 3 h before the digestat was recovered. Dry resin was washed with 3 x 500 µL PBS. Digestat and washes were combined and concentrated using Pierce Protein concentrator MWCO 10 kDa to give a solution of Fab and Fc in PBS(1X, pH 7.5).

Papain digestion, method 2 (M2): Immobilized papain (1 mL/mg mAb, 0.5 mL) was charged on a Pierce column, storage solution was removed by centrifugation and replaced with 500 µL of papain digest buffer (50 mM sodium phosphate (26 mM NaH_2PO_4 and 77 mM Na_2HPO_4), 150 mM NaCl, 1 mM EDTA pH 6.8) supplemented with 10 mM DTT. Resin was incubated at 25 °C under strong agitation (1100 rpm) for 60 min. The resin was then washed with six times with of papain digestion buffer (500 µL) and the mAb (5 mg in 500 µL digest buffer) was charged on the resin. Mixture was incubated at 37 °C under strong agitation (1100 rpm) for 16 h before the resin was flushed and washed with 3 x 500 µL of PBS. The digestat and washes were combined and concentrated using Pierce Protein concentrator MWCO 10 kDa to give a solution of Fab and Fc in PBS (1X, pH 7.5).

Protein A purification: Sample was purified on Protein A Plus Spin Columns 1 mL. Before its use, the column was left to warm at room temperature. Storage solution was flushed by centrifugation (1000 g, 1 min) and the resin was washed twice with protein A binding buffer (Phosphate 100 mM, NaCl 150 mM, pH 7.2). Sample's volume was adjusted to 1 mL before it was charged on the column which was gently agitated (end and over movement) for 10 min at room temperature. The column was then flushed and washed three times using 2 mL of protein A binding buffer. Flush and washes were collected, and buffer exchanged to PBS (1X, pH 7.5) using Thermo Scientific™ Pierce™ Protein Concentrators PES 10 K MWCO, 20 mL, 3 dilution-concentration cycles. Column was regenerated by washing twice with 3 mL of elution buffer (glycine 0.1 M, pH 2.5), 3 mL of PBS (1X, pH 7.5) and stored in 3 mL of PBS containing 0,01% NaN_3.

<u>mAb dependent methods:</u>

mAb	digestion				Protein A	AKTA	Fragment	M (Da)
	Pepsin	F(ab')$_2$	Papain					
			M1	M2				
trastuzumab	X	/	/	/	/	X	**F(ab')$_2$-tra**	97 296
trastuzumab	X	X	/	/	/	X	**F$_{tra}$**	47 637
avelumab	X	X	/	/	/	X	**F$_{ave}$**	46 855
durvalumab	/	/	X	/	/	X	**F$_{durva}$**	48 047
rituximab	/	/	/	X	X	/	**F$_{rit}$**	47 180
muromonab	/	/	X	/	X	/	**F$_{muro}$**	47 446

IV.2.b. Fab-BCN formation

Structure and calculated masses of the different adducts:

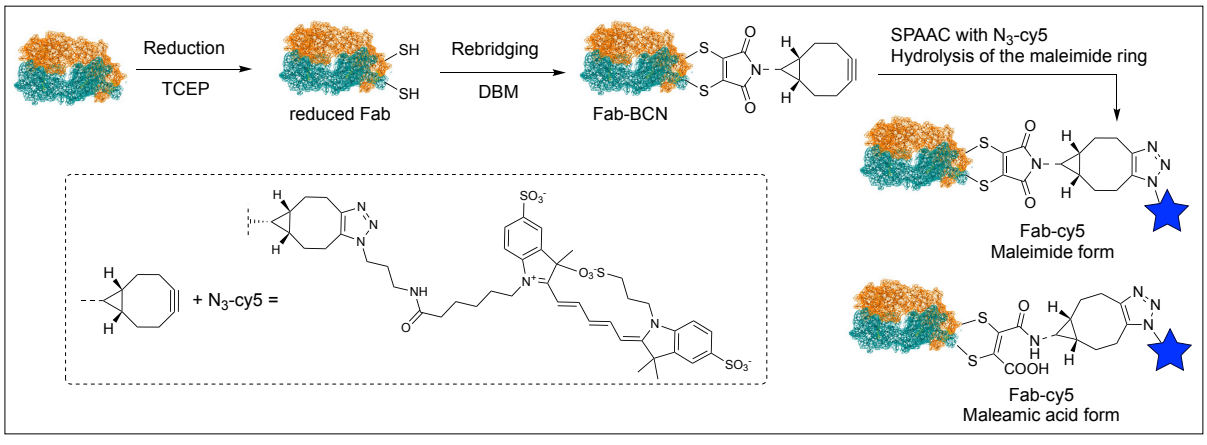

Reagent	Structure	Form	$M_{payload}$ (Da)
DBM-4	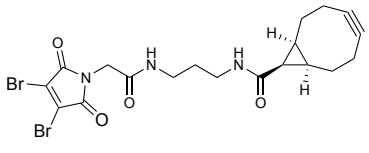	Maleimide	1184
		Maleamic acid	1202
DBM-3	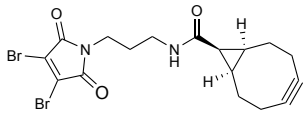	Maleimide	1127
		Maleamic acid	1145
DBM-2	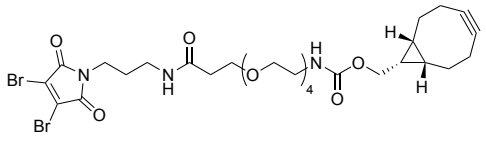	Maleimide	1405
		Maleamic acid	1423
DBM-1	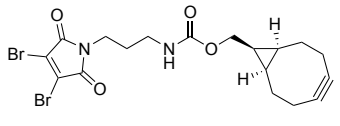	Maleimide	1157
		Maleamic acid	1175

Procedures:

Reduction: To a solution of Fab (105 µM in PBS 1X, pH 7.5) was added 5 mM EDTA (from a 0.5 M solution in H_2O) and 3,3',3''-phosphanetriyltripropionic acid (TCEP)(2 equiv. from a 0.02 M stock solution in mQ H_2O). The reaction mixture was incubated for 60 min at 37 °C before it was purified over biospins P6 pre-equilibrated with PBS (1X, pH 7.5) to give a solution of reduced Fab.

Reduction Fmuro: 50 equiv. of TCEP are required for the rebridging to be efficient.

Rebridging: To a solution of reduced Fab (105 µM in PBS (1X, pH 7.5)) was added the appropriate DBM (2 equiv. from a 0.01 M stock solution in DMSO). The reaction mixture was incubated for 20 min at 25 °C before it was purified over biospins P6 pre-equilibrated with PBS (1X, pH 7.5) to give a solution of rebridged Fab-BCN.

SPAAC : To the rebridged Fab-BCN, N_3-Cy5 (5 equiv. from a 0.01 M stock solution in DMSO) was added and sample was incubated at 25 °C for 16 h before it was purified over biospins P6 pre-equilibrated with PBS (1X, pH 7.5) to give a solution of Fab-Cy5.

Application to the different Fabs:

Fab	DBM	Conv. (%)	$M_{payload}$ (Da)
F_{tra}	DBM-4	100	1206
F_{rit}		100	1206
F_{ave}		100	1205
F_{durva}		100	1206
F_{muro}		100	1207
F_{rit}	DBM-3	100	1146
F_{rit}	DBM-2	89	1426
F_{rit}	DBM-1	74	1176

Native SEC-MS analysis:

F_{rit}-Cy5 rebridged using DBM-4.

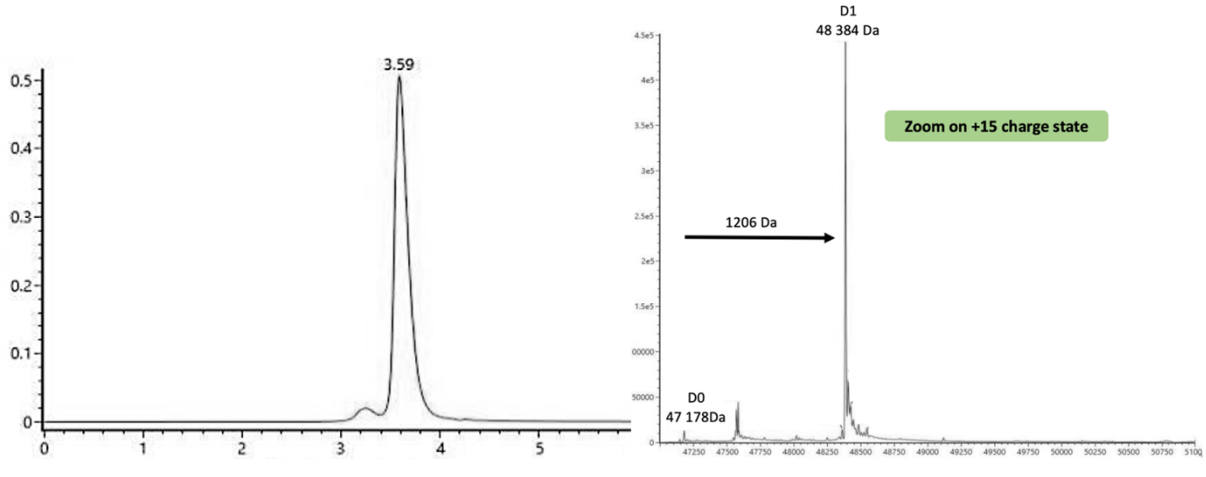

SDS-PAGE of different Fabs rebridged with DBM-4, under reducing conditions:

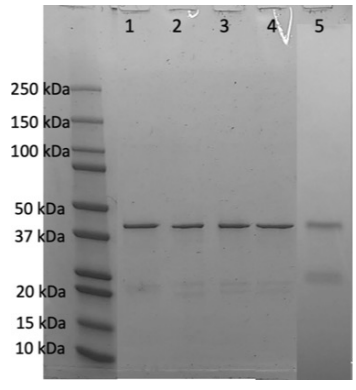

line	compound
1	F_{tra}-BCN
2	F_{rit}-BCN
3	F_{durva}-BCN
4	F_{ave}-BCN
5	F_{muro}-BCN

IV.2.c. BSA-BCN formation

Structure and calculated masses of the different adducts:

DBM	Form	$M_{payload}$ (Da)
DBM-1	Maleimide	1264
	Maleamic acid	1282
	Aspecific	1184
DBM-3	Maleimide	1485
	Maleamic acid	1503
	Aspecific	1405
DBM-4	Maleimide	1237
	Maleamic acid	1255
	Aspecific	1157

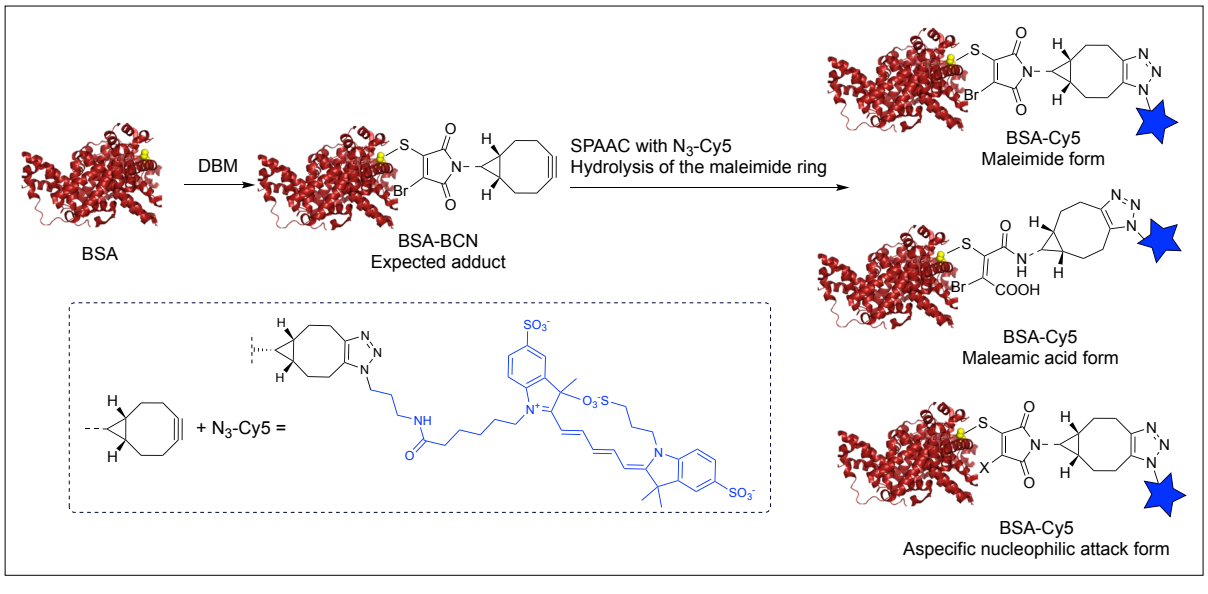

Native BSA analysis:

UV chromatogram: 2 main peaks were separated by SEC. The one with 2.51 min retention time was found to correspond to BSA-Dimer resulting from the formation of a disulfide bond between two BSA free cysteines. The peak with retention time of 2.85 (main product) was found to contain native BSA along with different species (see deconvoluted spectra).

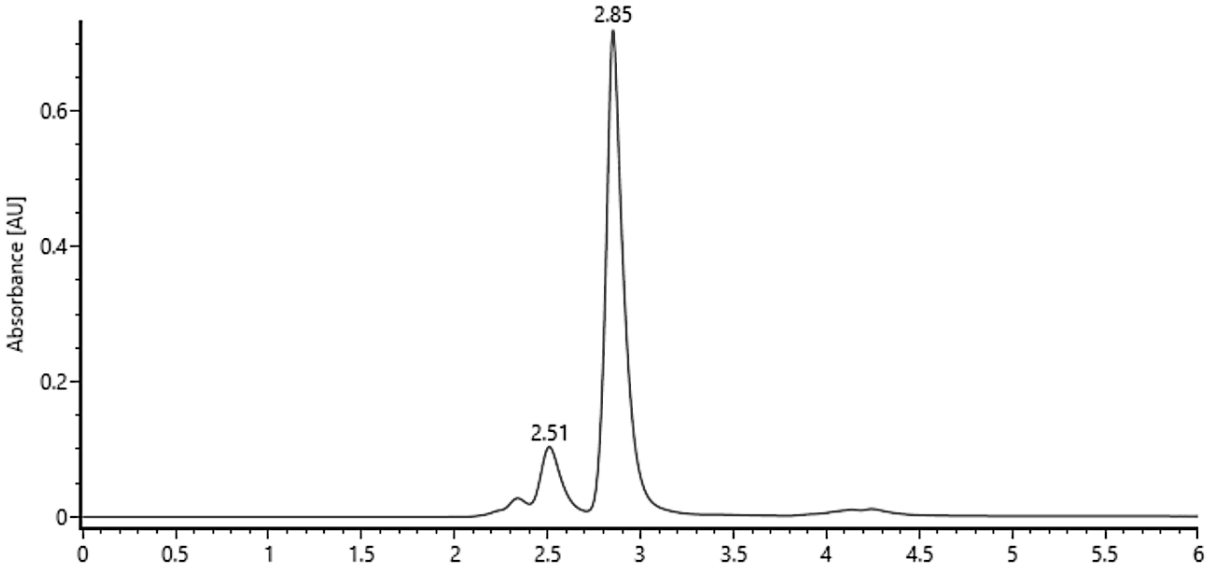

Deconvoluted spectrum of native BSA (2.85 min retention time): Native BSA is observed (M = 66 429 Da) as well as + 120 Da, + 167 Da and + 333 Da adducts.

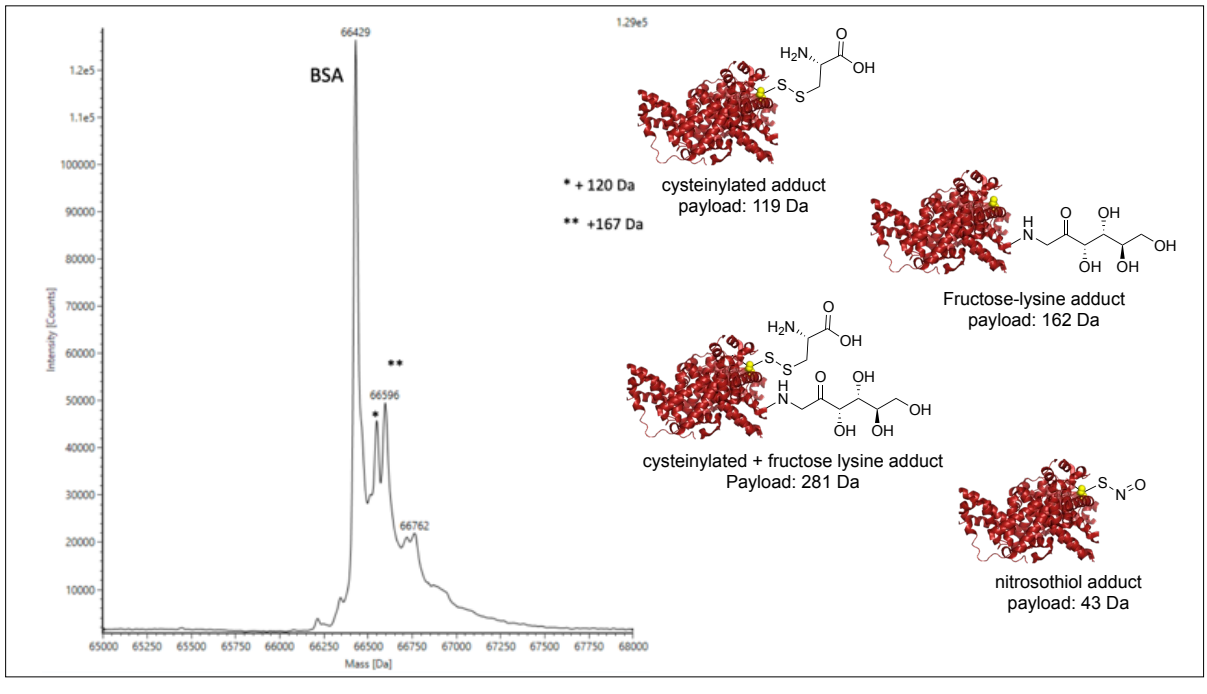

Procedures:

BCN-functionalization: 2 mg of BSA were diluted in 250 □L of PBS (1X, pH 7.5). The resulting solution was purified by SEC on an AKTA pure system (see preparative SEC in general procedure). The BSA containing fractions were combined and concentrated using vivaspin 30 kDa and buffer exchanged to PBS (1X, pH 6.5) to yield pure BSA. To a solution of pure BSA (50 □L from a 150 □M in PBS (1X, pH 6.5) was added 1 equiv. of DBM-4 (0.75 □L from a 0.01 M stock solution in DMSO) and the reaction mixture was incubated at 25 °C for 15 min before it was purified by gel filtration using biospins P6 pre-equilibrated with PBS (1X, pH 7.5) to afford a solution of BSA-BCN.

SPAAC reaction with N_3-Cy5: To the previously obtained solution of BSA-BCN, 5 equiv. of N_3-Cy5 were added (from a 0.01 M stock solution in DMSO) and the mixture was incubated at 25 °C overnight before it was purified by gel filtration using biospins P6 pre-equilibrated with PBS (1X, pH 7.5) to afford a solution of BSA-Cy5.

DBM variation:

DBM	[BSA] (□M)	Equiv.	pH	T (°C)	t (min)	Conv. (%)	% D2	$M_{payload}$ (Da)
DBM-4	150	2	7.5	25	20	100	20	D1: 1163 ; D2: 1241
		1	7.5	25	20	100	21	D1: 1159 ; D2: 1241
			6.5	25	20	100	17	D1: 1159 ; D2: 1241
			8.5	25	20	100	17	D1: 1160 ; D2: 1241
			6.5	37	15	100	10	D1: 1163 ; D2: 1240
	100	1	6.5	25	15	100	5	D1: 1157 ; 1240
	225	1	6.5	25	15	95	19	D1: 1159 ; D2: 1241
DBM-3	100	1	6.5	25	15	40	0	1423
	150	2	6.5	25	15	70	0	1409
DBM-1	100	1	6.5	25	15	100	0	1185

Native SEC-MS analysis on the BioAccord spectrometer:

BSA-cy5 rebridged with DBM-1 and functionalized with N_3-cy5.

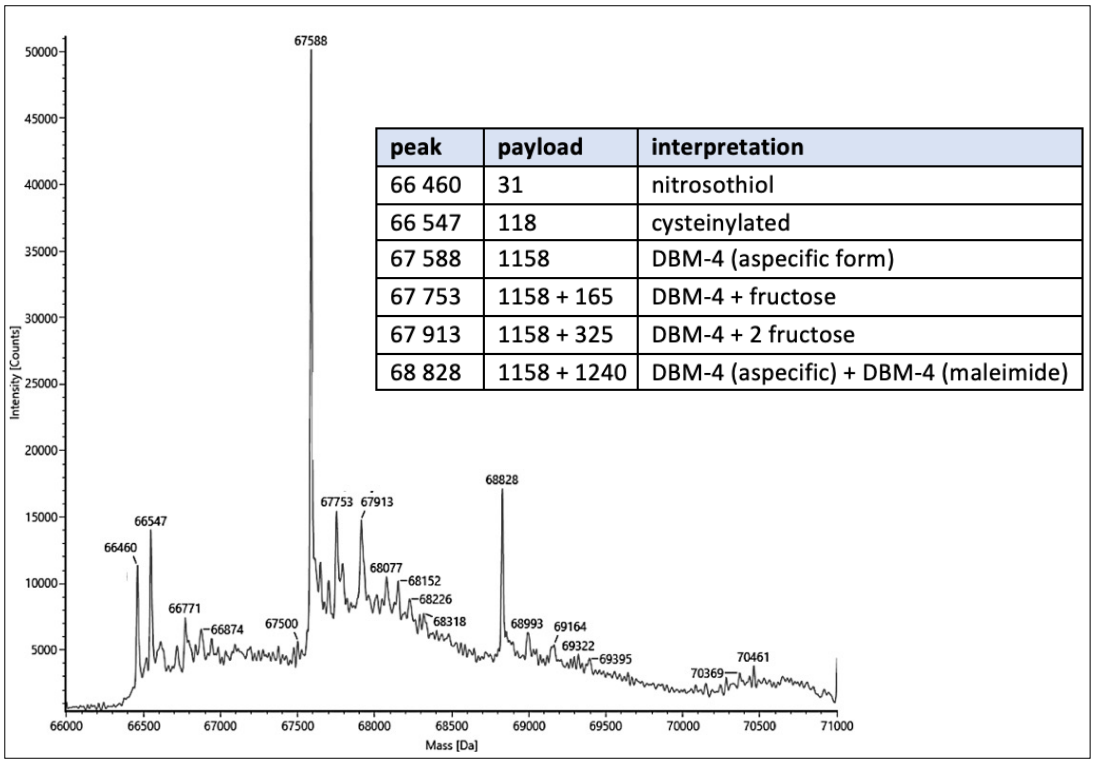

peak	payload	interpretation
66 460	31	nitrosothiol
66 547	118	cysteinylated
67 588	1158	DBM-4 (aspecific form)
67 753	1158 + 165	DBM-4 + fructose
67 913	1158 + 325	DBM-4 + 2 fructose
68 828	1158 + 1240	DBM-4 (aspecific) + DBM-4 (maleimide)

SDS-PAGE

BSA rebridged with DBM-1, under reducing conditions:

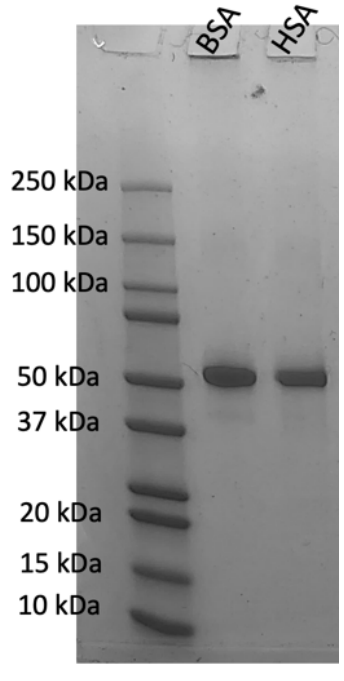

IV.2.d. BSA-trastuzumab formation:

Structure and calculated masses of the different formed adducts:

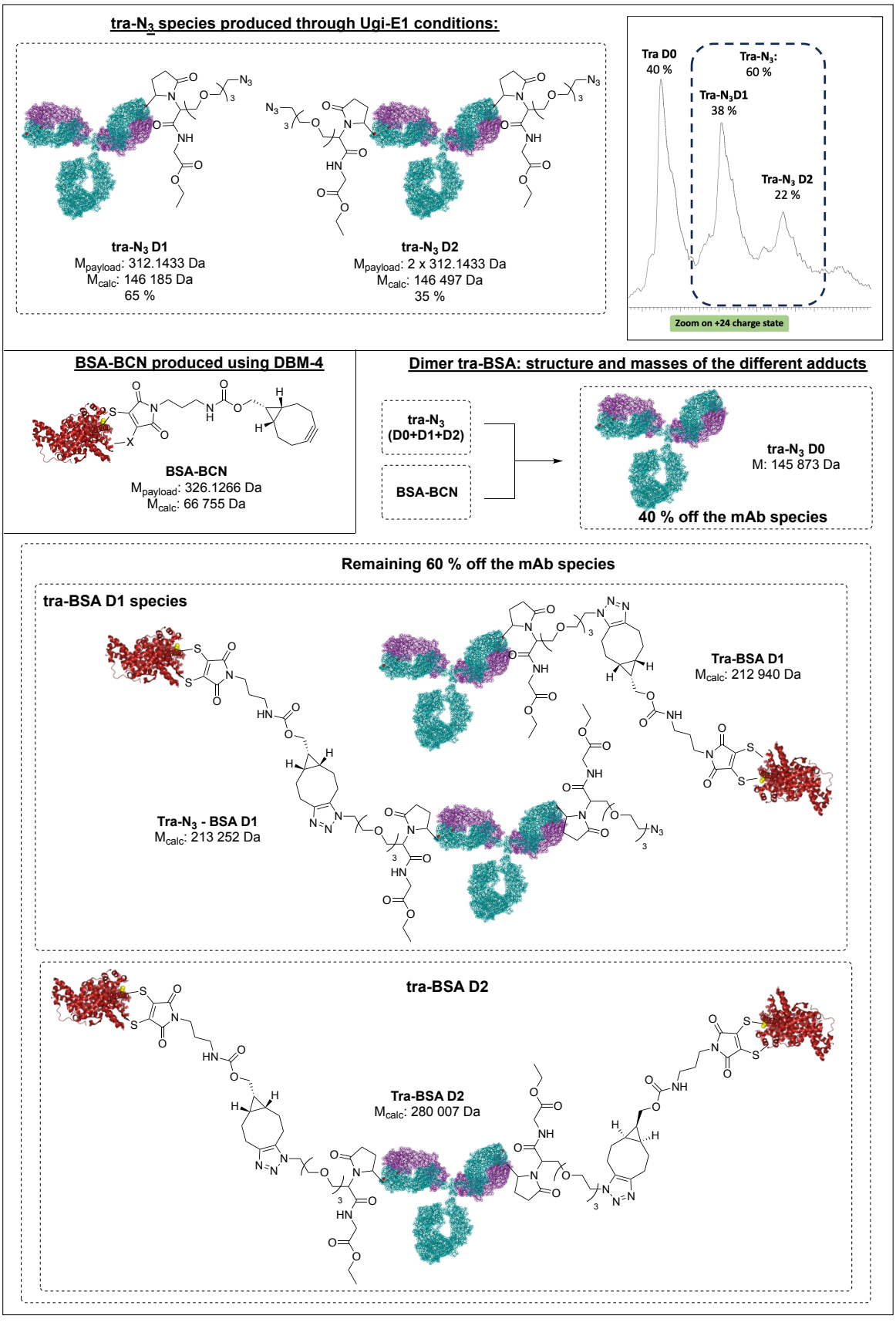

Procedures:

Tra-N_3 preparation: To 500 □L of trastuzumab (66 □M in PBS (1X, pH 7.5)), 45 equiv. of isocyanide **d** (15 □L from a 0.1 M stock solution in DMSO) and 45 equiv. of aldehyde **6** (15 □L from a 0.1 M stock solution in DMSO) were added. The solution was incubated at 25 °C for 16 h before NH_2OH (5 □L from a 50 w% solution in water) was added. After an extra hour incubation at 25 °C, the sample was purified by preparative SEC (2 x 250 □L injections). The mAb containing fractions were combined and concentrated using vivaspin 50 kDa to give concentrated solution of tra-N_3. Such concentrated solution can be stored up to 2 weeks without significant aggregate observation (native SEC-MS analysis).

BSA-BCN preparation: see BCN-functionalization procedure (IV.2.c).

SPAAC between tra-N_3 and BSA-BCN: To 2 nmol of tra-N_3 in PBS (1X, pH 7.5), 2 equiv. of BSA-BCN were added. PBS (1X, pH 7.5) was added to adjust the final tra concentration to 100 □M and the solution was incubated at 37 °C for 48 h before it was diluted to 100 □L using PBS. The resulting solution was deglycosylated and analysed by native SEC-MS.

Optimization of the SPAAC conditions:

The influence of the variation of the reaction's concentration, temperature and time was evaluated based on the UV chromatogram obtained after SEC analysis on an AKTA pure system (see analytical SEC in general procedure). The quantity of each species was calculated based on the area bellow the curve of each peak. Because the introduced quantity of BSA-BCN changed from an experiment to another we based the study on the amount of mAb species (peak 2, 3 and 4). Conversion was determined from the amount of trastuzumab remaining in the reaction media: 100 – (% peak 3 +% peak 4).

Tra-N_3 (□M)	BSA-BCN (□M)	T (°C)	t (h)	Conv. (%)	Peak 4 (%)
100	100	25	24	29	6
100	100	25	48	40	11
100	100	37	24	48	13
100	100	37	48	51	18
100	200	25	24	51	13
100	200	25	48	63	26
100	200	37	24	53	13
100	200	37	48	62	24
50	100	37	24	46	12
50	100	37	48	55	18
100	400	37	24	71	32
100	400	37	48	78	42

Example of UV chromatogram on the AKTÄ:

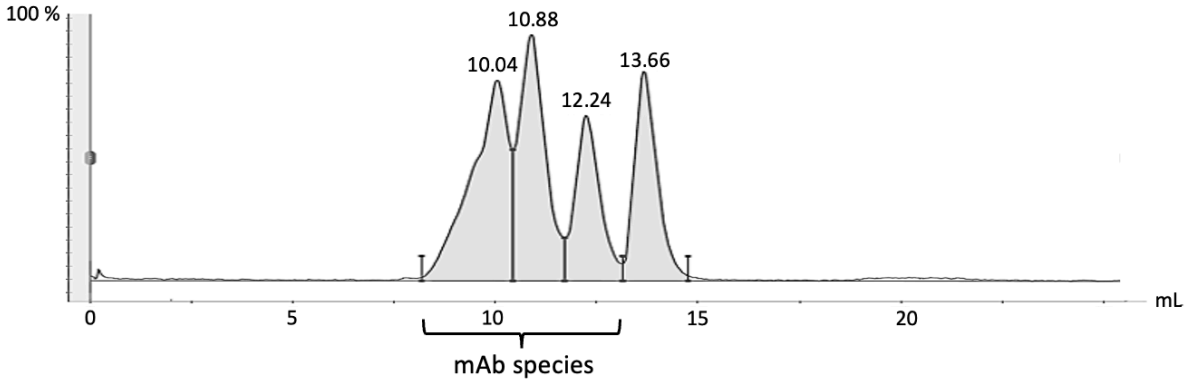

Isolation of tra-BSA:

Formation of tra-BSA, optimal conditons: To 2 nmol of AKTA purified tra-N_3 in PBS (1X, pH 7.5) was added 4 nmol of BSA-BCN (DBM-4). PBS (1X, pH 7.5) was added so a final concentration of 100 □M in tra-N_3 was reached and the resulting mixture was incubated at 25 °C for 48 h 100 □L of PBS (1X, pH 7.5) were added to the reaction mixture and the diluted solution was purified by preparative SEC. The middle fractions of peak 3 (elution volume: 10.88 mL) were combined and set aside. The border fractions (containing aggregate and D1 and D1 and tra-N_3) were combined and concentrated to a final volume 100 □L before they were purified again in the same conditions. The middle fractions of the D1 peak were combined with the previously obtained D1 fractions and concentrated using vivaspin 50 kDa. Pure tra-BSA was obtained with a 28% yield (C = 2.3 mg/mL, V = 52 □L, 0.56 nmol). Sample was deglycosylated and analyzed by native SEC-MS.

Analysis by native SEC-MS on the G2 spectrometer:

Analysis of the crude mixture resulting from the incubation of tra-N3 (70 □M), BSA-BCN-1 (210 □M) in PBS (1X, pH 7.5) at 37 °C for 24 h.

SEC UV chromatogram (abs at 280 nm):

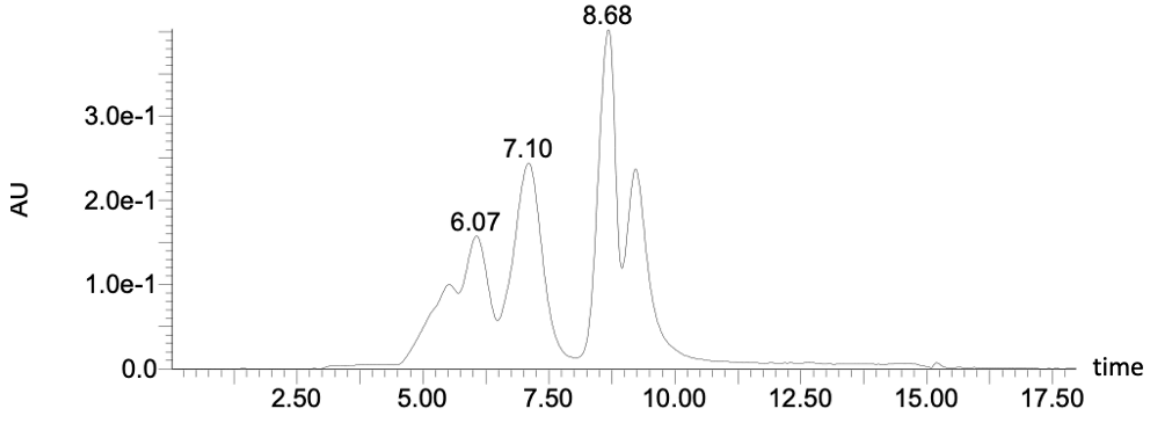

Peak 1 deconvoluted spectra: The first peak was found to contain BSA-BCN introduced in excess.

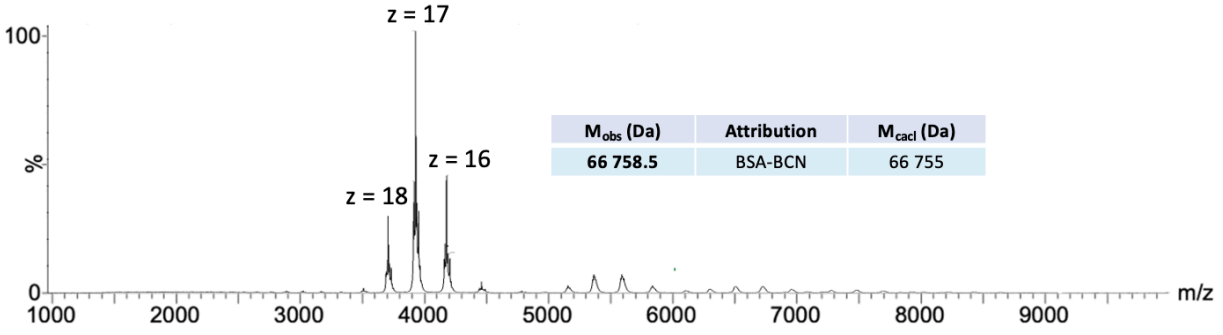

M_{obs} (Da)	Attribution	M_{cacl} (Da)
66 758.5	BSA-BCN	66 755

Peak 2 deconvoluted spectra: The second peak was found to contain a mixture of native trastuzumab, remaining from the mixture of tra-N_3 introduced as well as some BSA-BCN as observed in the first peak. This might come from a poor separation of the two species by SEC.

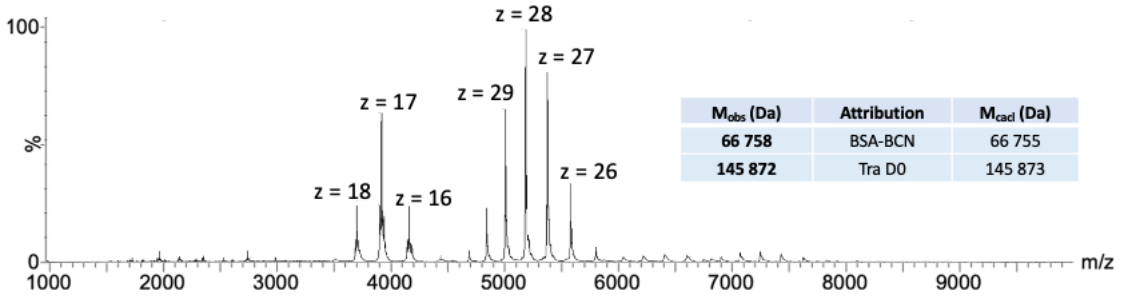

M_{obs} (Da)	Attribution	M_{cacl} (Da)
66 758	BSA-BCN	66 755
145 872	Tra D0	145 873

Peak 3 deconvoluted spectra: The third peak was found to contain a mixture of three different compounds. BSA-dimer (BSA_2) showing that BSA-BCN should be pre-purified before being used for the formation of the dimer. It was also found to contain a mixture of the desired dimer under two forms (tra-BSA and tra-N_3-BSA).

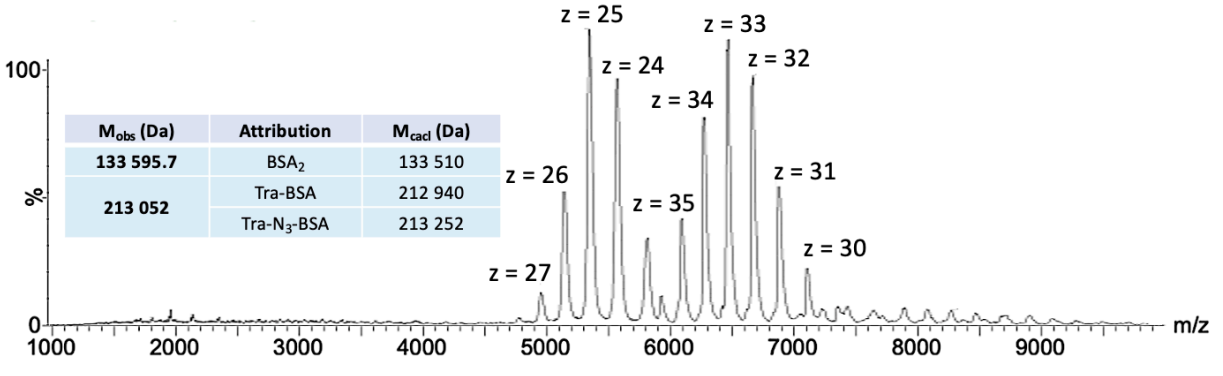

M_{obs} (Da)	Attribution	M_{cacl} (Da)
133 595.7	BSA_2	133 510
213 052	Tra-BSA	212 940
	Tra-N_3-BSA	213 252

Peak 4 deconvoluted spectra: The fourth peak was found to contain high molecular weight species that might fit to tra-N_3-BSA and tra-BSA_2 however high mass shifts were observed so no real conclusion could be taken based on this analysis.

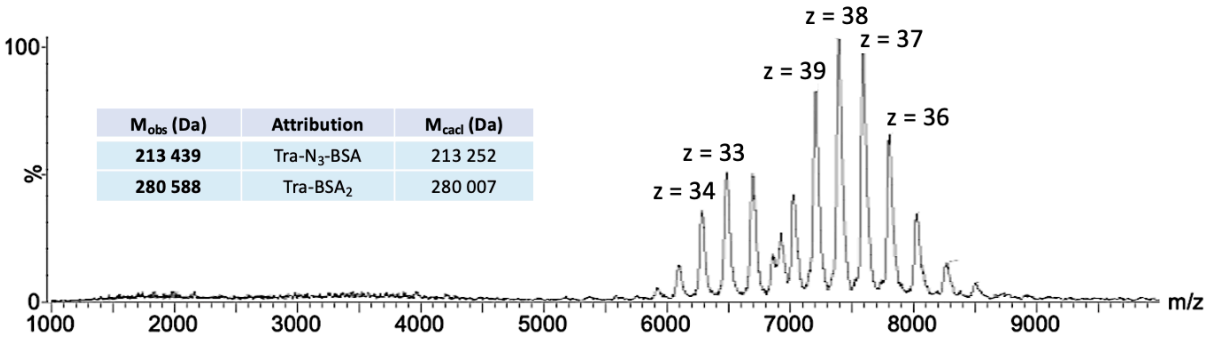

M_{obs} (Da)	Attribution	M_{cacl} (Da)
213 439	Tra-N_3-BSA	213 252
280 588	Tra-BSA_2	280 007

Analysis of the isolated tra-BSA resulting from the incubation of tra-N_3 (100 □M), BSA-BCN-1 (200 □M) in PBS (1X, pH 7.5) at 25 °C for 48 h.

UV-chromatogram:

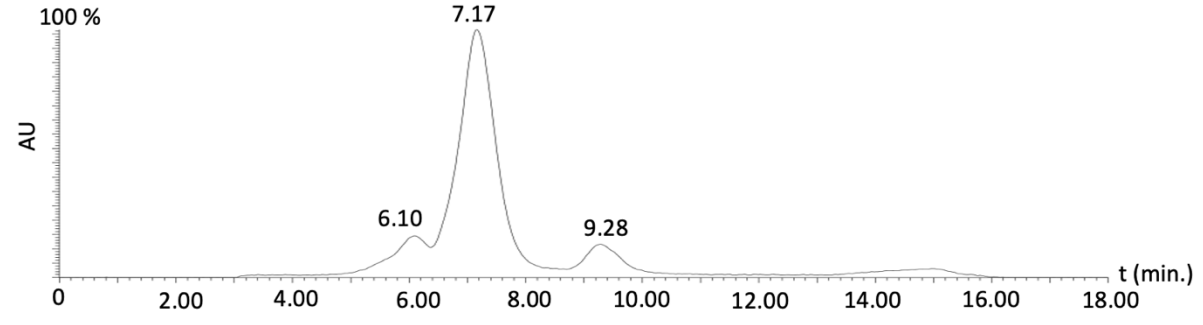

deconvoluted MS-spectra:

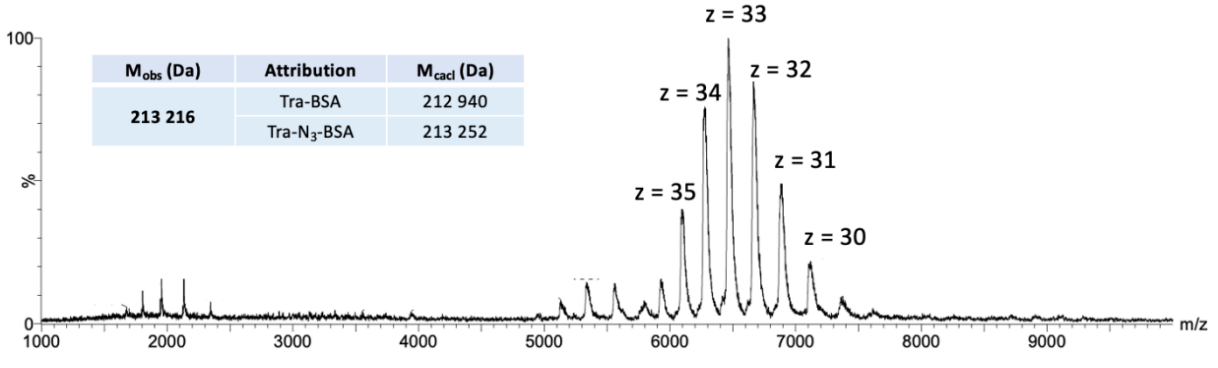

M_{obs} (Da)	Attribution	M_{cacl} (Da)
213 216	Tra-BSA	212 940
	Tra-N_3-BSA	213 252

IV.2.e. BsAb formation:

Structures and masses of the formed products:

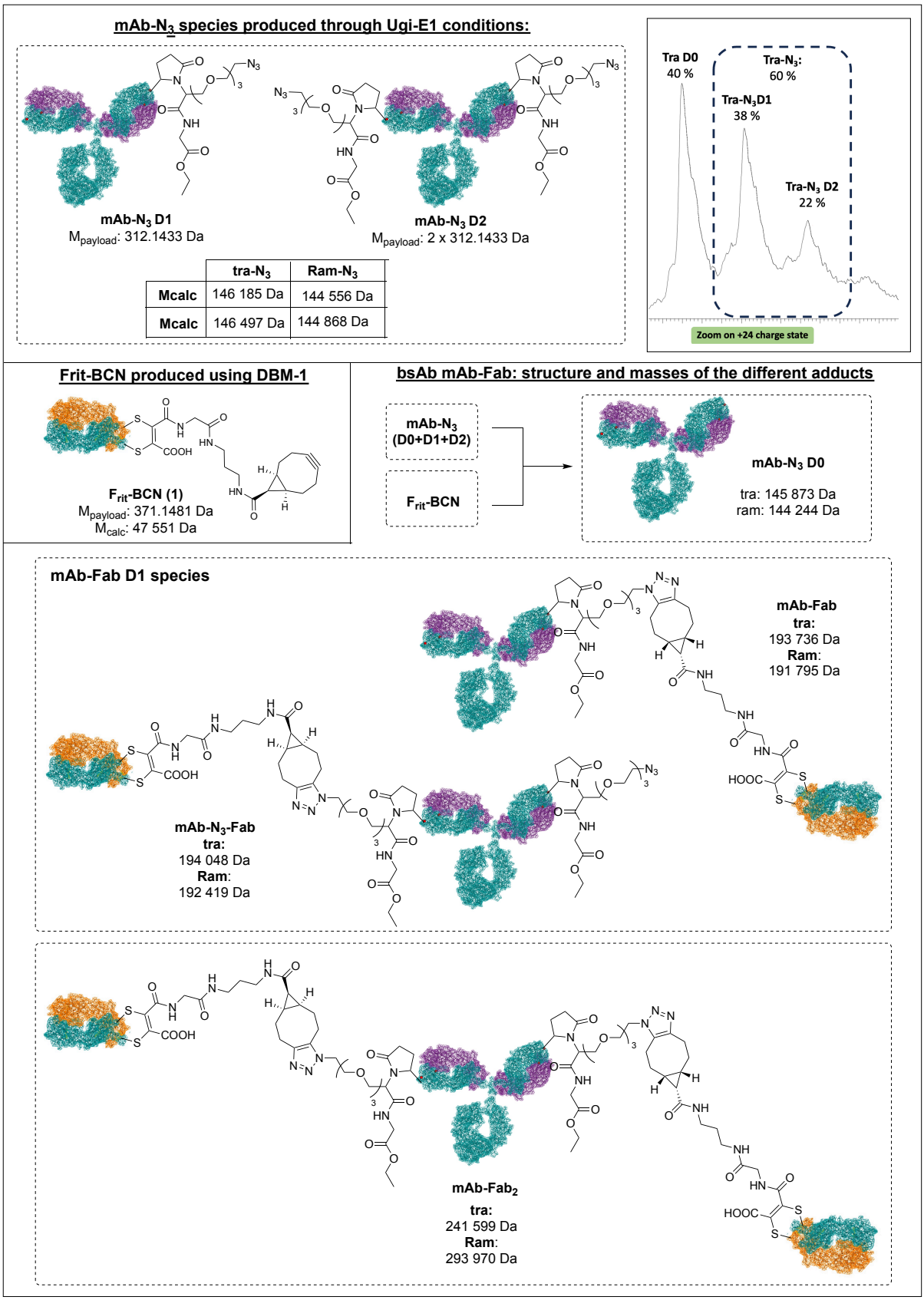

Procedures:

Tra-N_3 preparation: To 500 □L of trastuzumab (66 □M in PBS (1X, pH 7.5)), 45 equiv. of isocyanide **d** (15 □L from a 0.1 M stock solution in DMSO) and 45 equiv. of aldehyde **6** (15 □L from a 0.1 M stock solution in DMSO) were added. The solution was incubated at 25 °C for 16 h before NH_2OH (5 □L from a 50 w% solution in water) was added. After an extra hour incubation at 25 °C, the sample was purified by preparative SEC (2 x 250 □L injections). The mAb containing fractions were combined and concentrated using vivaspin 50 kDa to give concentrated solution of tra-N_3. Such concentrated solution can be stored up to 2 weeks without significant aggregate observation (native SEC-MS analysis).

F_{rit}-BCN preparation: To 100 □L of F_{rit} (106 □M in PBS (1X, pH 7.5, 5 mM EDTA)), 2 equiv. of TCEP (1 □L from a 0.02 M stock solution in mQ H_2O) were added. The resulting solution was incubated at 37 °C for 60 min before it was purified by gel filtration chromatography using biospins p-30 columns pre equilibrated with PBS (1X, pH 7.5) to give a solution of reduced mAb. To this solution, 2 equiv. of DBM (2 □L from a 0.01 M stock solution in DMSO) were added and the solution was incubated at 25 °C for 20 min before it was purified by gel filtration chromatography using biospins p-30 columns pre equilibrated with PBS (1X, pH 7.5) to give a solution of F_{rit}-BCN. F_{rit}-BCN was concentrated using vivaspin 10 kDa rinsed with PBS (1X, pH 7.5). Such solution can be stored up to 3 weeks without degradation of the protein (native SEC-MS analysis).

SPAAC between F_{rit}-BCN and tra-N_3 = bsAbs formation: To 2 nmol of tra-N_3, 2 equiv. of F_{rit}-BCN (4 nmol) were added and volume was adjusted to 100 □M of tra-N_3 using PBS (1X, pH 7.5). The resulting solution was incubated at 25 °C for 48 h before it was diluted to 100 □L using PBS (1X, pH 7.5). 1 □L was taken from this solution and SDS-PAGE was run, the following 99 □L were deglycosylated and analyzed by native SEC-MS.

Analysis:

Tra-F_{rit}, optimal conditions. (DBM-4)

UV chromatogram: 3 species were separated with 11.08 min retention time (peak 1, 23%), 7.78 min retention time (peak 2, 48%) and 7.10 min retention time (peak 3, 29%).

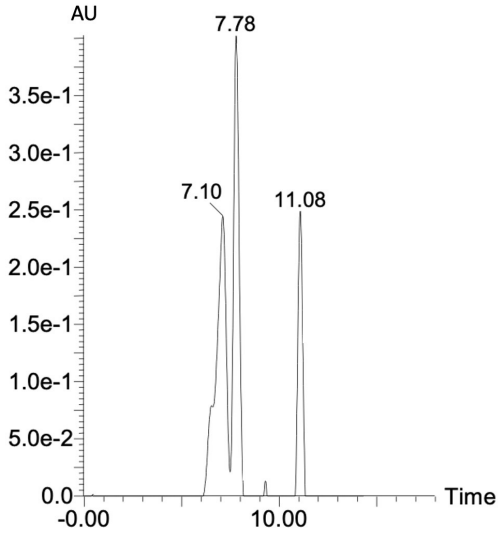

Peak 1 MS spectra: M_{obs} = 47 568 Da which corresponds to native F_{rit}-BCN (M_{calc} = 47 551 Da).

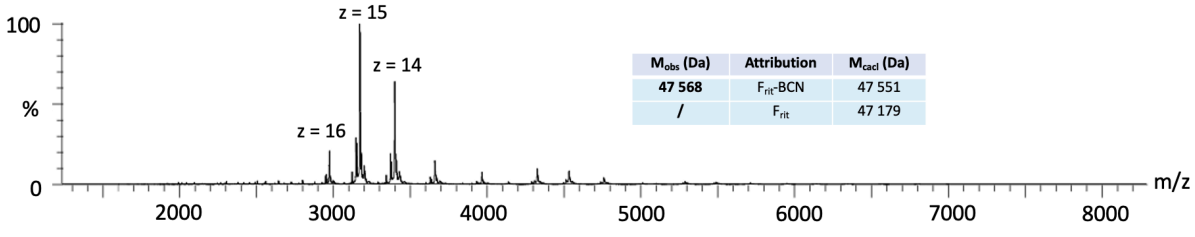

M_{obs} (Da)	Attribution	M_{cacl} (Da)
47 568	F_{rit}-BCN	47 551
/	F_{rit}	47 179

Peak 2 deconvoluted spectra: M_{obs} = 145 869 Da which correspond to native trastuzumab (M_{calc} = 145 873 Da)

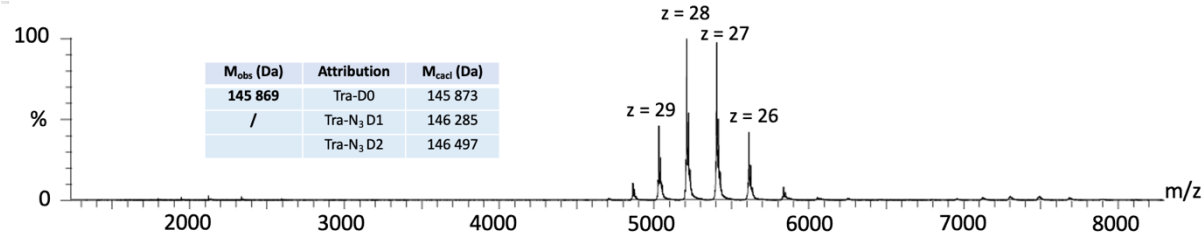

M_{obs} (Da)	Attribution	M_{cacl} (Da)
145 869	Tra-D0	145 873
/	Tra-N_3 D1	146 285
	Tra-N_3 D2	146 497

Peak 3 deconvoluted spectra: Mobs = 193 737 Da which corresponds to tra-F_{rit} M_{calc} = 193 736 Da)

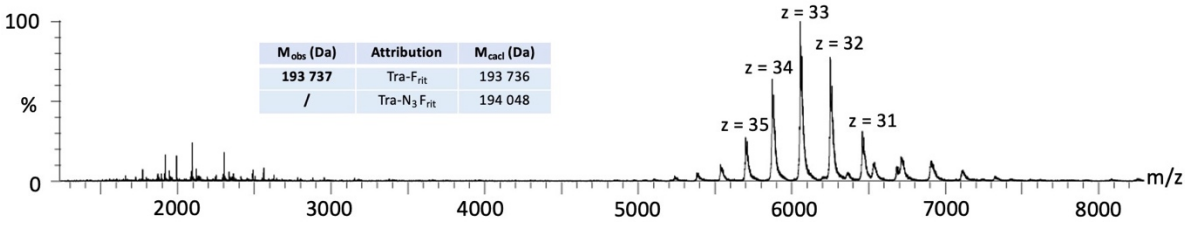

M_{obs} (Da)	Attribution	M_{cacl} (Da)
193 737	Tra-F_{rit}	193 736
/	Tra-N_3 F_{rit}	194 048

Having validated that our SPAAC conditions led to the formation of the desired Tra-F_{rit} bsAb, its isolation was performed by preparative SEC on an AKTÄ pure system (see general procedure)

<u>Isolation of Tra-F_{rit}:</u>

After SPAAC reaction, the crude reaction mixture was purified by preparative SEC. 3 species were separated, according to the UV chromatogram (abs 280 nM) peak 1 (elution volume =

16.24 mL, 19%) corresponding to F_{rit}-BCN was recovered, peak 2 (elution volume = 12.25 mL, 37%) corresponding to tra-N_3 was discarded and peak 3 (elution volume = 11.57 mL, 44%) was set aside. Border fractions of peak 3 (tube 8 and tube 11) were combined and purified a second time in the same manner. Middle fractions were combined with the previous peak 3 fractions and they were purified a second time (P2) leading to the isolation of a single peak (elution volume = 11.48 mL). Combined fractions were concentrated using vivaspin 50 kDa and pureTra.f_{rit} was obtained with 48% yield (C = 4.99 mg/mL, V = 69 □L, 1.8 nmol).

30 □g of the resulting tra.Frit solution were deglycosylated (see general procedure) and analyzed by SEC-native MS using the G2 spectrometer.

100 □g of tra-Frit were labelled with FITC and affinity for HER-2 receptor was evaluated on LigandTracer (see biological assay procedure).

pure Tra-Frit, produced via the optimal conditions. (DBM-4)

UV chromatogram of the first purification by SEC (P1):

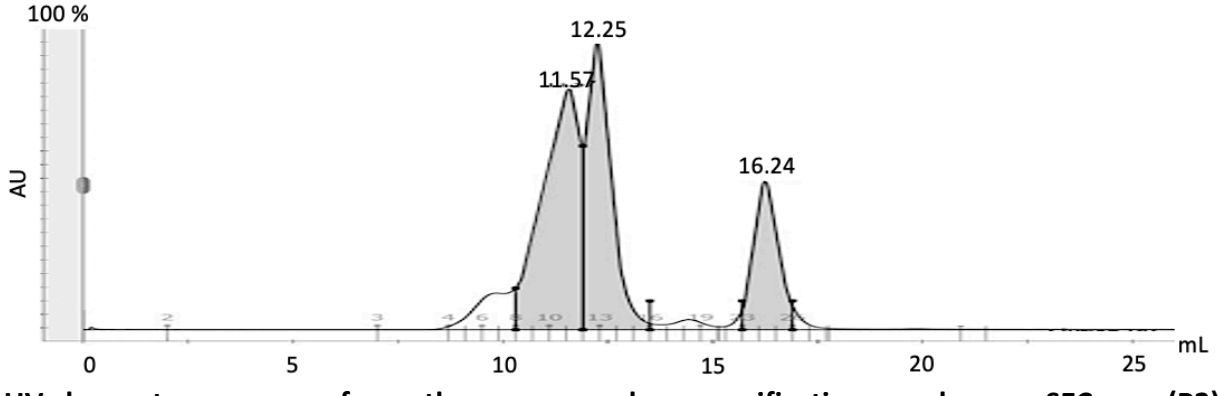

UV-chromatogram of the second purification by SEC (P2):

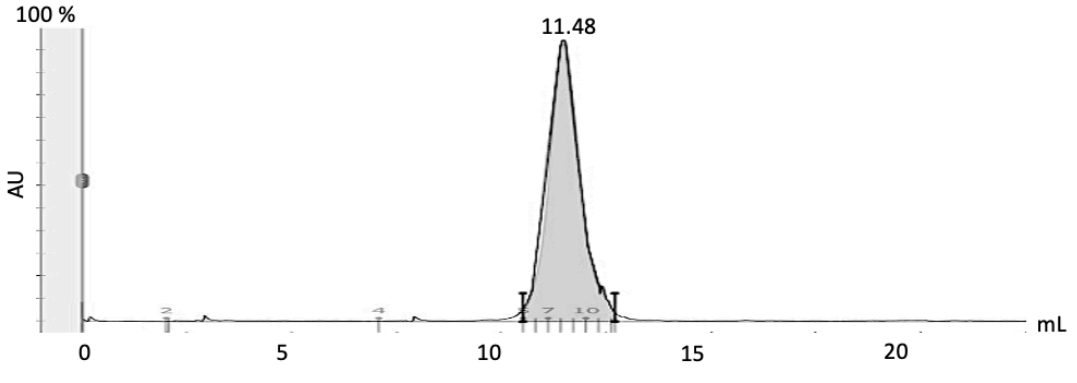

MS spectra: 2 species were found to co-elute at the same time (7.07 min) with M_1 = 193 750 Da and M_2 = 194 028 Da which were attributed to be respectively tra.F_{rit} (M_{calc} = 193 736 Da) and tra-N_3-F_{rit} (M_{calc} = 194 048 Da)

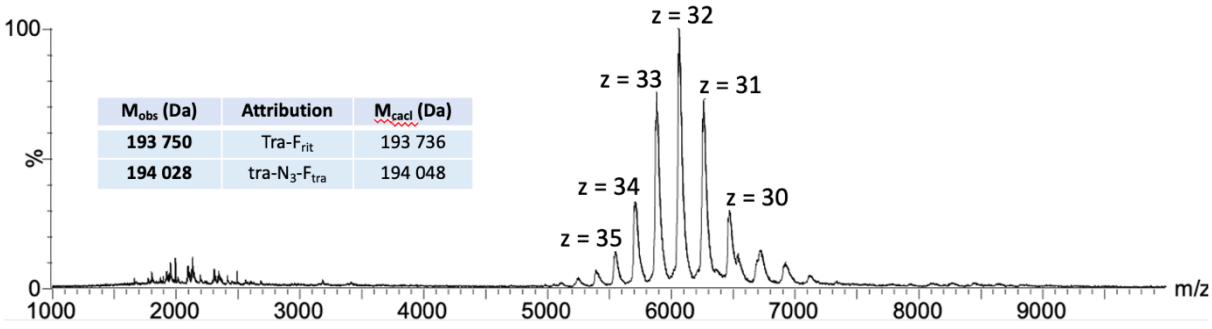

M_{obs} (Da)	Attribution	M_{cacl} (Da)
193 750	Tra-F_{rit}	193 736
194 028	tra-N_3-F_{tra}	194 048

Having successfully isolated and characterized the bsAb Tra-F_{rit} with 48% yield, the transferability of the method to the formation of other bsAbs was performed in the same manner by variation of either the mAb component or the Fab component.

Method transfer, variation of the Fab component:

Tra-F_{tra}: yield = 22%

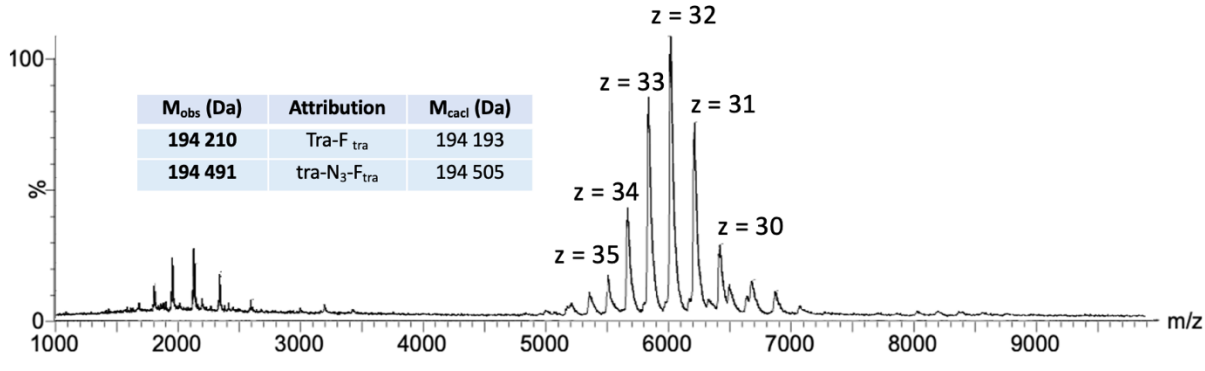

M_{obs} (Da)	Attribution	M_{cacl} (Da)
194 210	Tra-F_{tra}	194 193
194 491	tra-N_3-F_{tra}	194 505

Tra-F_{durva}: yield = 23%

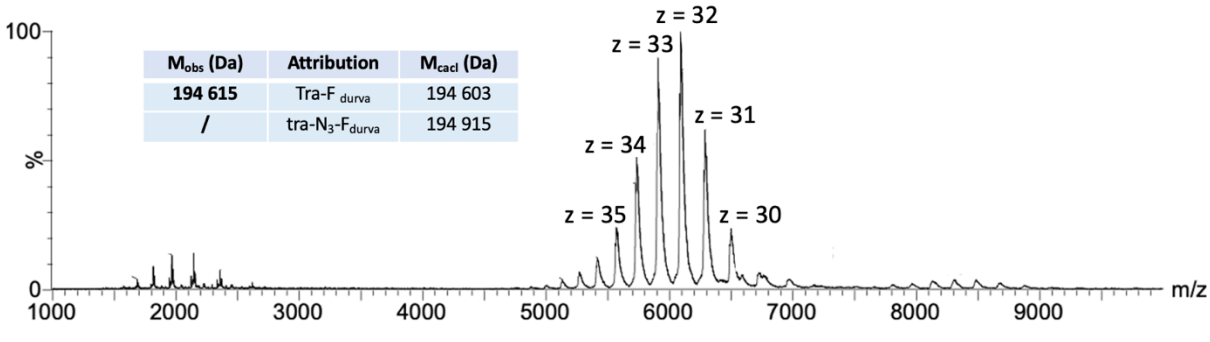

M_{obs} (Da)	Attribution	M_{cacl} (Da)
194 615	Tra-F_{durva}	194 603
/	tra-N_3-F_{durva}	194 915

Tra-F_{ave}: yield = 24%

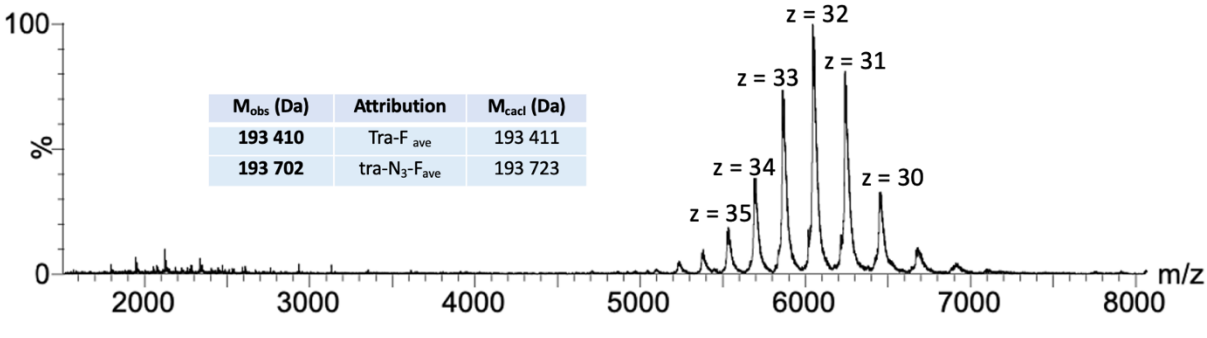

M_{obs} (Da)	Attribution	M_{cacl} (Da)
193 410	Tra-F_{ave}	193 411
193 702	tra-N_3-F_{ave}	193 723

Tra-F_{muro}: yield = 20%

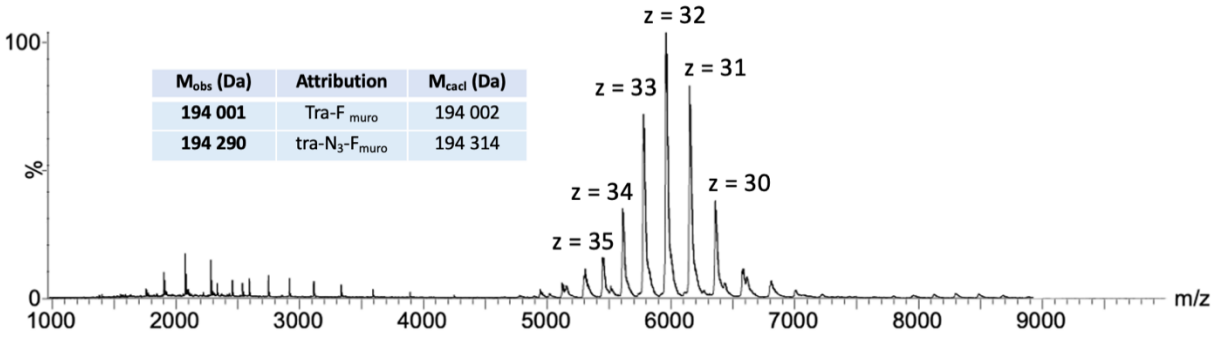

M_{obs} (Da)	Attribution	M_{cacl} (Da)
194 001	Tra-F_{muro}	194 002
194 290	tra-N_3-F_{muro}	194 314

Method transfer, variation of the mAb component:

Ram-F_{tra}: yield = 20%

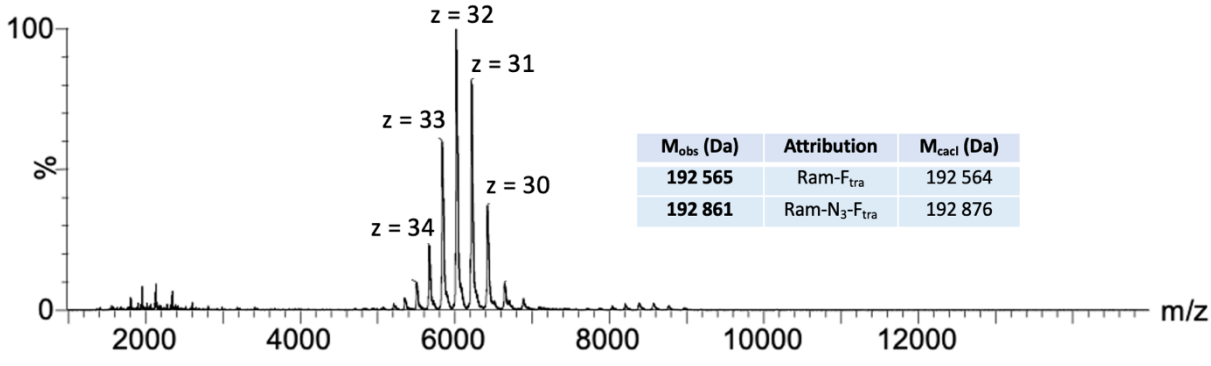

M_{obs} (Da)	Attribution	M_{cacl} (Da)
192 565	Ram-F_{tra}	192 564
192 861	Ram-N_3-F_{tra}	192 876

F(ab')2tra-F_{muro}: yield = 33%

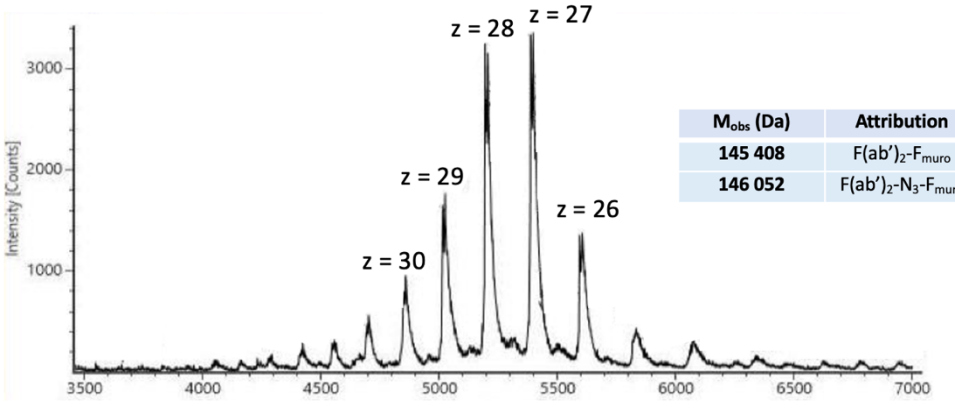

M_{obs} (Da)	Attribution	M_{cacl} (Da)
145 408	$F(ab')_2$-F_{muro}	145 425
146 052	$F(ab')_2$-N_3-F_{muro}	146 049

Method transfer, variation of the DBM reagent:

T.F$_{rit}$ (DBM-2): Observed heterogeneity seems higher with this rebridging agent. 3 different species are observed corresponding to $_{Frit}$ light chain (LC) probably due to the analysis, the expected bsAb as well as a high molecular weight species which do not fit with the expected bsAb D2.

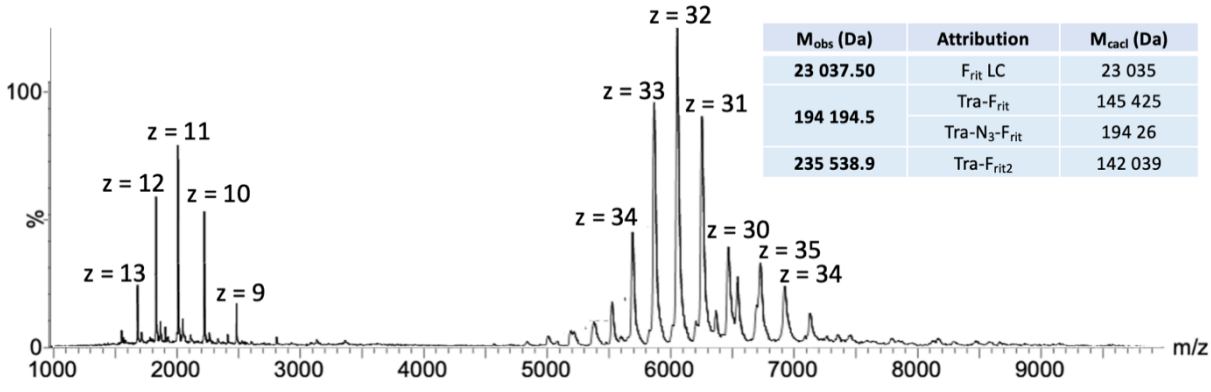

M_{obs} (Da)	Attribution	M_{cacl} (Da)
23 037.50	F_{rit} LC	23 035
194 194.5	Tra-F_{rit}	145 425
	Tra-N_3-F_{rit}	194 26
235 538.9	Tra-F_{rit2}	142 039

T.F$_{rit}$ (DBM-1): Observed heterogeneity seems higher with this rebridging agent. 3 different species are observed corresponding to F_{rit} light chain (LC) probably due to the analysis, the expected bsAb as well as a high molecular weight species which do not fit with the expected bsAb D2.

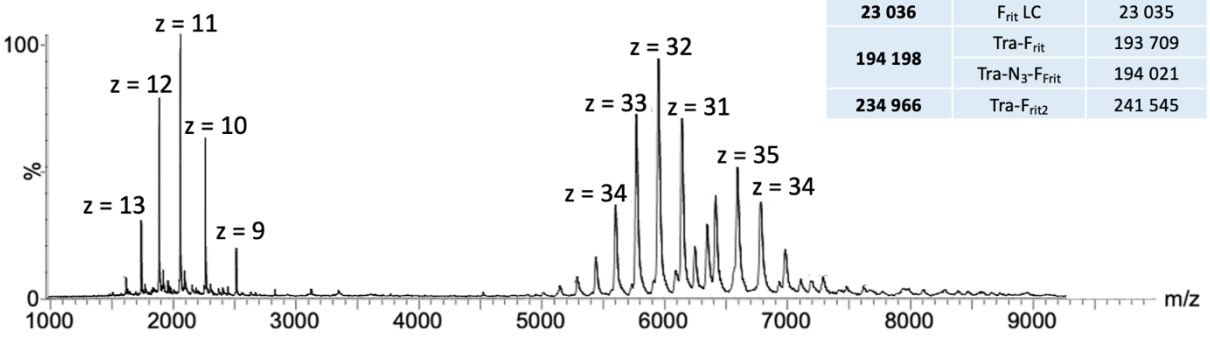

M_{obs} (Da)	Attribution	M_{cacl} (Da)
23 036	F_{rit} LC	23 035
194 198	Tra-F_{rit}	193 709
	Tra-N_3-F_{Frit}	194 021
234 966	Tra-F_{rit2}	241 545

VI. Biological assay

Cell culture for ligand tracer:

Human breast adenocarcinoma cells SK-BR-3 (ATCC HTB-30) and MDA-MB-231 (ATCC HTB-26) were grown in Dulbecco's Modified Eagles Medium – DMEM - containing 4.5 g/L glucose. The medium was supplemented with 10% foetal veal serum (FVS) and 100 U/mL penicillin and 100 µg/mL streptomycin. Cells were maintained in a 5% CO2 humidified atmosphere at 37 °C. SK-BR-3 cells overexpress HER2 protein, and MDA-MB-231 cells are used as negative controls and background. The day before the experiment on Ligand Tracer Green (Ridgeview Instruments), cells were seeded as 600 µL droplets with 8×10^5 cells/mL at 1 cm from the edge in 10 x 22 mm cell culture treated dishes (Starlab, Hamburg, Germany) and incubated at 37 °C overnight. Three droplets were prepared with SK-BR-3 and one with MDA-MB-231. Prior to kinetic measurement, the media was carefully removed and 3 mL of fresh media were added to the dish.

Time-resolved analysis of ligand binding assays:

The interaction of the fluorescein-labelled protein with living cells in real-time using Ligand Tracer Green (Ridgeview instruments). The Petri dish on which cells were grown was placed on inclined rotating support of the instrument, with the Blue/Green detector placed on its upper part. First, a baseline signal was collected for 20 to 30 min. Then the fluorescein-labelled protein was added in two steps at increasing concentration (10 nM and 30 nM). The inclination of the Petri dish allows the addition of the labelled compound outside of the detection area. For each rotation of the Petri dish, the signal from the four areas containing cells (three spots for SK-BR-3, one for MDA-MB-231) is recorded. Measurements last 15 s each, without time in between each of them in order to accelerate the association phase's measurement because cells were found to detach from the dish after around 7 h of experiment. This results in three background-subtracted real-time binding curves, which represent the specific binding of the fluorescein-labelled compound to the positive cell line (SK-BR-3). For each concentration the incubation was performed until a sufficient curvature was obtained for the subsequent extraction of kinetic parameters. Dissociation of the ligand was recorded after replacing the incubation solution with 3 ml of fresh medium. Signals from cell and reference areas are recorded during every rotation, resulting in a background-subtracted binding curve. Binding traces were analysed with the evaluation software TraceDrawer 1.8.1 (Ridgeview Instruments) in order to determine ka, kd and KD according to the Langmuir, or "one-to-one", binding model.

compound	DoL	k_{on} ($10^4.M^{-1}.s^{-1}$)	koff (10^{-5} s^{-1})	K_D (nM)
tra	1.3	2.00	1.37	0.65
Tra-N_3	1.2	2.40	1.00	0.45
Tra.F_{tra}	3.0	2.60	1.70	0.50
Tra.F_{rit}	1.2	1.30	0.46	0.35
Tra.F_{ave}	2.5	1.47	0.73	0.49
Tra.F_{durva}	2.4	1.20	0.48	0.39
Tra.F_{muro}	1.1	1.48	0.65	0.44
Tra.BSA	3.0	1.54	2.17	1.5
Ram.F_{tra}	0.9	78.0	2.25	2.9
F_{Tra}	2.0	2.24	2.20	0.97
F(ab')$_2$Tra-F_{muro}	2.0	1.81	0.75	0.42
F(ab')$_2$Tra	1.3	0.73	0.36	0.50

Flow cytometry for HER-2 occupancy of tra-F_{muro}:

HCC1954 cells were incubated with 2 µg/mL of tra-F_{muro} for 1h at 4°C under gentle agitation. Following two washes with PBS supplemented with 10% of foetal calf serum (FCS), HCC1954 cells were incubated with 1 µg of PE-stained anti-human IgG Fc antibody or with the respective PE-conjugated isotype control for 45 min on ice. Cells were then washed with PBS-FCS 10%, resuspended in PBS and analyzed using a BD ACCURI™ C6 Plus Flow cytometer, analyzing at least 10000 events per sample. All data shown is representative of three independent experiments and expressed as means ± SD.

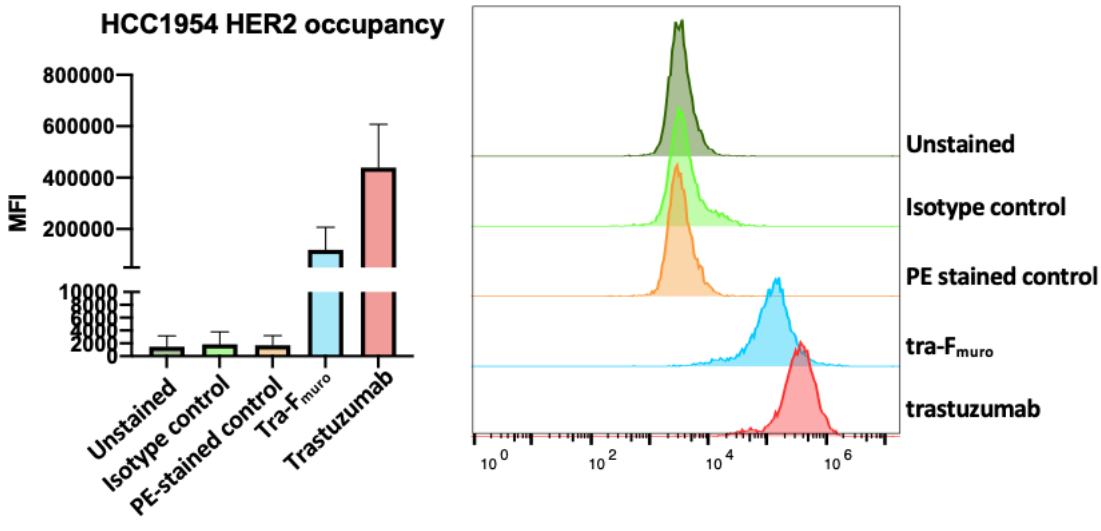

Flow cytometry for CD3 occupancy of tra-F_{muro} and F(ab')$_2$tra-F_{muro}:

Jurkat cells were incubated with 2 µg/mL of tra-F_{muro} or F(ab')$_2$tra-F_{muro} for 1h at 4°C under gentle agitation. Following two washes with with 10% of FCS, Jurkat cells were incubated with 1 µg of APC-stained anti-CD3 antibody or the respective APC-stained isotype control, for 45 min on ice. Cells were then washed with PBS-FCS 10%, resuspended in PBS and analysed using a BD ACCURI™ C6 Plus Flow cytometer, analyzing at least 10000 events per sample. All data shown is representative of three independent experiments and expressed as means ± SD.

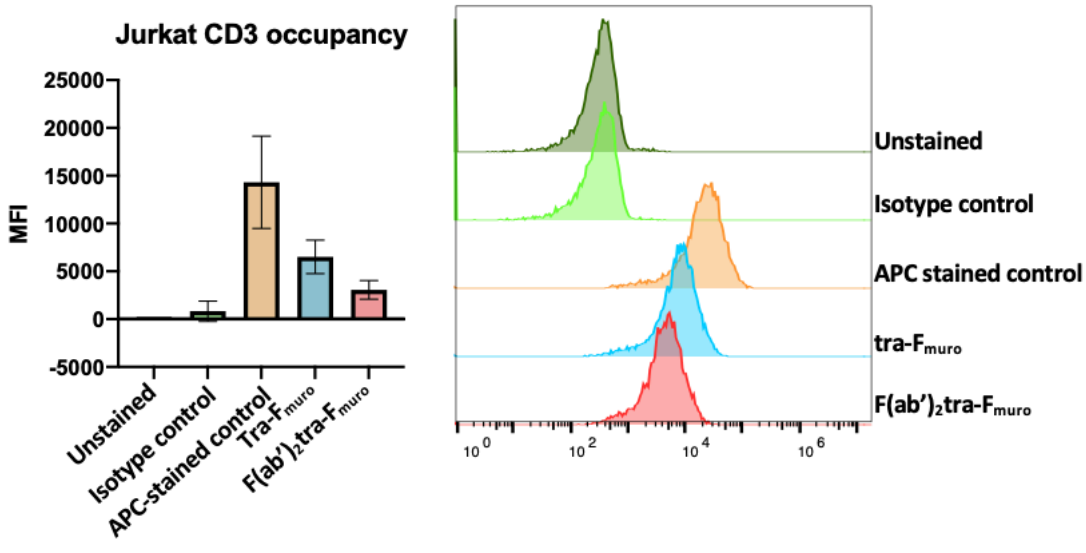

Evaluation of in vitro activity of tra-F_{muro} and F(ab')$_2$tra-F_{muro}:

To confirm that the bsAbs could activate T cells in vitro, IC_{50} of the both constructs was evaluated by performing 72 h dose-response studies. T cell-HCC1954 cell cocultures at E:T ratio of 10:1 were treated with increasing concentrations of tra-F_{muro} (9.9 pM – 2.53 nM) or F(ab')$_2$tra-F_{muro} (13.7 pM – 3.5 nM). Cancer cell viability was assessed after 72 h and expressed as % of viability of untreated control. All data shown is representative of three independent experiments performed using three different donors and expressed as means ± SD.

Tra-F_{muro}:

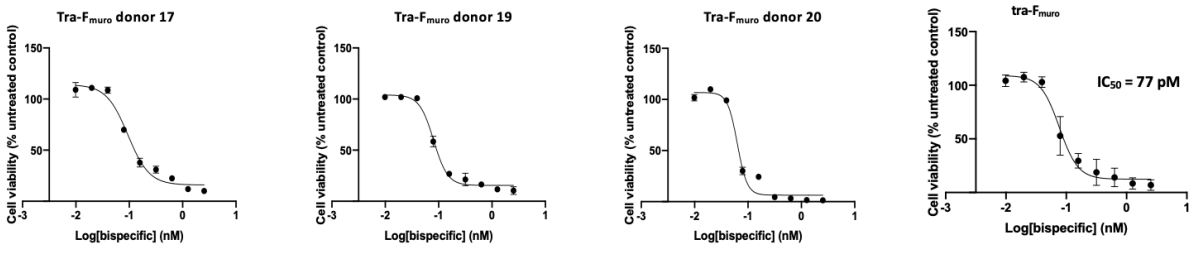

F(ab')$_2$Tra-F_{muro}:

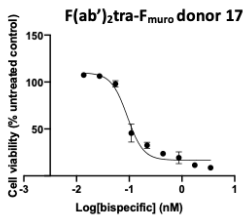
F(ab')2tra-Fmuro donor 17
Cell viability (% untreated control)
150
100
50
-3
-2
-1
0
1
Log[bispecific] (nM)

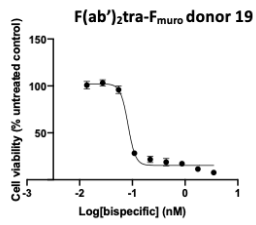
F(ab')2tra-Fmuro donor 19
Cell viability (% untreated control)
150
100
50
-3
-2
-1
0
1
Log[bispecific] (nM)

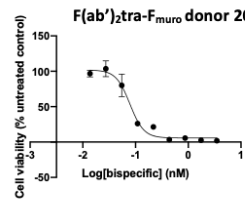
F(ab')2tra-Fmuro donor 20
Cell viability (% untreated control)
150
100
50
-50
-3
-2
-1
0
1
Log[bispecific] (nM)

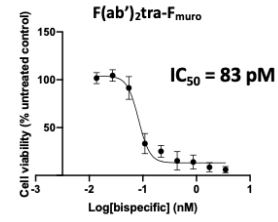
F(ab')2tra-Fmuro
IC50 = 83 pM
Cell viability (% untreated control)
150
100
50
-3
-2
-1
0
1
Log[bispecific] (nM)

Résumé

I. Introduction

La bioconjugaison est la formation d'une liaison covalente entre une biomolécule (dans notre cas, une protéine) et n'importe quelle autre molécule. Le principal défi de ce domaine est inhérent à la physicochimie des protéines : ce sont des espèces polynucléophiles essentiellement stables en solution aqueuse et qui ne peuvent supporter que de faibles variations de températures, de concentrations ou de pH. Les méthodes permettant la conjugaison de protéines peuvent être divisées en deux catégories selon leur degré de sélectivité. Elles sont classiquement réparties entre méthodes chimiosélectives, c'est-à-dire ciblant sélectivement une des fonctions chimiques présentes sur la protéine, et site-sélectives, c'est-à-dire ciblant une position précise de la protéine en se basant sur son environnement, son accessibilité ou sa réactivité.

II. Application des reactions multicomposantes a la bioconjugaison.

Durant ces travaux de thèse, l'adaptation de réactions multicomposantes a la bioconjugaison a été évalué. Ces réactions chimiques impliquent au moins trois réactifs qui réagissent ensemble de manière séquentielle pour former sélectivement un seul composé, avec peu de produits secondaires. Ces propriétés en font d'excellents candidats pour la modification de molécules aussi complexes que les protéines. Ainsi le remplacement de l'un (ou plusieurs) de ces réactifs par une fonction chimique présente de manière native à la surface des protéines s'est avéré efficace a la fois pour le développement de méthodes de conjugaison chimio- et site-selectives.

II.1. Robsinson Schöpf MCR

Dans une première partie, nous avons évalué l'adaptation de la réaction de Robinson-Schöpf pour la modification sélective des résidus de lysine de trastuzumab, un anticorps monoclonal (mAb) thérapeutique utilisé dans le traitement du cancer du sein HER-2 positif. Cette réaction, menant à la formation de tropinone à partir de méthyl amine **1**, de succinaldéhyde **2** et d'acide 3-oxoglutarique **3**, peut être réalisée en conditions aqueuses légèrement acides (pH 5.0) moyennant un chauffage à 40 °C (Schéma 1).

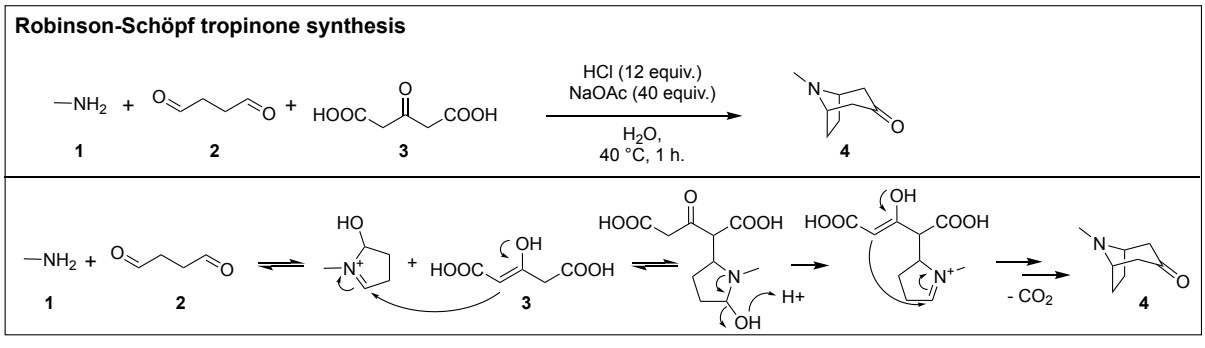

Schéma 1: Robinson Schöpf reaction

L'adaptation de ces conditions sur trastuzumab a montré que, si la formation de la tropinone est possible sur protéine, elle est en compétition avec de nombreux autres mécanismes (Tableau 1). Nous nous sommes donc engagés dans l'optimisation de ces conditions réactionnelles afin de pouvoir sélectionner la formation exclusive de cet adduit tropinone. Si nos tentatives sont restées infructueuses, nous avons néanmoins pu identifier l'une des principales réactions secondaires ayant lieu dans ces conditions. Cette réaction, menant à la formation d'un pyrrole sur les amines de la protéine, provient de la double addition/déshydratation du succinaldehyde introduit dans le milieu réactionnel. Nous avons même pu développer des conditions menant à la seule formation de cet adduit avec une bonne conversion (60%) et un bon degré de conjugaison (1.3). Les pyrroles pouvant réagir en tant que diène dans les réactions de Diels-Alder, nous pouvons imaginer une fonctionnalisation plus poussée de ce mAb en utilisant le dienophile approprié.

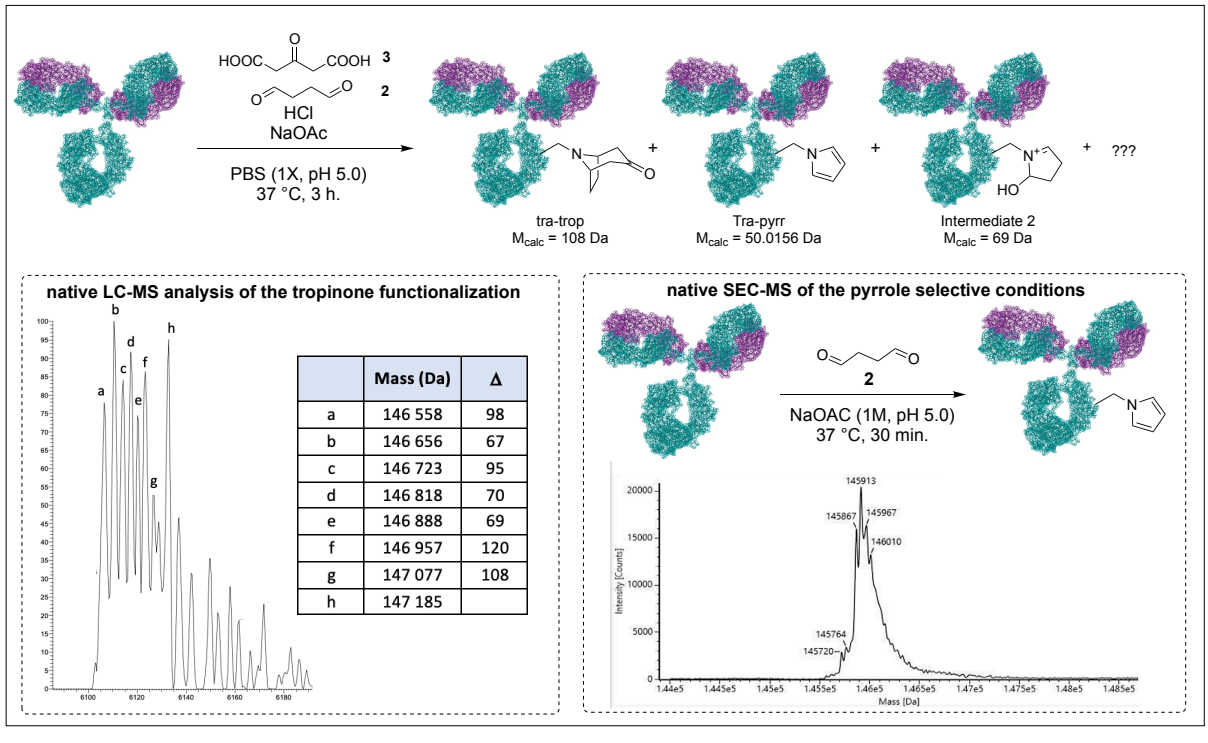

Tableau 1: Analysis of the heterogeneous conjugate obtained using the Robinson-Schöpf reaction to label trastuzumab. Conditions developped for the selective pyrrole formation.

II.2. Réaction de Ugi 4C-3CR

Ensuite, nous nous sommes focalisés sur les travaux de notre équipe, publiés en 2020, proposant d'utiliser la réaction de Ugi pour la modification de trastuzumab.[119] La réaction de Ugi est une réaction multi-composante impliquant une amine primaire, un carbonyle, un isonitrile et un acide carboxylique.[146] Le mécanisme proposé, décrit dans le Schéma 2, consiste tout d'abord en la condensation du carbonyle **5** avec l'amine **6** afin de former l'imine **7**, en équilibre avec l'ion iminium **10** après protonation par l'acide carboxylique **8**. Suite à l'addition de l'isonitrile **9**, l'isonitrilium formé réagit avec le carboxylate **11** pour former le

carboximidate **12** qui, après un réarrangement de Mumm irréversible, forme l'α-aminoacylamide **13 (**Schéma 2).[152,149]

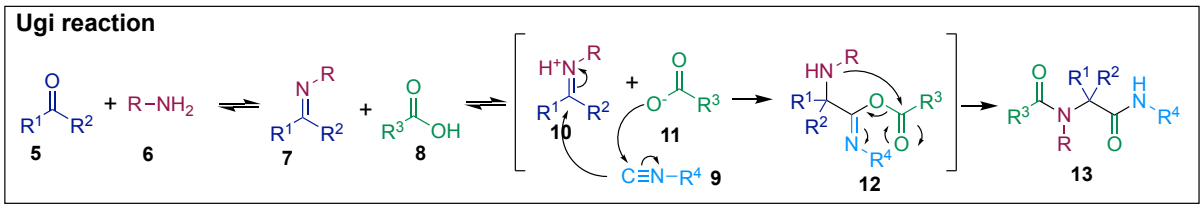

Schéma 2: Presumed mechanism of the Ugi reaction.

Appliquée à la bioconjugaison, cette réaction emploie l'anticorps comme source à la fois d'acide carboxylique et d'amine primaire, au travers des chaines latérales de ses acides aminés constitutifs : les résidus d'acide aspartique/glutamique et de lysine, respectivement. L'addition d'un carbonyle et d'un isonitrile à une solution tamponnée d'anticorps mène donc à une conjugaison « inter-résidu », suivant le mécanisme décrit ci-dessus. La forte proximité spatiale de deux résidus lysines et aspartates/glutamates étant la condition sine qua non pour pouvoir observer une potentielle conjugaison, la réaction d'Ugi devrait nous permettre de réduire le nombre potentiel de sites réactifs et donc de développer une méthode site-sélective.

II.2.a. Reproductibilité de la méthode

En nous basant sur cette hypothèse, nous avons réussi à développer des conditions optimales — i.e., 45 équivalents d'aldéhyde et d'isonitrile dans le PBS (1x, pH 7.5) à 25 °C pendant 16 heures — permettant la modification irréversible de trastuzumab. De plus, les réactifs utilisés ont permis le développement d'une approche dite « plug-and-play » : la réaction de Ugi (l'étape dite « plug ») est utilisée pour introduire, via l'aldéhyde **14** (Figure 1), un groupement azoture servant de point d'accroche à n'importe quelle charge utile d'intérêt porteuse d'un alcyne tendu (l'étape « play »), via l'utilisation d'une réaction dite SPAAC (*strain-promoted azide-alkyne cycloaddition*). Une étude approfondie par LC-MS/MS a permis de démontrer qu'un seul site à la surface de trastuzumab était modifié selon le mécanisme attendu (K126-E123), en compétition avec une modification Ugi dite « intra-résidu », prenant place au niveau des résidus aspartate et glutamate *N*-terminaux de la protéine. Dans le cas de cette dernière modification, la source d'amine est l'amine-α *N*-terminale, conduisant ainsi à la formation de β- et γ-lactames par cyclisation avec la chaîne latérale acide carboxylique. La modification de trois résidus d'acides glutamiques suivant une réaction de Passerini, différant de la réaction de Ugi uniquement par le fait qu'elle n'emploie pas d'amine, ont en outre pu être identifiées (Figure 1), empêchant de qualifier cette approche de site-sélective. Cependant, une étude mécanistique a alors été entreprise afin de tenter de comprendre les règles gouvernant

ces réactions à la surface des protéines dans le but de développer des conditions permettant de favoriser un seul des mécanismes de conjugaison observés.

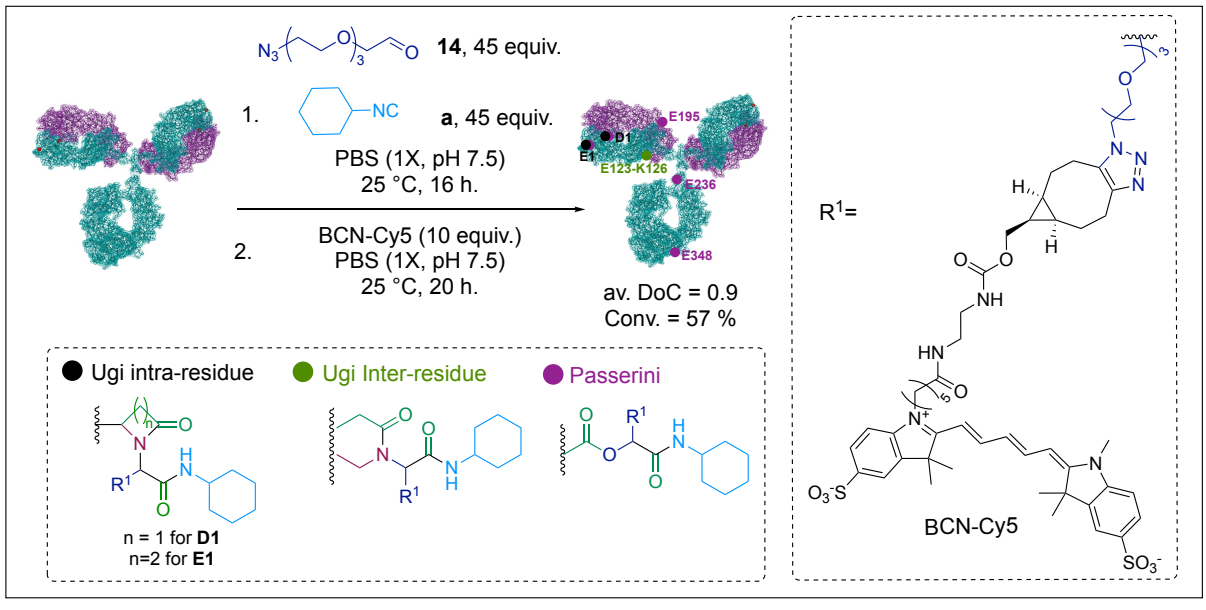

Figure 1: modification de trastuzumab par réaction de Ugi en utilisant les réactifs **14** et **a** suivis d'une SPAAC avec du BCN-sulfocy5. Les degrés de conjugaison moyen (av. DoC) et la conversion ont été déterminés par analyse de masse native et les sites de modification ainsi que la structure des modifications par LC-MS/MS.

II.2.b. Variation du carbonyle utilisé

En nous basant sur l'hypothèse que les trois mécanismes observés pouvaient venir d'une sur-réactivité de l'aldéhyde, nous avons évalué si l'introduction du carbonyle sous une forme d'imine stabilisée pouvait mener à la sélection d'un unique mécanisme de conjugaison, ne faisant intervenir que les acides carboxyliques constitutifs de trastuzumab.

Dans un premier temps, nous avons synthétisé le chlorooxime **15**, dérivé de l'aldehyde **14**. La réaction de **15** avec trastuzumab s'est avérée extrêmement rapide puisqu'une conversion et un degré de conjugaison similaire à ceux obtenus dans les résultats préliminaires ont été observés après une incubation de seulement 2 heures a 4 °C (Figure 2). Cependant, cette réactivité s'est avérée indépendante de la présence d'un isonitrile dans le milieu réactionnel suggérant un tout autre mécanisme que celui envisagé. Nous avons donc réalisé une étude mécanistique de la réaction qui nous a indiqué que la conjugaison observée provenait simplement de l'attaque nucléophile d'un résidu, probablement un acide aspartique, un acide glutamique ou une

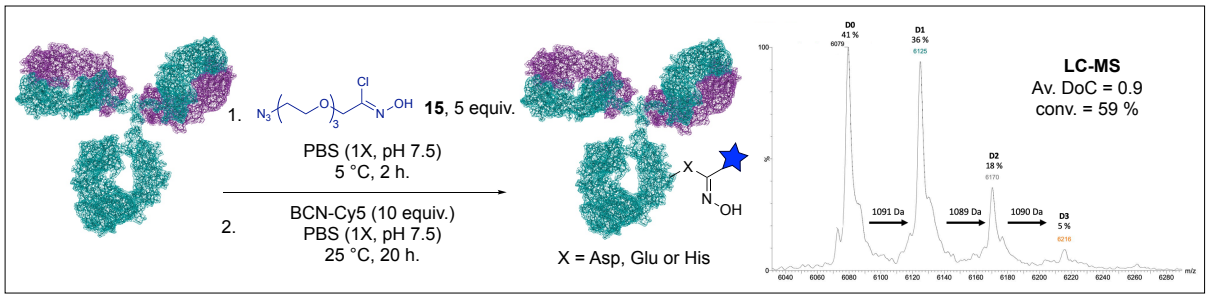

Figure 2: Réactivité du chlorooxime 15 sur trastuzumab

histidine, sur le chlorooxime. Si cette réactivité est en contradiction avec certains exemples de la littérature, et qu'une étude de peptide mapping plus poussée est nécessaire pour confirmer les acides aminés impliqués dans la conjugaison, elle reste néanmoins source d'une conjugaison remarquablement homogène sur trastuzumab.

Dans un second temps, la réactivité sur trastuzumab de l'hydrazone **16** en présence de l'isonitrile **a** a été évaluée (Figure 3). Dans des conditions similaires à celles développées dans les résultats préliminaires, cette combinaison de réactif s'est avérée moins efficace que la combinaison de l'aldéhyde **14** et du même isonitrile. Si cette efficacité moindre peut être corrélée à un gain de sélectivité, il était important de d'abord comprendre le mécanisme suivit par cette modification. En effet, nous n'avons pas trouvé de mention dans la littérature de l'utilisation de ce type de réactif dans des réactions multi-composantes. Les expériences menées ont en effet indiqué que l'hydrazone **16** réagit dans un premier temps avec les amines présentes à la surface de la protéine, suivant un mécanisme de transamination et que, en présence d'un acide carboxylique à proximité, la réaction de Ugi attendue a lieu. Si nos expériences n'ont pas pu écarter la possibilité qu'une partie de l'hydrazone introduite est hydrolysée, il est certain que cette réaction, si elle a lieu, est minoritaire. Le mécanisme de transamination est néanmoins très intéressant puisqu'il empêche toute réaction de Passerini de se produire, réduisant l'hétérogénéité associée à la réaction de Ugi sur anticorps. Cependant les faibles conversions observées nous ont poussées à poursuivre notre étude de la réaction de Ugi en étudiant l'influence de la variation d'autres paramètre, toujours en quête du développement de conditions plus sélectives.

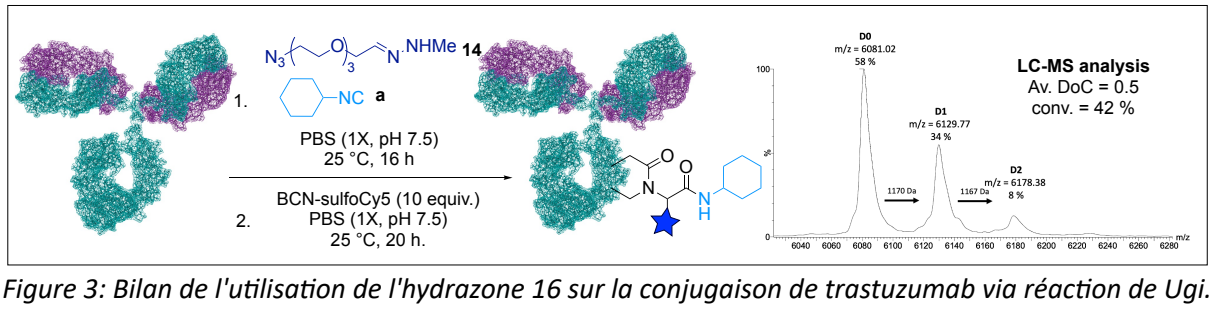

Figure 3: Bilan de l'utilisation de l'hydrazone 16 sur la conjugaison de trastuzumab via réaction de Ugi.

II.2.c. Variation de la chaine latérale de l'isonitrile

Afin de valider la répétabilité et la reproductibilité des résultats précédemment publiés, les conditions de Ugi optimales utilisant l'aldéhyde **14** et l'isonitrile **a** ont été répétées et analysées par peptide mapping. À ce stade, la seule variation expérimentale correspondait au remplacement du BCN-sulfocy5 par un BCN-iminobiotine lors de l'étape « play » afin de limiter la précipitation des conjugués précédemment observée. Dans ces conditions, les principaux sites identifiés furent les résidus aspartate et glutamate situés aux extrémités *N*-terminales, modifiés via une réaction de Ugi « intra-résidu » ainsi que par une réaction de Passerini, accompagnés de quelques modifications « inter-résidus » (K65-D62 et K277-E275). Une première stratégie envisagée pour favoriser un mécanisme par rapport à l'autre a alors été de varier le pH : le pK_a des amines-ε différant de celui des amines-α (10.5 et 7.7,[178] respectivement), une variation de pH devrait favoriser un site par rapport à l'autre. Cependant,

dans la gamme de pH pouvant être tolérée par la protéine (de 5.5 à 8.5), il n'a pas été possible de favoriser un site ou un mécanisme par rapport à un autre. Le grand nombre d'expériences mené lors de cette étude a cependant permis de déceler une tendance : lorsqu'un degré de conjugaison < 1 est atteint, seule la modification des résidus N-terminaux est observée cependant sans sélectivité de mécanisme.

Ensuite, l'influence de la structure des réactifs, aussi bien de l'isonitrile que du carbonyle, a été étudiée. Les résultats, confirment la tendance observée précédemment avec une modification majoritaire des résidus *N*-terminaux, et des conversions (conv.) et des degrés de conjugaison moyens (av. DoC) similaires. Le couple aldéhyde **14** et isonitrile **b** a particulièrement retenu notre attention puisque, dans ce cas précis, lorsqu'un degré de conjugaison ≤ 1 est obtenu, non seulement l'unique modification de l'acide glutamique *N*-terminal E1 est observée, mais en plus elle semble suivre uniquement un mécanisme de Ugi-intra-résidu (Fig 4). Lorsqu'un degré de conjugaison supérieur est atteint, la réaction semble redevenir uniquement site sélective. Il convient cependant de noter que des concentrations plus élevées en trastuzumab (15 mg/mL au lieu de 10 mg/mL) ont permis de conserver un certain degré de sélectivité, cette fois-ci pour l'ensemble des quatre résidus *N*-terminaux. À ce stade, nous pouvons donc conclure que nous avons développé deux jeux de conditions réactionnelles pour la modification site-sélective du trastuzumab, reposant sur la structure des réactifs employés ainsi que la concentration de la protéine en solution. De plus, nous avons pu appliquer ces résultats à la modification de deux autres anticorps monoclonaux utilisés en thérapie, ramucirumab et bevacizumab, tout en conservant la sélectivité pour les résidus *N*-terminaux. En revanche, lors de l'utilisation de ces conditions sur l'anticorps chimérique humain-murin rituximab, une conversion et un DoC similaire ont été observés mais aucun site de modification n'a pu être identifié par LC-MS/MS,

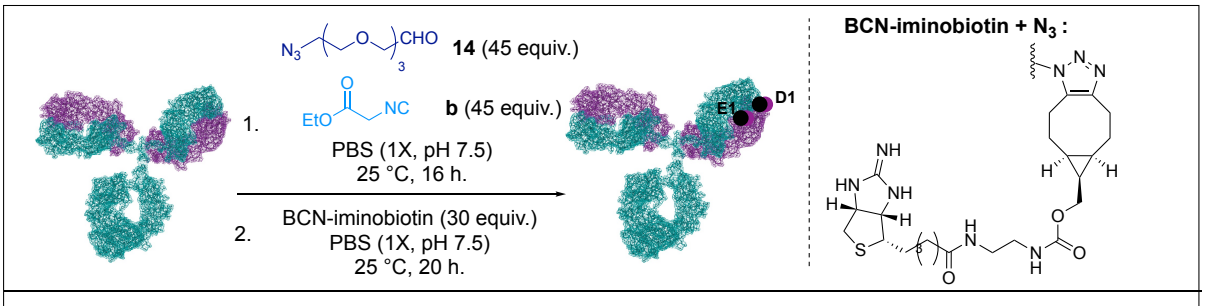

mAb	[mAb] (mg/mL)	conv. (%)	av. DoC	LC-MS/MS
trastuzumab	10	60	0.9	● E1 ● E1/D1 DoC > 1
trastuzumab	10	83	1.8	● E1/D1 ● D1
rituximab	10	45	1.5	/
ramucirumab	10	52	0.8	● E1 ● E1/D1
bevacizumab	10	44	0.6	● E1

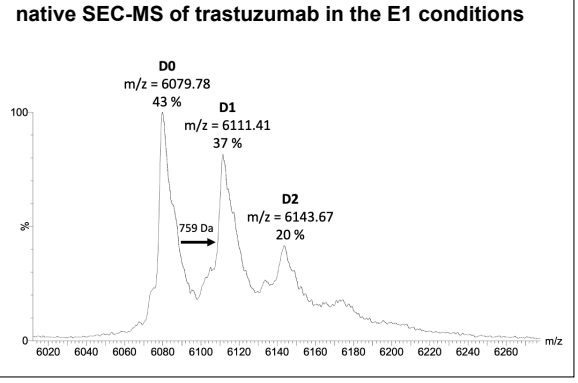

Figure 4: Bilan des conditions E1-selectives pour la modification de divers mAb.

suggérant potentiellement une trop faible abondance de peptides marqués et donc une plus grande variété de sites de conjugaison.

III. Formation et caractérisation d'anticorps bispécifiques

Ayant développé une méthode robuste, répétable et modulable de modification précise d'anticorps, nous avons souhaité tirer profit de celle-ci afin de produire des complexes protéiques homogènes et moléculairement définis. Ainsi, il a été imaginé que les conjugués azotures obtenus par réaction de Ugi pourraient être mis en présence d'une protéine ou d'un fragment de protéine porteur d'une fonction BCN, afin notamment de développer des anticorps bispécifiques (bsAbs). Les bsAbs sont des composés combinant les propriétés de deux anticorps et donc portant deux ou plusieurs paratopes différents. Ils ont particulièrement été explorés au cours des dernières années car ils sont décrits comme permettant de potentialiser l'effet antitumoral d'un anticorps seul mais aussi de diminuer de potentiels phénomènes de résistance.[182] En outre, par rapport au développement parallèle de deux mAbs différents (thérapie combinée), le coût du développement et des essais cliniques peut techniquement être divisé par deux dans le cas des bsAbs. Historiquement, la production des bsAbs repose essentiellement sur la fusion somatique de deux lignées d'hybridomes,[189,188] bien que la principale méthode de production actuelle repose sur le génie génétique, avec l'insertion symétrique au niveau des extrémités *N*- ou *C*-terminales d'une séquence de paratope choisie lors de la production de la protéine.[232] Si cette dernière méthode a permis la production de la plupart des bispécifiques actuellement en étude clinique, des stratégies chimiques commencent à émerger, offrant une production alternative moins coûteuse et plus flexible.[103,233]

D'un point de vue structurel, nous avons décidé de nous concentrer sur la production de constructions de type IgG-Fab. En effet, les Fab (fragment de liaison de l'antigène) sont des fragments d'anticorps composés d'une chaîne légère et d'une partie tronquée de la chaîne lourde, reliées entre elles par une seule liaison disulfure. Étant plus petits et donc plus faciles à fonctionnaliser, tout en conservant la capacité de reconnaissance de l'antigène de leur mAb parent, les Fabs sont extrêmement intéressants pour la production de bsAbs. Comme la réaction d'Ugi permet d'obtenir un mAb fonctionnalisé par un azoture de manière homogène, nous devions tout d'abord accéder à un Fab fonctionnalisé par un BCN de manière sélective pour réagir avec lui. Pour ce faire, nous avons opté pour une stratégie de pontage utilisant des réactifs de type dibromomaléimide (DBM). Appelés « maléimides de nouvelle génération », ces réactifs permettent la conjugaison covalente et simultanée des deux cystéines constitutives du seul pont disulfure accessible du fragment Fab.[213,212] Nous avons obtenu le BCN-dibromomaléimide DBM-A en trois étapes avec un rendement modéré (26%). DBM-A s'est avéré très efficace puisqu'il a permis de rebridger totalement les différents Fab disponible en seulement 20 minutes. La SPAAC entre le trastuzumab modifié par Ugi – tra-N_3 — et le F_{rit}-BCN a ensuite été évaluée dans différentes conditions et analysée par chromatographie d'exclusion

stérique. Alors que la variation de la température (de 25 °C à 37 °C) ne semble pas exercer une influence marquée sur la formation du bsAb (Tra-F_{rit}), un impact de la concentration en protéines et du temps de réaction a été clairement observé. Enfin, il a été constaté que l'incubation de 100 µM de trastu-E1 et de 200 µM de F_{rit}-BCN dans du PBS (1x, pH 7.5) à 25 °C pendant 48 heures a conduit à la consommation complète du trastuzumab conjugué (Figure 5). En outre, nous avons été ravis d'observer la formation du bsAb tra-Frit attendu, confirmé par analyse en SEC-MS native. En concentrant l'échantillon injecté et en effectuant des doubles purifications, nous avons cependant réussi à isoler le bsAb pure avec un rendement de 48% (calculé à partir de la quantité de tra-N_3 introduite), un processus qui a pu être exécuté à différentes échelles, de 200 µg à 1 mg de trastuzumab conjugué de départ. Le bsAb isolé qui en résulte a été analysé par SEC-MS native, qui a confirmé qu'il correspondait à l'espèce attendue. Sur la base de cette méthode, six différents bsAbs ont été produits, purifiés et caractérisés. Tous ont ensuite été marqués à la fluorescéine (FITC) pour mesurer leur affinité envers la lignée cellulaire SKBR-3, surexprimant le récepteur HER-2 ciblé par trastuzumab. Plus précisément, les valeurs k_{on}, k_{off} et K_D ont été calculées en utilisant la technologie LigandTracer de Ridgeview Instruments selon le modèle de liaison de Langmuir, ou "one-to-one", avec les cellules MDA-MB-231 comme contrôle négatif. Nous avons été heureux d'observer que le K_D global des bsAbs incorporant le trastuzumab comme anticorps était comparable à celui du trastuzumab natif – de 0.35 à 0.50 nM pour les bsAbs contre 0.65 nM pour le trastuzumab natif en utilisant la même méthode. Cela suggère que, même si le mAb est modifié au niveau de son paratope, la

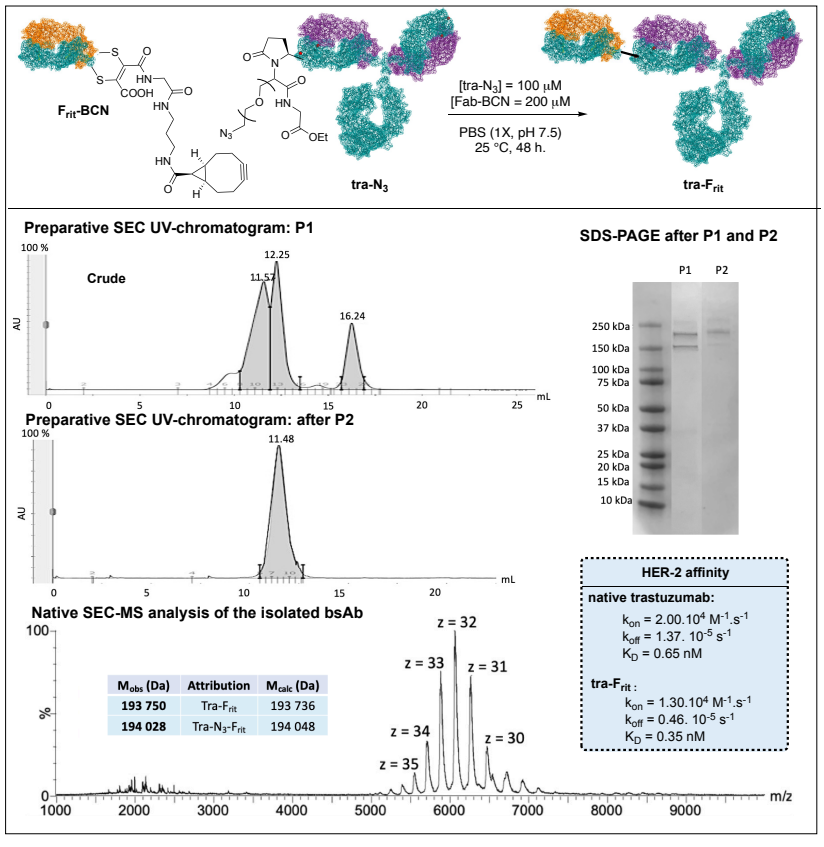

Figure 5: Les différentes étapes de la production d'un anticorps bispécifique basé sur les conditions E1 selectives de la réaction de Ugi.

conjugaison par réaction de Ugi n'altère pas l'affinité de celui-ci pour sa cible. De plus, une excellente affinité de 29 pM a été observée lorsque la seule composante pouvant reconnaître le récepteur HER-2 était le Fab du bsAb, suggérant que les affinités des deux anticorps sont bel et bien combinées.

De plus, parmi les différentes combinaisons réalisées, le format Tra-F_{muro} présente un intérêt particulier puisqu'il combine la reconnaissance pour le récepteur HER-2 (portée par trastuzumab) et celle pour le récepteur CD3 (portée par muromonab), présent à la surface des lymphocytes T. La combinaison de ces deux entités sur un bsAb permet de développer un outil thérapeutique permettant de recruter les lymphocytes T du patient pour détruire la tumeur, un format de bsAb nommé biTE, pour *bispecific T-cell Engager*, et considéré comme particulièrement prometteur.[234,235] Grâce a nos collaborateurs de la Queen's university of Belfast et les resultats, notre biTE a pu être évalué sur des lymphocytes T provenant de donneurs volontaires. Nous avons été très heureux d'observer une excellente occupation des récepteurs HER-2 et CD3 par tra-Fmuro (évaluée en cytométrie de flux) ainsi qu'une excellente toxicité de 77 pM (Figure 6).

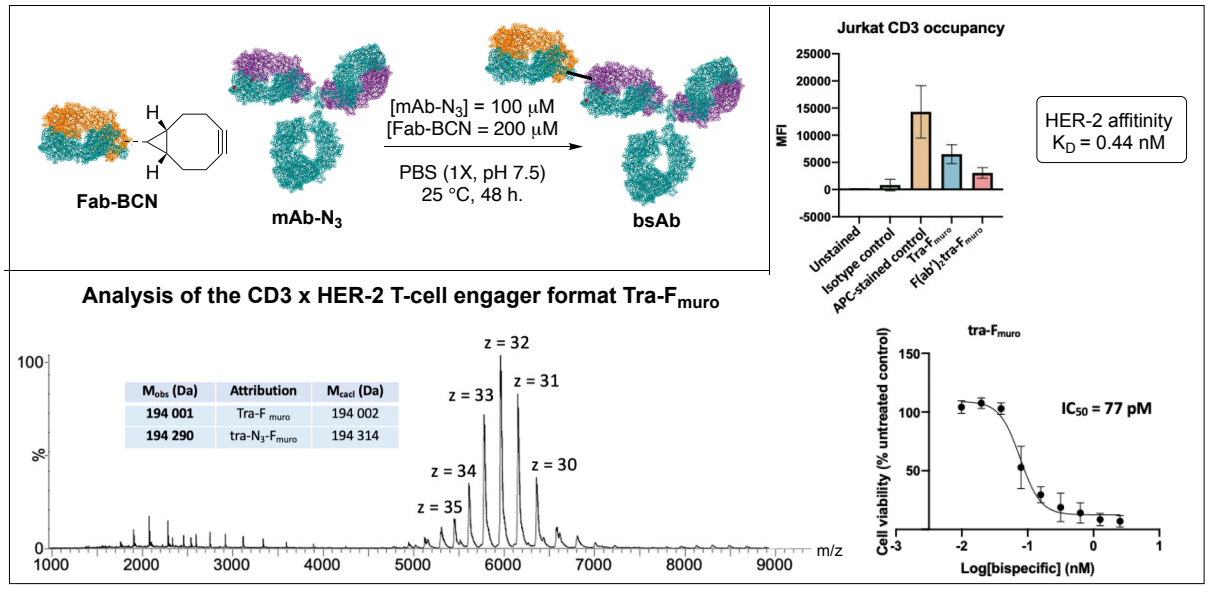

Figure 6: Caractérisation de l'activité du bispécifique T cell engager produit via la réaction de Ugi E1-selective.

IV. Conclusion

Au cours de la première partie de mon doctorat, j'ai pu développer et optimiser différentes méthodes pour la modification de protéines, basées sur l'utilisation de réactions multicomposantes.

Dans un premier, en s'inspirant de la réaction de Robinson-Schöpf, l'introduction d'un motif sur trastuzumab a été entreprise. Si la fonctionnalisation attendue n'a pas pu être obtenue,

l'exploitation d'une réaction secondaire, menant à la formation d'adduits pyrroles sur les lysines de la protéine a pu être développée.

En s'appuyant sur la réaction de Ugi, deux nouveaux réactifs de conjugaison ont été synthétisés. Le premier, un chlorooxime, s'est avéré extrêmement efficace pour la modification des protéines, cependant cette réactivité semble se reposer uniquement sur son fort caractère électrophile et la modification observée, bien qu'homogène ne suit pas le mécanisme attendu. L'utilisation de ce réactif pour la modification sélective des aspartates et des glutamates de la protéine est en cours d'investigation.

Ensuite, une hydrazone a été évaluée, toujours comme source de carbonyl dans le cadre de la réaction de Ugi. Ce réactif s'est avéré moins réactif qu'un aldéhyde analogue, cependant il est probable que cette baisse de réactivité soit liée a un gain de sélectivité de la réaction. En effet, en présence d'un aldéhyde et d'un isonitrile, notre protéine modèle trastuzumab, semble être modifiée non seulement par la réaction de Ugi mais aussi par la réaction de Passerini, menant a un mélange d'adduits final. Dans le cas de l'hydrazone, seul le mecanisme de Ugi a lieu, réduisant donc l'hétérogénéité observée.

Finalement la variation des chaines latérales des isonitriles utilisés, en présence d'un aldéhyde a permis d'observer la modification non seulement résidu sélective (E1) mais aussi Ugi-sélective de trastuzumab. Cette méthode a pu être étendue à d'autres anticorps monoclonaux.
De part son caractère de plug-and-play, le conjugué sélectivement modifié présente une fonction azide permettant sa fonctionnalisation avec, virtuellement n'importe quel objet, pourvu qu'il soit fonctionnalisé avec un alcyne tendu.

Afin d'exploiter cette propriété a son maximum, nous avons généré divers Fab, fonctionalisé avec un BCN, permettant ainsi la génération d'anticorps bispécifiques. Les tests réalisés montrent que les bsAbs produits en utilisant cette méthode présentent en effet une affinité pour les deux cibles visées. Nous avons même eu l'occasion de former des complexes permettant l'activation dirigée du système immunitaire, menant à une toxicité de l'ordre de 77 pM.

Bibliography

(1) Hermanson, G. T. Introduction to Bioconjugation. In *Bioconjugate Techniques*; Elsevier, 2013; pp 1–125. https://doi.org/10.1016/B978-0-12-382239-0.00001-7.
(2) Means, G. E.; Feeney, R. E. Chemical Modifications of Proteins: History and Applications. *Bioconjug. Chem.* **1990**, *1* (1), 2–12. https://doi.org/10.1021/bc00001a001.
(3) Fields, R. [38] The Rapid Determination of Amino Groups with TNBS. In *Methods in Enzymology*; Elsevier, 1972; Vol. 25, pp 464–468. https://doi.org/10.1016/S0076-6879(72)25042-X.
(4) Ellman, G. L. Tissue Sulfhydryl Groups. *Arch. Biochem. Biophys.* **1959**, *82* (1), 70–77. https://doi.org/10.1016/0003-9861(59)90090-6.
(5) Slawiński, P.; Karpińska, B.; Wrebiakowski, H. [Bartlett's test in the statistical determination of amino acids using an automatic analyzer]. *Pol. Arch. Weter.* **1975**, *17* (4), 737–748.
(6) Edman, P.; Högfeldt, E.; Sillén, L. G.; Kinell, P.-O. Method for Determination of the Amino Acid Sequence in Peptides. *Acta Chem. Scand.* **1950**, *4*, 283–293. https://doi.org/10.3891/acta.chem.scand.04-0283.
(7) Latterich, M.; Corbeil, J. Label-Free Detection of Biomolecular Interactions in Real Time with a Nano-Porous Silicon-Based Detection Method. *Proteome Sci.* **2008**, *6* (1), 31. https://doi.org/10.1186/1477-5956-6-31.
(8) Stachowiak, K.; Dyckes, D. F. Peptide Mapping Using Thermospray LC/MS Detection: Rapid Identification of Hemoglobin Variants. *Pept. Res.* **1989**, *2* (4), 267.
(9) Hernandez-Alba, O.; Houel, S.; Hessmann, S.; Erb, S.; Rabuka, D.; Huguet, R.; Josephs, J.; Beck, A.; Drake, P. M.; Cianférani, S. A Case Study to Identify the Drug Conjugation Site of a Site-Specific Antibody-Drug-Conjugate Using Middle-Down Mass Spectrometry. *J. Am. Soc. Mass Spectrom.* **2019**, *30* (11), 2419–2429. https://doi.org/10.1007/s13361-019-02296-2.
(10) Vreeland, W. N.; Barron, A. E. Functional Materials for Microscale Genomic and Proteomic Analyses. *Curr. Opin. Biotechnol.* **2002**, *13* (2), 87–94. https://doi.org/10.1016/S0958-1669(02)00292-6.
(11) Balls, A. K.; Jansen, E. F. Stoichiometric Inhibition of Chymotrypsin. In *Advances in Enzymology - and Related Areas of Molecular Biology*; Nord, F. F., Ed.; John Wiley & Sons, Inc.: Hoboken, NJ, USA, 2006; pp 321–343. https://doi.org/10.1002/9780470122587.ch8.
(12) Small, D. H.; Chubb, I. W. Identification of a Trypsin-Like Site Associated with Acetylcholinesterase by Affinity Labelling with [^{3} H]Diisopropyl Fluorophosphate. *J. Neurochem.* **1988**, *51* (1), 69–74. https://doi.org/10.1111/j.1471-4159.1988.tb04836.x.
(13) Weerapana, E.; Wang, C.; Simon, G. M.; Richter, F.; Khare, S.; Dillon, M. B. D.; Bachovchin, D. A.; Mowen, K.; Baker, D.; Cravatt, B. F. Quantitative Reactivity Profiling Predicts Functional Cysteines in Proteomes. *Nature* **2010**, *468* (7325), 790–795. https://doi.org/10.1038/nature09472.
(14) Sakamoto, S.; Hamachi, I. Ligand-Directed Chemistry for Protein Labeling for Affinity-Based Protein Analysis. *Isr. J. Chem.* **2023**, *63* (3–4), e202200077. https://doi.org/10.1002/ijch.202200077.
(15) Oli, A. N.; Rowaiye, A. B. Vaccine Types and Reverse Vaccinology. In *Vaccinology and Methods in Vaccine Research*; Elsevier, 2022; pp 31–55. https://doi.org/10.1016/B978-0-323-91146-7.00013-5.
(16) Vliegenthart, J. F. G. Carbohydrate Based Vaccines. *FEBS Lett.* **2006**, *580* (12), 2945–2950. https://doi.org/10.1016/j.febslet.2006.03.053.
(17) Peters, C.; Brown, S. Antibody–Drug Conjugates as Novel Anti-Cancer Chemotherapeutics. *Biosci. Rep.* **2015**, *35* (4), e00225. https://doi.org/10.1042/BSR20150089.

(18) Samantasinghar, A.; Sunildutt, N. P.; Ahmed, F.; Soomro, A. M.; Salih, A. R. C.; Parihar, P.; Memon, F. H.; Kim, K. H.; Kang, I. S.; Choi, K. H. A Comprehensive Review of Key Factors Affecting the Efficacy of Antibody Drug Conjugate. *Biomed. Pharmacother.* **2023**, *161*, 114408. https://doi.org/10.1016/j.biopha.2023.114408.
(19) Beck, A.; Goetsch, L.; Dumontet, C.; Corvaïa, N. Strategies and Challenges for the next Generation of Antibody–Drug Conjugates. *Nat. Rev. Drug Discov.* **2017**, *16* (5), 315–337. https://doi.org/10.1038/nrd.2016.268.
(20) Schumacher, D.; Hackenberger, C. P. R.; Leonhardt, H.; Helma, J. Current Status: Site-Specific Antibody Drug Conjugates. *J. Clin. Immunol.* **2016**, *36* (S1), 100–107. https://doi.org/10.1007/s10875-016-0265-6.
(21) *Www.Antibodysociety.Org/Antibody-Therapeutics-Product-Data*. www.antibodysociety.org/antibody-therapeutics-product-data (accessed 2023-08-21).
(22) Gautier, V.; Boumeester, A. J.; Lössl, P.; Heck, A. J. R. Lysine Conjugation Properties in Human IgGs Studied by Integrating High-Resolution Native Mass Spectrometry and Bottom-up Proteomics. *PROTEOMICS* **2015**, *15* (16), 2756–2765. https://doi.org/10.1002/pmic.201400462.
(23) Sornay, C.; Vaur, V.; Wagner, A.; Chaubet, G. An Overview of Chemo- and Site-Selectivity Aspects in the Chemical Conjugation of Proteins. *R. Soc. Open Sci.* **2022**, *9* (1), 211563. https://doi.org/10.1098/rsos.211563.
(24) Hermanson, G. T. Functional Targets for Bioconjugation. In *Bioconjugate Techniques*; Elsevier, 2013; pp 127–228. https://doi.org/10.1016/B978-0-12-382239-0.00002-9.
(25) Jentoft, N.; Dearborn, D. G. Labeling of Proteins by Reductive Methylation Using Sodium Cyanoborohydride. *J. Biol. Chem.* **1979**, *254* (11), 4359–4365. https://doi.org/10.1016/S0021-9258(17)30016-9.
(26) Baslé, E.; Joubert, N.; Pucheault, M. Protein Chemical Modification on Endogenous Amino Acids. *Chem. Biol.* **2010**, *17* (3), 213–227. https://doi.org/10.1016/j.chembiol.2010.02.008.
(27) Algar, W. R. A Brief Introduction to Traditional Bioconjugate Chemistry. In *Chemoselective and Bioorthogonal Ligation Reactions*; Algar, W. R., Dawson, P. E., Medintz, I. L., Eds.; Wiley-VCH Verlag GmbH & Co. KGaA: Weinheim, Germany, 2017; pp 1–36. https://doi.org/10.1002/9783527683451.ch1.
(28) Boutureira, O.; Bernardes, G. J. L. Advances in Chemical Protein Modification. *Chem. Rev.* **2015**, *115* (5), 2174–2195. https://doi.org/10.1021/cr500399p.
(29) Koniev, O.; Wagner, A. Developments and Recent Advancements in the Field of Endogenous Amino Acid Selective Bond Forming Reactions for Bioconjugation. *Chem Soc Rev* **2015**, *44* (15), 5495–5551. https://doi.org/10.1039/C5CS00048C.
(30) Gildersleeve, J. C.; Oyelaran, O.; Simpson, J. T.; Allred, B. Improved Procedure for Direct Coupling of Carbohydrates to Proteins via Reductive Amination. *Bioconjug. Chem.* **2008**, *19* (7), 1485–1490. https://doi.org/10.1021/bc800153t.
(31) Smith, G. P. Kinetics of Amine Modification of Proteins. *Bioconjug. Chem.* **2006**, *17* (2), 501–506. https://doi.org/10.1021/bc0503061.
(32) Dovgan, I.; Ursuegui, S.; Erb, S.; Michel, C.; Kolodych, S.; Cianférani, S.; Wagner, A. Acyl Fluorides: Fast, Efficient, and Versatile Lysine-Based Protein Conjugation via Plug-and-Play Strategy. *Bioconjug. Chem.* **2017**, *28* (5), 1452–1457. https://doi.org/10.1021/acs.bioconjchem.7b00141.
(33) Berndt, D. C.; Faburada, A. L. Reaction of Acyl Azide and Amines. Kinetics and Mechanism. *J. Org. Chem.* **1982**, *47* (21), 4167–4169. https://doi.org/10.1021/jo00142a033.
(34) Ślósarczyk, A. T.; Ramapanicker, R.; Norberg, T.; Baltzer, L. Mixed Pentafluorophenyl and O-Fluorophenyl Esters of Aliphatic Dicarboxylic Acids: Efficient Tools for Peptide and Protein Conjugation. *RSC Adv* **2012**, *2* (3), 908–914. https://doi.org/10.1039/C1RA00530H.
(35) Anderson, G. W.; Zimmerman, J. E.; Callahan, F. M. The Use of Esters of N-

Hydroxysuccinimide in Peptide Synthesis. *J. Am. Chem. Soc.* **1964**, *86* (9), 1839–1842. https://doi.org/10.1021/ja01063a037.
(36) Pham, G. H.; Ou, W.; Bursulaya, B.; DiDonato, M.; Herath, A.; Jin, Y.; Hao, X.; Loren, J.; Spraggon, G.; Brock, A.; Uno, T.; Geierstanger, B. H.; Cellitti, S. E. Tuning a Protein-Labeling Reaction to Achieve Highly Site Selective Lysine Conjugation. *ChemBioChem* **2018**, *19* (8), 799–804. https://doi.org/10.1002/cbic.201700611.
(37) Sarrett, S. M.; Rodriguez, C.; Rymarczyk, G.; Hosny, M. M.; Keinänen, O.; Delaney, S.; Thau, S.; Krantz, B. A.; Zeglis, B. M. Lysine-Directed Site-Selective Bioconjugation for the Creation of Radioimmunoconjugates. *Bioconjug. Chem.* **2022**, *33* (9), 1750–1760. https://doi.org/10.1021/acs.bioconjchem.2c00354.
(38) Jensen, K. B.; Mikkelsen, J. H.; Jensen, S. P.; Kidal, S.; Friberg, G.; Skrydstrup, T.; Gustafsson, M. B. F. New Phenol Esters for Efficient PH-Controlled Amine Acylation of Peptides, Proteins, and Sepharose Beads in Aqueous Media. *Bioconjug. Chem.* **2022**, *33* (1), 172–179. https://doi.org/10.1021/acs.bioconjchem.1c00528.
(39) Radzicka, A.; Wolfenden, R. Rates of Uncatalyzed Peptide Bond Hydrolysis in Neutral Solution and the Transition State Affinities of Proteases. *J. Am. Chem. Soc.* **1996**, *118* (26), 6105–6109. https://doi.org/10.1021/ja954077c.
(40) Cuatrecasas, P.; Parikh, I. Adsorbents for Affinity Chromatography. Use of N-Hydroxysuccinimide Esters of Agarose. *Biochemistry* **1972**, *11* (12), 2291–2299. https://doi.org/10.1021/bi00762a013.
(41) Hermanson, G. T. The Reactions of Bioconjugation. In *Bioconjugate Techniques*; Elsevier, 2013; pp 229–258. https://doi.org/10.1016/B978-0-12-382239-0.00003-0.
(42) Riggs, J. L.; Downs, C. M. Isothiocyanate Compounds as Fluorescent Labeling Agents for Immune Serum. *Am. J. Pathol.* **1958**, *34*, 1081–1097.
(43) Jorbágy, A.; Király, K. Chemical Characterization of Fluorescein Isothiocyanate-Protein Conjugates. *Biochim. Biophys. Acta BBA - Gen. Subj.* **1966**, *124* (1), 166–175. https://doi.org/10.1016/0304-4165(66)90325-4.
(44) Tuls, J.; Geren, L.; Millett, F. Fluorescein Isothiocyanate Specifically Modifies Lysine 338 of Cytochrome P-450scc and Inhibits Adrenodoxin Binding. *J. Biol. Chem.* **1989**, *264* (28), 16421–16425. https://doi.org/10.1016/S0021-9258(19)84723-3.
(45) Yi, S.; Wei, S.; Wu, Q.; Wang, H.; Yao, Z. Azaphilones as Activation-Free Primary-Amine-Specific Bioconjugation Reagents for Peptides, Proteins and Lipids. *Angew. Chem. Int. Ed.* **2022**, *61* (6). https://doi.org/10.1002/anie.202111783.
(46) Wolkersdorfer, A. M.; Jugovic, I.; Scheller, L.; Gutmann, M.; Hahn, L.; Diessner, J.; Lühmann, T.; Meinel, L. PEGylation of Human Vascular Endothelial Growth Factor. *ACS Biomater. Sci. Eng.* **2023**, acsbiomaterials.3c00253. https://doi.org/10.1021/acsbiomaterials.3c00253.
(47) Tully, M.; Hauptstein, N.; Licha, K.; Meinel, L.; Lühmann, T.; Haag, R. Linear Polyglycerol for N-Terminal-Selective Modification of Interleukin-4. *J. Pharm. Sci.* **2022**, *111* (6), 1642–1651. https://doi.org/10.1016/j.xphs.2021.10.032.
(48) Sanjayan, C. G.; Jyothi, M. S.; Sakar, M.; Balakrishna, R. G. Multidentate Ligand Approach for Conjugation of Perovskite Quantum Dots to Biomolecules. *J. Colloid Interface Sci.* **2021**, *603*, 758–770. https://doi.org/10.1016/j.jcis.2021.06.088.
(49) Dziemidowicz, K.; Brocchini, S.; Williams, G. R. A Simple Route to Functionalising Electrospun Polymer Scaffolds with Surface Biomolecules. *Int. J. Pharm.* **2021**, *597*, 120231. https://doi.org/10.1016/j.ijpharm.2021.120231.
(50) Longo, B.; Zanato, C.; Piras, M.; Dall'Angelo, S.; Windhorst, A. D.; Vugts, D. J.; Baldassarre, M.; Zanda, M. Design, Synthesis, Conjugation, and Reactivity of Novel *Trans,Trans* -1,5-Cyclooctadiene-Derived Bioorthogonal Linkers. *Bioconjug. Chem.* **2020**, *31* (9), 2201–2210. https://doi.org/10.1021/acs.bioconjchem.0c00375.
(51) Dovgan, I.; Hentz, A.; Koniev, O.; Ehkirch, A.; Hessmann, S.; Ursuegui, S.; Delacroix,

S.; Riomet, M.; Taran, F.; Cianférani, S.; Kolodych, S.; Wagner, A. Automated Linkage of Proteins and Payloads Producing Monodisperse Conjugates. *Chem. Sci.* **2020**, *11* (5), 1210–1215. https://doi.org/10.1039/C9SC05468E.
(52) Kreusser, J.; Ninni, L.; Jirasek, F.; Hasse, H. Adsorption of Conjugates of Lysozyme and Fluorescein Isothiocyanate in Hydrophobic Interaction Chromatography. *J. Biotechnol.* **2022**, *360*, 133–141. https://doi.org/10.1016/j.jbiotec.2022.10.015.
(53) Schnaible, V.; Przybylski, M. Identification of Fluorescein-5'-Isothiocyanate-Modification Sites in Proteins by Electrospray-Ionization Mass Spectrometry. *Bioconjug. Chem.* **1999**, *10* (5), 861–866. https://doi.org/10.1021/bc990039x.
(54) Chen, X.; Muthoosamy, K.; Pfisterer, A.; Neumann, B.; Weil, T. Site-Selective Lysine Modification of Native Proteins and Peptides via Kinetically Controlled Labeling. *Bioconjug. Chem.* **2012**, *23* (3), 500–508. https://doi.org/10.1021/bc200556n.
(55) Poole, L. B. The Basics of Thiols and Cysteines in Redox Biology and Chemistry. *Free Radic. Biol. Med.* **2015**, *80*, 148–157. https://doi.org/10.1016/j.freeradbiomed.2014.11.013.
(56) Cal, P. M. S. D.; Bernardes, G. J. L.; Gois, P. M. P. Cysteine-Selective Reactions for Antibody Conjugation. *Angew. Chem. Int. Ed.* **2014**, *53* (40), 10585–10587. https://doi.org/10.1002/anie.201405702.
(57) Sechi, S.; Chait, B. T. Modification of Cysteine Residues by Alkylation. A Tool in Peptide Mapping and Protein Identification. *Anal. Chem.* **1998**, *70* (24), 5150–5158. https://doi.org/10.1021/ac9806005.
(58) Müller, T.; Winter, D. Systematic Evaluation of Protein Reduction and Alkylation Reveals Massive Unspecific Side Effects by Iodine-Containing Reagents. *Mol. Cell. Proteomics* **2017**, *16* (7), 1173–1187. https://doi.org/10.1074/mcp.M116.064048.
(59) Tallon, A.; Xu, Y.; West, G.; Am Ende, C.; Fox, J. *Thiomethyltetrazines Are Reversible Covalent Cysteine Warheads Whose Dynamic Behavior Can Be "Switched off" via Bioorthogonal Chemistry Inside Live Cells*; preprint; Chemistry, 2023. https://doi.org/10.26434/chemrxiv-2023-w0p5m.
(60) Liu, Y.; Liu, J.; Zhang, X.; Guo, C.; Xing, X.; Zhang, Z.-M.; Ding, K.; Li, Z. Oxidant-Induced Bioconjugation for Protein Labeling in Live Cells. *ACS Chem. Biol.* **2023**, *18* (1), 112–122. https://doi.org/10.1021/acschembio.2c00740.
(61) Chen, F.; Zheng, M.; Nobile, V.; Gao, J. Fast and Cysteine-Specific Modification of Peptides, Proteins and Bacteriophage Using Chlorooximes. *Chem. – Eur. J.* **2022**, *28* (20). https://doi.org/10.1002/chem.202200058.
(62) Ravasco, J. M. J. M.; Faustino, H.; Trindade, A.; Gois, P. M. P. Bioconjugation with Maleimides: A Useful Tool for Chemical Biology. *Chem. – Eur. J.* **2019**, *25* (1), 43–59. https://doi.org/10.1002/chem.201803174.
(63) Partis, M. D.; Griffiths, D. G.; Roberts, G. C.; Beechey, R. B. Cross-Linking of Protein by ω-Maleimido AlkanoylN-Hydroxysuccinimido Esters. *J. Protein Chem.* **1983**, *2* (3), 263–277. https://doi.org/10.1007/BF01025358.
(64) Gorin, G.; Martic, P. A.; Doughty, G. Kinetics of the Reaction of N-Ethylmaleimide with Cysteine and Some Congeners. *Arch. Biochem. Biophys.* **1966**, *115* (3), 593–597. https://doi.org/10.1016/0003-9861(66)90079-8.
(65) Brewer, C. F.; Riehm, J. P. Evidence for Possible Nonspecific Reactions between N-Ethylmaleimide and Proteins. *Anal. Biochem.* **1967**, *18* (2), 248–255. https://doi.org/10.1016/0003-2697(67)90007-3.
(66) Gennari, A.; Wedgwood, J.; Lallana, E.; Francini, N.; Tirelli, N. Thiol-Based Michael-Type Addition. A Systematic Evaluation of Its Controlling Factors. *Tetrahedron* **2020**, *76* (47), 131637. https://doi.org/10.1016/j.tet.2020.131637.
(67) Saito, F.; Noda, H.; Bode, J. W. Critical Evaluation and Rate Constants of Chemoselective Ligation Reactions for Stoichiometric Conjugations in Water. *ACS Chem. Biol.* **2015**, *10* (4), 1026–1033. https://doi.org/10.1021/cb5006728.

(68) Schelté, P.; Boeckler, C.; Frisch, B.; Schuber, F. Differential Reactivity of Maleimide and Bromoacetyl Functions with Thiols: Application to the Preparation of Liposomal Diepitope Constructs. *Bioconjug. Chem.* **2000**, *11* (1), 118–123. https://doi.org/10.1021/bc990122k.
(69) Baldwin, A. D.; Kiick, K. L. Tunable Degradation of Maleimide–Thiol Adducts in Reducing Environments. *Bioconjug. Chem.* **2011**, *22* (10), 1946–1953. https://doi.org/10.1021/bc200148v.
(70) Fontaine, S. D.; Reid, R.; Robinson, L.; Ashley, G. W.; Santi, D. V. Long-Term Stabilization of Maleimide–Thiol Conjugates. *Bioconjug. Chem.* **2015**, *26* (1), 145–152. https://doi.org/10.1021/bc5005262.
(71) Kalia, D.; Pawar, S. P.; Thopate, J. S. Stable and Rapid Thiol Bioconjugation by Light-Triggered Thiomaleimide Ring Hydrolysis. *Angew. Chem. Int. Ed.* **2017**, *56* (7), 1885–1889. https://doi.org/10.1002/anie.201609733.
(72) Wang, Y.; Xie, F.; Liu, L.; Xu, X.; Fan, S.; Zhong, W.; Zhou, X. Development of Applicable Thiol-Linked Antibody–Drug Conjugates with Improved Stability and Therapeutic Index. *Drug Deliv.* **2022**, *29* (1), 754–766. https://doi.org/10.1080/10717544.2022.2039807.
(73) Kasper, M.; Glanz, M.; Stengl, A.; Penkert, M.; Klenk, S.; Sauer, T.; Schumacher, D.; Helma, J.; Krause, E.; Cardoso, M. C.; Leonhardt, H.; Hackenberger, C. P. R. Cysteine-Selective Phosphonamidate Electrophiles for Modular Protein Bioconjugations. *Angew. Chem. Int. Ed.* **2019**, *58* (34), 11625–11630. https://doi.org/10.1002/anie.201814715.
(74) Stieger, C. E.; Park, Y.; de Geus, M. A. R.; Kim, D.; Huhn, C.; Slenczka, J. S.; Ochtrop, P.; Müchler, J. M.; Süssmuth, R. D.; Broichhagen, J.; Baik, M.; Hackenberger, C. P. R. DFT-Guided Discovery of Ethynyl-Triazolyl-Phosphinates as Modular Electrophiles for Chemoselective Cysteine Bioconjugation and Profiling. *Angew. Chem. Int. Ed.* **2022**, *61* (41). https://doi.org/10.1002/anie.202205348.
(75) Ochtrop, P.; Jahzerah, J.; Machui, P.; Mai, I.; Schumacher, D.; Helma, J.; Kasper, M.-A.; Hackenberger, C. P. R. Compact Hydrophilic Electrophiles Enable Highly Efficacious High DAR ADCs with Excellent *in Vivo* PK Profile. *Chem. Sci.* **2023**, *14* (9), 2259–2266. https://doi.org/10.1039/D2SC05678J.
(76) Yang, Y.; Fischer, N. H.; Oliveira, M. T.; Hadaf, G. B.; Liu, J.; Brock-Nannestad, T.; Diness, F.; Lee, J.-W. Carbon Dioxide Enhances Sulphur-Selective Conjugate Addition Reactions. *Org. Biomol. Chem.* **2022**, *20* (22), 4526–4533. https://doi.org/10.1039/D2OB00831A.
(77) Jun, J. V.; Petri, Y. D.; Erickson, L. W.; Raines, R. T. Modular Diazo Compound for the Bioreversible Late-Stage Modification of Proteins. *J. Am. Chem. Soc.* **2023**, *145* (12), 6615–6621. https://doi.org/10.1021/jacs.2c11325.
(78) Petri, Y. D.; Gutierrez, C. S.; Raines, R. T. Chemoselective Caging of Carboxyl Groups for On-Demand Protein Activation with Small Molecules. *Angew. Chem. Int. Ed.* **2023**, e202215614. https://doi.org/10.1002/anie.202215614.
(79) Chan, A. O.-Y.; Ho, C.-M.; Chong, H.-C.; Leung, Y.-C.; Huang, J.-S.; Wong, M.-K.; Che, C.-M. Modification of N-Terminal α-Amino Groups of Peptides and Proteins Using Ketenes. *J. Am. Chem. Soc.* **2012**, *134* (5), 2589–2598. https://doi.org/10.1021/ja208009r.
(80) Mikkelsen, J. H.; Gustafsson, M. B. F.; Skrydstrup, T.; Jensen, K. B. Selective N-Terminal Acylation of Peptides and Proteins with Tunable Phenol Esters. *Bioconjug. Chem.* **2022**, *33* (4), 625–633. https://doi.org/10.1021/acs.bioconjchem.2c00045.
(81) Hanaya, K.; Yamoto, K.; Taguchi, K.; Matsumoto, K.; Higashibayashi, S.; Sugai, T. Single-Step N-Terminal Modification of Proteins via a Bio-Inspired Copper(II)-Mediated Aldol Reaction. *Chem. – Eur. J.* **2022**, *28* (47). https://doi.org/10.1002/chem.202201677.
(82) MacDonald, J. I.; Munch, H. K.; Moore, T.; Francis, M. B. One-Step Site-Specific Modification of Native Proteins with 2-Pyridinecarboxyaldehydes. *Nat. Chem. Biol.* **2015**, *11* (5), 326–331. https://doi.org/10.1038/nchembio.1792.

(83) Bandyopadhyay, A.; Cambray, S.; Gao, J. Fast and Selective Labeling of N-Terminal Cysteines at Neutral PH via Thiazolidino Boronate Formation. *Chem. Sci.* **2016**, *7* (7), 4589–4593. https://doi.org/10.1039/C6SC00172F.
(84) Faustino, H.; Silva, M. J. S. A.; Veiros, L. F.; Bernardes, G. J. L.; Gois, P. M. P. Iminoboronates Are Efficient Intermediates for Selective, Rapid and Reversible N-Terminal Cysteine Functionalisation. *Chem. Sci.* **2016**, *7* (8), 5052–5058. https://doi.org/10.1039/C6SC01520D.
(85) Li, K.; Wang, W.; Gao, J. Fast and Stable N-Terminal Cysteine Modification through Thiazolidino Boronate Mediated Acyl Transfer. *Angew. Chem. Int. Ed.* **2020**, *59* (34), 14246–14250. https://doi.org/10.1002/anie.202000837.
(86) Silva, M. J. S. A.; Cavadas, R. A. N.; Faustino, H.; Veiros, L. F.; Gois, P. M. P. Interactive Bioconjugation at *N* -Terminal Cysteines by Using *O* -Salicylaldehyde Esters towards Dual Site-Selective Functionalization. *Chem. – Eur. J.* **2022**, *28* (67). https://doi.org/10.1002/chem.202202377.
(87) Silva, M. J. S. A.; Faustino, H.; Coelho, J. A. S.; Pinto, M. V.; Fernandes, A.; Compañón, I.; Corzana, F.; Gasser, G.; Gois, P. M. P. Efficient Amino-Sulfhydryl Stapling on Peptides and Proteins Using Bifunctional NHS-Activated Acrylamides. *Angew. Chem. Int. Ed.* **2021**, *60* (19), 10850–10857. https://doi.org/10.1002/anie.202016936.
(88) Istrate, A.; Geeson, M. B.; Navo, C. D.; Sousa, B. B.; Marques, M. C.; Taylor, R. J.; Journeaux, T.; Oehler, S. R.; Mortensen, M. R.; Deery, M. J.; Bond, A. D.; Corzana, F.; Jiménez-Osés, G.; Bernardes, G. J. L. Platform for Orthogonal *N* -Cysteine-Specific Protein Modification Enabled by Cyclopropenone Reagents. *J. Am. Chem. Soc.* **2022**, *144* (23), 10396–10406. https://doi.org/10.1021/jacs.2c02185.
(89) Purushottam, L.; Adusumalli, S. R.; Singh, U.; Unnikrishnan, V. B.; Rawale, D. G.; Gujrati, M.; Mishra, R. K.; Rai, V. Single-Site Glycine-Specific Labeling of Proteins. *Nat. Commun.* **2019**, *10* (1), 2539. https://doi.org/10.1038/s41467-019-10503-7.
(90) Sahu, T.; Kumar, M.; T. K., S.; Joshi, M.; Mishra, R. K.; Rai, V. Residue-Specific N-Terminal Glycine to Aldehyde Transformation Renders Analytically Pure Single-Site Labeled Proteins. *Chem. Commun.* **2022**, *58* (89), 12451–12454. https://doi.org/10.1039/D2CC04196K.
(91) Akkapeddi, P.; Azizi, S.-A.; Freedy, A. M.; Cal, P. M. S. D.; Gois, P. M. P.; Bernardes, G. J. L. Construction of Homogeneous Antibody–Drug Conjugates Using Site-Selective Protein Chemistry. *Chem. Sci.* **2016**, *7* (5), 2954–2963. https://doi.org/10.1039/C6SC00170J.
(92) Mitra, S.; Lawton, R. G. Reagents for the Crosslinking of Proteins by Equilibrium Transfer Alkylation. *J. Am. Chem. Soc.* **1979**, *101* (11), 3097–3110. https://doi.org/10.1021/ja00505a043.
(93) Schumacher, F. F.; Nunes, J. P. M.; Maruani, A.; Chudasama, V.; Smith, M. E. B.; Chester, K. A.; Baker, J. R.; Caddick, S. Next Generation Maleimides Enable the Controlled Assembly of Antibody–Drug Conjugates *via* Native Disulfide Bond Bridging. *Org Biomol Chem* **2014**, *12* (37), 7261–7269. https://doi.org/10.1039/C4OB01550A.
(94) Nunes, J. P. M.; Morais, M.; Vassileva, V.; Robinson, E.; Rajkumar, V. S.; Smith, M. E. B.; Pedley, R. B.; Caddick, S.; Baker, J. R.; Chudasama, V. Functional Native Disulfide Bridging Enables Delivery of a Potent, Stable and Targeted Antibody–Drug Conjugate (ADC). *Chem. Commun.* **2015**, *51* (53), 10624–10627. https://doi.org/10.1039/C5CC03557K.
(95) Bryden, F.; Maruani, A.; Savoie, H.; Chudasama, V.; Smith, M. E. B.; Caddick, S.; Boyle, R. W. Regioselective and Stoichiometrically Controlled Conjugation of Photodynamic Sensitizers to a HER2 Targeting Antibody Fragment. *Bioconjug. Chem.* **2014**, *25* (3), 611–617. https://doi.org/10.1021/bc5000324.
(96) Behrens, C. R.; Ha, E. H.; Chinn, L. L.; Bowers, S.; Probst, G.; Fitch-Bruhns, M.; Monteon, J.; Valdiosera, A.; Bermudez, A.; Liao-Chan, S.; Wong, T.; Melnick, J.; Theunissen, J.-W.; Flory, M. R.; Houser, D.; Venstrom, K.; Levashova, Z.; Sauer, P.; Migone, T.-S.; Van Der Horst, E. H.; Halcomb, R. L.; Jackson, D. Y. Antibody–Drug Conjugates (ADCs) Derived

from Interchain Cysteine Cross-Linking Demonstrate Improved Homogeneity and Other Pharmacological Properties over Conventional Heterogeneous ADCs. *Mol. Pharm.* **2015**, *12* (11), 3986–3998. https://doi.org/10.1021/acs.molpharmaceut.5b00432.
(97) Maruani, A.; Smith, M. E. B.; Miranda, E.; Chester, K. A.; Chudasama, V.; Caddick, S. A Plug-and-Play Approach to Antibody-Based Therapeutics via a Chemoselective Dual Click Strategy. *Nat. Commun.* **2015**, *6* (1), 6645. https://doi.org/10.1038/ncomms7645.
(98) Robinson, E.; Nunes, J. P. M.; Vassileva, V.; Maruani, A.; Nogueira, J. C. F.; Smith, M. E. B.; Pedley, R. B.; Caddick, S.; Baker, J. R.; Chudasama, V. Pyridazinediones Deliver Potent, Stable, Targeted and Efficacious Antibody–Drug Conjugates (ADCs) with a Controlled Loading of 4 Drugs per Antibody. *RSC Adv.* **2017**, *7* (15), 9073–9077. https://doi.org/10.1039/C7RA00788D.
(99) Bahou, C.; Richards, D. A.; Maruani, A.; Love, E. A.; Javaid, F.; Caddick, S.; Baker, J. R.; Chudasama, V. Highly Homogeneous Antibody Modification through Optimisation of the Synthesis and Conjugation of Functionalised Dibromopyridazinediones. *Org. Biomol. Chem.* **2018**, *16* (8), 1359–1366. https://doi.org/10.1039/C7OB03138F.
(100) Lee, M. T. W.; Maruani, A.; Baker, J. R.; Caddick, S.; Chudasama, V. Next-Generation Disulfide Stapling: Reduction and Functional Re-Bridging All in One. *Chem. Sci.* **2016**, *7* (1), 799–802. https://doi.org/10.1039/C5SC02666K.
(101) Lee, M. T. W.; Maruani, A.; Richards, D. A.; Baker, J. R.; Caddick, S.; Chudasama, V. Enabling the Controlled Assembly of Antibody Conjugates with a Loading of Two Modules without Antibody Engineering. *Chem. Sci.* **2017**, *8* (3), 2056–2060. https://doi.org/10.1039/C6SC03655D.
(102) Maruani, A.; Szijj, P. A.; Bahou, C.; Nogueira, J. C. F.; Caddick, S.; Baker, J. R.; Chudasama, V. A Plug-and-Play Approach for the *De Novo* Generation of Dually Functionalized Bispecifics. *Bioconjug. Chem.* **2020**, *31* (3), 520–529. https://doi.org/10.1021/acs.bioconjchem.0c00002.
(103) Thoreau, F.; Rochet, L. N. C.; Baker, J. R.; Chudasama, V. Enabling the Formation of Native MAb, Fab′ and Fc-Conjugates Using a Bis-Disulfide Bridging Reagent to Achieve Tunable Payload-to-Antibody Ratios (PARs). *Chem. Sci.* **2023**, *14* (14), 3752–3762. https://doi.org/10.1039/D2SC06318B.
(104) Thoreau, F.; Szijj, P. A.; Greene, M. K.; Rochet, L. N. C.; Thanasi, I. A.; Blayney, J. K.; Maruani, A.; Baker, J. R.; Scott, C. J.; Chudasama, V. Modular Chemical Construction of IgG-like Mono- and Bispecific Synthetic Antibodies (SynAbs). *ACS Cent. Sci.* **2023**, *9* (3), 476–487. https://doi.org/10.1021/acscentsci.2c01437.
(105) Koniev, O.; Dovgan, I.; Renoux, B.; Ehkirch, A.; Eberova, J.; Cianférani, S.; Kolodych, S.; Papot, S.; Wagner, A. Reduction–Rebridging Strategy for the Preparation of ADPN-Based Antibody–Drug Conjugates. *MedChemComm* **2018**, *9* (5), 827–830. https://doi.org/10.1039/C8MD00141C.
(106) Walsh, S. J.; Iegre, J.; Seki, H.; Bargh, J. D.; Sore, H. F.; Parker, J. S.; Carroll, J. S.; Spring, D. R. General Dual Functionalisation of Biomacromolecules *via* a Cysteine Bridging Strategy. *Org. Biomol. Chem.* **2020**, *18* (22), 4224–4230. https://doi.org/10.1039/D0OB00907E.
(107) Walsh, S. J.; Omarjee, S.; Galloway, W. R. J. D.; Kwan, T. T.-L.; Sore, H. F.; Parker, J. S.; Hyvönen, M.; Carroll, J. S.; Spring, D. R. A General Approach for the Site-Selective Modification of Native Proteins, Enabling the Generation of Stable and Functional Antibody–Drug Conjugates. *Chem. Sci.* **2019**, *10* (3), 694–700. https://doi.org/10.1039/C8SC04645J.
(108) Counsell, A. J.; Walsh, S. J.; Robertson, N. S.; Sore, H. F.; Spring, D. R. Efficient and Selective Antibody Modification with Functionalised Divinyltriazines. *Org. Biomol. Chem.* **2020**, *18* (25), 4739–4743. https://doi.org/10.1039/D0OB01002B.
(109) Hanby, A. R.; Walsh, S. J.; Counsell, A. J.; Ashman, N.; Mortensen, K. T.; Carroll, J. S.; Spring, D. R. Antibody Dual-Functionalisation Enabled through a Modular

Divinylpyrimidine Disulfide Rebridging Strategy. *Chem. Commun.* **2022**, *58* (67), 9401–9404. https://doi.org/10.1039/D2CC02515A.
(110) Dannheim, F. M.; Walsh, S. J.; Orozco, C. T.; Hansen, A. H.; Bargh, J. D.; Jackson, S. E.; Bond, N. J.; Parker, J. S.; Carroll, J. S.; Spring, D. R. All-in-One Disulfide Bridging Enables the Generation of Antibody Conjugates with Modular Cargo Loading. *Chem. Sci.* **2022**, *13* (30), 8781–8790. https://doi.org/10.1039/D2SC02198F.
(111) Chrzastek, A.; Thanasi, I. A.; Irving, J. A.; Chudasama, V.; Baker, J. R. Dual Reactivity Disulfide Bridging Reagents; Enabling New Approaches to Antibody Fragment Bioconjugation. *Chem. Sci.* **2022**, *13* (39), 11533–11539. https://doi.org/10.1039/D2SC04531A.
(112) Rosen, C. B.; Kodal, A. L. B.; Nielsen, J. S.; Schaffert, D. H.; Scavenius, C.; Okholm, A. H.; Voigt, N. V.; Enghild, J. J.; Kjems, J.; Tørring, T.; Gothelf, K. V. Template-Directed Covalent Conjugation of DNA to Native Antibodies, Transferrin and Other Metal-Binding Proteins. *Nat. Chem.* **2014**, *6* (9), 804–809. https://doi.org/10.1038/nchem.2003.
(113) Adusumalli, S. R.; Rawale, D. G.; Thakur, K.; Purushottam, L.; Reddy, N. C.; Kalra, N.; Shukla, S.; Rai, V. Chemoselective and Site-Selective Lysine-Directed Lysine Modification Enables Single-Site Labeling of Native Proteins. *Angew. Chem. Int. Ed.* **2020**, *59* (26), 10332–10336. https://doi.org/10.1002/anie.202000062.
(114) Hansen, R. A.; Märcher, A.; Gothelf, K. V. One-Step Conversion of NHS Esters to Reagents for Site-Directed Labeling of IgG Antibodies. *Bioconjug. Chem.* **2022**, *33* (10), 1811–1817. https://doi.org/10.1021/acs.bioconjchem.2c00392.
(115) Sahu, T.; Chilamari, M.; Rai, V. Protein Inspired Chemically Orthogonal Imines for Linchpin Directed Precise and Modular Labeling of Lysine in Proteins. *Chem. Commun.* **2022**, *58* (11), 1768–1771. https://doi.org/10.1039/D1CC05559C.
(116) Forte, N.; Benni, I.; Karu, K.; Chudasama, V.; Baker, J. R. Cysteine-to-Lysine Transfer Antibody Fragment Conjugation. *Chem. Sci.* **2019**, *10* (47), 10919–10924. https://doi.org/10.1039/C9SC03825F.
(117) Reddy, N. C.; Molla, R.; Joshi, P. N.; T. K., S.; Basu, I.; Kawadkar, J.; Kalra, N.; Mishra, R. K.; Chakrabarty, S.; Shukla, S.; Rai, V. Traceless Cysteine-Linchpin Enables Precision Engineering of Lysine in Native Proteins. *Nat. Commun.* **2022**, *13* (1), 6038. https://doi.org/10.1038/s41467-022-33772-1.
(118) Adusumalli, S. R.; Rawale, D. G.; Singh, U.; Tripathi, P.; Paul, R.; Kalra, N.; Mishra, R. K.; Shukla, S.; Rai, V. Single-Site Labeling of Native Proteins Enabled by a Chemoselective and Site-Selective Chemical Technology. *J. Am. Chem. Soc.* **2018**, *140* (44), 15114–15123. https://doi.org/10.1021/jacs.8b10490.
(119) Sornay, C.; Hessmann, S.; Erb, S.; Dovgan, I.; Ehkirch, A.; Botzanowski, T.; Cianférani, S.; Wagner, A.; Chaubet, G. Investigating Ugi/Passerini Multicomponent Reactions for the Site-Selective Conjugation of Native Trastuzumab**. *Chem. – Eur. J.* **2020**, *26* (61), 13797–13805. https://doi.org/10.1002/chem.202002432.
(120) Matos, M. J.; Oliveira, B. L.; Martínez-Sáez, N.; Guerreiro, A.; Cal, P. M. S. D.; Bertoldo, J.; Maneiro, M.; Perkins, E.; Howard, J.; Deery, M. J.; Chalker, J. M.; Corzana, F.; Jiménez-Osés, G.; Bernardes, G. J. L. Chemo- and Regioselective Lysine Modification on Native Proteins. *J. Am. Chem. Soc.* **2018**, *140* (11), 4004–4017. https://doi.org/10.1021/jacs.7b12874.
(121) Armstrong, R. W.; Combs, A. P.; Tempest, P. A.; Brown, S. D.; Keating, T. A. Multiple-Component Condensation Strategies for Combinatorial Library Synthesis. *Acc. Chem. Res.* **1996**, *29* (3), 123–131. https://doi.org/10.1021/ar9502083.
(122) Biggs-Houck, J. E.; Younai, A.; Shaw, J. T. Recent Advances in Multicomponent Reactions for Diversity-Oriented Synthesis. *Curr. Opin. Chem. Biol.* **2010**, *14* (3), 371–382. https://doi.org/10.1016/j.cbpa.2010.03.003.
(123) Horváth, I. T.; Anastas, P. T. Innovations and Green Chemistry. *Chem. Rev.* **2007**, *107*

(6), 2169–2173. https://doi.org/10.1021/cr078380v.
(124) Strecker, A. Ueber die künstliche Bildung der Milchsäure und einen neuen, dem Glycocoll homologen Körper; *Ann. Chem. Pharm.* **1850**, *75* (1), 27–45. https://doi.org/10.1002/jlac.18500750103.
(125) Laurent, A.; Gerhardt, C. F. Diverses Combinaisons Azotées du Benzoïle. 1838, pp 181–195.
(126) Hantzsch, A. Ueber die Synthese pyridinartiger Verbindungen aus Acetessigäther und Aldehydammoniak. *Justus Liebigs Ann. Chem.* **1882**, *215* (1), 1–82. https://doi.org/10.1002/jlac.18822150102.
(127) Biginelli, P. Ueber Aldehyduramide Des Acetessigäthers. *Berichte Dtsch. Chem. Ges.* **1891**, *24* (1), 1317–1319. https://doi.org/10.1002/cber.189102401228.
(128) Mannich, C.; Krösche, W. Ueber ein Kondensationsprodukt aus Formaldehyd, Ammoniak und Antipyrin. *Arch. Pharm. (Weinheim)* **1912**, *250* (1), 647–667. https://doi.org/10.1002/ardp.19122500151.
(129) Passerini, M.; Simone, L. Composto del p-isonitrilazobenzolo con acetone e acido acetico. *Gazzeta Chimica Italiana*. 51st ed. Gazz. Chim. Ital. 1921, pp 126–129.
(130) Graebin, C. S.; Ribeiro, F. V.; Rogério, K. R.; Kümmerle, A. E. Multicomponent Reactions for the Synthesis of Bioactive Compounds: A Review. *Curr. Org. Synth.* **2019**, *16* (6), 855–899. https://doi.org/10.2174/1570179416666190718153703.
(131) Mishra, A. P.; Bajpai, A.; Rai, A. K. 1,4-Dihydropyridine: A Dependable Heterocyclic Ring with the Promising and the Most Anticipable Therapeutic Effects. *Mini-Rev. Med. Chem.* **2019**, *19* (15), 1219–1254. https://doi.org/10.2174/1389557519666190425184749.
(132) Santos, V. G.; Godoi, M. N.; Regiani, T.; Gama, F. H. S.; Coelho, M. B.; de Souza, R. O. M. A.; Eberlin, M. N.; Garden, S. J. The Multicomponent Hantzsch Reaction: Comprehensive Mass Spectrometry Monitoring Using Charge-Tagged Reagents. *Chem. Weinh. Bergstr. Ger.* **2014**, *20* (40), 12808–12816. https://doi.org/10.1002/chem.201303065.
(133) Katritzky, A. R.; Ostercamp, D. L.; Yousaf, T. I. The Mechanism of the Hantzsch Pyridine Synthesis: A Study by 15N and 13C NMR Spectroscopy. *Tetrahedron* **1986**, *42* (20), 5729–5738. https://doi.org/10.1016/S0040-4020(01)88178-3.
(134) Hantzsch, A. Neue Bildungsweise von Pyrrolderivaten. *Berichte Dtsch. Chem. Ges.* **1890**, *23* (1), 1474–1476. https://doi.org/10.1002/cber.189002301243.
(135) Gewald, K.; Schinke, E.; Böttcher, H. Heterocyclen Aus CH-aciden Nitrilen, VIII. 2-Amino-thiophene Aus Methylenaktiven Nitrilen, Carbonylverbindungen Und Schwefel. *Chem. Ber.* **1966**, *99* (1), 94–100. https://doi.org/10.1002/cber.19660990116.
(136) Russowsky, D.; Canto, R. F. S.; Sanches, S. A. A.; D'Oca, M. G. M.; de Fátima, A.; Pilli, R. A.; Kohn, L. K.; Antônio, M. A.; de Carvalho, J. E. Synthesis and Differential Antiproliferative Activity of Biginelli Compounds against Cancer Cell Lines: Monastrol, Oxo-Monastrol and Oxygenated Analogues. *Bioorganic Chem.* **2006**, *34* (4), 173–182. https://doi.org/10.1016/j.bioorg.2006.04.003.
(137) Chakrabarti, J. K.; Hotten, T. M.; Tupper, D. E. Process for Preparing 2-Methyl-Thieno-Benzodiazepine. US6008216A.
(138) Thomas, J.; Jana, S.; Sonawane, M.; Fiey, B.; Balzarini, J.; Liekens, S.; Dehaen, W. A New Four-Component Reaction Involving the Michael Addition and the Gewald Reaction, Leading to Diverse Biologically Active 2-Aminothiophenes. *Org. Biomol. Chem.* **2017**, *15* (18), 3892–3900. https://doi.org/10.1039/c7ob00707h.
(139) Cummings, T. F.; Shelton, J. R. Mannich Reaction Mechanisms. *J. Org. Chem.* **1960**, *25* (3), 419–423. https://doi.org/10.1021/jo01073a029.
(140) Van Marle, C. M.; Tollens, B. Ueber Formaldehyd-Derivate Des Acetophenons. *Berichte Dtsch. Chem. Ges.* **1903**, *36* (2), 1351–1357. https://doi.org/10.1002/cber.19030360207.
(141) Bae, H. Y.; Kim, M. J.; Sim, J. H.; Song, C. E. Direct Catalytic Asymmetric Mannich

Reaction with Dithiomalonates as Excellent Mannich Donors: Organocatalytic Synthesis of (R)-Sitagliptin. *Angew. Chem. Int. Ed Engl.* **2016**, *55* (36), 10825–10829. https://doi.org/10.1002/anie.201605167.
(142) Heravi, M.; Zadsirjan, V.; Savadjani, Z. Applications of Mannich Reaction in Total Syntheses of Natural Products. *Curr. Org. Chem.* **2014**, *18* (22), 2857–2891. https://doi.org/10.2174/1385272819666141014212254.
(143) Robinson, R. A synthesis of tropinone. 111th ed. Journal of the Chemical Society, Transactions July 13, 1917, pp 762–768.
(144) Schöpf, C. Die Synthese von Naturstoffen, insbesondere von alkaloiden, under physiologischen Bedingungen und ihre Bedeutung für die Frage der Entstehung einiger pflanzlicher Naturstoffe in der Zelle. *Angewandte Chemie*. October 2, 1937, pp 779–790.
(145) Petasis, N. A.; Akritopoulou, I. The Boronic Acid Mannich Reaction: A New Method for the Synthesis of Geometrically Pure Allylamines. *Tetrahedron Lett.* **1993**, *34* (4), 583–586. https://doi.org/10.1016/S0040-4039(00)61625-8.
(146) Dömling, A.; Ugi, I. Multicomponent Reactions with Isocyanides. *Angew. Chem.* **2000**, *39* (18), 3168–3210. https://doi.org/10.1002/1521-3773(20000915)39:18<3168::AID-ANIE3168>3.0.CO;2-U.
(147) Baker, R. H.; Stanonis, D. The Passerini Reaction. III. Stereochemistry and Mechanism [1,2]. *J. Am. Chem. Soc.* **1951**, *73* (2), 699–702. https://doi.org/10.1021/ja01146a060.
(148) Moran, E. J.; Armstrong, R. W. Highly Convergent Approach to the Synthesis of the Epoxy-Amide Fragment of the Azinomycins. *Tetrahedron Lett.* **1991**, *32* (31), 3807–3810. https://doi.org/10.1016/S0040-4039(00)79381-6.
(149) Ugi, I. The ?-Addition of Immonium Ions and Anions to Isonitriles Accompanied by Secondary Reactions. *Angew. Chem. Int. Ed. Engl.* **1962**, *1* (1), 8–21. https://doi.org/10.1002/anie.196200081.
(150) Ugi, I. Recent Progress in the Chemistry of Multicomponent Reactions. *Pure Appl. Chem.* **2001**, *73* (1), 187–191. https://doi.org/10.1351/pac200173010187.
(151) Qiu, G.; Ding, Q.; Wu, J. Recent Advances in Isocyanide Insertion Chemistry. *Chem. Soc. Rev.* **2013**, *42* (12), 5257–5269. https://doi.org/10.1039/c3cs35507a.
(152) Denmark, S. E.; Fan, Y. Catalytic, Enantioselective α-Additions of Isocyanides: Lewis Base Catalyzed Passerini-Type Reactions. *J. Org. Chem.* **2005**, *70* (24), 9667–9676. https://doi.org/10.1021/jo050549m.
(153) Gedey, S.; Van der Eycken, J.; Fülöp, F. Liquid-Phase Combinatorial Synthesis of Alicyclic Beta-Lactams via Ugi Four-Component Reaction. *Org. Lett.* **2002**, *4* (11), 1967–1969. https://doi.org/10.1021/ol025986r.
(154) Ilyin, A.; Kysil, V.; Krasavin, M.; Kurashvili, I.; Ivachtchenko, A. V. Complexity-Enhancing Acid-Promoted Rearrangement of Tricyclic Products of Tandem Ugi 4CC/Intramolecular Diels-Alder Reaction. *J. Org. Chem.* **2006**, *71* (25), 9544–9547. https://doi.org/10.1021/jo061825f.
(155) Vázquez-Vera, Ó.; Segura-Olvera, D.; Rincón-Guevara, M.; Gutiérrez-Carrillo, A.; García-Sánchez, M.; Ibarra, I.; Lomas-Romero, L.; Islas-Jácome, A.; González-Zamora, E. Synthesis of New 5-Aryl-Benzo[f][1,7]Naphthyridines via a Cascade Process (Ugi-3CR/Intramolecular Aza-Diels-Alder Cycloaddition)/Aromatization. *Molecules* **2018**, *23* (8), 2029. https://doi.org/10.3390/molecules23082029.
(156) El Kaim, L.; Gizolme, M.; Grimaud, L.; Oble, J. Direct Access to Heterocyclic Scaffolds by New Multicomponent Ugi-Smiles Couplings. *Org. Lett.* **2006**, *8* (18), 4019–4021. https://doi.org/10.1021/ol061605o.
(157) Joshi, N. S.; Whitaker, L. R.; Francis, M. B. A Three-Component Mannich-Type Reaction for Selective Tyrosine Bioconjugation. *J. Am. Chem. Soc.* **2004**, *126* (49), 15942–15943. https://doi.org/10.1021/ja0439017.
(158) Romanini, D. W.; Francis, M. B. Attachment of Peptide Building Blocks to Proteins

Through Tyrosine Bioconjugation. *Bioconjug. Chem.* **2008**, *19* (1), 153–157. https://doi.org/10.1021/bc700231v.
(159) Chilamari, M.; Purushottam, L.; Rai, V. Site-Selective Labeling of Native Proteins by a Multicomponent Approach. *Chem. - Eur. J.* **2017**, *23* (16), 3819–3823. https://doi.org/10.1002/chem.201605938.
(160) Chilamari, M.; Kalra, N.; Shukla, S.; Rai, V. Single-Site Labeling of Lysine in Proteins through a Metal-Free Multicomponent Approach. *Chem. Commun.* **2018**, *54* (53), 7302–7305. https://doi.org/10.1039/C8CC03311K.
(161) Sim, Y. E.; Nwajiobi, O.; Mahesh, S.; Cohen, R. D.; Reibarkh, M. Y.; Raj, M. Secondary Amine Selective Petasis (SASP) Bioconjugation. *Chem. Sci.* **2020**, *11* (1), 53–61. https://doi.org/10.1039/C9SC04697F.
(162) Goldstein, L.; Freeman, A.; Sokolovsky, M. Chemically Modified Nylons as Supports for Enzyme Immobilization. Polyisonitrile-Nylon. *Biochem. J.* **1974**, *143* (3), 497–509. https://doi.org/10.1042/bj1430497a.
(163) Camacho, C.; Matías, J. C.; García, D.; Simpson, B. K.; Villalonga, R. Amperometric Enzyme Biosensor for Hydrogen Peroxide via Ugi Multicomponent Reaction. *Electrochem. Commun.* **2007**, *9* (7), 1655–1660. https://doi.org/10.1016/j.elecom.2007.03.013.
(164) Mohammadi, M.; Ashjari, M.; Garmroodi, M.; Yousefi, M.; Karkhane, A. A. The Use of Isocyanide-Based Multicomponent Reaction for Covalent Immobilization of Rhizomucor Miehei Lipase on Multiwall Carbon Nanotubes and Graphene Nanosheets. *RSC Adv.* **2016**, *6* (76), 72275–72285. https://doi.org/10.1039/C6RA14142K.
(165) Mohammadi, M.; Ashjari, M.; Dezvarei, S.; Yousefi, M.; Babaki, M.; Mohammadi, J. Rapid and High-Density Covalent Immobilization of Rhizomucor Miehei Lipase Using a Multi Component Reaction: Application in Biodiesel Production. *RSC Adv.* **2015**, *5* (41), 32698–32705. https://doi.org/10.1039/C5RA03299G.
(166) Mohammadi, M.; Habibi, Z.; Gandomkar, S.; Yousefi, M. A Novel Approach for Bioconjugation of Rhizomucor Miehei Lipase (RML) onto Amine-Functionalized Supports; Application for Enantioselective Resolution of Rac-Ibuprofen. *Int. J. Biol. Macromol.* **2018**, *117*, 523–531. https://doi.org/10.1016/j.ijbiomac.2018.05.218.
(167) Ziegler, T.; Gerling, S.; Lang, M. Preparation of Bioconjugates through an Ugi Reaction. *Angew. Chem. Int. Ed.* **2000**, *39* (12), 2109–2112. https://doi.org/10.1002/1521-3773(20000616)39:12<2109::AID-ANIE2109>3.0.CO;2-9.
(168) Méndez, Y.; Chang, J.; Humpierre, A. R.; Zanuy, A.; Garrido, R.; Vasco, A. V.; Pedroso, J.; Santana, D.; Rodríguez, L. M.; García-Rivera, D.; Valdés, Y.; Vérez-Bencomo, V.; Rivera, D. G. Multicomponent Polysaccharide–Protein Bioconjugation in the Development of Antibacterial Glycoconjugate Vaccine Candidates. *Chem. Sci.* **2018**, *9* (9), 2581–2588. https://doi.org/10.1039/C7SC05467J.
(169) Humpierre, A. R.; Zanuy, A.; Saenz, M.; Garrido, R.; Vasco, A. V.; Pérez-Nicado, R.; Soroa-Milán, Y.; Santana-Mederos, D.; Westermann, B.; Vérez-Bencomo, V.; Méndez, Y.; García-Rivera, D.; Rivera, D. G. Expanding the Scope of Ugi Multicomponent Bioconjugation to Produce Pneumococcal Multivalent Glycoconjugates as Vaccine Candidates. *Bioconjug. Chem.* **2020**, *31* (9), 2231–2240. https://doi.org/10.1021/acs.bioconjchem.0c00423.
(170) Burks, J. E.; Espinosa, L.; LaBell, E. S.; McGill, J. M.; Ritter, A. R.; Speakman, J. L.; Williams, M.; Bradley, D. A.; Haehl, M. G.; Schmid, C. R. Development of a Manufacturing Process for Zatosetron Maleate. *Org. Process Res. Dev.* **1997**, *1* (3), 198–210. https://doi.org/10.1021/op970101q.
(171) Joshi, P. N.; Rai, V. Single-Site Labeling of Histidine in Proteins, on-Demand Reversibility, and Traceless Metal-Free Protein Purification. *Chem. Commun.* **2019**, *55* (8), 1100–1103. https://doi.org/10.1039/C8CC08733D.
(172) Miyashita, H.; Chikazawa, M.; Otaki, N.; Hioki, Y.; Shimozu, Y.; Nakashima, F.; Shibata, T.; Hagihara, Y.; Maruyama, S.; Matsumi, N.; Uchida, K. Lysine Pyrrolation Is a

Naturally-Occurring Covalent Modification Involved in the Production of DNA Mimic Proteins. *Sci. Rep.* **2014**, *4* (1), 5343. https://doi.org/10.1038/srep05343.
(173) Pirali, T.; Mossetti, R.; Galli, S.; Tron, G. C. Stereospecific Synthesis of *Syn* -α-Oximinoamides by a Three-Component Reaction of Isocyanides, *Syn* -Chlorooximes, and Carboxylic Acids. *Org. Lett.* **2011**, *13* (14), 3734–3737. https://doi.org/10.1021/ol201397x.
(174) Giustiniano, M.; Novellino, E.; Tron, G. Nitrile N-Oxides and Nitrile Imines as New Fuels for the Discovery of Novel Isocyanide-Based Multicomponent Reactions. *Synthesis* **2016**, *48* (17), 2721–2731. https://doi.org/10.1055/s-0035-1561672.
(175) Mercalli, V.; Giustiniano, M.; Del Grosso, E.; Varese, M.; Cassese, H.; Massarotti, A.; Novellino, E.; Tron, G. C. Solution-Phase Parallel Synthesis of Aryloxyimino Amides via a Novel Multicomponent Reaction among Aromatic (*Z*)-Chlorooximes, Isocyanides, and Electron-Deficient Phenols. *ACS Comb. Sci.* **2014**, *16* (11), 602–605. https://doi.org/10.1021/co5000882.
(176) Mercalli, V.; Meneghetti, F.; Tron, G. C. Isocyanide-Mediated Multicomponent Synthesis of *C* -Oximinoamidines. *Org. Lett.* **2013**, *15* (22), 5902–5905. https://doi.org/10.1021/ol403062m.
(177) Schäfer, R. J. B.; Monaco, M. R.; Li, M.; Tirla, A.; Rivera-Fuentes, P.; Wennemers, H. The Bioorthogonal Isonitrile–Chlorooxime Ligation. *J. Am. Chem. Soc.* **2019**, *141* (47), 18644–18648. https://doi.org/10.1021/jacs.9b07632.
(178) Grimsley, G. R.; Scholtz, J. M.; Pace, C. N. A Summary of the Measured p *K* Values of the Ionizable Groups in Folded Proteins. *Protein Sci.* **2008**, *18*, 247–251. https://doi.org/10.1002/pro.19.
(179) Hermanto, S.; Yusuf, M.; Mutalib, A.; Hudiyono, S. Molecular Dynamic Simulation of Trastuzumab F(Ab') $_2$ Structure in Corporation with HER2 as a Theranostic Agent of Breast Cancer. *J. Phys. Conf. Ser.* **2017**, *835*, 012005. https://doi.org/10.1088/1742-6596/835/1/012005.
(180) Nisonoff, A.; Wissler, F. C.; Lipman, L. N. Properties of the Major Component of a Peptic Digest of Rabbit Antibody. *Science* **1960**, *132*, 1770–1771.
(181) Fudenberg, H., H.; Drews, G.; Nisonoff, A. Serologic Demonstration of Dual Specificity of Rabbit Bivalent Hybrid Antibody. *J. Exp. Med.* **1964**, *119* (1), 151–156. https://doi.org/10.1084/jem.119.1.151.
(182) Kontermann, R. Dual Targeting Strategies with Bispecific Antibodies. *mAbs* **2012**, *4* (2), 182–197. https://doi.org/10.4161/mabs.4.2.19000.
(183) Dhimolea, E.; Reichert, J. M. World Bispecific Antibody Summit, September 27–28, 2011, Boston, MA. *mAbs* **2012**, *4* (1), 4–13. https://doi.org/10.4161/mabs.4.1.18821.
(184) Labrijn, A. F.; Parren, P. W. H. I. Hitting Ebola, to the Power of Two. *Science* **2016**, *354* (6310), 284–285. https://doi.org/10.1126/science.aaj2036.
(185) Spiess, C.; Zhai, Q.; Carter, P. J. Alternative Molecular Formats and Therapeutic Applications for Bispecific Antibodies. *Mol. Immunol.* **2015**, *67* (2), 95–106. https://doi.org/10.1016/j.molimm.2015.01.003.
(186) Mullard, A. Bispecific Antibody Pipeline Moves beyond Oncology. *Nat. Rev. Drug Discov.* **2017**, *16* (10), 667–668. https://doi.org/10.1038/nrd.2017.187.
(187) Staerz, U. D.; Kanagawa, O.; Bevan, M. J. Hybrid Antibodies Can Target Sites for Attack by T Cells. *Nature* **1985**, *314* (6012), 628–631. https://doi.org/10.1038/314628a0.
(188) Milstein, C.; Cuello, A. C. Hybrid Hybridomas and Their Use in Immunohistochemistry. *Nature* **1983**, *305* (5934), 537–540. https://doi.org/10.1038/305537a0.
(189) Köhler, G.; Milstein, C. Continuous Cultures of Fused Cells Secreting Antibody of Predefined Specificity. *Nature* **1975**, *256* (5517), 495–497. https://doi.org/10.1038/256495a0.
(190) Köhler, G.; Howe, S. C.; Milstein, C. Fusion between Immunoglobulin-Secreting and Nonsecreting Myeloma Cell Lines. *Eur. J. Immunol.* **1976**, *6* (4), 292–295. https://doi.org/10.1002/eji.1830060411.

(191) Ridgway, J. B. B.; Presta, L. G.; Carter, P. 'Knobs-into-Holes' Engineering of Antibody C_H3 Domains for Heavy Chain Heterodimerization. *Protein Eng. Des. Sel.* **1996**, *9* (7), 617–621. https://doi.org/10.1093/protein/9.7.617.
(192) Kuglstatter, A.; Stihle, M.; Neumann, C.; Müller, C.; Schaefer, W.; Klein, C.; Benz, J.; Roche Pharmaceutical Research and Early Development. Structural Differences between Glycosylated, Disulfide-Linked Heterodimeric Knob-into-Hole Fc Fragment and Its Homodimeric Knob-Knob and Hole-Hole Side Products. *Protein Eng. Des. Sel. PEDS* **2017**, *30* (9), 649–656. https://doi.org/10.1093/protein/gzx041.
(193) Merchant, A. M.; Zhu, Z.; Yuan, J. Q.; Goddard, A.; Adams, C. W.; Presta, L. G.; Carter, P. An Efficient Route to Human Bispecific IgG. *Nat. Biotechnol.* **1998**, *16* (7), 677–681. https://doi.org/10.1038/nbt0798-677.
(194) Stutz, C.; Blein, S. A Single Mutation Increases Heavy-Chain Heterodimer Assembly of Bispecific Antibodies by Inducing Structural Disorder in One Homodimer Species. *J. Biol. Chem.* **2020**, *295* (28), 9392–9408. https://doi.org/10.1074/jbc.RA119.012335.
(195) Schaefer, W.; Regula, J. T.; Bähner, M.; Schanzer, J.; Croasdale, R.; Dürr, H.; Gassner, C.; Georges, G.; Kettenberger, H.; Imhof-Jung, S.; Schwaiger, M.; Stubenrauch, K. G.; Sustmann, C.; Thomas, M.; Scheuer, W.; Klein, C. Immunoglobulin Domain Crossover as a Generic Approach for the Production of Bispecific IgG Antibodies. *Proc. Natl. Acad. Sci.* **2011**, *108* (27), 11187–11192. https://doi.org/10.1073/pnas.1019002108.
(196) Birch, J. R.; Racher, A. J. Antibody Production. *Adv. Drug Deliv. Rev.* **2006**, *58* (5–6), 671–685. https://doi.org/10.1016/j.addr.2005.12.006.
(197) Chan, A. C.; Carter, P. J. Therapeutic Antibodies for Autoimmunity and Inflammation. *Nat. Rev. Immunol.* **2010**, *10* (5), 301–316. https://doi.org/10.1038/nri2761.
(198) Kim, C. H.; Axup, J. Y.; Dubrovska, A.; Kazane, S. A.; Hutchins, B. A.; Wold, E. D.; Smider, V. V.; Schultz, P. G. Synthesis of Bispecific Antibodies Using Genetically Encoded Unnatural Amino Acids. *J. Am. Chem. Soc.* **2012**, *134* (24), 9918–9921. https://doi.org/10.1021/ja303904e.
(199) Hudak, J. E.; Barfield, R. M.; de Hart, G. W.; Grob, P.; Nogales, E.; Bertozzi, C. R.; Rabuka, D. Synthesis of Heterobifunctional Protein Fusions Using Copper-Free Click Chemistry and the Aldehyde Tag. *Angew. Chem. Int. Ed.* **2012**, *51* (17), 4161–4165. https://doi.org/10.1002/anie.201108130.
(200) Patterson, J. T.; Gros, E.; Zhou, H.; Atassi, G.; Kerwin, L.; Carmody, L.; Zhu, T.; Jones, B.; Fu, Y.; Kaufmann, G. F. Chemically Generated IgG2 Bispecific Antibodies through Disulfide Bridging. *Bioorg. Med. Chem. Lett.* **2017**, *27* (16), 3647–3652. https://doi.org/10.1016/j.bmcl.2017.07.021.
(201) Carlring, J.; De Leenheer, E.; Heath, A. W. A Novel Redox Method for Rapid Production of Functional Bi-Specific Antibodies For Use in Early Pilot Studies. *PLoS ONE* **2011**, *6* (7), e22533. https://doi.org/10.1371/journal.pone.0022533.
(202) Gupta, J.; Hoque, M.; Ahmad, M. F.; Khan, R. H.; Saleemuddin, M. Acid PH Promotes Bispecific Antibody Formation by the Redox Procedure. *Int. J. Biol. Macromol.* **2019**, *125*, 469–477. https://doi.org/10.1016/j.ijbiomac.2018.12.063.
(203) Karpovsky, B.; Titus, J. A.; Stephany, D. A.; Segal, D. M. Production of Target-Specific Effector Cells Using Hetero-Cross-Linked Aggregates Containing Anti-Target Cell and Anti-Fc Gamma Receptor Antibodies. *J. Exp. Med.* **1984**, *160* (6), 1686–1701. https://doi.org/10.1084/jem.160.6.1686.
(204) Snider, D. P.; Segal, D. M. Targeted Antigen Presentation Using Crosslinked Antibody Heteroaggregates. *J. Immunol. Baltim. Md 1950* **1987**, *139* (5), 1609–1616.
(205) Ring, D. B.; Hsieh-Ma, S. T.; Shi, T.; Reeder, J. Antigen Forks: Bispecific Reagents That Inhibit Cell Growth by Binding Selected Pairs of Tumor Antigens. *Cancer Immunol. Immunother.* **1994**, *39* (1), 41–48. https://doi.org/10.1007/bf01517179.
(206) Reusch, U.; Sundaram, M.; Davol, P. A.; Olson, S. D.; Davis, J. B.; Demel, K.; Nissim,

J.; Rathore, R.; Liu, P. Y.; Lum, L. G. Anti-CD3 × Anti-Epidermal Growth Factor Receptor (EGFR) Bispecific Antibody Redirects T-Cell Cytolytic Activity to EGFR-Positive Cancers *In Vitro* and in an Animal Model. *Clin. Cancer Res.* **2006**, *12* (1), 183–190. https://doi.org/10.1158/1078-0432.CCR-05-1855.
(207) Anderson, P.; Crist, W.; Hasz, D.; Carroll, A.; Myers, D.; Uckun, F. G19.4(Alpha CD3) x B43(Alpha CD19) Monoclonal Antibody Heteroconjugate Triggers CD19 Antigen-Specific Lysis of t(4;11) Acute Lymphoblastic Leukemia Cells by Activated CD3 Antigen-Positive Cytotoxic T Cells. *Blood* **1992**, *80* (11), 2826–2834. https://doi.org/10.1182/blood.V80.11.2826.2826.
(208) Glennie, M. J.; McBride, H. M.; Worth, A. T.; Stevenson, G. T. Preparation and Performance of Bispecific F(Ab' Gamma)2 Antibody Containing Thioether-Linked Fab' Gamma Fragments. *J. Immunol. Baltim. Md 1950* **1987**, *139* (7), 2367–2375.
(209) Morais, M.; Forte, N.; Chudasama, V.; Baker, J. R. Application of Next-Generation Maleimides (NGMs) to Site-Selective Antibody Conjugation. In *Bioconjugation*; Massa, S., Devoogdt, N., Eds.; Methods in Molecular Biology; Springer New York: New York, NY, 2019; Vol. 2033, pp 15–24. https://doi.org/10.1007/978-1-4939-9654-4_2.
(210) Smith, M. E. B.; Schumacher, F. F.; Ryan, C. P.; Tedaldi, L. M.; Papaioannou, D.; Waksman, G.; Caddick, S.; Baker, J. R. Protein Modification, Bioconjugation, and Disulfide Bridging Using Bromomaleimides. *J. Am. Chem. Soc.* **2010**, *132* (6), 1960–1965. https://doi.org/10.1021/ja908610s.
(211) Lyon, R. P.; Setter, J. R.; Bovee, T. D.; Doronina, S. O.; Hunter, J. H.; Anderson, M. E.; Balasubramanian, C. L.; Duniho, S. M.; Leiske, C. I.; Li, F.; Senter, P. D. Self-Hydrolyzing Maleimides Improve the Stability and Pharmacological Properties of Antibody-Drug Conjugates. *Nat. Biotechnol.* **2014**, *32* (10), 1059–1062. https://doi.org/10.1038/nbt.2968.
(212) Morais, M.; Nunes, J. P. M.; Karu, K.; Forte, N.; Benni, I.; Smith, M. E. B.; Caddick, S.; Chudasama, V.; Baker, J. R. Optimisation of the Dibromomaleimide (DBM) Platform for Native Antibody Conjugation by Accelerated Post-Conjugation Hydrolysis. *Org. Biomol. Chem.* **2017**, *15* (14), 2947–2952. https://doi.org/10.1039/C7OB00220C.
(213) Castañeda, L.; Wright, Z. V. F.; Marculescu, C.; Tran, T. M.; Chudasama, V.; Maruani, A.; Hull, E. A.; Nunes, J. P. M.; Fitzmaurice, R. J.; Smith, M. E. B.; Jones, L. H.; Caddick, S.; Baker, J. R. A Mild Synthesis of N-Functionalised Bromomaleimides, Thiomaleimides and Bromopyridazinediones. *Tetrahedron Lett.* **2013**, *54* (27), 3493–3495. https://doi.org/10.1016/j.tetlet.2013.04.088.
(214) Dommerholt, J.; Schmidt, S.; Temming, R.; Hendriks, L. J. A.; Rutjes, F. P. J. T.; van Hest, J. C. M.; Lefeber, D. J.; Friedl, P.; van Delft, F. L. Readily Accessible Bicyclononynes for Bioorthogonal Labeling and Three-Dimensional Imaging of Living Cells. *Angew. Chem. Int. Ed.* **2010**, *49* (49), 9422–9425. https://doi.org/10.1002/anie.201003761.
(215) Rady, T.; Mosser, M.; Nothisen, M.; Erb, S.; Dovgan, I.; Cianférani, S.; Wagner, A.; Chaubet, G. Bicyclo[6.1.0]Nonyne Carboxylic Acid for the Production of Stable Molecular Probes. *RSC Adv.* **2021**, *11* (58), 36777–36780. https://doi.org/10.1039/D1RA07905K.
(216) Cresswell, C.; Newcombe, A. R.; Davies, S.; Macpherson, I.; Nelson, P.; O'Donovan, K.; Francis, R. Optimal Conditions for the Papain Digestion of Polyclonal Ovine IgG for the Production of Biotherapeutic Fab Fragments. *Biotechnol. Appl. Biochem.* **2005**, *42* (2), 163. https://doi.org/10.1042/BA20050020.
(217) Lewis, S. D.; Johnson, F. A.; Ohno, A. K.; Shafer, J. A. Dependence of the Catalytic Activity of Papain on the Ionization of Two Acidic Groups. *J. Biol. Chem.* **1978**, *253* (14), 5080–5086. https://doi.org/10.1016/S0021-9258(17)34660-4.
(218) Ramos-de-la-Peña, A. M.; González-Valdez, J.; Aguilar, O. Protein A Chromatography: Challenges and Progress in the Purification of Monoclonal Antibodies. *J. Sep. Sci.* **2019**, *42* (9), 1816–1827. https://doi.org/10.1002/jssc.201800963.
(219) Lefranc, M.-P.; Pommié, C.; Kaas, Q.; Duprat, E.; Bosc, N.; Guiraudou, D.; Jean, C.;

Ruiz, M.; Da Piédade, I.; Rouard, M.; Foulquier, E.; Thouvenin, V.; Lefranc, G. IMGT Unique Numbering for Immunoglobulin and T Cell Receptor Constant Domains and Ig Superfamily C-like Domains. *Dev. Comp. Immunol.* **2005**, *29* (3), 185–203. https://doi.org/10.1016/j.dci.2004.07.003.
(220) Liu, H.; May, K. Disulfide Bond Structures of IgG Molecules: Structural Variations, Chemical Modifications and Possible Impacts to Stability and Biological Function. *mAbs* **2012**, *4* (1), 17–23. https://doi.org/10.4161/mabs.4.1.18347.
(221) Gu, S.; Wen, D.; Weinreb, P. H.; Sun, Y.; Zhang, L.; Foley, S. F.; Kshirsagar, R.; Evans, D.; Mi, S.; Meier, W.; Pepinsky, R. B. Characterization of Trisulfide Modification in Antibodies. *Anal. Biochem.* **2010**, *400* (1), 89–98. https://doi.org/10.1016/j.ab.2010.01.019.
(222) Peters, T. Serum Albumin. *Adv. Protein Chem.* **1985**, *37*, 161–245. https://doi.org/10.1016/s0065-3233(08)60065-0.
(223) Kratz, F. Albumin as a Drug Carrier: Design of Prodrugs, Drug Conjugates and Nanoparticles. *J. Control. Release Off. J. Control. Release Soc.* **2008**, *132* (3), 171–183. https://doi.org/10.1016/j.jconrel.2008.05.010.
(224) Elzoghby, A. O.; Samy, W. M.; Elgindy, N. A. Albumin-Based Nanoparticles as Potential Controlled Release Drug Delivery Systems. *J. Control. Release Off. J. Control. Release Soc.* **2012**, *157* (2), 168–182. https://doi.org/10.1016/j.jconrel.2011.07.031.
(225) Steinhauser, I. M.; Langer, K.; Strebhardt, K. M.; Spänkuch, B. Effect of Trastuzumab-Modified Antisense Oligonucleotide-Loaded Human Serum Albumin Nanoparticles Prepared by Heat Denaturation. *Biomaterials* **2008**, *29* (29), 4022–4028. https://doi.org/10.1016/j.biomaterials.2008.07.001.
(226) Ulbrich, K.; Hekmatara, T.; Herbert, E.; Kreuter, J. Transferrin- and Transferrin-Receptor-Antibody-Modified Nanoparticles Enable Drug Delivery across the Blood-Brain Barrier (BBB). *Eur. J. Pharm. Biopharm. Off. J. Arbeitsgemeinschaft Pharm. Verfahrenstechnik EV* **2009**, *71* (2), 251–256. https://doi.org/10.1016/j.ejpb.2008.08.021.
(227) Wang, J.; Zhang, B. Bovine Serum Albumin as a Versatile Platform for Cancer Imaging and Therapy. *Curr. Med. Chem.* **2018**, *25* (25), 2938–2953. https://doi.org/10.2174/0929867324666170314143335.
(228) Chen, C. B.; Hammo, B.; Barry, J.; Radhakrishnan, K. Overview of Albumin Physiology and Its Role in Pediatric Diseases. *Curr. Gastroenterol. Rep.* **2021**, *23* (8), 11. https://doi.org/10.1007/s11894-021-00813-6.
(229) Cysteinylation of Proteins. In *Co□ and Post-Translational Modifications of Therapeutic Antibodies and Proteins*; John Wiley & Sons, Inc.: Hoboken, NJ, USA, 2019; pp 35–38. https://doi.org/10.1002/9781119053354.ch4.
(230) Wiame, E.; Delpierre, G.; Collard, F.; Van Schaftingen, E. Identification of a Pathway for the Utilization of the Amadori Product Fructoselysine in Escherichia Coli. *J. Biol. Chem.* **2002**, *277* (45), 42523–42529. https://doi.org/10.1074/jbc.M200863200.
(231) Fernhoff, N. B.; Derbyshire, E. R.; Marletta, M. A. A Nitric Oxide/Cysteine Interaction Mediates the Activation of Soluble Guanylate Cyclase. *Proc. Natl. Acad. Sci.* **2009**, *106* (51), 21602–21607. https://doi.org/10.1073/pnas.0911083106.
(232) Müller, D.; Kontermann, R. E. Bispecific Antibodies for Cancer Immunotherapy: Current Perspectives. *BioDrugs* **2010**, *24* (2), 89–98. https://doi.org/10.2165/11530960-000000000-00000.
(233) Mei, L.; Zappala, F.; Tsourkas, A. Rapid Production of Bispecific Antibodies from Off-the-Shelf IgGs with High Yield and Purity. *Bioconjug. Chem.* **2022**, *33* (1), 134–141. https://doi.org/10.1021/acs.bioconjchem.1c00476.
(234) Baeuerle, P. A.; Reinhardt, C. Bispecific T-Cell Engaging Antibodies for Cancer Therapy. *Cancer Res.* **2009**, *69* (12), 4941–4944. https://doi.org/10.1158/0008-5472.CAN-09-0547.
(235) Trabolsi, A.; Arumov, A.; Schatz, J. H. T Cell–Activating Bispecific Antibodies in

Cancer Therapy. *J. Immunol.* **2019**, *203* (3), 585–592.https://doi.org/10.4049/jimmunol.1900496.

Valentine VAUR

EDSC
École Doctorale des Sciences Chimiques

Développement de nouvelles méthodes de conjugaison chimiques pour la modification site-sélective de protéines natives

Résumé

La modification chimique de protéines a été largement étudié lors des dernières décennies, en particulier dans le domaine thérapeutique. Les protéines étant des poly-nucléophiles, leur modification homogène demeure un défi majeur du domaine. Les travaux présentés ici proposent de cibler en même temps deux résidus d'une protéine via la réaction de Ugi. Ainsi la protéine est utilisée à la fois comme source d'amine primaire et d'acide carboxylique. Après introduction de diverses combinaisons d'isocyanides et d'aldéhydes dans le milieu, la formation de l'adduit attendu a pu être observé mais sa formation s'est avéré être en compétition avec un adduit intra-résidu au niveau des aspartates et glutamates *N*-terminaux des anticorps monoclonaux utilisés. Une étude mécaniste approfondie nous a permis de développer des conditions permettant la modification exclusive des résidus E1 et D1. Ensuite, nous avons illustré l'intérêt d'un tel niveau de sélectivité en produisant de manière rapide et homogène des complexes de haut poids moléculaire tels que des anticorps bispécifiques.

Mots-clés : anticorps, bioconjugation, réactions multicomposantes, anticorps bispécifiques.

Abstract

The development of chemical methods for the site-selective modification of proteins have been widely investigated for the past decades, especially in the therapeutic field. Because of their poly-nucleophilic nature, site-selective modification of proteins can be highly challenging and careful choice of the targeted amino acid(s) must be made. We recently developed an Ugi based dual residue targeting strategy for the labeling of human and humanized mAbs. In our case the mAb is used as source for both primary amine and carboxylic acid and the introduction of various isocyanides and aldehydes in the media led to the formation of the expected inter residue adduct in competition with an intra residue adduct on the highly conserved N-terminal aspartates and glutamates residues. In depth mechanistic study of the reaction allowed to develop *N*-ter selective conditions. Then, we showed that such selectively labeled mAb allowed the rapid and efficient formation of high molecular weight complexes such as bispecific antibodies. More precisely we managed to form a bispecific T cell engager which showed great occupancy of both target receptors and good cytotoxic activity.

Keywords: antibodies, bioconjugation, multicomponent reactions, bispecific antibodies